SMART MATERIALS BASED ON THERMORESPONSIVE POLYMERS

Qilu ZHANG

2014

Submitted in partial fulfillment of the requirements

For the degree of Doctor of Science

Promoter:

Prof. Richard Hoogenboom

Department of Organic and Macromolecular Chemistry, Ghent University

Qilu Zhang

Smart materials based on thermoresponsive polymers

Dissertation, Ghent University, Belgium

Qilu Zhang was funded by the Chinese Scholarship Council (2010629042) and Special Research Fund (BOF) of Ghent University (BOF11/CHN/009).

ACKNOWLEDGEMENTS

I would like to thank my promoter, Professor Richard Hoogenboom. The works presented in this thesis would not have been possible without his support and guidance over the last four years. I really appreciate his effort and patience in training me in scientific thinking, research and writing skills. Also highly appreciated are the illuminating discussions with him, which offer me outstanding trainings to become an independent scientist.

I would also like to extend my gratitude to my master advisor Professor Xiaoyan Ma, who has helped and inspired me a lot when I was lost.

I truly thank my current and former colleagues in *supra-group* for their help, scientific discussions and collaborations, and more importantly, for the friendship. They are Victor, Lenny, Gertjan, Dr. Zhou, Zhanyao, Dr. Monnery, Kanykei, Dr. Lava, Daniel, JIM and Jim, Dr. Maji, Dr. Glassner, Bart, Glenn, Joachim, Alessandro …… Special thanks go to my student Filippo, Sibel, Berin for their contributions to my thesis.

I would like to acknowledge all my collaborators, especially Professor Bruno De Geest and his students Zhiyue, Nane and Benoit from Department of Pharmaceutics, Ghent University; Professor Patrick Theato and Philipp from University of Hamburg and Professor Jong-Dal Hong from University of Incheon.

I would also like to thank the faculty of the Department of Organic and Macromolecular Chemistry, especially Mr. Tom Parlevliet, Mr. Jos Van den Begin, Mr. Tim Courtin, Mrs. Ingrid Denaene, Mrs. Carine Laurent, Mrs. Veerle Van de Velde and Mrs. Queenie Van Muylem for their kind assistance over the last four years.

I would like to thank my Chinese friends in Ghent, especially Woody, Yuechao, Michael, Angela, Zhiyue, Hui, Ji, Jing, Amy, Ming, Guangzhi and Qun for sharing food and happiness. Special thanks go to Chaobo, Shaoren, Ranhua, Lei, Yuanyuan and Yingjie for the wonderful life in CHiSAG 2011. Without them, my life in Ghent would be so boring.

My endless thanks go to my parents for their unconditional love and giving me the best possible education.

Last but certainly not least, I want to express my love and thanks to my wife Meng for her love and accompany and my new born son Bill for coming into my life.

Qilu

September 2014

Ghent

TABLE OF CONTENT

Outline and aims of this thesis

Thermoresponsive polymers are polymers that undergo phase transition upon heating or cooling to the lower critical solution temperature (LCST) or upper critical solution temperature (UCST), which have been widely used as smart materials in a variety of fields, including biomedicine, temperature sensing and nanotechnology. To extent the application of thermoresponsive polymers as smart materials, this thesis will focus on the synthesis, thermoresponsive behavior and potential applications of a series of thermoresponsive (co)polymers. The research starts with the evaluation and improvement of synthesis and characterization methods, i.e. reversible addition-fragmentation chain transfer (RAFT) polymerization and determination of phase transition temperature by turbidimetry. After this optimization of the synthesis and characterization of thermoresponsive polymers, the research focused on the development of novel thermoresponsive smart materials with UCST behavior, multi-responsive materials as well as co-assembly of different responsive polymers. With regard to applications, pH degradable polymers have been developed for drug delivery purposes and polymeric temperature sensors with a broad temperature sensing regime were targeted. For most of the systems, polyacrylates or polymethacrylates with functional side chains are used since the polymerization of such monomers can be easily controlled. Moreover, the commercial availability of a wide range of (meth)acrylate monomers also make them an excellent choice for manipulating polymer structure.

In order to accomplish these tasks, this thesis is divided into 8 chapters.

Chapter 1 provides an overview of current developments of thermoresponsive polymers with specific focus on polymers with upper critical solution temperature (UCST) behavior in alcohol/water solvent mixture and polymeric thermometers.

When studying thermoresponsive polymers, advanced polymerization techniques and accurate phase transition temperature determination is essential. Therefore, **Chapter 2** will describe a one-pot consecutive method for RAFT polymerization and facile *in situ* end group transformation resulting in inert well-defined polymers. In addition, our investigations on the influence and optimization of the parameters used for turbidimetry measurements of thermoresponsive polymer solutions are described.

The main parts of this thesis deal with the investigation of tuning the thermoresponsive behaviors as well as potential applications of thermoresponsive polymers. Since polymers with LCST behavior, which represents the majority of the thermoresponsive polymers, have already been in depth studied, this thesis mainly focuses on UCST polymers to show their importance and unique properties. In **Chapter 3**, the tuning

of the UCST behavior by introduction of comonomers or by UV light irradiation is investigated based on a simple polymer system, namely poly(methyl methacrylate) in ethanol/water solvent mixtures. In **Chapter 4**, we attempted to study the UCST behavior of polymer in aqueous solution based on the intra and/or inter electrostatic interaction of the polymer. Hence, a series of polyampholytes were synthesized by stoichiometric copolymerization of cationic and anionic monomers. However, the interaction between the negative and positive charges is not strong enough to result in the UCST behavior of the copolymer in pure water. Upon addition of alcohol as co-nonsolvent, the copolymers were found to show phase transition upon cooling indicating UCST behavior in alcohol/water solvent mixtures.

Apart from showing a single LCST and UCST phase transition behavior, polymers can also exhibit both LCST and UCST behaviors. Such double thermoresponsive polymers are quite rare, yet interesting for the fabricating of smart systems. In **Chapter 5**, the tuning of the double thermoresponsive behavior is investigated employing poly(*N*,*N*-dimethylaminoethyl methacrylate) (PDMAEMA) as model polymer, which exhibit both UCST and LCST phase transition in the presence of trivalent metal anions. Subsequently, a triple thermoresponsive schizophrenic diblock copolymer based on the double thermoresponsive behavior of PDMAEMA as well as LCST behavior of PDEGMA will be described to show the versatility of this kind of thermoresponsive polymer.

In **Chapter 6**, we focus on the cooperative behavior of thermoresponsive polymers, which was found to be attractive for the fine-tuning of the transition temperatures of polymers by a simple mixing strategy. The cooperative behavior of copoly(2-oxazoline)s with various T_{CP}s ranging from 25 to 90 ^{o}C was firstly investigated as a complementarity of the already reported polymer library. Then the cooperative behavior was extended to the co-assembly behavior of statistical thermoresponsive copolymers and a hydrophilic block copolymer with one thermoresponsive block. The influence of the hydrophilicity and concentration of the thermoresponsive polymer on the co-assembly behavior will be reported.

The last two chapters focus on the potential application of thermoresponsive polymers as smart materials. In **Chapter 7**, we will report the synthesis and properties of a series of novel dual pH- and temperature-responsive copolymers. The application for pH induced release of cargos and protein conjugation aiming for dual responsive protein will also be discussed. In addition, optimization of the dual responsive copolymers by controlling the copolymer architecture and utilizing a less stable pH-labile linear acetal instead of its cyclic analogue will be discussed.

Finally, results on the development of polymeric temperature sensor with a broad temperature sensing regime in aqueous solution will be reported in **Chapter 8**.

Chapter 1 Introduction

Abstract: This chapter highlighted recent development of thermoresponsive polymers, i.e. polymers that undergo a reversible phase transition from a molecularly dissolved state to an aggregated state in response to temperature changes. In particular, polymers undergo phase separation at upper critical solution temperature (UCST) in alcohol/water solvent mixtures (section 1.2) and thermoresponsive polymers used for temperature sensors (section 1.3) will be detailed discussed.

Compared to polymers that undergo a lower critical solution temperature (LCST) phase transition in aqueous solution, polymers exhibiting the reversed UCST behavior in aqueous solution have been much less documented as it is more challenging to achieve this behavior in aqueous solutions. Furthermore, the high sensitivity of UCST behavior to minor variation in polymer structure and solution composition hampered the development of applications based on these polymers (Seuring and Agarwal, 2012). However, polymers with UCST transition in aqueous alcohol/water solvent mixtures are more commonly reported and exhibit promising properties for the preparation of 'smart' materials. In this section, the theory and development of such polymers with UCST behavior in alcohol/water solvent mixtures will be discussed. By highlighting the reported examples of UCST polymers in alcohol/water solvent mixtures, we hope to demonstrate the versatility and potential that such UCST polymers possess as biomedical and 'smart' materials.

Polymeric temperature sensors based on the combination of solvatochromic dyes and thermoresponsive polymers will also be discussed. The concepts and synthesis of such polymeric sensors will be explained, followed by a discussion on how polymer structures influence the sensory properties. Finally, selected potential applications of these polymeric temperature sensors will be highlighted.

1.1 Stimuli-responsive polymers

Stimuli-responsive or "*smart*" polymers undergo dramatic property changes in response to small changes in the environment, such as temperature, pH, light or the presence of small molecules.[1-16] Proteins can be regarded as the smart polymers from Nature. The primary structure of these poly(amino acid)s controls their folding into 3D protein structures providing a wide range of functions ranging from, e.g., catalysis (enzymes) to switching of permeation (ion channels). Inspired by Nature, polymer scientists have developed artificial stimuli-responsive polymers to mimic this behavior and, although far less sophisticated than proteins, have made exciting progress in the last decades.

External stimuli for responsive polymers can be either physical or chemical signals. Physical signals could be, e.g., temperature, light or pressure, while pH, ionic strength, small molecules or proteins are examples of chemical signals. The environmental change can alter the molecular interactions between polymeric chains and solutes leading to a change of hydrogen bonding, hydrophobic interactions or ionic interactions of polymeric systems causing a response in the physical state of the system. For most of the 'smart' polymer systems, the removal or reversal of the stimulus can result in a reversion to the original physical state.

1.2 Polymers with UCST in alcohol/water solvent mixtures

Amongst the various applicable stimuli, temperature is most extensively exploited in the field of 'smart' polymers. Temperature responsive polymers, also called thermoresponsive polymers are polymers that respond with a solution phase transition to a change in the environmental temperature.[1, 8, 17] Because of the sophisticated and highly reversible responsive behavior, thermoresponsive polymers have found variety of applications in, e.g., drug delivery system, smart surface modification, nanotechnology and catalysis.[1-3, 8, 18-22] The first reported and most studied thermoresponsive polymer is poly(*N*-isopropylacrylamide) (PNIPAM), which exhibit phase transition from soluble state to aggregation at lower critical solution temperature (LCST).[23-25] Apart from PNIPAM, other LCST polymers like poly(oligo(ethylene glycol) (meth)acrylate)s,[20, 26-29] poly(2-oxazoline)s,[3, 30] poly(vinyl ether)s[31] or polypeptides[32, 33] have also been widely studied and have found various applications as smart materials. In comparison to the widely reported LCST polymers, polymers with the reverse behavior, i.e. polymers that are solubilized above the upper critical solution temperature (UCST) in aqueous solutions, have been much less documented since on one hand it is more challenging to achieve this behavior in aqueous solutions and on the other hand the UCST transition temperature is very sensitive to the environment.[17] In contrast to the commonly observed LCST behavior of polymers in water based on entropy driven dehydration, UCST behavior in water requires strong supramolecular attraction of the polymer chains. Upon heating the supramolecuar interactions are weakened leading to an enthalpy driven solubility phase transition, i.e. solubilization of the polymer chains. The main types of reported polymers with UCST behavior in water are zwitterionic polymers,[34, 35] polymers with strong

intermolecular hydrogen bonding[36] and polymer solutions with supramolecular crosslinking additives.[37-40] For most of these systems, the UCST behavior is very sensitive to, e.g. (co)polymer composition, electrolytes or concentration, which greatly limits the broad application of these polymers.[17] As an alternative, UCST polymers in organic solvent or in water-organic binary solvents mixtures have shown attractive properties.[41-46]

Ethanol/water solvent mixtures are environmentally friendly solvents that exhibit interesting abnormal properties due to the presence of hydration shells around the ethanol molecules.[47-49] For instance, the presence of such hydration shells has been reported to result in solubility maxima for drug molecules in water/ethanol mixtures with certain ratios.[50, 51] Benefiting from the non-ideal solvent mixture and its large change in polarity with varying temperatures, thermoresponsive polymers with UCST behavior have been developed for which the transition temperature depends on the structure of the alcohol and the composition of the alcohol/water binary solvent. Such UCST systems with low toxicity solvents have promising potential for, *e.g.*, personal care, medical or pharmaceutical applications. In addition, the responsive behavior of such polymers could be well controlled by solvent composition, which allows tuning of the self-assembly of copolymers bearing such UCST polymer block(s).[52, 53] Nonetheless, surprisingly few publications have appeared in recent years concerning UCST behavior of polymers in alcohol/water solvent mixtures, especially compared to the large amount of publications regarding LCST polymers. Two reasons may be ascribed to the low activity of this field: i) the importance of such ternary systems has been underestimated and overlooked; and ii) the alcohol-water-polymer ternary systems are very complicated and not well understood. Hence, this review aims at highlighting the recent progress in this area and to discuss the fundamentals of such UCST polymer systems based on recent literature, serving to enhance awareness and interest in the development of UCST polymers in alcohol/water solvent mixtures.

In this section, we will first briefly explain important concepts, such as the structure of binary alcohol/water systems, co-(non)solvency and UCST behavior of polymers in such binary solvent mixtures (section 1.2.1). The remainder of the review will provide an overview of the recent literature of UCST polymers in alcohol/water systems, organized based on co-solvency behavior (section 1.2.2) and co-nonsolvency behavior (section 1.2.3). Finally, polymers with reported UCST behavior in pure alcohol will be discussed (section 1.2.4) as these polymers are very likely to also exhibit UCST behavior in alcohol/water mixtures.

1.2.1 General concepts

In this section some basic concepts that are important for UCST polymer systems will be briefly explained. The structure of alcohol/water solvent mixtures will be firstly described followed by the explanation of two important concepts regarding solvent mixtures, namely co-solvency and co-nonsolvency

effects, as well as their applicability in polymer solutions. Finally, the basic concepts of UCST behavior of polymers in alcohol/water solvent mixtures will be discussed.

1.2.1.1 Structure of alcohol/water binary systems

Before discussing the mixtures of alcohol and water, it is necessary to know the structure of pure water since then the alcohol can be considered as a solute in water. However, the structure of pure liquid water has not yet been fully understood, although some models have been reported to explain its unusual properties.[54-57] Among these models, Frank and Wen's view of hydrogen bonding in liquid water is highly accepted,[58] as it can explain most of the properties of water, e.g. high dielectric constant, heat capacity, viscosity and thermal conductivity. According to this model, each oxygen atom can form four tetrahedral-like hydrogen bonds with protons originated from other water molecules. Hence, the H_2O molecules in pure liquid water are highly ordered self-stabilizing, three-dimensional, hydrogen-bonded clusters. Only less than 1% of the molecules are not connected to the bulk H-bond network as suggested by molecular simulation.[59]

The addition of an alcohol into water can disrupt the network of hydrogen-bonded water molecules resulting in a non-ideal solvent mixture. In general, when a small amount of low polarity organic solvent is added to water, these solute molecules are surrounded by cages of water molecules, being known as hydrophobic hydration. Hydration of alcohols is commonly, structurally interpreted in terms of the classical "iceberg" picture of Frank and Evans.[47, 49] Within this framework, it is suggested that the water molecules surrounding a nonpolar moiety are rearranging into a low-entropy cage with stronger hydrogen bonds. However, the hydrophobic hydration is broken with more solute added leading to phase separation. A more hydrophobic solute demands a larger number of water molecules to hydrate it and hence is more likely to cause rupture of its hydration shell. The presence of such hydration shells has been reported to result in solubility maxima for drug molecules in water/ethanol mixtures.[50, 60, 61] In case of thermoresponsive polymers in ethanol/water solvent mixtures, the hydration shells could lead to a solubility maximum of the polymer solute.[62, 63]

Molecular dynamic studies have shown that upon the addition of ethanol to water, the H-bond network of water gradually becomes less dense leading to the formation of disconnected water clusters (see Figure 1-1).[48] The cluster analysis shows that with increasing amount of ethanol in the water, more of the hydrogen-bonded water connections are broken leading to the presence of smaller water clusters and eventually free water molecules. More specifically, at $X_{EtOH} = 0.90$, up to 69% of the water component is present as free molecules and only 22%, 5% and 2% as water dimers, trimers and tetramers, respectively, indicating the complete disruption of the hydrogen bonding network of water. The disaggregation of the water-water clusters has been suggested to facilitate the solubility of poly(methyl methacrylate) (PMMA) and rendered the maximum solubility of the polymer in the solvent mixture with the highest fraction of individual water

molecules.[64, 65] The solvent mixtures of methanol and water have also been investigated by neutron-diffraction revealing that a major fraction of monomeric water molecules is present at a methanol fraction of 0.7.[66] Similarly, with isopropanol or *n*-propanol molar fraction of 0.7 in water, the tetrahedral-like network structure of water is scarcely formed.[67, 68]

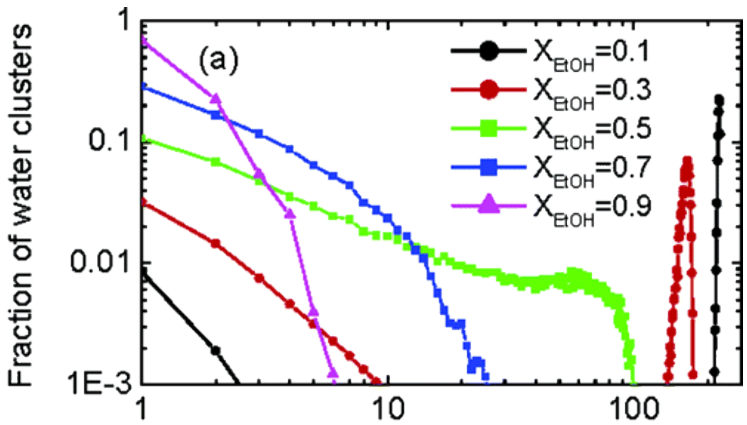

Figure 1-1 Molar contribution of H-bonded clusters in terms of their sizes for pure-water clusters in ethanol/water solvent mixtures. reproduce from ref.[48] Copyright © 2005, American Chemical Society.

1.2.1.2 Cosolvency and co-nonsolvency

Back to about half a century ago, Shultz and Flory[69] as well as Wolf and Blaum[70] have already demonstrated that the solubility of polymers can be affected in an unpredictable way using binary solvent mixtures resulting in improved solubility compared with the individual solvents. In terms of polymer solution in alcohol/water solvent mixtures, this co-solvency effect has been found for several polymers, such as PMMA.[62, 64] In contrast, the binary solvent mixture can also induce decreased solubility of polymers compared with the individual solvents, which is termed as the co-nonsolvent effect. The two types of solvent systems will be explained in this section.

The co-solvency effect widely exists in aqueous polymer solutions. For example, poly(12-acryloyloxydodecanoic acid-co-acrylic acid) gels were reported to swell with increasing content of ethanol (x) in ethanol/water binary solvent until x = 50-60 *vol*%.[71] In addition, solubility maxima have been reported for thermoresponsive polymeric gels based on 2-hydroxyethyl methacrylate and acetoacetoxyethyl methacrylate in ethanol/water solvent mixtures with around 40–50 mol-% ethanol.[62] In the latter system, the co-solvency effect was ascribed to the formation of water-alcohol-polymer contacts in the solution lowering the free energy of the system (as shown in Figure 1-2). Dissolution of the polymer occurs when a sufficient number of water-alcohol contacts have formed in the vicinity of a polymer chain to allow it to be drawn into solution by the formation of sufficient water-alcohol-polymer contacts. Increasing either the amount of water or

alcohol in the mixture will destroy the stability of the water-alcohol-polymer contacts leading to lower solubility, as neither water-polymer nor alcohol-polymer contacts are energetically favorable.

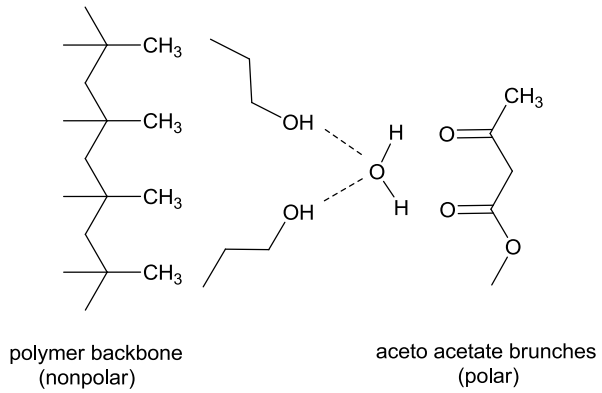

Figure 1-2 Schematic representation of the proposed co-solvency mechanism of the PAAEM in a water-alcohol mixture.[62]

In contrast, the solubility maximum of PMMA in ethanol/water solvent mixtures appears at around 85 wt% of ethanol. This has been ascribed to the preferential water-hydrogen bonding to the ester moieties of the polymer as most of the water is present as single, non-clustered molecules in this ethanol concentration regime leading to favorable water-polymer hydrogen bonding (Scheme 1-1).[48, 52, 65, 72] The formation of this hydration-shell around the carbonyl groups of the polymer is supported by small angle neutron scattering indicating the presence of a single deuterated water molecule per PMMA repeat unit.[52] The solubility of PMMA decreases with higher water content due to the formation of larger water clusters that need to be broken for hydration of the polymers. In contrast, with addition of more alcohol, the hydration of the polymer becomes less efficient as less water is present leading to a decrease of solubility.

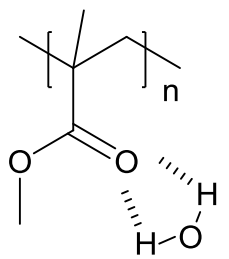

Scheme 1-1 The structure of the proposed hydrated PMMA in alcohol/water solvent mixtures

Although successfully explaining the enhanced solubility of the polymer at a certain alcohol/water ratio, both of the proposed mechanisms neglect the influence of the polarity of the polymer when analyzing the polymer-water or polymer-alcohol interactions, hence failing to explain a shift in the alcohol/water ratio of the best solvent mixture for different polymers. In fact, the polymer in the ternary system could be considered as a ‘macro-solute’ that is dissolved in the alcohol/water solvent mixture. Due to the large volume of the polymer chain, full hydrophobic hydration cannot be achieved making the polymer insoluble in pure

water. Alcohol molecules with both polar and apolar functionality can act as compatibilizer in the solution to assist the dissolution. Alternatively, polymers that are not readily soluble in alcohols and have strong hydrogen bond accepting moieties can be hydrated in alcohol/water solvent mixtures, whereby the hydrating water molecules act as compatibilizer to dissolve the polymer in the alcohol. As a result, the solubility of the polymer can be enhanced by the solvation effects of both water and alcohol via water-polymer and alcohol-polymer contacts. The water-polymer contact is favored by strong water-polymer interactions and relatively weak water-water and water-alcohol hydrogen bonding, which are highly influenced by the composition of alcohol/water solvent mixture. Accordingly, the best solvent mixture for the polymer is determined by both the composition of alcohol/water solvent mixtures and the polarity of polymer. For instance, the solubility maximum of poly(methyl acrylate) (PMA) in ethanol/water solvent mixtures appears at much lower ethanol fraction (around 70 wt%) compared to PMMA (80 wt%) due to its higher polarity.[73]

The co-nonsolvency effect refers to the fact that the solubility of a solute in a mixture of good solvents decreases or even vanishes.[74, 75] For example, PNIPAM with low molecular weight is soluble in both water and in ethanol/methanol at room temperature, while it tends to be insoluble in mixtures of the two solvents giving rise to a UCST-type reentrant-phase diagram.[75-80]

The molecular level mechanism of such co-nonsolvency effects in alcohol/water solutions is not well understood yet, although many papers have been published on this subject. Theoretical calculations based on the Flory-Huggins thermodynamic theory suggest that the reentrant behavior results from the perturbation of the alcohol–water interaction parameter in the presence of PNIPAM. Accordingly, alcohol–water complexes are formed that dominate the hydrogen bonds in the bad solvent mixtures suppressing PNIPAM solubilization.[76-78] The formation of different water-methanol complexes was confirmed by light scattering and FTIR spectroscopy[81, 82] indicating that as the methanol content increases, the composition of the complexes gradually changes from $(CH_3OH)(H_2O)_5$ to $(CH_3OH)(H_2O)$. However, Tanaka[83, 84] proposed a different mechanism based on molecular simulations, which suggested that the competition between PNIPAM-water and PNIPAM-alcohol hydrogen bonding and subsequent cooperative solvation are responsible for the co-nonsolvency effect of this ternary system. SANS measurements performed with PNIPAM dissolved in D_2O/MeOD mixtures revealed a good agreement with these theoretical calculations.[85]

1.2.1.3 UCST behavior of polymers in alcohol/water solvent mixtures

Thermoresponsive polymers are polymers that undergo a reversible phase transition from a molecularly dissolved state to an aggregated state in response to temperature changes. When the phase separation occurs at lower temperatures, this is referred to as UCST behavior while the reversed phase behavior is known as LCST behavior. As shown in Figure 1-3, the LCST is defined as the minimum temperature of the binodal (or the coexistence curve) of the phase diagram, while the UCST is defined as the maximum temperature of the

binodal (or the coexistence curve). The terms UCST or LCST are sometimes misused as cloud point temperature (T_{CP}), which refers to the temperature at which the phase transition of a polymer solution at a specific concentration occurs from the soluble state to the collapsed aggregated state, accompanied by clouding of the solution. As shown in Figure 1-3, T_{CP} is a phase transition temperature at a specific polymer concentration, which can be located at any position of bimodal curve. In other words, the UCST is the lowest value of T_{CP} in the phase diagram, although it should be noted that often the T_{CP} does not exactly coincide with the binodal curve.[86]

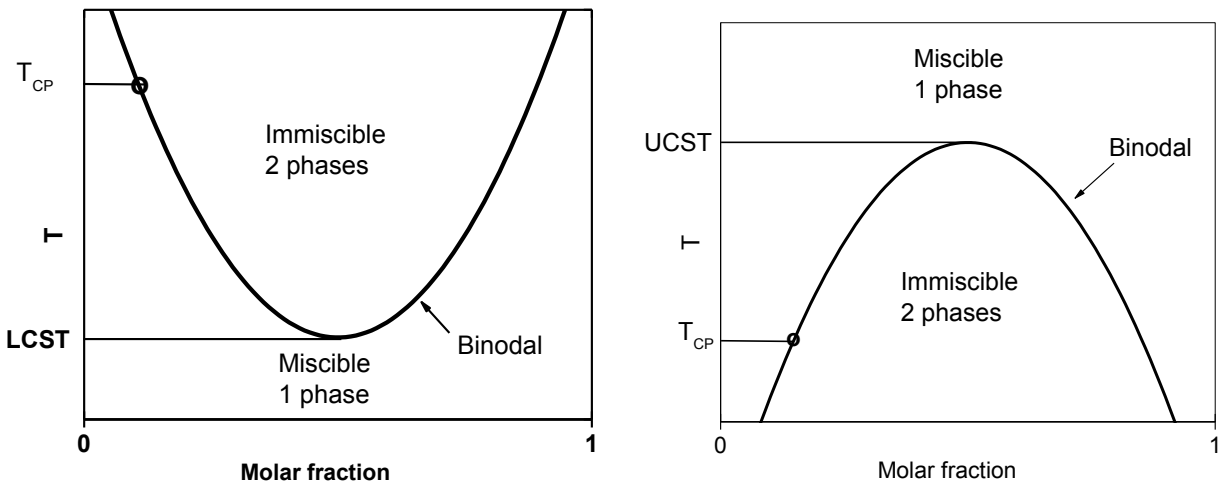

Figure 1-3 Phase diagram for a polymer solution exhibiting an LCST and UCST.

T_{CP} is one of the most important parameters of a thermoresponsive polymer in solution when considering its applications under certain conditions. Fortunately, the T_{CP} of UCST polymers can be accurately controlled by various parameters. For instance, the chemical structure determines the UCST of the polymer as well as T_{CP} at a specific concentration. The copolymerization with hydrophobic (increase in T_{CP}) or hydrophilic (decrease in T_{CP}) comonomers or end group transformations can intrinsically determine the UCST of a polymer.[87-89] In addition, increasing molecular weight can increase the T_{CP} caused by enhanced intermolecular interactions.[89, 90] UCST transition temperatures of polymers can also vary in the presence of additives.[90-93] Liu et.al reported that the influence of anions on the UCST behavior of PNIPAM in an ethanol/water solvent mixture with $X_{Ethanol}$=26 mol% follows the Hofmeister series (Figure 1-4).[90] The authors suggest that either the anion adsorption on PNIPAM chains or the anionic polarization of hydrogen bonding between water and PNIPAM causes the increase of the UCST transition temperature. The addition of co-solvent or co-nonsolvent also strongly influences the thermoresponsive behavior of a polymer, which will be explained in the following sections.

Unlike in physical chemistry where scientists use molar fraction to describe the composition of alcohol/water dual solvent systems, weight percent (wt%) or volume percent (vol%) have also frequently been used in the literature concerning UCST behavior of polymers in alcohol/water solvent mixtures. To keep the accuracy of the original reports, those units are not uniformed in this review. Instead, the relationships of molar fraction with wt% and vol% are provided in Figure 1-5 to facilitate comparison of the values reported in different publications.

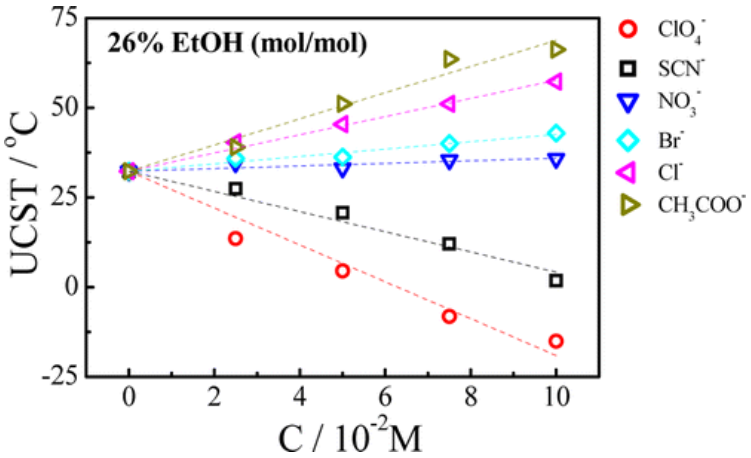

Figure 1-4 Change in T_{CP} of PNIPAM as a function of salt concentration (C) for the anions in the ethanol/water solvent mixture at x_E of 26% with Na^+ as the common cation, where the polymer concentration is fixed at 5.0 mg mL^{-1}. Reproduced from ref,[90] Copyright © 2013, American Chemical Society.

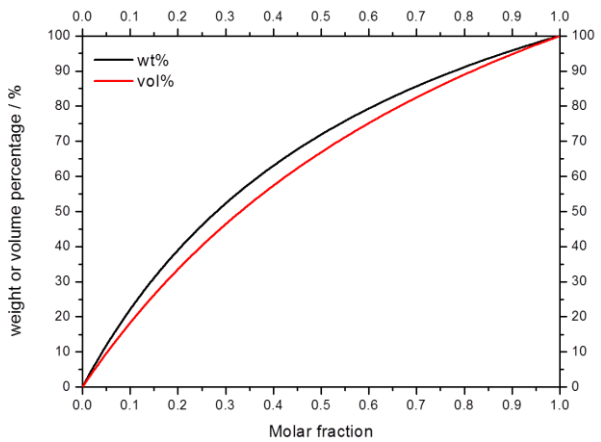

Figure 1-5 Weight or volume percentage plots versus molar fraction of ethanol in ethanol/water solvent mixtures at 25°C.

1.2.2 Polymers with UCST behavior in alcohol/water co-solvent systems

1.2.2.1 Poly(methyl methacrylate) (PMMA)

PMMA (Scheme 1-1) is insoluble in both water and ethanol at ambient temperature, although a UCST was reported for PMMA in pure methanol as well as in pure ethanol at ~87 °C or above.[64] The polymer, however, shows a lower UCST phase transition temperature when adding water to the alcohol indicating a better solubility.[52, 64, 65, 72, 87, 94-96]

A typical UCST phase diagram of PMMA in ethanol/water solvent mixtures exhibits a 'U' shape, as shown in Figure 1-6.[65, 87] The phase behavior is highly influenced by the composition of the solvent mixture, i.e. the T_{CPC} (cloud point upon cooling) and T_{CPH} (clearance point upon heating) values of the polymer in ethanol decrease when the amount of water is increased until the maximum solubility at an ethanol content of around 80 wt-% is reached. This maximum solubility of 80 wt% ethanol was ascribed to the presence of individual non-clustered water molecules leading to very efficient hydration of the polymers. Moreover, the hysteresis between cooling and heating reversed by variation of the ethanol content, i.e. in the case of the good solvent mixture, the dissolution upon heating occurs at a higher temperature than the precipitation upon cooling. The lower T_{CPC} compared with the T_{CPH} was explained by the difficulty to hydrate the hydrophobic PMMA clusters upon heating while during cooling the polymer chains are already hydrated.[48]

In addition to the composition of the solvent, the UCST behavior is also strongly influenced by molecular weight of the polymer.[65, 72] The T_{CPC} of the polymer solutions in ethanol/water mixtures increases dramatically with increasing molar mass of PMMA indicating strong molar mass dependence of the UCST behavior which is typical for UCST polymers in aqueous solution resulting from strong intra-polymer interactions.[17] Importantly, the shape of the UCST phase diagram with regard to solvent composition is unaffected by polymer molar mass indicating that the UCST behavior is indeed governed by the mixed solvent properties. Concentration also plays a vital role in determining the T_{CPC} and T_{CPH}. The transition temperatures increase with increasing polymer concentration,[65] which can be ascribed to an increase in polymer-polymer interactions in solution, commonly observed in the low polymer concentration regime.[97, 98]

UCST behavior of PMMA copolymers with either hydrophilic or hydrophobic comonomers prepared by post-polymerization of activated poly(MMA-*co*-pentafluorophenyl methacrylate) (PMMA–PFPMA) was reported in ethanol/water mixtures.[87] The results indicate that only 6 mol-% of the methacrylamide comonomer can result in a dramatic change of the UCST behavior of PMMA in ethanol/water solvent mixtures, i.e. the introduction of hydrophilic moieties increases the solubility of PMMA in aqueous ethanol leading to a decrease in T_{CP}, while hydrophobic substituents decrease the solubility of PMMA leading to higher T_{CP} in solvent mixtures with a low ethanol content and increase the solubility in solvent mixtures with a high ethanol content. Inspired by these results, photochromic azobenzene moieties have also been

incorporated in the side chains of PMMA via the post-polymerization modification of activated PMMA–PFPMA leading to a dual responsive polymer that combines light responsiveness with UCST behavior in aqueous ethanol/water solvent mixtures.[87] The T_{CP} of the polymer solutions was found to decrease after UV-irradiated due to the higher dipole moment of the *cis*-isomer of the azobenzene moiety enhancing the copolymer solubility indicating UV-tunable UCST behavior. Furthermore, the UV responsiveness strongly depends on the solvent composition revealing a higher decrease in T_{CP} after UV-irradiation in ethanol-water solvent mixtures with higher water content (See Figure 1-7). The solvent dependence of light-responsiveness was explained by the competition for hydrogen bonding of water and ethanol with the azo-group.

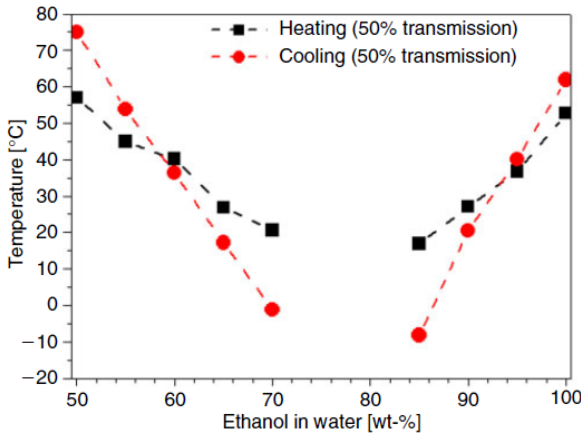

Figure 1-6 Clearance points upon heating and cloud points upon cooling as a function of ethanol content in 0.5 wt-% aqueous solutions of PMMA (Mn=14k). Reproduced from ref[65], Copyright © 2010 CSIRO Publishing

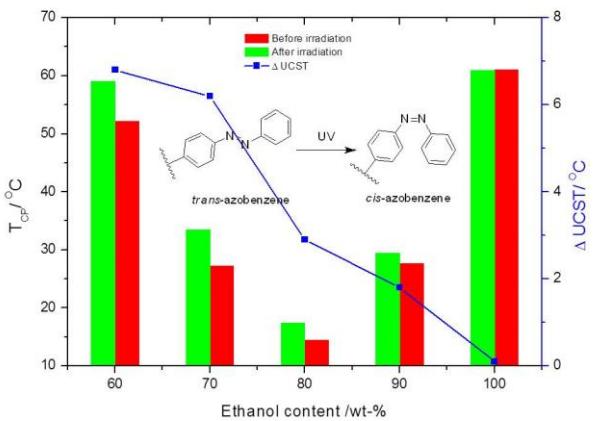

Figure 1-7 Cloud point temperatures upon cooling as a function of ethanol content for 2 mg/ml aqueous solutions of azobenzene containing PMMA before and after 1h of UV irradiation, the blue data points show the difference in cloud point temperature before and after UV irradiation (ΔUCST). Reproduced from ref[99], Copyright © 2014 2014 Elsevier Ltd.

UCST behavior of PMMA in other lower aliphatic alcohols, e.g. methanol, 1-propanol, 2-propanol and *t*-butanol has also been reported revealing increased solubility, i.e. lower T_{CP}, with increasing size of the alkyl group.[65, 72]

Due to the structural similarity of poly(methyl acrylate) (PMA) and PMMA, it is not surprising that PMA also exhibits a UCST transition in ethanol/water solvent mixtures.[73] Thermoresponsive micelles were then obtained in ethanol/water solvent mixtures for PMA-b-polystyrene (PS) and PS-b-PMA block copolymers above the UCST of PMA. Dynamic light scattering (DLS) and transmission electron microscopy (TEM) of the block copolymer solutions in 70/30 and 80/20 wt % ethanol–water mixtures showed that thermoresponsive micellar aggregates were formed when the solution was cooled below the UCST transition temperature of the PMA block (Figure 1-8).

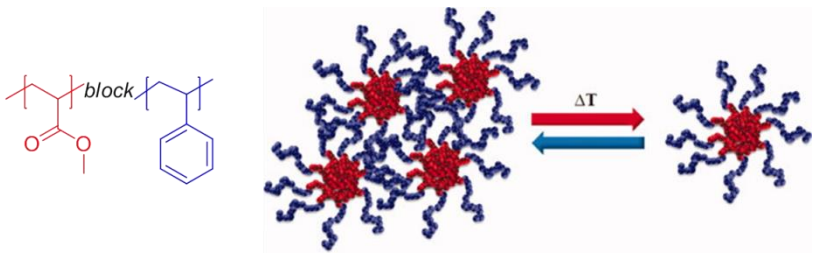

Figure 1-8 Structure of PMA-*b*-PS block copolymer and schematical representation of the micellization process of the polymer on heating. Reproduced from Ref.,[73] Copyright © 2011 Wiley Periodicals, Inc.

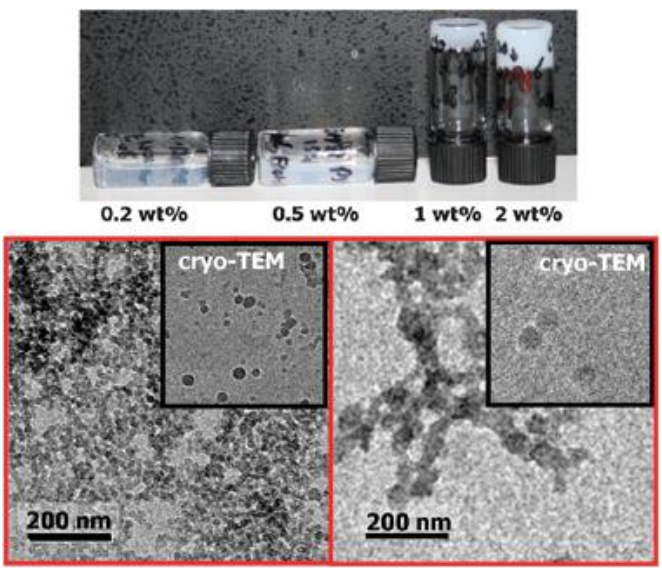

Figure 1-9 Top: pictures of the vial inversion test for micellar solutions of PS_{88}-b-$PMMA_{80}$ in an ethanol–water 80/20 wt% mixture with different polymer concentrations. Bottom: TEM images of PS_{88}-b-$PMMA_{80}$ (left) and PS_{112}-b-$PMMA_{2800}$ (right) micelles at 0.2 wt% concentration. The insets show the corresponding cryo-TEM images (same scale). Reproduced from Ref.[52] with permission from The Royal Society of Chemistry.

Due to the reversible and easy tunable UCST phase transition of PMMA in ethanol/water as well as the environmentally friendly nature of this solvent mixture, the thermoresponsive nature of this system has already been employed in nanotechnology and material science. The self-assembly of double hydrophobic PS_{88}-*b*-$PMMA_{80}$ block copolymers was demonstrated in an ethanol/water solvent mixture with 80 wt-% of ethanol.[52] At polymer concentrations below 0.2 wt-%, individual spherical micelles were obtained from polymers with equal sizes of both blocks due to the relatively large radius of gyration (Rg) of the fully hydrated PMMA chains as revealed by SANS. Interestingly, when the polymer concentration was increased to only 1 wt-%, a thermoresponsive micellar gel was formed ascribed due to the large Rg of the PMMA block facilitating interactions between the individual micelles (Figure 1-9).

PMMA copolymers functionalized with a UV/vis or fluorescent dye were also developed to act as soluble temperature sensors in ethanol or ethanol/water solvent mixtures.[100] The UCST transition of PMMA in combination with solvatochromic dyes was found to result in a much broader temperature sensing regime compared to sensors based on LCST polymers, proposed to result from the enthalpic UCST phase transition versus the entropy driven LCST phase transition.

1.2.2.2 Poly(2-alkyl/aryl-2-oxazoline)s

Poly(2-alkyl/aryl-2-oxazoline)s (PAOx) represent a class of (co)polymers comprising a tertiary amide group in the repeat unit and variable side chains.[30, 101] Various 2-oxazoline-based monomers can be polymerized via a living cationic ring-opening polymerization (CROP) mechanism (Scheme 1-2) resulting in PAOx with well controlled structures. Due to the livingness of the polymerization, the use of functional electrophilic initiators as well as nucleophilic end-capping agents enables the synthesis of both α- and ω-end-functionalized polymers. In addition, by tuning monomer reactivity or the order of adding monomers, statistical, block or gradient copolymers can be obtained.

PAOx with short side chains are either fully soluble or show LCST phase transition in ethanol/water solvent mixtures, but extending the hydrophobic side chain length to a butyl group induces UCST behavior depending on the content of ethanol (see Figure 1-10).[102] The ethanol content required to induce UCST transitions increases with increasing hydrophobicity of the polymer side chains. The evolution of the UCST cloud points was ascribed to the hydrophilic-hydrophobic balance of the side groups of the polymers on the one hand and the ethanol-water solvent structure on the other hand.

PAOx with aromatic substituents, PPhOx and PBnOx, also exhibit UCST behavior in ethanol/water solvent mixtures. The higher hydrophobicity of the PBnOx is clearly evidenced by the higher cloud points as well as a shift of the transitions to higher ethanol content. Furthermore, it is observed that these polymer show similar behavior as the PAOx comprising side-chains with intermediate hydrophobicity, i.e. PPentOx and PHexOx.

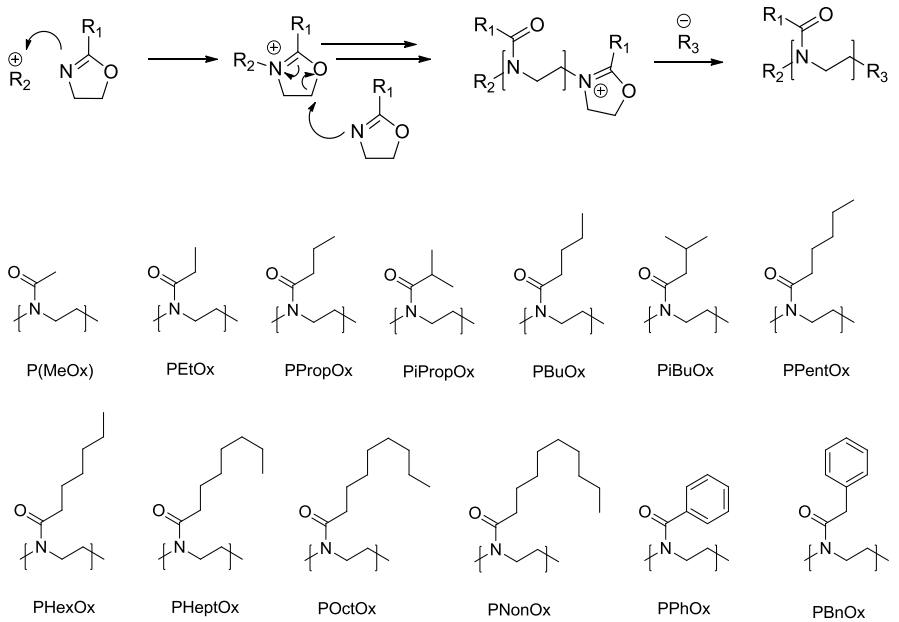

Scheme 1-2 Representation of the CROP of 2-oxazolines and the polymers synthesized for UCST screening

Quasi-diblock statistical copolymers based on 2-phenyl-2-oxazoline (PhOx; hydrophobic) and 2-methyl-2-oxazoline (MeOx; hydrophilic) or 2-ethyl-2-oxazoline (EtOx; hydrophilic) have been synthesized via statistical copolymerization by CROP.[103] Due to the higher reactivity of the MeOx and EtOx compared to the PhOx, the monomers were distributed in a quasi-diblock copolymer architecture, i.e. the copolymers have a first block of nearly pure MeOx or EtOx with PhOx incorporated as a gradient block in which the composition gradually changes from MeOx or EtOx to PhOx. Solubility screening of the MeOx–PhOx and EtOx–PhOx copolymers revealed that both of the two series of copolymers exhibit UCST behavior at high amount of PhOx in ethanol/water solvent mixtures with high content of ethanol.[104] The solubility maxima of those copolymers were found at an ethanol content of around 80 wt%. In addition, a remarkable observation was made for the $EtOx_{50}$–$PhOx_{50}$ copolymer in an aqueous solution with 40 wt% ethanol revealing both a LCST and a subsequent UCST, so-called closed-loop coexistence (see Figure 1-11). Similar screening with random copolymers of EtOx and 2-nonyl-2-oxazoline (NonOx) in binary water–ethanol mixtures has revealed that copolymers containing 60 and 70 mol% NonOx exhibited UCST transitions in aqueous solvent mixtures with 80 wt % ethanol.[105]

The potential applications of the widely tunable solubility of PAOx in ethanol/water solvent mixtures have already been demonstrated. Schlaad et al. have found that poly(2-isobutyl-2-oxazoline) (P*i*BuOx) and PNonOx can crystallize in ethanol/water solvent mixtures below its T_{CP} to produce nanosized materials with hierarchical structure.[106] The crystallization of P*i*BuOx is affected by polymer concentration, temperature and the solvent composition could lead to crystals with different morphologies.

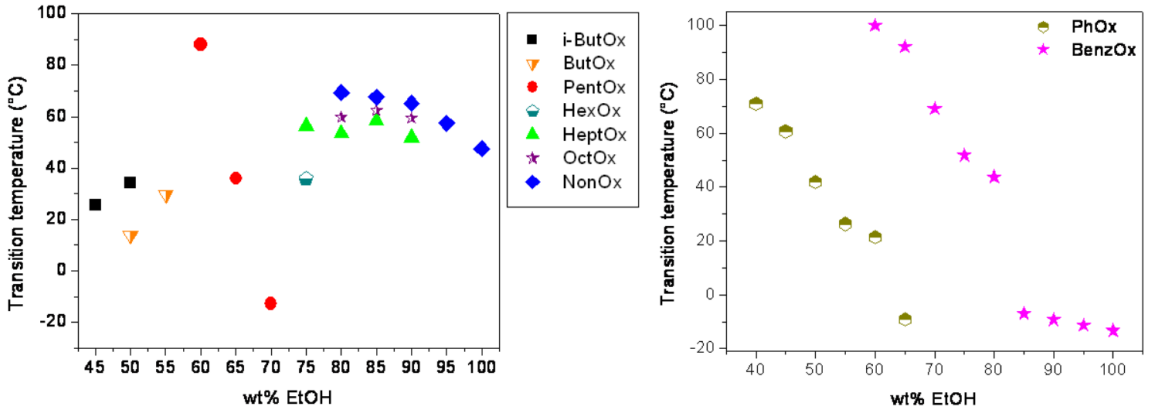

Figure 1-10 Cloud points as function of wt% ethanol for the UCST transitions of the poly(2-alkyl-2-oxazoline)s (left) as well as poly(2-phenyl-2-oxazoline) (PhOx) and poly(2-benzyl-2-oxazoline) (BenzOx) (right) determined at 5 mg/ml. Reproduced from Ref.[102]

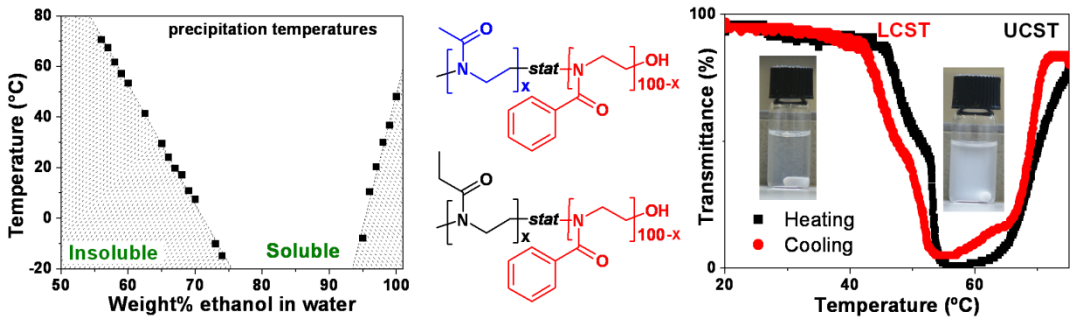

Figure 1-11 Transmittance as a function of temperature for pEtOx50–PhOx50 in 40 wt.% ethanol in water demonstrating a LCST transition as well as an UCST. Reproduced from Ref.[104] with permission from The Royal Society of Chemistry.

By fine-adjusting of the ethanol fraction of the aqueous ethanol dual solvent system, Hoogenboom et al.52 have reported a schizophrenic copolymer based on gradient copolymers of NonOx and PhOx in ethanol–water solvent mixtures (see Figure 1-12). The self-assembly of the copolymer could be finely tuned by temperature as well as subtle changes in the solvent composition leading to both switching and reversing of the formed micelles.

Pathway dependent self-assembly of PAOx copolymers in ethanol/water solvent mixtures has been demonstrated using tri- and tetrablock copoly(2-oxazoline)s composed of solvophilic EtOx and/or MeOx blocks, a solvophobic NonOx block as well as a PhOx block, of which the solubility can be switched from solvophilic in ethanol/water solvent mixtures with 60 wt% of ethanol to solvophobic in ethanol/water with 40 wt% of ethanol.[107] The size and morphology obtained from the self-assembly of the block copolymers in ethanol/water solvent mixtures could be tuned by the solvophobic content of the copolymers and the block order as well as the solvent composition. In particular, MPN and EPN triblock copolymers were found to

form spherical micelles together with larger, irregularly shaped, aggregates in ethanol/water 60/40% w/w solvent mixtures, while coexistence of spherical micelles and cylindrical micelles was observed in ethanol/water 40/60% w/w solvent mixtures. Interestingly, dilution with water of the MPN/EPN micellar solution in ethanol/water 60/40% w/w to 40/60% w/w resulted in a collapse of the PhOx block onto the NonOx core leading to a core–shell structure indicating an pathway dependent self-assembly behavior (see Figure 1-13).

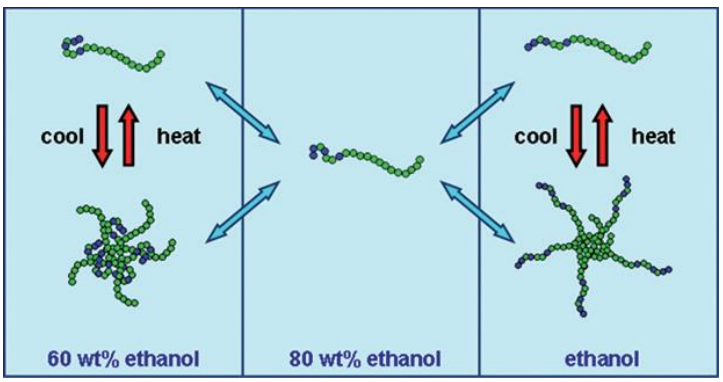

Figure 1-12 Schematic overview of the temperature- and solvent-dependent self-assembly of the PNonOx10-stat-PPhOx90 gradient copolymer in ethanol–water mixtures. Blue = NonOx; green = PhOx. Reproduced from Ref.[52] with permission from The Royal Society of Chemistry

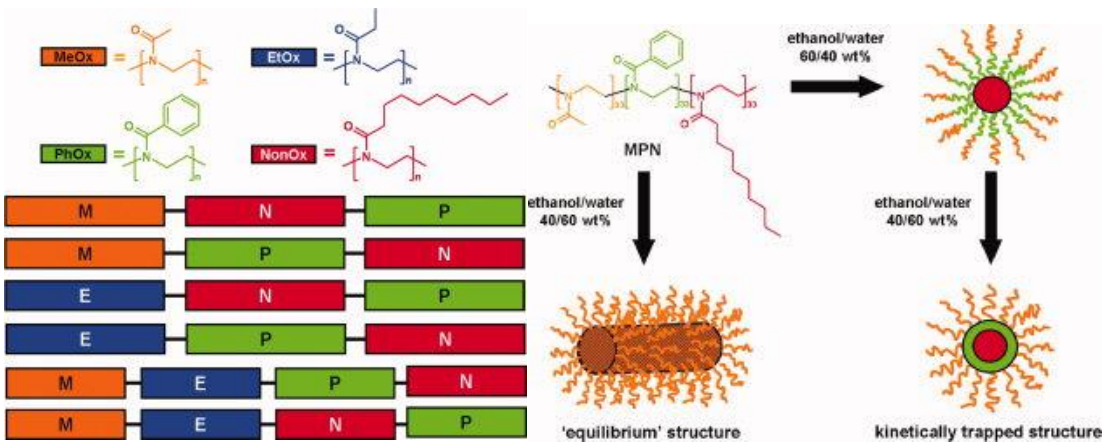

Figure 1-13 a) Schematic representation of the studied triblock and tetrablock copoly(2-oxazoline)s; and b) Schematic representation of the micelles formed by the triblock copolymer in ethanol/water 60/40% w/w mixture and after addition of water to reach an ethanol/water 40/60% w/w composition. Reproduced from Ref.[107] Copyright © 2010 Wiley Periodicals, Inc.

1.2.2.3 Poly(ethylene glycol) and its derivatives

Poly(ethylene glycol) (PEG) has been widely used as hydrophilic biomaterials due to its low toxicity and more importantly the 'stealth' behavior, i.e. it suppresses recognition by the immune system.[108] Apart from PEGylation,[109, 110] polymers with short PEG side chains have also been intensively studied as LCST polymers and bio-materials, with poly[oligo(ethylene glycol) methyl ether (meth)acrylate] being mostly studied.[3, 20, 26, 27] However, only little is known about the UCST behavior of PEG and its derivatives. PEG was reported to have a UCST phase transition in water only at elevated temperature and high pressures.[111] More recently, it was reported that PEG also exhibits a UCST transition in pure ethanol at temperatures ranging from about -80 to 10 ^{o}C depending on the concentration, which is, however, only a UCST-like phase transition driven by crystallization of PEG upon cooling and not by liquid-liquid phase separation.[112] The UCST behavior of polymers with PEG side-chains in alcohols have been recently reported by Theato, Roth and coworkers (See Scheme 1-3) and will be further detailed in the following.

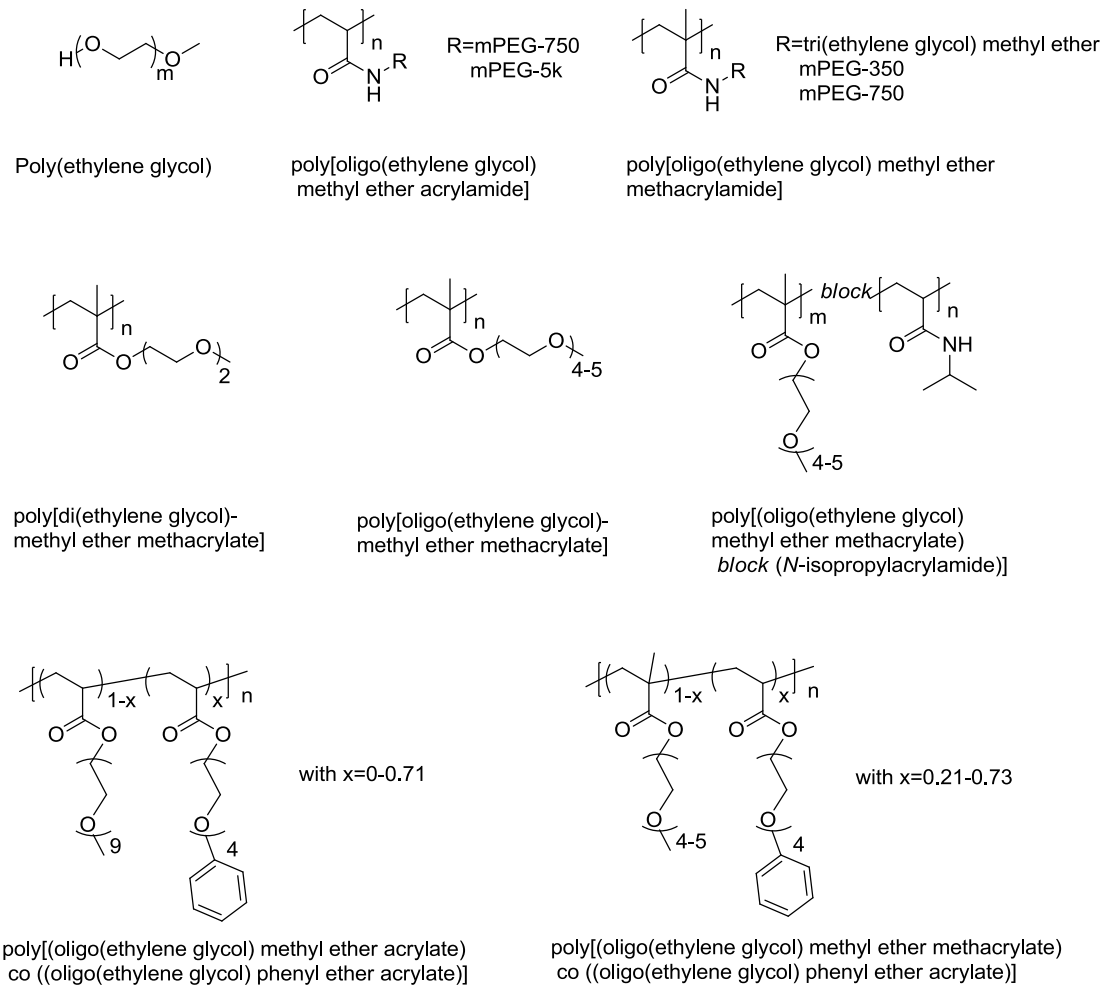

Scheme 1-3 Poly(ethylene glycol) and its derivatives that exhibit UCST behavior in alcohols or alcohol/water solvent mixtures.

Poly[di(ethylene glycol) methyl ether methacrylate] (PDEGMA) was reported to exhibit a UCST phase transition in ethanol and isopropanol with strong dependence on the polymer molecular weight.[113] The T_{CP} of $PDEGMA_{29}$ in isopropanol (2.0 wt %) decreases from 27.8 to 17.8 ^{o}C with the addition of only 1 wt% of water indicating a co-solvency effect. When the water content increased to 5 wt%, the polymer becomes completely soluble in either the ethanol/water or isopropanol/water solvent mixtures.

UCST-type behavior of poly[oligo(ethylene glycol) methyl ether methacrylate] (POEGMA, with ethylene glycol DP=4-5) was investigated in alcohols by Roth et.al.[89] Alcohols with different aliphatic groups including ethanol and isopropanol were investigated as solvents revealing reversible and sharp UCST transitions. Co-solvency effect was also observed upon addition of water to the isopropanol solution of the polymer as indicated by a decreasing cloud point for the UCST transition. POEGMAs with defined architectures such as block or star polymers can easily be synthesized by controlled radical polymerization or living polymerization.[114-117] The stimulus responsive behavior of such more complex POEGMA copolymers in a wide range of alcohols can thus allow the investigation of temperature controlled self-assembly of those copolymers. For instance, Roth et.al[53, 118] have synthesized double thermoresponsive block copolymers, POEGMA-b-PNIPAM, POEGMA-b-poly(N,N-diethylacrylamide) (POEGMA-b-PDEAM) and POEGMA-b-[PNIPAM-co-poly(pentafluorophenyl acrylate)] (POEGMA-b-(PNIPAM-co-PPFPA)) through RAFT polymerization. Based on the UCST behavior of POEGMA in 1-octanol and the LCST behavior of PNIPAM or PDEAM in water, the block copolymers were found to form temperature induced micelles and inverted micelles in the mentioned solvents, respectively. In a next step, inverted micelles with PNIPAM-co-PPFPA as corona in 1-octanol were shell crosslinked using a diamine and subsequently transferred into water yielding cage-like structures with a swollen POEGMA cores and a cross-linked PNIPAM shell (See Figure 1-14). The shell reversibly collapsed onto the cores when heated above the LCST of PNIPAM providing particles with novel architecture and the potential to encapsulate and release guest molecules by a thermal trigger.

The UCST behavior of poly(oligo(ethylene glycol) methyl ether acrylate) (POEGMA, with ethylene glycol DP=8-9) with even longer PEG side chains was also reported in isopropanol with a T_{CP} at about 11.8 ^{o}C.[88] The T_{CP} of POEGMA can be increased by copolymerization with commercially available oligo(ethylene glycol) phenyl ether acrylate (PhOEGA) up to 73 ^{o}C depending on the ratio of the two monomers. The incorporated phenyl ethers are assumed to decrease solubility by promoting attractive polymer–polymer interactions and lowering the entropy of mixing upon dissolution in isopropanol. The incorporated phenyl ethers were also found to affect solubility in ethanol/water solvent mixtures. For copolymers with 71% of PhOEGA, a five region phase diagram was obtained with co-solvency effect in mixtures of 35 to 45 vol-% water in ethanol, as shown in Figure 1-15.

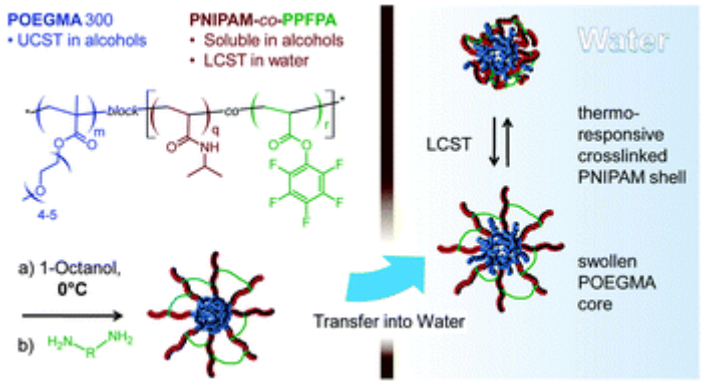

Figure 1-14 Schematics representation of the shell crosslinking reaction of POEGMA-b-(PNIPAM-co-PPFPA) micelles with 1,8-diaminooctane and behavior of shell cross-linked, swollen core micelles in water. Reproduced from Ref.,[53] with permission from The Royal Society of Chemistry

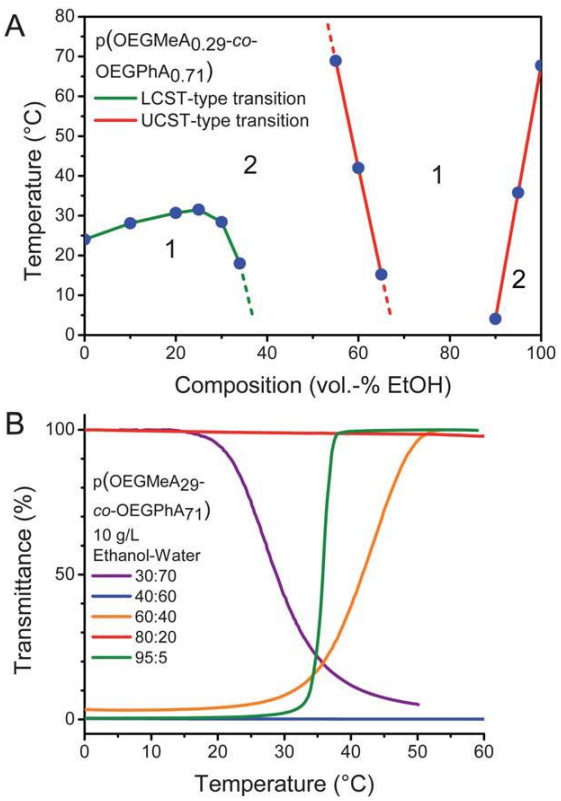

Figure 1-15 (A) Phase diagram of P(OEGMeA$_{0.29}$-*co*-OEGPhA$_{0.71}$) in ethanol/water solvent mixtures. (B) Representative transmittance curves for the five different regimes in the phase diagram. Reproduced from Ref.,[88] with permission from The Royal Society of Chemistry

The PEG (meth) acrylamide analogous were synthesized by postpolymerization of poly(pentafluorophenyl (meth)acrylate) with α-amino, ω-methoxy functionalized di(ethylene glycol), tri(ethylene glycol), and PEG-350, PEG-750, and PEG-5k.[118] It was found that these polymers with long ethylene glycol side chains exhibit UCST behavior in either isopropanol or n-octanol (for polymer acrylamide, longer than PEG-750, while for

polymethacrylamide longer than tri(ethylene glycol)). The T_{CP} increases with an increasing ethylene glycol side chain length, but were found to be essentially independent on the alcohol chain length with polymers exhibiting higher UCST transition temperatures. Cytotoxicity tests on MRC5 fibroblast cells of the di- and tri(ethylene glycol) methyl ether acrylamide homopolymers revealed no toxicity up to concentrations of 10.0 g/L indicating this series polymer are ideal candidates for biomedical applications.

1.2.2.4 Other polymers exhibiting UCST behavior in alcohol/water co-solvent systems

Boyko et al. have reported the UCST behavior of a poly(acetoacetoxyethyl methacrylate) (PAAEM) gel in binary ethanol/water solvent mixtures.[62] A solubility maximum was observed with solvent mixture at around 40–50 mol% of ethanol, which was ascribed to the formation of water-cages around the hydrophobic ethanol molecules. The solubility maximum shifted to about 30 mol-% of alcohol in n-propanol/water solvent mixtures due to the higher hydrophobicity of n-propanol. The UCST of PAAEM could be lowered by copolymerization with hydroxyethyl methacrylate (HEMA) leading to a decrease of T_{CP} in a linear order from 75 to 10 ^{o}C when HEMA content was increased to about 90 mol% .

Theato and coworkers have recently reported a series of poly(*N*-alkyl-2-cyanohex-4-enamide) (PACHE) prepared by post-polymerization modification of poly(1-cyano-1-pentafluorophenoxycarbonyl-2-vinylcyclopropane) (See Scheme 1-5).[119, 120] All of these synthetic polymers, except PACHE1, were found to show UCST transition in ethanol and ethanol/water solvent mixtures. For PACHE3 and PACHE4, the addition of water first decreases T_{CP}, which then increased with more water, while for PACHE5 and PACHE6, no decrease of the UCST was observed but a steady increase of the transition temperature with the water content in ethanol was found. The R group of the polymers was, thus, found to influence the UCST behavior depending on the solvent composition, i.e. an increased hydrophobicity of the polymer shifts the UCST in ethanol to lower temperatures; while the trend was reversed when water is added to the ethanol mixture (see Figure 1-16). PACHE1 does not show a phase transition in ethanol or ethanol/water solvent mixtures, however, a phase transition in methanol and methanol/water solvent mixtures was observed instead. Interestingly, favored solely by the structure and length of the n-propyl side chains, PACHE2 was found to feature both UCST and physical gelation in specific solvent compositions.[119]

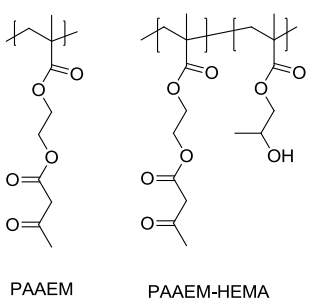

Scheme 1-4 Structures of PAAEM and PAAEM-HEMA copolymer

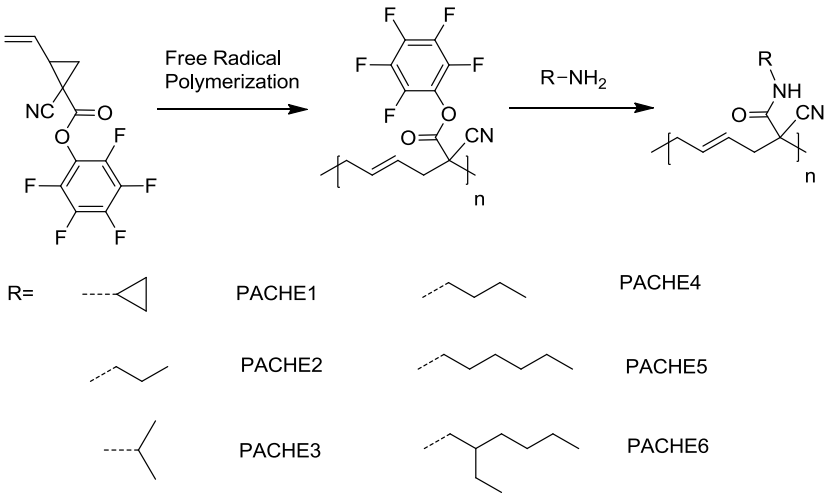

Scheme 1-5 The synthesis and chemical structures of poly(*N*-alkyl-2-cyanohex-4-enamide)s that exhibit UCST behavior in alcohols or aqueous alcohols[119, 120]

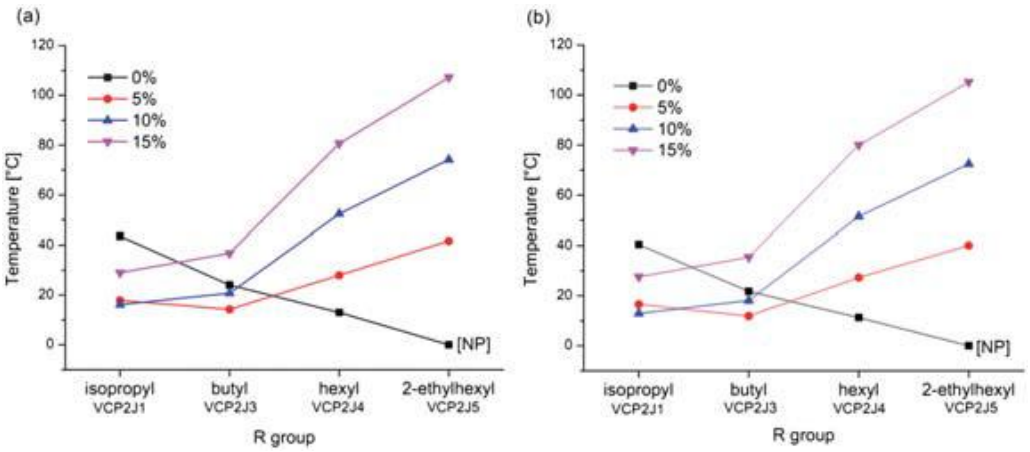

Figure 1-16 T_{CP}s in ethanol/water solvent mixtures of PACHE as a function of side chain amide moieties. (a) T_{CP}s upon heating and (b) T_{CP}s upon cooling. NP=no precipitation. Reproduced from Ref.[120], with permission from The Royal Society of Chemistry

Poly(trimethylene ether) glycol (PO3G, Scheme 1-6) with low molecular weight was reported to show UCST behavior in water in the temperature range between 30 and 80 ^{o}C depending on the concentration of the polymer.[121] Addition of ethanol or isopropanol was found to lower the UCST transition temperature of the polymer indicating a co-solvency effect. The commercially available PO3G is prepared by acid catalyzed polycondensation of Bio-PDO^{TM}, a renewably sourced monomer from a bacterial fermentation process making this 100% renewable great promising for applications in personal care products.

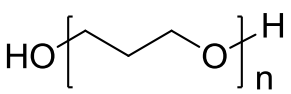

Scheme 1-6 Structure of PO3G.

1.2.3 **Polymers** with **UCST in water/alcohol co-nonsolvent system**

1.2.3.1 Poly(N-isopropylacrylamide)

PNIPAM (Scheme 1-7) is widely known as polymer with LCST behavior in water.[23, 24] Due to the excellent properties, PNIPAM is considered as the gold standard of thermoresponsive polymers and has been used for various purposes.[25, 31, 122-124] The phase behavior of PNIPAM in alcohol /water solvent mixtures was firstly studied by adding alcohols to PNIPAM–water solutions leading to s shift of the T_{CP}.[75] In general, the LCST transition temperature of PNIPAM is decreased by addition of methanol and a further addition of the alcohol promotes an increased phase transition temperature. Similar experiments carried out using a PNIPAM gel instead of linear PNIPAM revealed an abrupt decrease in its swelling degree, termed 'reentrant phase transition'.[125]

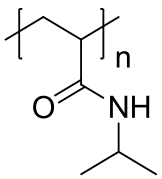

Scheme 1-7 Structure of PNIPAM.

Costa et.al reported the UCST behavior of PNIPAM in binary ethanol/water solvent mixtures with an ethanol molar fraction *x* between 0.28 and 0.35, a clear example of the co-nonsolvency effect (see Figure 1-17).[63] Further addition of ethanol leads to complete dissolution of the polymer. The UCST phase transition of PNIPAM in solvent mixtures of water with 1-propanol or 2-propanol appears at a lower mole fraction of alcohol (x=0.21) than with ethanol. PNIPAM in methanol/water solvent mixtures does not exhibit a UCST behavior since the hydrophobic group of methanol is too small to compete with hydrogen bonding with the hydroxyl group. Hore et.al have reproduced and extended the phase diagram in d-ethanol/d-water solvent mixtures by SANS experiments for PNIPAM.[126] The conformation of the polymer chains was determined by monitoring of the radius of gyration. It was found that polymer chains tend to swell with increasing temperature except close to the boundary of the d-ethanol rich area of the phase diagram (40% d-water) where they observed shrinkage. In addition, three Flory−Huggins interaction parameters, PNIPAM/d-water, PNIPAM/d-ethanol and d-water/d-ethanol, were obtained based on the SANS data.

1.2.3.2 Poly[N-(4-vinylbenzyl)-N,N-dialkylamine]

Poly[*N*-(4-vinylbenzyl)-*N,N*-dialkylamine] (Scheme 1-8) represent a series of polymers with tunable hydrophobicity depending on the alkyl chains.[90, 113] These polymers could be prepared by RAFT polymerization of styrenic monomers with different N-substituents and exhibit LCST and/or UCST in alcohols and in alcohol/water mixtures depending on the *N*-substitution of polymer and the structure of the

alcohol. Poly[*N*-(4-vinylbenzyl)-*N*,*N*-dibutylamine] (PVBA, Mn=8.1kDa) was found to show UCST behavior in pure n-propanol and n-propanol/water solvent mixtures with 10 wt% of water. The addition of water increased the T_{CP} from 48.0 to 75.0 ℃ (2.0 wt % polymer) indicating the co-nonsolvency effect.[90] Poly[*N*-(4-vinylbenzyl)−*N*,*N*-diethylamine] (PVEA) with shorter alkyl groups only shows UCST behavior in pure isopropanol. The copolymer becomes completely soluble upon addition of only 1 wt% of water to the polymer isopropanol solution. However, water was found to be a co-nonsolvent in the system with a water content higher than 15 wt% indicated by the appearance of an LCST transition as well as a decrease of the T_{CP} when the water content is increased.[113]

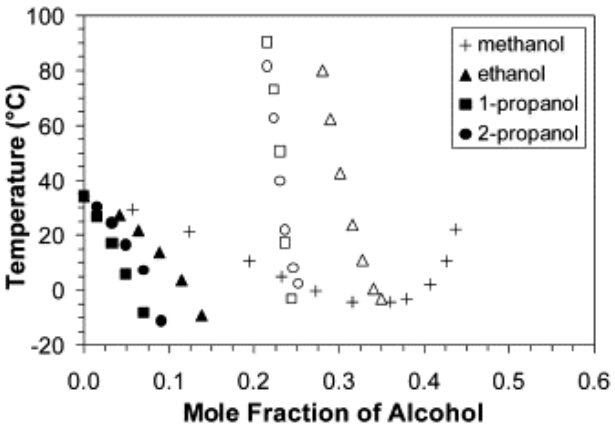

Figure 1-17 Phase transition temperatures of PNIPAM in several water–alcohol solutions. Filled symbols represent LCST behavior and open symbols represent UCST behavior. Reproduced from Ref.[63] Copyright © 2002 Elsevier Ltd.

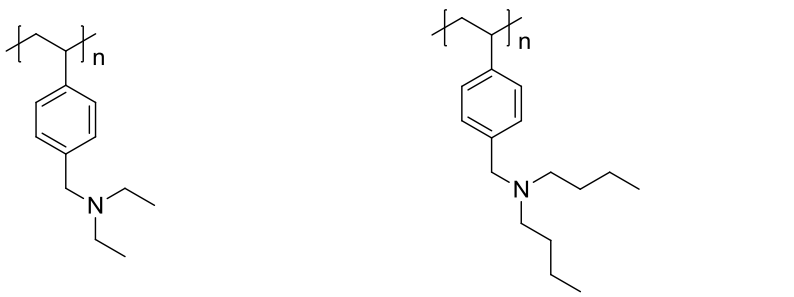

Poly[*N*-(4-vinylbenzyl)-*N*,*N*-diethylamine] Poly[*N*-(4-vinylbenzyl)-*N*,*N*-dibutylamine]

Scheme 1-8 Structures of poly[*N*-(4-vinylbenzyl)-*N*,*N*-dialkylamine].

1.2.3.3 Polyampholyte

Poly(2-methacryloyloxyethyl phosphorylcholine) (PMPC, Scheme 1-9) is a polyampholyte bearing both positive and negative charges in its phosphorylcholine group.[127] The polymer is well soluble in either water or ethanol, while it exhibits UCST behavior in the mixture of the two solvent at x_{org} = *ca*.0.35–0.80 due to the co-nonsolvency effect. Co-nonsolvency was also observed for n-propanol/water solutions and isopropanol/water solutions in a wide x_{org} range.

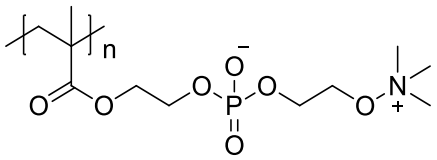

Scheme 1-9 Chemical structure of poly(2-methacryloyloxyethyl phosphorylcholine).

1.2.4 Polymers with UCST behavior in pure alcohols

Apart from the previously described polymers that show UCST behavior in alcohol/water solvent mixtures, there are also some reports on polymers that show UCST behavior in pure alcohols.[45, 128-130] These polymers are also of interest for this review because they may also exhibit UCST in alcohol/water solvent mixtures, which are not yet explored. Some of these polymers are highlighted in this section.

Many poly(vinyl ether)s (PVE, Scheme 1-10) exhibit LCST thermoresponsive behavior in water in the physiological temperature range depending on the hydrophilic/hydrophobic balance making these polymers of interest in biomedical applications.[21, 31] Poly(2-methoxy-ethyl vinyl ether) (PMOVE) prepared via living cationic polymerization was reported to show a LCST T_{CP} at about 70 ^{o}C in aqueous solution.[131] The thermoresponsive behavior could be finely tuned by copolymerization with hydrophobic octadecyl vinyl ether (ODVE) leading to polymers that also exhibit UCST behavior in alcohols.[44] More specifically, UCST phase transitions were found for the random copolymers $ODVE_{60}$-*r*-$MOVE_{240}$ and $ODVE_{40}$-*r*-$MOVE_{260}$ in ethanol and methanol, respectively, depending on the composition of the copolymer. Copolymers of the hydrophobic ODVE with *N*-phenyl maleimide (PhMI) were also reported to be thermoresponsive polymers[132] revealing UCST behavior in 1-butanol and 1-hexanol. A fluorine-containing copolymer poly((isobutyl vinyl ether)-*r*-(2-(4,4,5,5,6,6,7,7,8,8,9,9,9-tridecafluorononyloxy)ethyl vinyl ether)) ($IBVE_{190}$-r-$13FVE_{40}$) was also synthesized by living cationic polymerization[45] and the resulting copolymer was found to exhibit an UCST type of phase transition in ethanol.

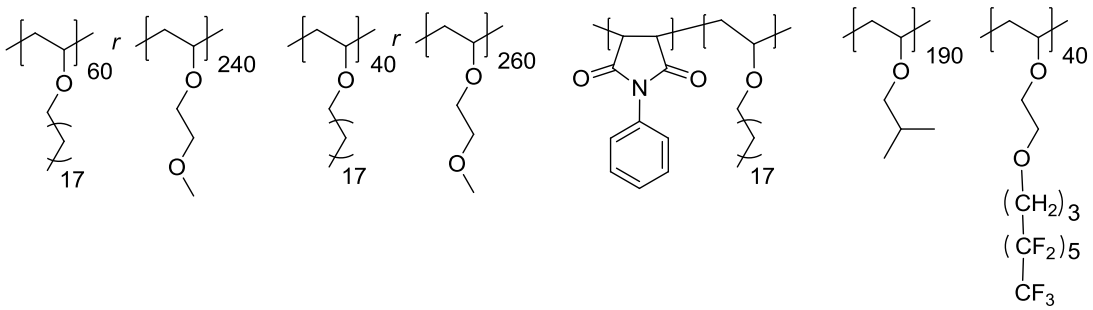

Scheme 1-10 Structures of PVEs that show UCST behavior in alcohols.

A series of polyacrylates (Scheme 1-11) were prepared by radical polymerization using functionalized acrylate monomers originated from the Passerini three-component reaction (Passerini-3CR) of acrylic acid and a variety of aldehydes and isocyanides as reported by Meier.[133] The properties of the 'Passerini' polyacrylates could be well tuned depending on the reagents used for Passerini reaction. Favored by balanced hydrophilicity/hydrophobicity, poly(1-(benzylamino)-1-oxopropan-2-yl acrylate) (PBAOPA) and poly(methyl 4-(2-(acryloyloxy)propanamido)butanoate) (PMAPAB) were found to exhibit UCST behavior in ethanol at 55−74 and 6−19 ^{o}C, respectively, while poly(methyl 4-(2-(acryloyloxy)propanamido)butanoate) (PMAPAB) and poly(1-(cyclohexylamino)-1-oxopropan-2-yl acrylate) (PCAOPA) exhibit UCST transitions in methanol at −37 to −20 and 6−27 ^{o}C respectively. The Passerini-3CR was reported have an excellent atom economy and to be an highly efficient tool for the synthesis of acrylate monomers[134] making this series of thermoresponsive polymer even more attractive for future applications.

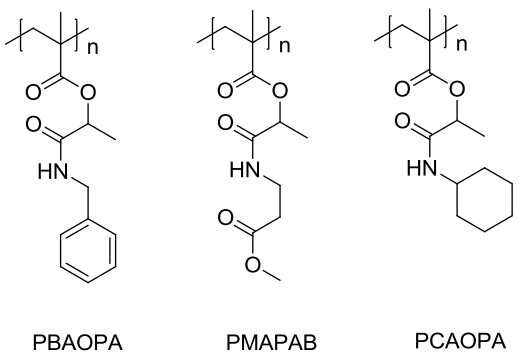

Scheme 1-11 Structures of 'Passerini' polyacrylates that exhibit UCST behavior in alcohol

Poly(2-methoxyethyl methacrylate) (PMEMA) is well soluble in methanol. However, PMEMA brush decorated magnetic nanoparticles, namely Fe_3O_4@PMEMA (Figure 1-18), were reported to show UCST behavior in methanol indicated by the transition of the nanoparticle solution from a turbid suspension to a brownish transparent dispersion.[135] Surprisingly, the cloud point is lower for particles with longer polymer arms, oppositional to the UCST behavior of free polymers. This unique behavior of Fe_3O_4@PMEMA was ascribed to the crowded and stretched polymer chains attached on the surface of the nanoparticles leading to less beneficial entropic contribution to the solvation process. It is expected that this effect is less relevant for long chains, as the free volume of chain segments increases with rising distance to the solid core.

1.3 Temperature sensors based on thermoresponsive polymers

The use of polymers is finding a permanent place in sensor development as their chemical and physical properties can be tailored over a wide range of characteristics.[136-138] Great progress has been made in the last 20 years for the development of polymeric sensors, especially systems that make use of stimuli-responsive polymers that sharply respond with a solution phase transition to environmental parameter changes such as the temperature, pH value, UV/Vis light or chemical changes.[138] The unique properties and easy accessibility

of polymeric sensors enable their development as important alternative sensoric materials in areas such as biology, diagnostics, and chemical analysis.[136, 138-140]

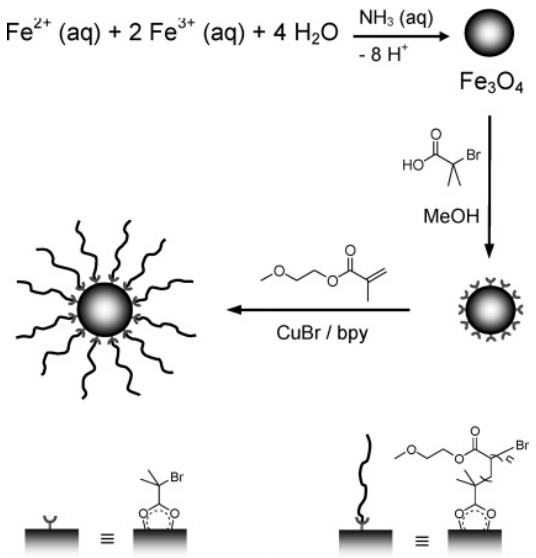

Figure 1-18 Synthesis of Fe_3O_4@PMEMA Hybrid Nanoparticles. Reproduce from ref,[135] Copyright © 2013, American Chemical Society.

For temperature sensing purposes, the temperature induced solution phase transition of a polymer can be translated into a sensory signal by incorporating solvatochromic dyes[141, 142] that specifically change their optical or emissive properties in response to polarity changes in the local environmental (Figure 1-19). Such a polymer sensor system is composed of two key parts: (1) A thermoresponsive polymer that undergoes a phase transition due to changes in the environmental temperature, in particular polymers with a lower critical solution temperature (LCST) are mostly used that dissolve at lower temperatures and precipitate upon heating;[1] (2) The chromophore can be a fluorescence or visible solvatochromic dye that generates an output signal that can be quantitatively detected. In aqueous solution, the chromophore changes its absorbance or emission behavior upon variation of the microenvironment from being exposed to water in the soluble polymer state to being in contact with the less polar collapsed polymer globules. For visible solvatochromic dyes, the change of signal can be either variation of absorption intensity or maximum absorption wavelength. In terms of fluorescent dyes, more information can be provided because numerous parameters like fluorescence decay times, fluorescence intensity, quenching efficiency, energy transfer and fluorescence polarization can be determined as output signals.

The combination of thermoresponsive polymers and solvatochromic dyes has provided the resulting thermometers benificial properties originating from both components: 1) the solubility and temperature sensing regime of the sensor materials can be easily tuned by varying the ratio of hydrophobic/hydrophilic monomers; 2) the polymer can provide structural stability and easy processability (e.g. coating or formation

of nanoparticles); and 3) embedding of the chromophore into the polymeric matrix can dramatically reduce photobleaching and chemical reactions of the dye. Due to their excellent properties, polymeric temperature sensors have been considered as very promising thermometers and have received significant interest over the last two decades. Numerous publications have appeared and such systems have been summarized in some recent reviews.[138, 143]

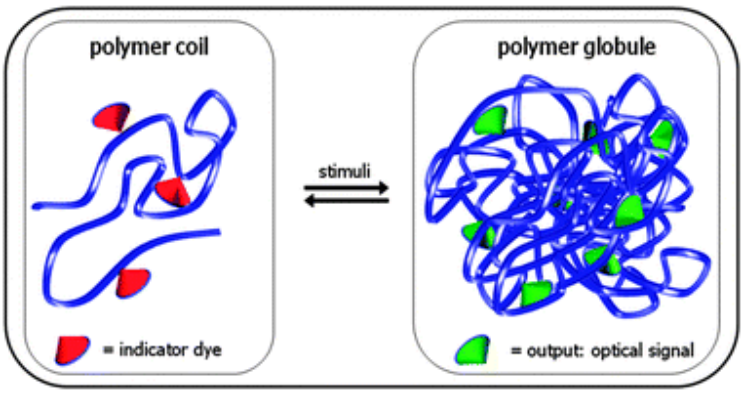

Figure 1-19 Schematic representation of the polymeric sensors based on polymer phase transitions (coil-to-globule) and solvatochromic dyes. Reproduced from ref.[143], with permission from The Royal Society of Chemistry

The first reported examples of thermoresponsive polymers modified with (solvatochromic) chromophores as indicator dyes were designed for a new method to study the polymer phase transitions. At the end of the eighties, Irie and Kungwatchakun[144] studied azobenzene containing poly(*N*-isopropylacrylamide) (PNIPAM) copolymers as photoresponsive systems and Binkert et al.[145] reported a fluorescein labeled PNIPAM to investigate the local mobility of the polymer chains during the phase transition by fluorescence spectroscopy. Fundamental studies on fluorophores as indicators for stimuli-responsive polymers were reported by the Winnik group[146] in 1990 and shortly after by Schild and Tirrell[147] based on PNIPAM in combination with the solvatochromic fluorescent chromophore pyrene. Both groups used the non-radiative energy transfer between donor and acceptor chain labels to explore the interpolymer interactions and the changes of the chain dimensions during the coil-to-globule transition. Since 2003 a large number of fluorescent/solvatochromic dye containing polymers have been developed based on these initially reported concepts. These dye functional polymers are studied for two purposes: (i) the development of new polymeric sensor systems and (ii) to gain in depth understanding of polymer chain conformations and/or phase transitions.[148, 149]

1.3.1 Polymers used for temperature sensors

Polymers used for temperature sensors can simply act as physical support for small molecule temperature probes to enhance their stability and processability.[150] However, increasing attention has been paid to complex thermometers based on the combination of solvatochromic dyes and a wide range of

thermoresponsive polymers (Scheme 1-12) that sharply respond with a solubility phase transition to environmental temperature changes.[151] In this chapter, we will focus on the latter system where the thermosensitivity of the polymers is responsible for the temperature sensing. For the development of polymeric temperature sensors in which the polymer only acts as immobilizing matrix of sensory probes, the reader is referred to a recent review.[152]

1.3.1.1 Synthesis of dye-functionalized polymer

The synthetic approach to incorporate an organic dye into a polymer chain has been widely investigated, and has been summarized in recent reviews.[153, 154] Basically, there are two major synthetic pathways to prepare dye-functionalized polymers: i) using dye-functionalized monomers or an initiator/chain transfer agent during polymerization;[153-155] or ii) the functionalization of the polymer by post-polymerization modification[156, 157] using e.g. an activated ester or an efficient ‘‘click’’ reaction.[100, 158, 159] Both of the strategies are very well suited for the preparation of dye-functionalized (co)polymers also allowing the preparation of different polymer architectures.

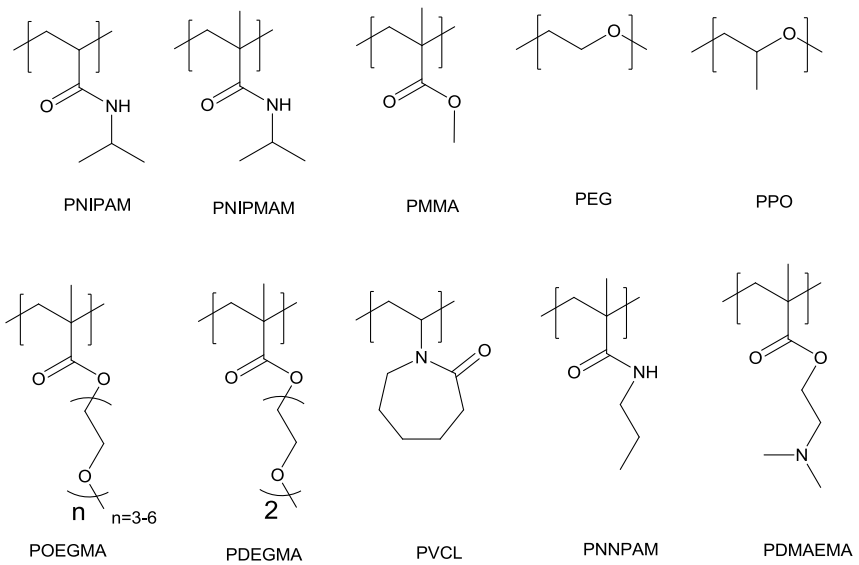

Scheme 1-12 Chemical structures of thermoresponsive polymers employed for the synthesis of polymeric thermosensors described in this section

The synthesis of dye-functional polymers is usually performed by free radical polymerization due to its high tolerance to functional groups compared to other polymerization techniques. In the last years controlled radical polymerization methods (CRP) were also performed if well-defined polymer architecture, composition or chain length is desired for the target polymer. Among the reported CRP techniques, atom transfer radical polymerization (ATRP)[114, 160, 161] or reversible addition-fragmentation chain transfer polymerization (RAFT)[116, 117] are mostly used for the construction of polymers defined. Besides linear

polymer chains, dye functionalized polymers with other architectures like block,[162, 163] comb-like[164-166] or star[167] structures can be realized by these methods. Difunctional monomers are sometimes added to an emulsion polymerization to form nanogel or microgel particles. As a limitation of this direct dye-incorporation strategy, the dye-functional monomer must be compatible with the polymerization method.

In the post-polymerization modification approach, an activated copolymer is required, which can comprise, *e.g.* activated esters,[157] like the pentafluorophenyl (meth)acrylate or N-((meth)acryloxy) succinimide, or 'clickable' groups,[158, 159] such as acetylene or azide. The dye modification of end groups originating from the initiator or chain transfer agent with dye has been used to generate polymer with dyes as end group(s). The advantage of post-polymerization modification is that the "activated copolymer'' represents a universal scaffold for versatile dye functionalization (e.g. two different chromophores for FRET[168]) allowing easy evaluation and comparison of the optical properties of similar polymers with different chromophores.

1.3.1.2 Classification of polymers used for temperature sensors

The polymeric thermometers as discussed in this chapter are based on thermoresponsive polymers, i.e. polymers that undergo a reversible phase transition from a molecularly dissolved hydrated state in aqueous solution (hydrophilic) to a dehydrated state (hydrophobic) in response to temperature changes (See Scheme 1-13). This sharp coil-to-globule transition has a strong influence on the microenvironment of the repeating units of the polymer as the (majority of) water molecules are expelled from the collapsed globules during the phase transition and, therefore, a hydrophilic-to-hydrophobic change occurs in the microenvironment of the polymer. By attaching a solvatochromic chromophore to the polymer chain, this microenvironmental polarity change can be translated into a colorimetric or fluorescent sensing output signal.

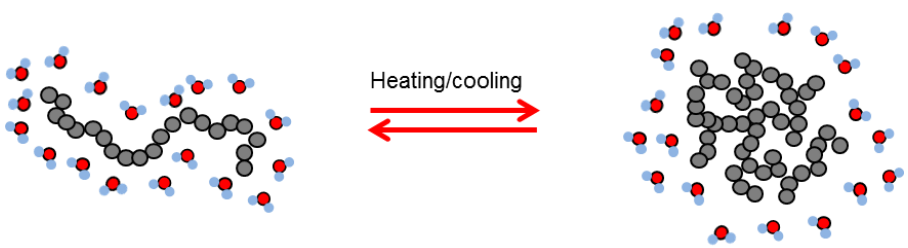

Scheme 1-13. Schematic representation of the temperature induced collapse of a thermoresponsive polymer in aqueous solution

There are two types of thermoresponsive polymers in solution: When the phase separation occurs at elevated temperatures, this is referred to as lower critical solution temperature (LCST) behavior while the reversed phase behavior is known as upper critical solution temperature (UCST) behavior. The phase transition is often accompanied by a transition from a clear solution to a cloudy solution, and the temperature

at which this transition occurs is called the cloud point temperature (T_{CP}). In general, the LCST phase transition is an entropic event driven by release of hydrating water molecules upon heating while the UCST transition is an enthalpic event driven by stronger inter-polymer attraction at lower temperatures.

The most commonly studied and firstly reported thermoresponsive polymer in aqueous solution is poly(*N*-isopropylacrylamide) (PNIPAM) with an LCST of *ca.* 32 °C,[24, 169] which is close to human body temperature. Its phase transition temperature is relatively insensitive to changes in concentration and pH making it quite robust. Moreover, the low toxicity of PNIPAM has made it possible to be used for biomedical applications. Hence, it is not surprising that PNIPAM is the most popular thermoresponsive polymer for developing polymeric temperature sensors.[144, 146, 170-177] In addition to PNIPAM, other analogous polyacrylamides, e.g. poly(*N*-n-propylacrylamide) (PNNPAM), and poly(*N*-isopropylmethacrylamide) (PNIPMAM), have also been reported as basis for temperature sensing copolymers.[173, 178-180] However, both homo- and copolyacrylamides exhibit very high glass transition temperatures, which has been reported to lead to vitrification of the highly concentrated polymer phase during phase separation, potentially inducing hysteresis between heating and cooling.[181] This translates into a typical limitation of PNIPAM as polymeric matrix of thermometer, i.e. differences in the output signal, for the same temperature value, depending on whether the temperature is increasing or decreasing.

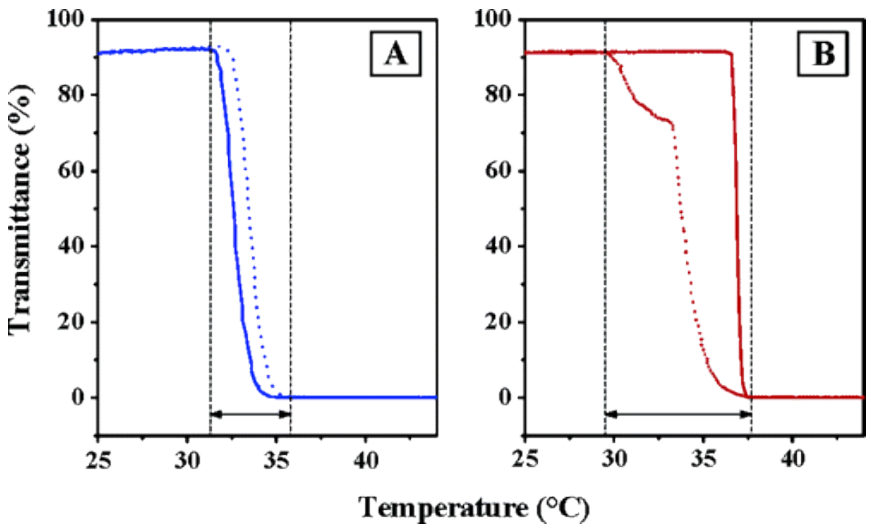

Figure 1-20 1 Transmittance as a function of temperature measured for aqueous solutions of (A) P(DEGMA-*co*-OEGMA) and (B) PNIPAM. Solid lines, heating cycles; Dotted lines, cooling cycles. Reprinted with permission from ref. [28] Copyright © 2006, American Chemical Society.

Recently, poly(oligoethylene glycol (meth)acrylate)s (POEG(M)A)s with low Tg have been introduced as thermoresponsive alternatives to PNIPAM showing excellent reversibility of the phase transition without hysteresis (see Figure 1-20).[20, 26-28, 182] In addition, the phase transition temperature can easily be tuned by copolymerization of different commercially available OEG(M)A monomers. These polymers, furnished by

'stealthy' oligoethylene glycol side chains, also show superb biocompatibility making them very well suited for biomedical applications, similar to PNIPAM. Hence, POEG(M)As have frequently been employed as thermoresponsive polymeric matrices for thermometer in recent years.[183-187]

Apart from PNIPAM and POEG(M)A, various other LCST polymers have also been reported as polymeric matrices for thermometers, such as poly[2-(*N*,*N*-dimethyl amino)ethyl methacrylate] (PDMAEMA), [176] poly(propylene oxide) (PPO)[188] and poly(*N*-vinylcaprolactam) (VCL)[166].

As a limitation, the temperature sensing regime of LCST-based sensors is often limited to a narrow temperature range (around 10 to 20 ^{o}C) resulting from the sharp entropic LCST phase transition. Instead of the entropy driven phase separation that occurs for LCST polymers, the upper critical solution temperature (UCST) polymer phase transition is mostly driven by enthalpy causing a broader transition range. As a result, temperature sensors based on UCST polymers are expected to give a broader temperature sensing regime compared with LCST polymers. However, polymers with UCST transitions have been rarely used for thermometers, possibly due to the fact that polymers that show UCST behavior in aqueous solution are quite rare.[17] Nevertheless, based on the UCST transition of PMMA in ethanol/water solvent mixtures,[52, 65, 87] Hoogenboom et al. have reported temperature sensors by incorporating disperse red 1 (DR1) or pyrene.[100] These sensors indeed had a much broader temperature sensing regime of 30 ^{o}C compared to those based on LCST polymers that typically have a temperature sensing regime of 10 ^{o}C.

1.3.1.3 Chemical structure of thermoresponsive polymer thermometers

The chemical structure of the polymer used for the thermometer acts as the chemical environment of the incorporated solvatochromic dyes, both in the hydrated soluble state and the dehydrated collapsed state.[184, 189] Hence, the chemical structure of the polymer has a great influence on the sensory properties of the thermometer, e.g. temperature response range and fluorescence intensity.

Laschewsky and Neher[189] have recently investigated structure-related differences in the solvatochromic shift and sensing behavior of PNIPAM, POEGMA and POEGA modified with naphthalimide as solvatochromic fluorescent dye. (Figure 1-21). Due to the LCST phase transition of PNIPAM, the fluorescence intensity of the dye was dramatically increased, whereas the emission properties of the dye are rather unaffected when OEG-based polyacrylate and methacrylate sensors undergo the temperature induced phase transition. These observed differences were ascribed to the difference of the local micro-environment of the dye. The PNIPAM chains can form much denser agglomerates, compared to the OEG-based copolymers, due to strong intramolecular and intermolecular hydrogen bonds at temperatures above the LCST. In addition, the hydrophilic OEG side chains of POEG(M)As hinder efficient dehydration of the collapsed polymer globules upon heating resulting in a smaller change of the polarity of the microenviroment of the dye. Similar conclusions were made when employing a different solvatochromic fluorescent dye,

namely 7-(diethylamino)-3-carboxy-coumarin (DEAC).[187] The dye is mostly insensitive to the polymer phase transition of a dye-functionalized P($DEGMA_{81}$-co-$OEGMA_{19}$) copolymer. In contrast, analogues PNIPAM-based sensors exhibit drastically increased emission intensity after heating above the LCST.

The influence of polymer chemical structure on sensing behavior has also been reported by Hoogenboom et al.[184] The authors have shown that PDEGMA decorated with DR1 revealed dual pH and temperature sensing behavior with both an absorption intensity and peak shift output. When replacing the di(ethylene glycol) side chains with more hydrophilic OEG side chains, the temperature induced absorption peak shift of the incorporated polarity sensitive dye was lost, ascribed to less efficient dehydration of the more hydrophilic POEGMA.

Ionic components can be introduced in thermoresponsive polymeric materials via the monomer or initiator in the expectation that electrostatic repulsion would prevent the formation of large aggregates in the dehydrated state, which can cause hysteresis between heating and cooling. Gota et al.[190] have investigated the influence of incorporating an ionic component in fluorescent polymeric thermometers. Polymer thermometers consisting of only N-alkylacrylamide and the fluorescent dye show rather low temperature resolution in their functional ranges due to the occurrence of inter polymer aggregation, whereas much high temperature resolution (< 0.2 ^{o}C) is obtained by adding an ionic component as comonomer during polymerization. Such an ionic fluorescent nanogel was then applied for intracellular thermometry in living cells.[191, 192] With increasing temperature, the thermoresponsive ionic gel produces stronger fluorescence in the cytoplasm, allowing monitoring temperature differences of less than 0.5 ℃ without any interference due to precipitation or interaction with cellular components. An even higher temperature resolution of 0.18-0.58 ^{o}C was achieved by application of fluorescence lifetime imaging as output signal.

1.3.1.4 Architectures of thermoresponsive polymer thermometers

The simplest polymer structure for use in thermometers is just a linear thermoresponsive homopolymer decorated with a solvatochromic dye. In real applications, however, the solution will be become turbid during sensing due to the aggregation of such homopolymer chains leading to lower transmittance of the solution. Moreover, precipitation of the copolymer could happen when the hydrophobic collapsed polymer globules are not stabilized sufficiently by hydrophilic species. To avoid such drawbacks of simple homopolymer structures as well as to introduce functionalities, more complex polymeric structures, like cross-linked particles, block and brush copolymers, have been developed for polymer temperature sensor applications.

Dye incorporated nano- or micro-particle sensors[171, 174, 193-195] are usually prepared by (mini-)emulsion radical polymerization in the presence of cross-linkers and ionic species. The resulting particles, dispersed in aqueous solution, undergo a temperature induced swollen-to-shrunken transition, as normally noticed by a

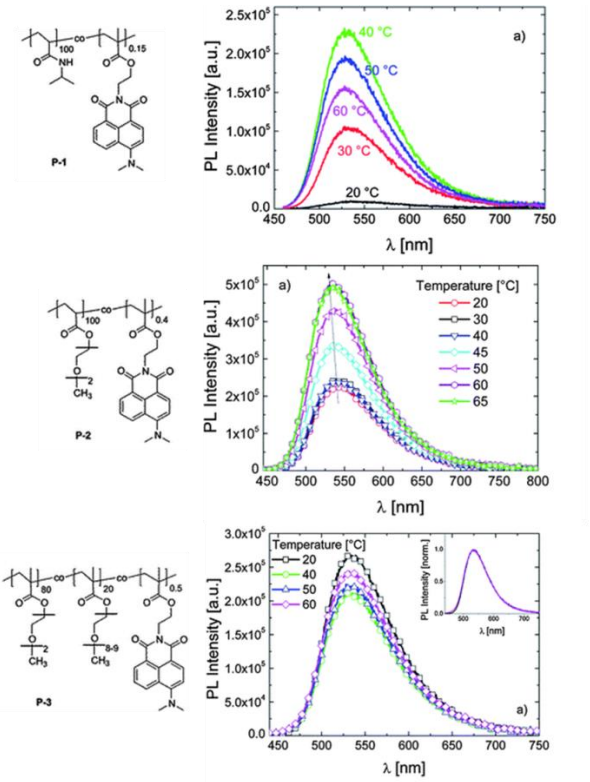

Figure 1-21 The fluorescence spectra of naphthalimide functionalized PNIPAM, $PMEO_2A$ and P(DEGMA-*co*-OEGMA) in PBS (0.1 g L^{-1}) at various temperatures. Reproduced from ref.[189] with permission from The Royal Society of Chemistry

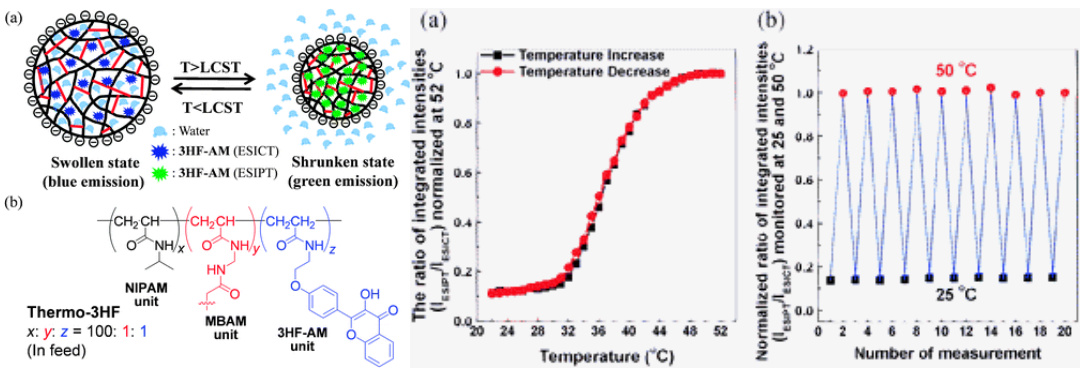

Figure 1-22 Highly reversible fluorescent nanothermometer, Thermo-3HF, based on cross-linked polymeric nanoparticles. Reproduced from ref.[194] with permission from The Royal Society of Chemistry

decrease in particle size. Such systems have frequently been used for temperature imaging, as the phase transition temperature is insensitive to the concentration of the sensory materials. Moreover, instead of macroscopic aggregation of linear polymer chains, the shrunken state of cross-linked particles remains dispersed leading to a higher reversibility. For instance, Chen et al.[194] have synthesized a cross-linked

PNIPAM-based fluorescent nanothermometer, Thermo-3HF (3HF refers to 3-hydroxyflavones) (Figure 1-22). Single-run and multiple-run reversibility experiments of Thermo-3HF revealed no hysteresis during the heating and cooling cycles and no declining signal during multiple-run tests. The high temperature resolution and excellent reversibility was attributed to the highly hydrophilic, ionic surface originated from the anionic initiator used for the radical emulsion polymerization. The electrostatic repulsion prevents individual nanogels from incurring severe intermolecular aggregation through electrostatic repulsion.

Block copolymers with one thermoresponsive block are also interesting for sensing applications.[188, 196-200] The dye can be incorporated in different parts of the block copolymer chain making the polymer very robust for different tasks. Han et al.[196] have reported the sensory amphiphilic copolymer, poly(NIPAM-*b*-1-(4-vinyl benzyl)-2-naphthyl-benzimidazole) (poly(NIPAM-b-VBNBI)). This copolymer can self-assembly into micelles in aqueous solution with the hydrophobic dye containing block as core and the thermoresponsive block PNIPAM as corona. The system exhibited a reversible fluorescent response to change in temperature around the LCST of PNIPAM due to coil-to-globular induced micro-viscosity increase of the dye microenviroment. Another amphiphilic block copolymer, P{styrene-*co*-[4-(2-acryloyloxyethylamino)-7-nitro-2,1,3-benzoxadiazole]-*co*-[10-(2-methacryloxyethyl)-30,30-dimethyl-6-nitrospiro(2H-1-benzo-pyran-2,20-indoline)]}-*b*-P(NIPAM-*co*-RhBAM) P(St-*co*-NBDAE-*co*-SPMA) -b-P(NIPAM-*co*-RhBAM), bearing NBDAE and SPMA moieties in the hydrophobic polystyrene (PS) block and RhBAM moieties in the thermoresponsive PNIPAM block was reported by Liu et al.[162] A sensitive ratiometric fluorescent temperature sensor was obtained through thermo-induced collapse of the PNIPAM micellar corona owing to the closer proximity between the FRET donors (NBDAE) and acceptors (RhBAM). The FRET could be also adjusted by pH-induced ring opening of RhBAM leading to pH sensing by the micelles. The presence of the UV-active SPMA moieties in the core of the micelle renders additional features to the modulation for multicolor emission by light irradiation. The principal of this reversible three-state switching of fluorescence emission is shown in Figure 1-23. A drawback of such block copolymers consisting of a hydrophobic block and a thermoresponsive block is that macroscopic aggregation will occur during sensing. To overcome this aggregation, the double hydrophilic P(NIPAM-co-FITC)-b-P(OEGMA-co-RhBAM) block copolymer was synthesized.[163] In addition to ratiometric temperature sensing originating from FRET between FITC and RhBAM at pH < 6, the copolymer is also capable of sensing pH in the range 2-10 based on the pH responsiveness of the two dyes. Such double hydrophilic block copolymers go from unimers to micelles during sensing preventing macroscopic aggregation. A drawback of such systems is their strong concentration dependence as this influences the micellization, which can even be fully suppressed when concentration is lower than the critical micellization concentration.

In addition to these mostly employed linear homopolymers, cross-linked particles and block copolymers, other types of polymer architectures have also been reported as polymeric sensory scaffolds, such as a brush

polymer,[164] a polymer coating on nanoparticles,[201] a star polymer,[202] and a dendronized copolymer.[203] Even though such polymers bear unique functionalities, they have not widely been used for temperature sensors to date.

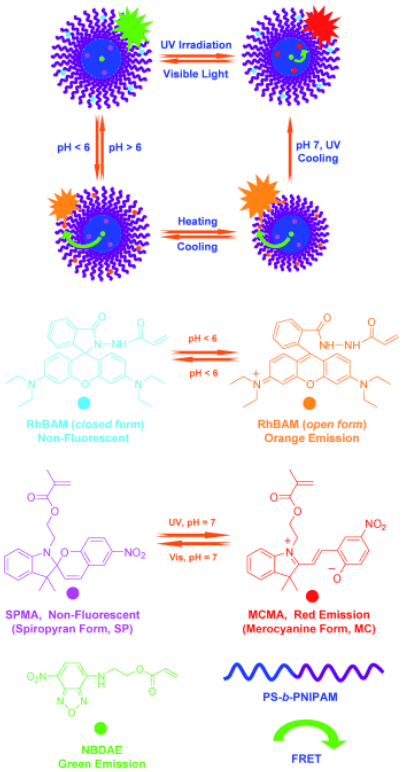

Figure 1-23 Schematic representation of a block copolymer based reversible three-state switchable multicolor luminescent system from P(St-co-NBDAE-co-SPMA)-b-P(NIPAM-co-RhBAM). Reprinted with permission from ref.[162] Copyright © 2010 Wiley Periodicals, Inc.

1.3.2 Potential applications of polymeric temperature sensors

In this section, the potential applications of polymeric temperature sensors are highlighted based on selected examples. Of course all reported polymeric thermometers can be used as sensors for detection of temperature. In this section, we will highlight some of the novel creative strategies and concepts for more advanced applications of the polymeric sensors. More specifically, recent studies demonstrated the extension of this temperature sensing concept towards intracellular temperature imaging, dual sensing, ion sensing and logic gates as will be discussed in the following.

1.3.2.1 Intracellular temperature detection

The temperature and its distribution in a living cell are very important parameters that relate to various cellular events and strongly influence biochemical reactions inside living cells. Hence, intracellular temperature mapping within a living cell is keenly desired in various field of life science. However, detection

of temperature with high resolution and accuracy in a living cell is still a challenge for conventional thermometers.[192] Recently, a series of high resolution thermometers based on dye functionalized polymers were developed, which have shown great promise on the detection and mapping of temperature. [191-193, 204-206]

Uchiyama et al. have pioneered the intracellular thermometry with a fluorescent nanogel thermometer based on the thermoresponsiveness of PNIPAM in combination with environmentally sensitive fluorophores.[191, 206, 207] The sensor encompasses thermoresponsive PNIPAM, the fluorescent benzoxadiazole dye and negatively charged units to enriche the hydrophilicity of the thermometer and to prevent interpolymer aggregation within a cell. The nanosensor undergoes strong fluorescence enhancement upon heating due to the temperature induced collapse of the gel inside the cytoplasm of a COS7 cell. The sensor system was then optimized by using fluorescence lifetime imaging microscopy, which has improved the spatial and temperature resolution of the thermometer down to 200 nm and 0.18–0.58 ℃, respectively (Figure 1-24).[192] In addition to the high resolution, the polymeric sensor holds high biocompatibility and negligible interactions were observed with cellular components making this system very attractive for application.

Yin et al. have extended the intracellar thermosensor concept to a system that responds to both temperature and pH.[193] The sensory polymeric gel was prepared by combining a thermoresponsive PNIPAM hydrogel and a pH-responsive fluorescent benzo[*de*]isoquinoline dye by copolymerization of NIPAM, the dye-functionalized monomer and a cross-linker. The resulting gel could sense temperature in living cells between 32 ^{o}C and 40 ^{o}C by flourescence intensity enhancement. In addition, due to the pH sensitivity of the dye, the fluorescence intensity decreased by increasing pH from 4.0 and 10.0 at 25 ^{o}C providing the possiblity of pH sensing. As a drawback, this temperature and pH sensing system can only sense temperature or pH separately. The dual sensing systems that probe temperature and pH simultaneously are highlighted in the next section.

1.3.2.2 Dual temperature and pH sensors

A dual sensor that simultaneously responds to temperature and pH value was synthesized by Hoogenboom et al. as illustrated in Figure 1-25.[184] The sensor is based on a thermoresponsive PDEGMA copolymer bearing DR1 as a solvatochromic dye in the side chain. This dual sensitive copolymer shows temperature responsiveness in the range from 10 to 20 ^{o}C due to the phase separation of the PDEGMA; and the chromophore exhibits a color change from 487 to 532 nm under acidic conditions due to protonation of the chromophore, while at basic conditions this shift is lost. By measuring a single absorption spectrum, the combination of the absorption maximum as well as the absorbance ratio of the DR1 dye provides information of both the temperature and pH value of the solution. In a similar approach, DR1 was incorporated in thermoresponsive dendronized polymer[203] and Liu et al. demonstrated that the dual sensing

behavior can be tuned by the generation of the dendronized polymers that affects the dye localization from the interior to the periphery of the collapsed polymer aggregates.

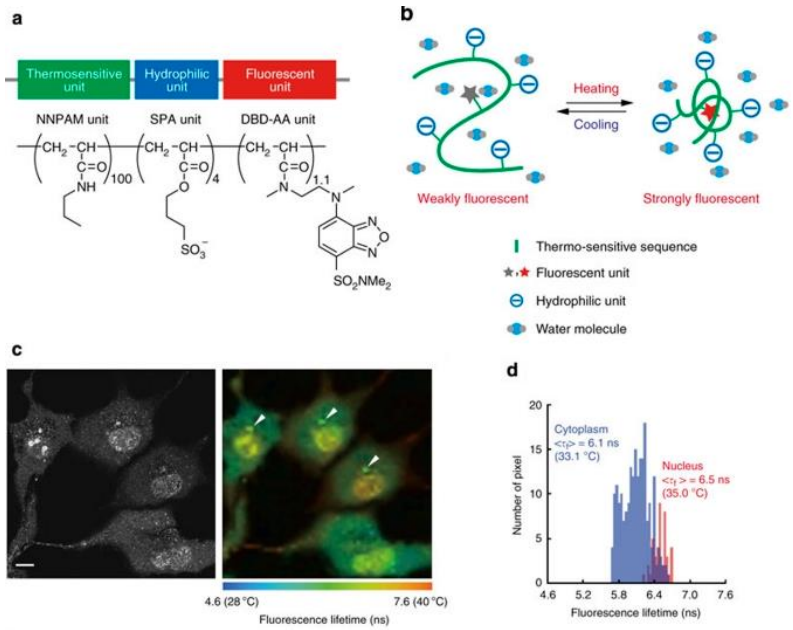

Figure 1-24 (a) Chemical structure and, (b) mechanism of PNIPAM nanogel used for intracellular temperature imaging. (c) Confocal fluorescence image and fluorescence lifetime image of FPT in a COS7 cell; and (d) Temperature of cytoplasm and nucleus detected by fluorescence lifetime in COS7 cells. Reprinted with permission from ref.[192] Copyright © 2012, Rights Managed by Nature Publishing Group.

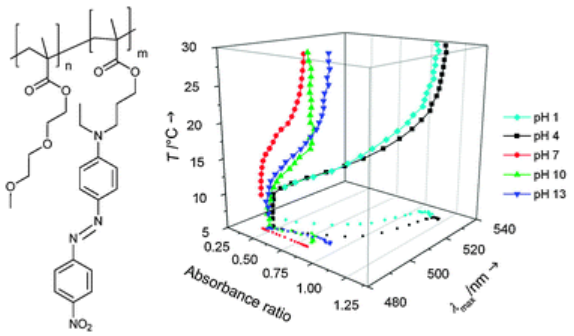

Figure 1-25 Dual sensor for temperature and pH value. Reprinted with permission from ref. [184] Copyright © 2009 Wiley Periodicals, Inc.

Dual temperature and pH sensors based on platinum(II) metallosupramolecular triblock copolymers with hydrophilic alkynyl ligands have been reported by Yam and coworkers (Figure 1-26)[199] yielding a NIR-emitting dual sensor for pH and temperature in the range of pH 4–10 and 20–50 ^{o}C. Such dual-responsive behavior was ascribed to the modulation of the self-assembly of the Pt complexes by temperature-induced micellization and the changes in the hydrophilicity as well as electrostatic interactions upon protonation/deprotonation of the CH_2NMe_2 (R1 in Figure 1-26) groups on the alkynyl ligand.

1.3.2.3 Ion sensors

Thermoresponsive PNIPAM microgel-based ratiometric fluorescent sensors for both K^+ ions and temperature were reported by Liu and coworkers (Figure 1-27).[208] The system shows facile modulation of FRET efficiency due to thermo-induced collapse and swelling of the thermoresponsive microgels functionalized with NBDAE as FRET donor and RhBEA as acceptor. Crown ether moieties were incorporated within the microgels to preferentially capture K^+ via the formation of 1:1 host-guest complexes, resulting in the enhancement of microgel hydrophilicity and elevated phase transition temperatures. Thus, the gradual addition of K^+ into microgel dispersions at intermediate temperatures, i.e. in between the phase transition temperatures of the microgels in the absence and presence of K^+ ions, respectively, can directly lead to the re-swelling of initially collapsed microgels. This process can also be monitored by changes in fluorescence intensity ratios, i.e. FRET efficiencies enabling efficient K^+ detection.

Heavy metal ion pollution poses a huge threat to human beings and our environment. However, the detection of heavy ions based on small fluorescent molecules is suffering from poor solubility and biocompatibility of the probe molecules. To conquer these drawbacks, polymeric ion sensors are being developed providing better solubility and similar or even higher sensitivity.[209, 210] A RhB hydrazide functionalized thermoresponsive block copolymer, PEO-*b*-P(NIPAM-*co*-RhBHA), was synthesized as Hg^{2+} sensor. In the dissolved state, the RhBHA can be ring-opened by Hg^{2+} ions to yield a highly fluorescent acyclic species leading to ion sensing. Dramatically improved detection sensitivity for Hg^{2+} ions could be achieved by thermo-induced micellization of the copolymer leading to fluorescence enhancement of RhBHA acyclic residues within the hydrophobic core. Similarly, the detection of Cu^{2+} ions by phenanthroline could be improved via thermo-induced microgel collapse.[210] In this system, the fluorescence intensity of phenanthroline incorporated microgels is quenched by complexion of Cu^{2+} ions, where by the quenching efficiency by Cu^{2+} ions is considerably enhanced in the collapsed microgel state.

Yan et al. have reported a porphyrin-containing triblock copolymer for dual sensing of metal ions and temperature.[211] The sensor exhibits full-color tunable behavior as a cation detector and colorimeter.

1.3.2.4 Logic gates

Logic gates that can (simultaneously) respond to multiple input signals with a single output signal are extremely interesting for developing molecular memory systems. The fabrication of logic gates based on dye-functionalized polymers has attracted significant attentions; especially temperature sensitive polymers due to the importance of temperature as input signal.[212-215] Uchiyama and Iwai et al. have developed a fluorescent polymeric AND logic gate with both temperature and pH as input signals (Figure 1-28).[213] The fluorescence intensity is enhanced by a thermo and/or pH induced phase transition, which serves as output signal of the logic gate. As shown in Figure 1-28, the fluorescence intensity (Output) of the copolymer is

distinctly high (1) only when (Input1, Input2) is (1, 1), that is when the temperature is 35 °C and pH is 9. In contrast, the fluorescence intensity holds a low level when (Input1, Input2) is (0, 0), (0, 1), or (1, 0).

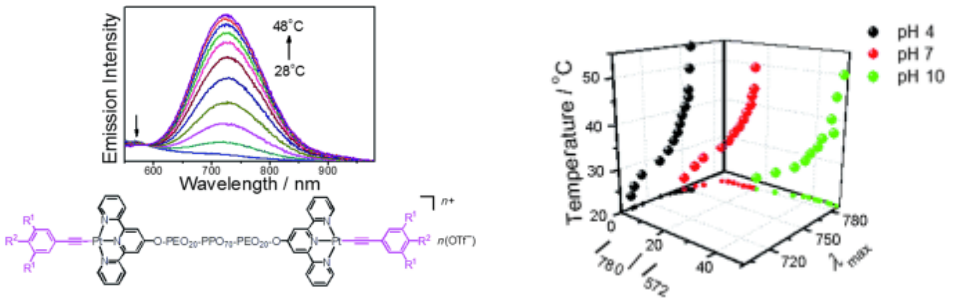

Figure 1-26 Dual temperature and pH sensor system based on metallosupramolecular triblock copolymers. Reprinted with permission from ref.[199] Copyright © 2013 Wiley Periodicals, Inc.

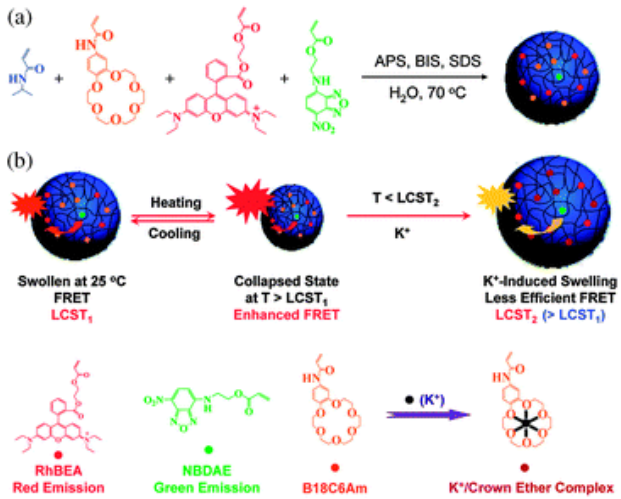

Figure 1-27 (a) Synthesis of thermoresponsive P(NIPAM-B18C6Am-NBDAE-RhBEA) microgels via emulsion polymerization; (b) Schematic illustration for temperature and K^+ ions responsive P(NIPAM-B18C6Am-NBDAE-RhBEA) microgel. Reprinted with permission from ref.[208] Copyright © 2010, American Chemical Society

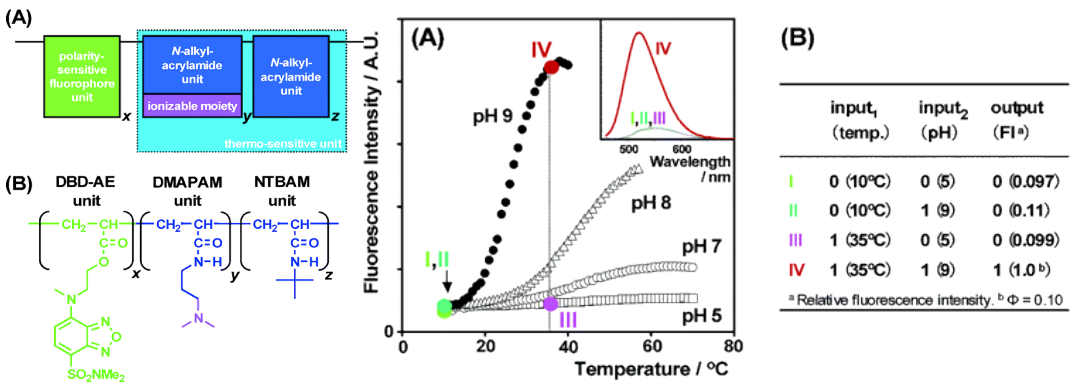

Figure 1-28 Logic gates based on poly(DBD-*co*-DMAPAM-co-NTBAM), chemical structure and working principal. Reprinted with permission from ref.[213] Copyright © 2004, American Chemical Society

1.4 Summary

The development of polymers exhibiting UCST phase transitions in alcohol/water solvent mixtures were highlight in this section. The low toxicity of the binary solvents, especially ethanol/water solvent mixtures, makes this system very promising for application in, e.g. personal care, medical or pharmaceutical areas. In addition, the solvent composition dependence of the solubility behavior of the polymers can provide another dimension to manipulate the self-assembly of (block) copolymers, which may lead to unique ordered nano-structures.

Polymeric temperature sensors have attracted increasing attention during the last decades mainly due to the wide applicability and importance of the temperature stimulus and the adaptability of the sensing behavior towards different applications. Polymeric thermometers based on the combination of solvatochromic dyes and thermoresponsive polymers that undergo a temperature induced phase transition are most common in current literature due to their uniquely controllable chemical and physical properties. This allows for a large variety of both output signals and sensor response regions with only limited changes to the polymeric design, such as the polymer architecture, identity and ratio of (co)monomers and the dye incorporation approach. Besides the new biomedical applications that are made possible due to the improvements discussed in this section, other recently emerging application areas include temperature imaging, logic gate operations, dual sensors, and metal ion detection.

Chapter 2 Methodology

Abstract: In this chapter, novel methods concerning the synthesis of well-defined polymers and the investigation of thermoresponsive behavior of polymers are developed.

In section 2.1, a one-pot procedure that straightforwardly combines RAFT polymerization and end group transformation to remove the RAFT end-groups was developed for the synthesis of well-defined polyacrylates and polyacrylamides. The procedure only requires the addition of an amine at the end of the standard RAFT polymerization procedure, which avoids the separation and purification of the intermediate polymers and hence extremely reduces the working time and utilized amount of solvent. Upon addition of the amines, thiol groups are formed by aminolysis of the thiocarbonylthio group, which undergo Michael addition with unreacted monomers leading to inert thiol-ether functionalized polymer.

In section 2.2, our investigations on the influence of the parameters used for turbidimetric analysis of thermoresponsive polymer solutions are described. Various parameters, such as concentration, heating rate, wavelength of incident light, stirring, position of temperature probe and type of cuvette were identified that can provide in depth information of the thermoresponsive behavior of polymers in solution on the one hand, but can also strongly influence the results, partially leading to erroneous interpretations and conclusions.

2.1 One-Pot preparation of inert well-defined polymers combining RAFT polymerization in situ and end group transformation

2.1.1 Introduction

Reversible addition-fragmentation chain transfer (RAFT) polymerization has been widely used to prepare well-defined polymers for various applications.[116, 117, 216-221] As an important controlled radical polymerization (CRP) technique, RAFT polymerization offers several advantages over free radical polymerization in the control of, e.g. polymer molecular weight and end-group functionality. One important feature of RAFT polymerization is that heavy metals are not required in the polymerization process making this technique of interest for biomedical applications.[196, 222-224] However, the thiocarbonylthio end-group of RAFT polymers is rather unstable, in particular under basic conditions or in the presence of primary or secondary amines and the degradable products have a strong odor limiting industrial applications. Hence, much attention has been paid to convert the unstable thiocarbonylthio functionality into an inactive and stable end-group.[220, 225, 226] For instance, Lima et al. have reported the aminolysis and subsequent Michael addition modification of RAFT termini leading to the stable thiol ether end groups.[227] Therefore, the thiocarbonylthio group of an isolated and purified RAFT polymer was first aminolyzed into a thiol by adding a primary amine, and after purification, the polymer with a thiol end group was modified via Michael addition with an acrylate to obtain the thiol ether functionalized polymer. Both of the two steps employ mild reaction conditions and produce good yields indicating promising potential for (biomedical) application. This two-step procedure was further simplified by Winnik et al.[228] who demonstrated that isolation of the intermediate thiol functionalized polymers is not required. As such, aminolysis of the thiocarbonylthio end-group was performed followed by addition of the acrylate to the solution leading to Michael addition making this technique more attractive for the synthesis of well-defined polymers. However, purification of the RAFT polymers with thiocarbonylthio group is still required.

To further optimize the procedure of end group transformation of RAFT polymers, we propose that, for polyacrylates and polyacrylamides, the end group transformation may be directly done *in situ* after RAFT polymerization, as shown in Scheme 2-1. The new procedure only requires the addition of an amine after a standard RAFT polymerization procedure. The amine can *in situ* aminolyze the thiocarbonylthio groups into thiols, which can immediately react via Michael addition with unreacted monomers still present in solution. This proposed *in situ* end-group removal procedure can extremely reduce the preparation time and the amount of solvent since only one purification step is required for preparing inert well-defined polymers. It should be noted that this method is limited to Michael addition of the same monomer as is being polymerized and will not allow introduction of other chain end functionalities. Surprisingly, this economic *in situ* end-group removal procedure has not been reported, to the best of our knowledge. The possible Michael addition of the added primary amine with acrylates or acrylamides may be the main concern that has stopped others

from developing such a method. Nonetheless, aminolysis of the thiocarbonylthio group is a fast reaction while Michael addition of acrylates to amines is relatively slow. As such, we speculated that addition of an excess of primary amine could lead to full aminolysis before the amine is consumed in Michael addition reactions. This direct *in situ* end-group modification method has been studied with four acrylates, i.e. butyl acrylate (BA), 2-methoxyethyl acrylate (MEA), di(ethylene glycol) methyl ether acrylate (mDEGA) and 2-hydroxyethyl acrylate (HEA)to demonstrate its versatility. In addition, inspired by their similar structure and reactivity, acrylamides were also tested and *N*-isopropylacrylamide (NIPAM) and *N*,*N*-dimethylacrylamide (DMAM) were chosen as representative examples. Methacrylates and methacrylamides have not been tested as they have rather low reactivity for Michael addition to the thiol end-groups.

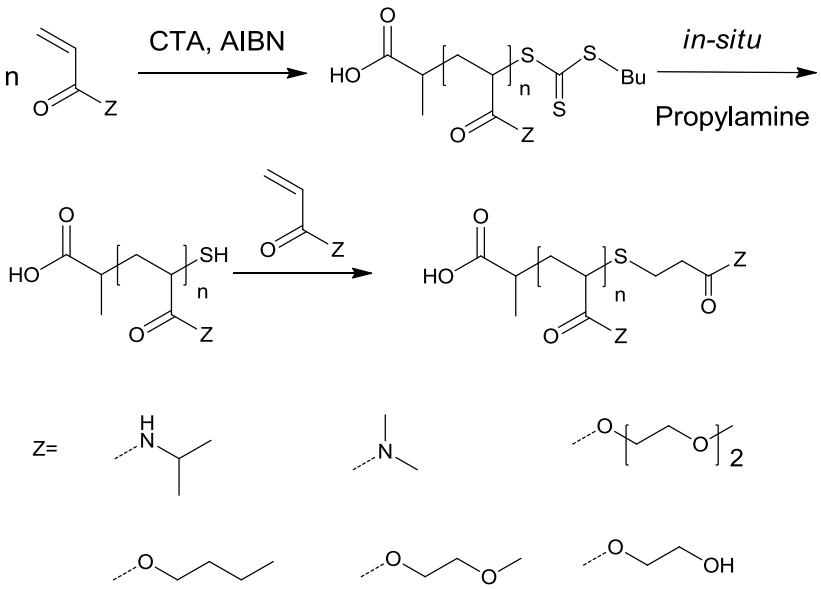

Scheme 2-1 Schematic representation of *in situ* end-group modification of well-defined polymers combining RAFT polymerization, aminolysis and Michael addition as well as the structures of the investigated monomers

2.1.2 Results and discussion

The *in situ* end-group removal reactions were explored in an automated parallel synthesizer. RAFT polymerizations were performed using a ratio of [monomer]: [CTA]: [initiator] equal to 100: 1: 0.1 at a monomer concentration of 2M at 70 ^{o}C. The polymerizations were stopped at approximately 60 % monomer conversions to ensure high chain-end functionality of the resulting polymers. After the polymerization, solutions were cooled down to room temperature followed by addition of 25 equivalents of propylamine (with respect to CTA) to every reaction vessel. Excess of propylamine was added because the potential occurrence of the amine-ene side-reaction will also consume part of the amine.

Polymers obtained before and after end group modification were characterized by size-exclusion chromatography (SEC) with refractive index (RI) detection, which revealed a minor change of the molecular

weight and dispersity (Đ) giving a first indication of successful end group modification (Figure 2-1). More importantly, no additional shoulders were present in the SEC traces of the polymers after end group transformation indicating the absence of disulfide formation after aminolysis. Next, ^{1}H NMR spectroscopy was performed to characterize the polymers before and after end group transformation (Data not shown) but no clear evidence was found to support the successful transformation of the end-groups, which can be ascribed to a too low content of end-groups in comparison to the polymer backbone as well as the overlap of characteristic end-group signals with polymer signals. Further characterizations were then performed by UV-Vis spectroscopy, SEC with UV detection and matrix assisted laser desorption/ionization time of flight mass spectrometry (MALDI-TOF MS) to assess the efficiency of the *in situ* end-group removal procedure. PDMAM and PBA were analyzed in most detail serving as representative examples for polyacrylamides and polyacrylates, respectively. For the other polymers, successful end-group removal was confirmed by SEC with both RI and UV detection.

The one-pot procedure combining RAFT polymerization and *in-situ* end group transformation was assessed by UV-Vis spectroscopy in the range of 400-480 nm, corresponding to the absorbance peak of the yellow trithiocarbonate group (see Figure 2-2, data for PDMAM, PBA before and after aminolysis as well as the CTA). For PDMAM, the disappearance of this absorption peak can be clearly observed after aminolysis indicating the high efficiency of the reaction. For PBA, however, the polymer after end-group modification still exhibits some absorption at these wavelengths, which may be attributed to the tail of ester group absorption peak. Importantly, the peak at 430 has also disappeared for PBA after the end-group modification procedure.

The next step to assess the success of the *in situ* end group transformation was performed by size exclusion chromatography (SEC) with a diode array detector (DAD). As shown in Figure 2-3 , the RAFT polymer PDMAM-CTA exhibits strong absorption at ca. 25 min, while no absorption can be detected at 450 nm after end-group removal, which confirms the complete removal of the trithiocarbonate group. In contrast to these results with DAD detection, SEC with refractive index detector (RID) revealed polymer signals from both PDMAM and PDMAM-CTA at almost the same time (Figure 2-1) demonstrating that the polymer is intact and that only the end-group has been removed. Similarly, the absorbance for PBA-CTA at 450 nm vanished after aminolysis revealing successful removal of the CTA functionality. The full absorbance spectra at the retention time of the polymers also suggest the complete end-group removal as indicated by the complete disappearance of the polymer signals (Figure 2-3).

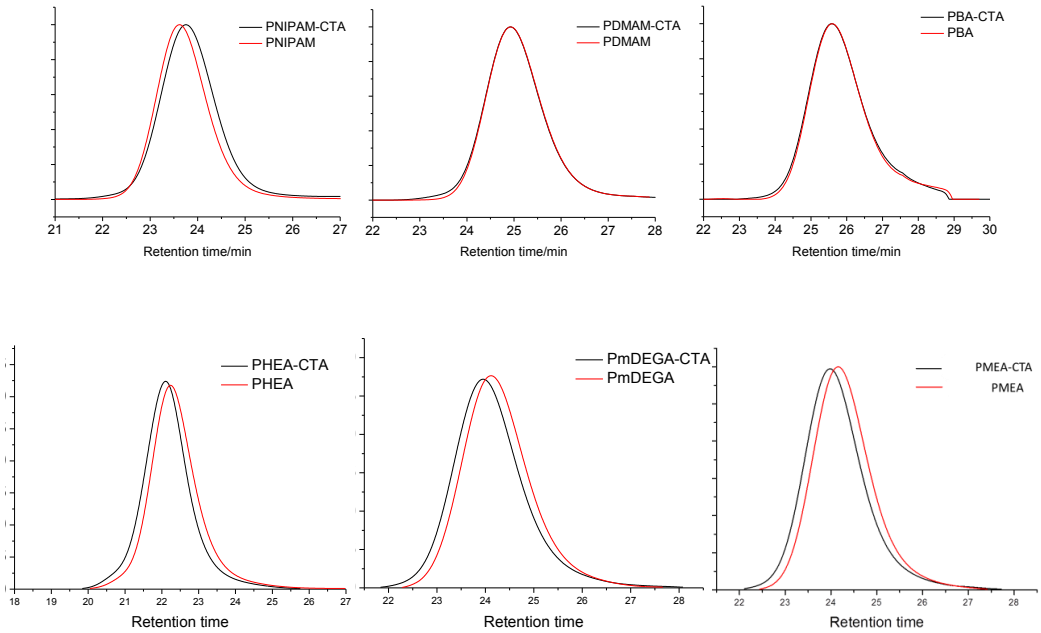

Figure 2-1 SEC traces of the synthesized polymers before and after *in-situ* end-group transformation

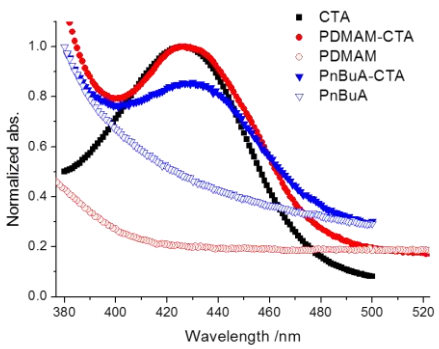

Figure 2-2 UV-vis spectra of PDMAM (red) and PBA (blue) before (solid) and after (hollow) end group transformation at a concentration of 10 mg/ml in chloroform; the spectrum of the pure CTA is also included (black).

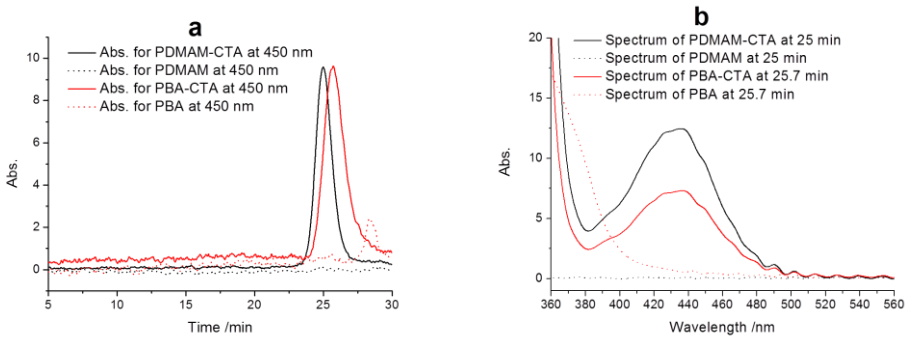

Figure 2-3 a) SEC traces collected at 450 nm, b) Absorption spectra collected by DAD for PDMAM and PBA before and after end-group transformation.

Table 2-1Overview of the synthesized polymers and their characterization data

Monomers	Conversion / %[a]	DP[a]	RAFT polymers		Polymers after end group transformation	
			Mn/kDa[b]	Đ[b]	Mn/kDa[b]	Đ[b]
NIPAM	75.8	76	14.6	1.09	15.3	1.09
DMAM	73.9	74	7.8	1.13	7.6	1.13
BA	55.1	55	4.8	1.24	4.9	1.22
HEA	71.5	72	32.3	1.14	28.5	1.16
mDEGA	63.7	64	12.0	1.18	11.3	1.15
MEA	59.6	60	12.1	1.15	11.3	1.13

[a]Conversion and DP were determined by gas chromatography with dimethylacetamide (DMA) as internal standard; [b]Number average molecular weight (Mn) and dispersity (Đ) were determined by DMA SEC.

To provide a final proof of the structure of the polymers obtained after the *in situ* end-group modification procedure, matrix-assisted laser desorption ionization time-of-flight mass spectrometry (MALDI-TOF-MS) was performed for all the polymers after end group transformation. Only PNIPAM, PDMAM and PBA after end-group modification could be successfully ionized and detected and no spectra could be obtained for PHEA, PMEA and PmDEGA most likely due to their high hydrophilicity, which appears to limit analysis by MALDI-TOF-MS. In addition, only low quality spectra for PNIPAM, PDMAM and PBA with RAFT end-groups were collected mostly like due to the presence of RAFT end-groups. As shown in Figure 2-4 for the mass spectrum of PDMAM, three major distributions are observed, all with an interval of 99.25 mass units corresponding to the DMAM repeat unit. The main peaks, for example m/z = 5579.32, can be attributed to the expected polymer species with a degree of polymerization of 54 and the thioether end group resulting from Michael addition, cationized by Na^+. The other major distributions, represented by the peaks with m/z= 5601.47 and 5634.48, can be ascribed to the sodium and potassium adducts of the polymer cationized by Na^+ and K^+, respectively (see Figure 2-4 for the proposed chemical structures). The MALDI spectrum of PBA reveals two main distributions with mass interval of 128.31 corresponding to the BA monomer (Figure 2-5). The two series of main peaks, for example m/z=4999.67 and 5021.08, can be identified as the expected polymer species with a degree of polymerization of 49, ionized with H^+ or Na^+ and a thiol-ether ω-end group. The mass spectrum of PNIPAM shown in Figure 2-6 also suggests the successful end group transformation.

2.1.3 Summary

A one-pot procedure for the preparation of well-defined polyacrylamides and polyacrylates combining RAFT polymerization and *in situ* end group transformation has been developed for straightforward preparation of inert poymers by RAFT polymerization. This one-pot procedure requires only the addition of excess primary amine at the end of the standard RAFT polymerization procedure, which eliminates the separation and purification of the intermediate polymers and hence leads to extreme reduction of the working time and utilized amount of solvents.

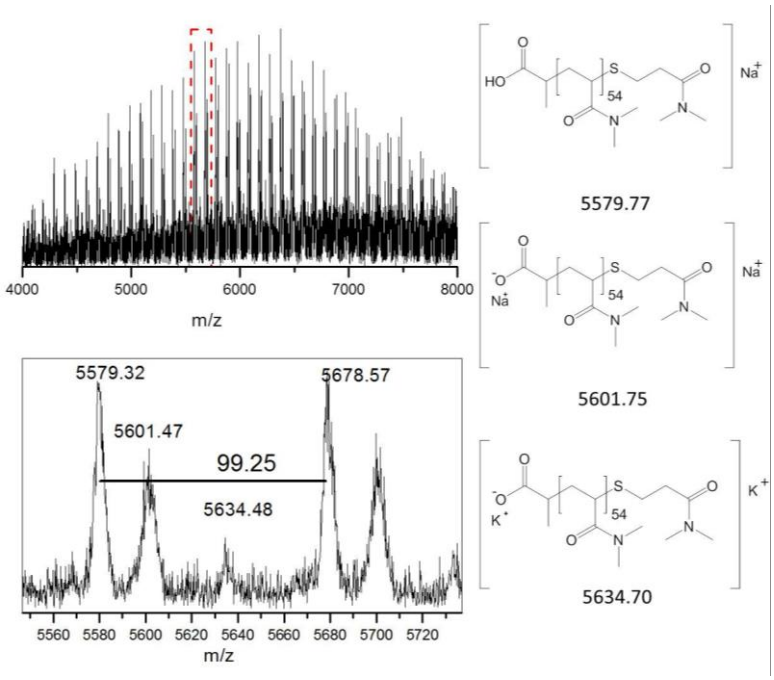

Figure 2-4 Matrix-assisted laser desorption ionization time-of-flight mass spectrum of PDMAM synthesized by one pot RAFT polymerization and *in situ* end group transformation. (Top: full view, Bottom: partial enlargement). Assigned structures and ions of the peaks in the enlarged view are shown on the right.

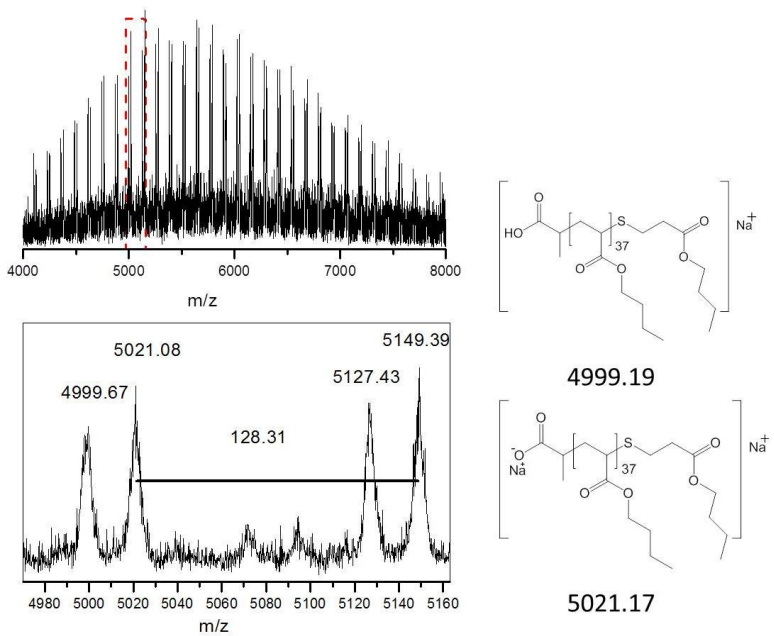

Figure 2-5 Matrix-assisted laser desorption ionization time-of-flight mass spectrum of PBA synthesized by one pot RAFT polymerization and *in situ* end group transformation. (Top: full view, Bottom: partial enlargement). Assigned structures and ions of the peaks in the enlarged view are shown on the right.

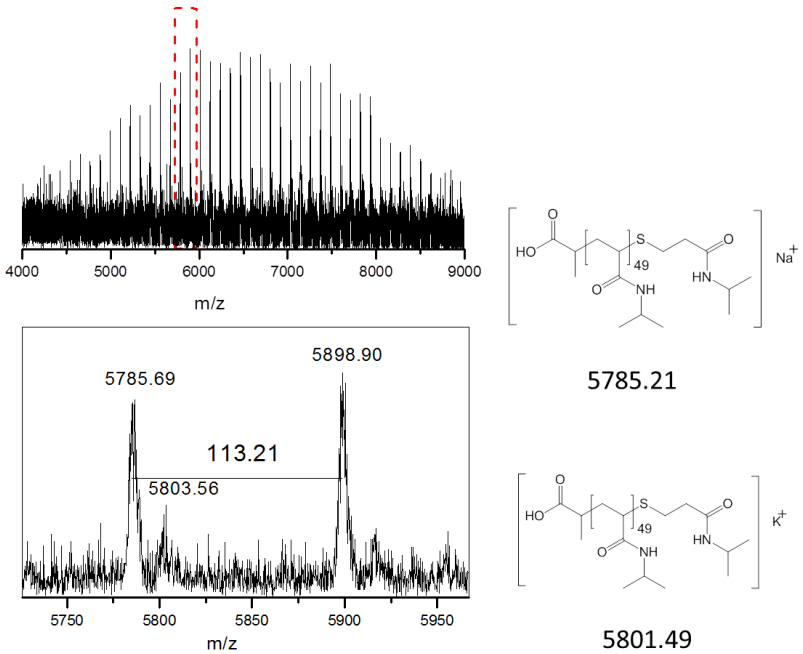

Figure 2-6 Matrix-assisted laser desorption ionization time-of-flight mass spectrum of PNIPAM synthesized by one pot RAFT polymerization and *in situ* end group transformation. (Top: full view, Bottom: partial enlargement). Assigned structures and ions of the peaks in the enlarged view are shown on the right.

2.1.4 Experimental Section

Materials and instrumentation

All chemicals and solvents are commercially available and were used as received unless otherwise stated. Dichloromethane (DCM), tetrahydrofuran (THF), propylamine, *N*,*N*-dimethylformamide (DMF), *N*,*N*-dimethylacetalamide (DMA) and hexane were obtained from Sigma Aldrich. Deuterated chloroform and methanol are supplied by Eurisotop. Azobis(isobutyronitrile) (AIBN) was recrystallized from diethyl ether and stored at -7 ^{o}C.

Reactions were performed using a Chemspeed ASW2000 automated synthesizer equipped with 8 parallel reactors with a volume of 16 mL, a Huber Petite Fleur thermostat for heating/cooling, a Huber Ministat 125 for reflux and a Vacuubrand PC3000 vacuum pump. Stock solutions of all components were prepared and bubbled with argon for at least 50 minutes before being introduced into the robot system and then kept under an argon atmosphere. The hood of the automated synthesizer was continuously flushed with nitrogen and the reactors were flushed with argon to ensure an inert atmosphere. Before starting the polymerizations, the reactors were degassed through ten vacuum–argon cycles. Stock solutions were transferred to the reactors using the liquid handling robot of the automated synthesizer leading to a polymerization mixture with the desired ratio of reagents and a total volume of 4 mL. Before the reactions, 50 µL samples were taken and

directly injected into 1.5 mL sample vials. More detailed automated parallel synthesis protocol has been described on ref.[229, 230]. After 80 min of polymerization, the reaction vessels were cooled to room temperature and 2 mL of the polymerization mixture was transferred to a sample vial for isolation of the CTA functionalized polymer, propylamine (25 eq relative to CTA) stock solution in DMF was then added to the vessels followed by 60 min of incubation for the aminolysis and end group transformation under argon atmosphere. The polymerization mixtures of PNIPAM, PDMA and PMEA (before and after end-group removal) were first precipitated by adding hexane/ether 50/50 vol/vol. The precipitates were then dissolved again in DCM and precipitated in hexane/ether 50/50 vol/vol for two more times. The polymerization mixtures of PHEA and PmDEGA (before and after end-group removal) were first dried under reduced pressure to remove the volatile solvent. The polymers were subsequently purified with PD10 column (preparative SEC) after addition of water. All polymers were dried at 50 ^{o}C under vacuum overnight before analysis. PBA samples were purified by casting in a petri dish followed by evaporating of the volatile monomer and solvent in a vacuum oven at 50 ^{o}C for 24 hours.

^{1}H NMR spectra were recorded on a Bruker 300 MHz FT-NMR spectrometer in deuterated solvents. Chemical shifts (δ) are given in ppm relative to TMS.

Size-exclusion chromatography (SEC) was performed on a Agilent 1260-series HPLC system equipped with a 1260 online degasser, a 1260 ISO-pump, a 1260 automatic liquid sampler, a thermostatted column compartment, a 1260 diode array detector (DAD) and a 1260 refractive index detector (RID). Analyses were performed on a PSS Gram30 column in series with a PSS Gram1000 column at 50 ^{o}C. DMAc containing 50 mM of LiCl was used as eluent at a flow rate of 0.6 ml/min. The SEC traces were analysed using the Agilent Chemstation software with the GPC add on. Molar mass and PDI values were calculated against PMMA standards.

UV-Vis spectra were collected on a Cary 100 Bio UV-Visible spectrophotometer. The polymers were dissolved in chloroform at a concentration of 10 mg/ml in quartz cuvettes. The temperature was kept at 25 ^{o}C during the measurement.

Matrix assisted laser desorption/ionization time of flight mass spectrometry (MALDI-TOF MS) was performed on an Applied Biosystems Voyager De STR MALDI-TOF mass spectrometer equipped with 2 m linear and 3 m reflector flight tubes, and a 355 nm Blue Lion Biotech Marathon solid state laser (3.5 ns pulse). All mass spectra were obtained with an accelerating potential of 20 kV in positive ion mode and in reflectron mode. The matrix used for all experiments was dithranol. Samples were prepared by mixing the solution of polymer (2.5 µL, 10 mg/mL in acetone), the matrix (20 µL, 10 mg/mL in acetone), and sodium trifluoroacetate (2.5µL, 1 mg/mL in acetone). Analyte solutions were prepared by mixing 10 µL of the matrix, 10 µL of the polymer and 1 µL of the salt solution. Subsequently, 0.5 µL of this mixture was spotted on the sample plate, and the spots were dried in air at room temperature. A poly(ethylene oxide) standard

(Mn= 2000 g/mol) was used for calibration. All data were processed using the Data Explorer 4.0.0.0 (Applied Biosystems) software package.

2.2 Thermoresponsive behavior of poly(2-oxazoline) and Poly(di(ethylene glycol) methyl ether methacrylate investigated by turbidimetry in water

2.2.1 Introduction

Thermoresponsive polymers are polymers that undergo a reversible phase transition from a molecularly dissolved state to an aggregated state in response to temperature changes.[1, 8, 13, 17, 21] When the phase separation occurs at decreased temperatures, this is referred to as upper critical solution temperature (UCST) behavior while the reversed phase behavior is known as lower critical solution temperature (LCST) behavior. These polymers have been widely studied for the last decades and found various applications as 'smart' materials.

For the application of thermoresponsive polymers in a particular condition, the phase transition temperature, or cloud point temperature (T_{CP}), is one of the most important parameters of a thermoresponsive polymer in solution. The T_{CP}s are highly tunable by chemical strategies like copolymerization[87, 231-233] and end group modification,[234] or physical strategies, like mixture[235] and ionic strength.[91, 92] The phase transition temperature can be determined by various techniques, such as turbidimetry,[87] ^{1}H NMR spectroscopy[40] or dynamic light scattering (DLS)[236, 237] leading to T_{CP}s using slightly definitions depending on the method used. For instance, with turbidimetry, T_{CP} is referred to as the transition from a homogeneous solution into a heterogeneous milky phase with a concentrated polymer phase and a diluted polymer phase. In contrast, DLS allows more sensitive determination of the onset of the phase transition by the appearance of large aggregates even when they do not yet course cloudy of the solution.

Turbidimetry has been used by various groups to determine the T_{CP}s of thermoresponsive polymer as it is the most straightforward and fastest method. However, the T_{CP} value obtained varies depending on the parameters used making it difficult to compare data reported by different groups, which on the one hand, make it difficult to compare the thermoresponsive behavior of polymers reported by different groups while, on the other hand, it can lead to non-accurate results. In this section, the influence of the turbidimetry measurement parameters on T_{CP} was surveyed using two different polymers serves as example. The influence of several parameters including polymer concentration, temperature ramp, wavelength of incident light, stirring, cuvette type and temperature sensor were investigated. In addition, we have shown that more information regarding the thermoresponsive behavior could be determined by varying the parameters during turbidimetry.

2.2.2 Results and discussions

Turbidimetry is an easy and straightforward technique to evaluate the thermoresponsive behavior of polymers and has been used by many researchers. The most important data obtained by turbidimetry are the transmittance or absorbance versus temperature plot and the cloud point temperature (T_{CP}) of the polymer often defined as the temperature where transmittance passes through 50 %. However, serious deviations could be expected when plotting absorbance versus temperature because the results are strongly depended on the sensitivity of the optical device used, in particular, when the absorption exceeds 1.5. This drawback of plotting absorbance data can be easily overcome by converting to transmittance (%T=100*10^(-Abs.)). For example, absorbance value higher than 1.5 only give a small variation in the converted transmittance in 3.2 to 0 %. Hence, all the discussions in this work are discussed based on the transmittance versus temperature plots.

Two different types of polymers, namely poly(di(ethylene glycol) methyl ether methacrylate (PDEGMA) and Aquazol 50 (Poly(2-ethyl-2-oxazoline, shorted as PEtOx, with Mw=50 kDa and Đ=3-4), were chose as representative examples for the thermoresponsive behavior investigation. The utilized PEtOx is an ill-defined thermoresponsive polymer with a molecular weight dependent LCST, while the LCST of the defined PDEGMA is barely influenced by its molecular weight. Besides, the transition temperature of the two polymers varies a lot, i.e. the T_{CP} of PDEGMA is around room temperature, while T_{CP} of PEtOx is around 65 ^{o}C.

Influence of the wavelength of incident light

For thermoresponsive polymers undergoing phase separation, the homogeneous clear solution phase separates into a concentrated polymer phase and which is dispersed in the diluted polymer phase. The phase transition is usually accompanied by a transition from a clear solution to a cloudy solution due to the large difference in refractive index between the two phases, which can be followed by measuring the light transmittance of the solution at different temperatures. A low transmittance (usually 0%) is obtained for polymer solutions in the phase separated state due to the scattering of the incident light by the polymer globules while the one-phase system below T_{CP} scatter negligible light leading to almost 100% transmittance. As such, the phase separation is accompanied by a drop in transmittance from 100% to 0%. According to the Rayleigh approximation, i.e. $I \alpha d^6$ and $I \alpha 1/\lambda^4$, where I = intensity of light scattered, d = particle diameter and λ = laser wavelength, the scattering of light is very sensitive to relatively large particles. Hence, variation of the λ of the incident light might provide information on the particle. As shown in Figure 2-7a, the transition of turbidimetry plots for PEtOx slightly shift to higher temperature with increasing incident light wavelength indicating the formation of smaller particles at the initial stage of phase separation followed by the formation of large particles with increasing temperature. This evolution of particle size with temperature might be related to the broad molar mass distribution of this PEtOx (Aquazol 50) sample leading to different

transition temperature for different fractions of the sample. In contrast, the phase transition of PDEGMA as detected by turbidimetry exhibits less or no dependence on the utilized wavelength indicating the direct formation of large particles (Figure 2-7b). Note that the incomplete drop of transmittance is due to precipitation of the high concentrated polymer phase droplets indicating the importance of visual inspection of the vials when unexpected turbidimetry curves are obtained.

Influence of heating ramp and polymer concentration

The turbidimetry plots for polymer solutions at different concentrations during heating at 0.1, 0.5, 1 and 5 K/min are plotted in Figure 2-8. The phase transition for both of the two polymers shift to higher temperature with faster heating, which is due to the relatively slower response of precipitation of polymer chains compared to the heating rate and/or a lag time in between heating of the sample holder and the solution. When looking into details of the two plots, different dependence on the heating ramp could be observed, i.e. PDEGMA is more sensitive to the heating ramp than PEtOx indicating a slower collapse, i.e. dehydration, of the PDEGMA chains. As such, variation of heating rates provides further information on the phase transition kinetics. Note that the transmittance goes up for PDEGMA heated at 0.1 K/min, which can be ascribed to the macroscopic precipitation of the polymer sample in the long heating process revealing one of the drawback of too slow heating/cooling for the sample solution.

The concentration dependence of the turbidimetry plots are plotted in Figure 2-9. In general the two polymers exhibit similar concentration dependence, i.e. the phase transition shifts to lower temperatures with higher concentrations, which is also widely reported in the literature.[1, 65, 238] This observation is related to the technique that only allows detection of relatively large phase separated droplets of which less are present at the initial stages of phase separation at lower concentrations. Besides, with samples at high concentration, sharp transition from 100% transmittance to 0% transmittance are obtained, while with diluted polymer solutions, the phase transition occurs over a broader temperature window, in particular for PEtOx indicating a more gradual collapse and coagulation of the polymer chains instead of a simultaneously process. The slower transition for PEtOx can be ascribed to the high dispersity of the polymer resulting in non-identical phase transition temperatures. The fast dropping of transmittance to 0 % at high concentration is due to the high mass of polymer present in the solution quickly leading to large high polymer concentration droplets that produce high turbidity.

The T_{CP} represents the phase transition temperature of the thermoresponsive polymer. However, different researchers define the position of T_{CP} on the transmittance versus temperature curve in different ways. Even with similar data collected by UV–Vis spectrometer with the same experimental settings, 4 different types of definition for T_{CP} are used by different researchers as listed by Chytrý and Ulbrich.[239] The lack of unity in the definitions makes it difficult to compare the data reported by different researchers.[5] Besides, T_{CP}s obtained

by some of the definitions are strongly depended on the sensitivity of optical device used and the presence of insoluble particles in the solution.[239]

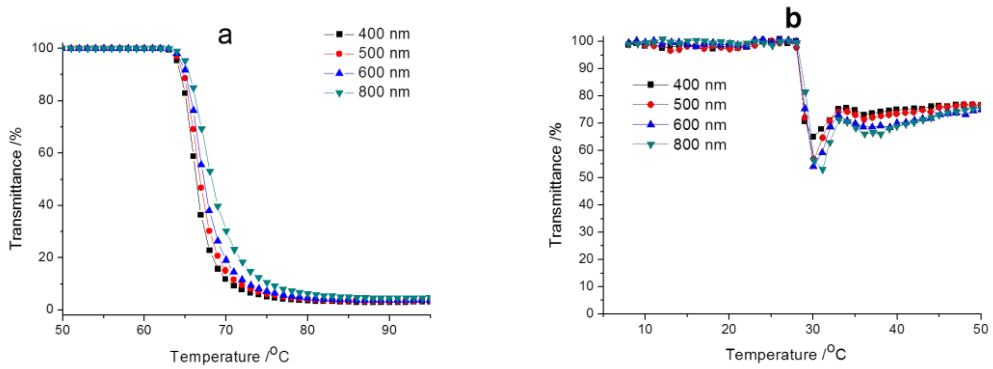

Figure 2-7 Transmittance verses temperature with different incident wavelengths of a) PEtOx (Aquazol 50) and b) PDEGMA in water at 1 mg/ml, at a temperature ramp of 0.1K/min, without stirring.

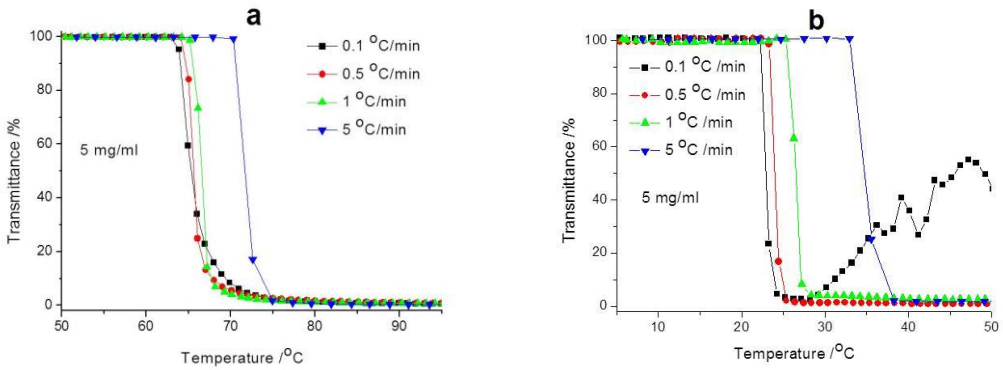

Figure 2-8 Transmittance versus temperature plots recorded with different temperature ramps of (a) PEtOx (Aquazol 50) in water at 5 mg/ml, with stirring and incident wavelength of 600 nm, and (b) PDEGMA in water at 5 mg/ml, with stirring and incident wavelength of 600 nm.

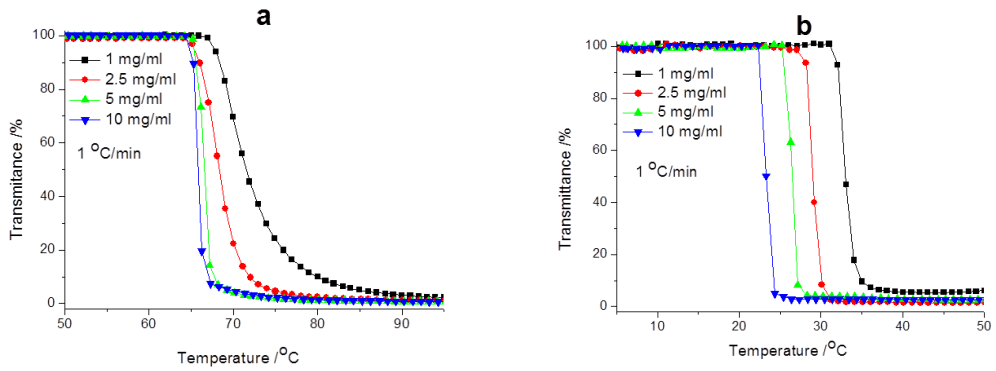

Figure 2-9 Transmittance verses temperature in different concentrations of (a) PEtOx (Aquazol 50) in water at temperature ramp at 1 °C/min, with stirring and incident wavelength of 600 nm and (b) PDEGMA in water at temperature ramp at 1 °C/min, with stirring and incident wavelength of 600 nm.

Two types of plots could be used to define the T_{CP}, i.e. absorbance versus temperature and transmittance versus temperature.[232] However, as explained above transmittance versus temperature is more accurate and will be further discussed here.

Based on the transmittance versus temperature plot, the T_{CP} is usually defined as the temperature of a certain stage of the drop in transmittance. The onset of decrease,[240] 10, 50 or 80% of transmittance have been reported as definition to determine T_{CP}. For thermoresponsive polymers with sharp transition from clear to cloudy, e.g. PDEGMA, these definitions give, however, only minor deviations in T_{CP}. However, for thermoresponsive polymers with broader UCST transitions or with broader molecular weight dependence LCST phase transitions, e.g. PEtOx (Aquazol 50), the transmittance decreases more gradually from 100% to 0% (also depending on concentration as shown above) leading to a large deviation in T_{CP} depending on the used definition (Table 2-2). An ideal definition of the cloud point should, on the one hand show no dependence on the sensitivity of the device or experience of experimentalist, while on the other hand it should be sensitive to the parameters used, e.g. concentration and heating rate. Therefore, it is proposed to use 50 % of transmittance as definition for T_{CP}.

Table 2-2 T_{CP}s of PEtOx (Aquazol 50) and PDEGMA at different concentrations based on different definitions at a heating rate of 5 K/min

Stage of transmittance	Concentration of PEtOx (Aquazol 50)				Concentration of PDEGMA			
	1 mg/ml	2.5 mg/ml	5 mg/ml	10 mg/ml	1 mg/ml	2.5 mg/ml	5 mg/ml	10 mg/ml
Onset of decrease	65.1	64.1	64.2	64.3	40.0	35.1	32.9	27.8
80 %	69.2	66.7	65.9	65.5	44.1	39.2	34.3	29.3
50 %	71.5	68.3	66.6	65.9	43.9	39.1	34.7	31.4
10 %	80.0	72.0	67.8	67.1	46.0	40.6	37.4	33.0

Influence of stirring

The influence of stirring was evaluated with PEtOx (Aquazol 50) at various concentrations and heating ramps. In order to compare the data obtained with and without stirring, T_{CP} upon heating are defined as the temperature at which the transmittance passes through 50%. As shown in Figure 2-10, a clear difference of T_{CP}s detected with and without stirring is found, which is most pronounced with heating ramps of 0.1 and 5 K/min. The T_{CP}s appears at relatively higher temperature with too fast heating (5 ^{o}C/min) due to not inefficient thermal conductivity, i.e. without stirring it takes longer to heat the solution leading to a longer lag time and higher over estimation of T_{CP}. In contrast, turbidimetry plots of T_{CP}s for polymer solution measured at 0.1 ^{o}C/min exhibit complex behavior due to the slow temperature change. Visual inspection of the cuvettes revealed that large polymer aggregates are formed during the measurement and these stick on

the wall of cuvettes due to the long time incubation of the precipitated polymer samples, both with and without stirring leading to inaccurate results.

Influence of cuvette and temperature sensor

The reliability of the temperature control is essential for the accuracy of the turbidimetry measurements. Apart from the heating/cooling ramp, several other parameters can also influence the temperature monitoring influencing the accuracy of T_{CP} determination by turbidimetry measurement performed in a UV-Vis spectrometer. For instance, the monitoring of temperature can be done with a sensor inside or outside of the cuvette, corresponding to the probe or block mode in the UV-Vis spectrometer. Furthermore, the type of cuvette influences heat transport from the block to the solution.

The T_{CP}s for PEtOx (Aquazol 50) and PDEGMA determined in different cuvettes with probe and block temperature sensor are plotted in Figure 2-12. As expected, the probe mode is most accurate and least dependent on the type of cuvette since it monitors directly the temperature of polymer solution. The T_{CP}s determined in quartz cuvette 1 (Figure 2-11), however, deviate a lot from others, which could be ascribed to the inefficient stirring of the polymer solution in the long and narrow chamber as well as the large amount of insulating quartz. For T_{CP}s determined by block mode, deviations are always presence due to the temperature difference inside and outside of the cuvettes. For different temperature ramps, a mediate heating/cooling rate at 0.5 ^{o}C/min gives the best results as indicated by the lowest deviation from the probe mode. It is logical that slow changing of temperature gives better results since it allows more efficient thermal transfer through the cuvette. The temperature ramp at 0.1 ^{o}C/min, however, exhibits higher deviation than that with 0.5 ^{o}C/min and a reversed hysteresis. The abnormal phenomenon can be ascribed to the formation of large globules and sticking of polymer globules on the wall of cuvette during the long measurement time as also discussed above. This assumption was confirmed by visual inspection of the cuvette during the measurement. The T_{CP}s obtained at 1 ^{o}C/min exhibit the highest deviation due to the relatively fast changing of temperature. The deviation of the T_{CP}s for different polymer samples also varies depending on the temperature. For PDEGMA, the T_{CP} values obtained by block mode are higher or lower than that obtained by probe mode depending on the temperature program, which is mainly due to the lag of the temperature inside the cuvettes. In contrast, T_{CP}s for PEtOx (Aquazol 50) detected by block mode are always higher than the results from probe mode. Apart from the lag of temperature inside the cuvette, cooling of the cuvette and cuvette holder of instrument by atmosphere may also lead to difference of the temperature inside and outside of the cuvette.

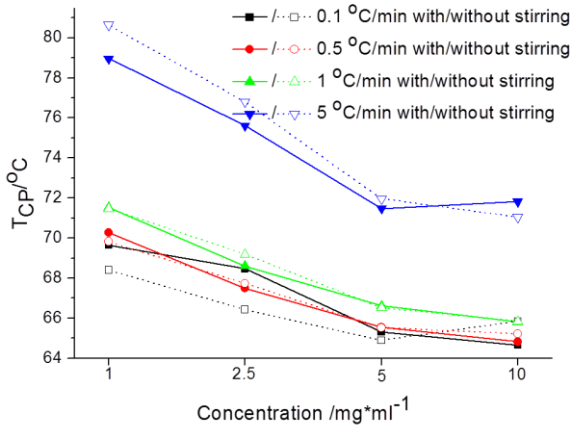

Figure 2-10 Dependence of T_{CP} of PEtOx (Aquazol 50) on the concentration determined with and without stirring

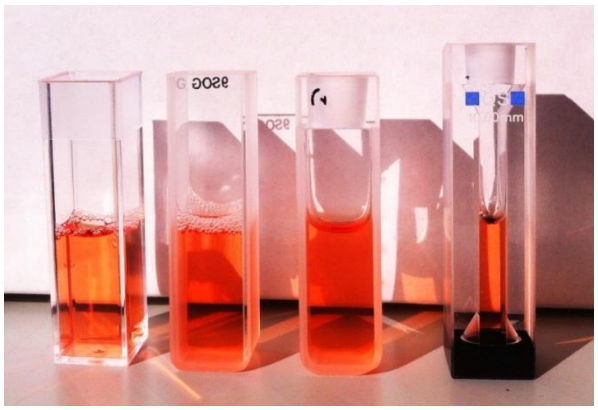

Figure 2-11 Different cuvettes used in the determination of turbidimetry on a UV-Vis spectrometer, dye solution was filled in the cuvette allowing a clear visual of the shape, from left to right: plastic, glass, quartz 2 and quartz 1cuvette

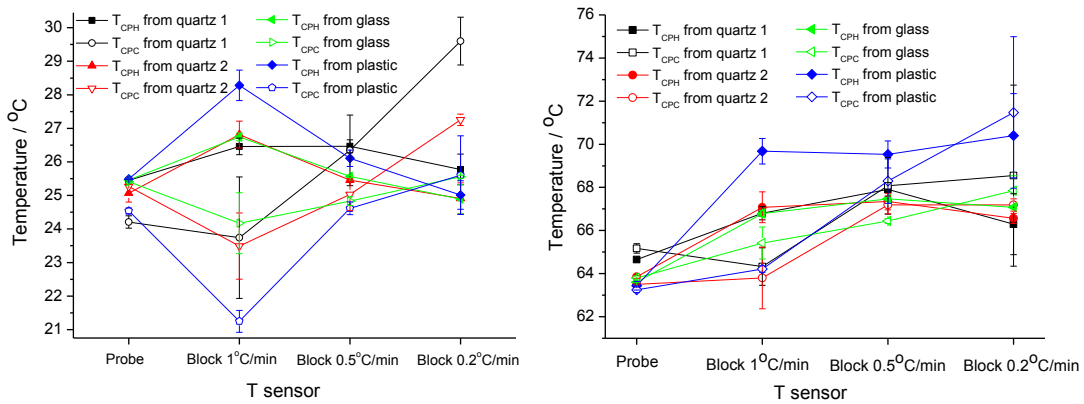

Figure 2-12 Dependence of cloud point temperature (CPH) and clearance point temperature (CPC) for PEtOx (Aquazol 50) and PDEGMA on the temperature sensor (probe and block) and ramp (1, 0.5 and 0.2 °C/min) with stirring.

However, the heating ramp of 1 ^{o}C/min has been employed for most of the publications. Hence, it would be valuable to relate the value obtained in block mode to the values obtained at probe mode as calibration. An easy and accurate way for the calibration is to relate the actual temperature of the solution (temperature detected by probe sensor) to the block temperature. Therefore, the temperatures detected by block and probe sensors in pure water and different cuvettes was recorded with a 1K/min temperature program controlled by the block T-sensor. Figure 2-13 shows the plot of probe temperature versus block temperature during heating and cooling in the plastic disposable cuvettes. The probe temperature in the cuvette firstly exhibited an initial slow heating stage, after which a kind of equilibration was reached as indicated by the linear dependence of probe temperature on block temperature, whereby the probe temperature is lower than the block temperature. Hence, a linear fit of block temperature versus probe temperature was performed as calibration for the block temperature. The fitted intercept and slope values for different cuvettes during heating or cooling are listed in Table 2-3. The adjusted determination coefficients (R square higher than 0.9999) obtained by linear fits indicate the strong and predictable relationship between the temperatures detected by the two temperature sensors.

To assess the proposed calibration and the parameters obtained, the T_{CPH} and T_{CPC} for PEtOx (Aquazol 50) and PDEGMA obtained by block mode with a ramp of 1 ^{o}C/min are recalibrated (Table 2-4). The recalibrated T_{CP}s are highly comparable with the T_{CP}s obtained by probe mode with an error lower than 0.5 ^{o}C for most of the cases. Exceptions are found for quartz cuvette 1 with errors higher than 1 ^{o}C most likely due to inefficient stirring.

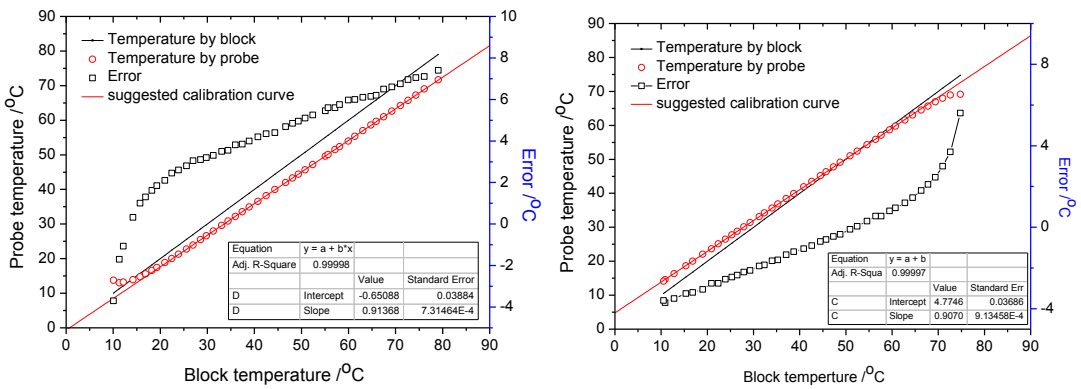

Figure 2-13 Suggested calibration curve for plastic cuvette during a) heating and b) cooling. Red circle represent the probe temperature versus block temperature; the error represented as open squares was calculated by probe temperature - block temperature.

Table 2-3 Calibration parameters for different cuvettes via heating and cooling

Cuvette/temperature program [a]	Intercept	Slope	R square
Q1/H	-0.97	0.96	0.99996
Q1/C	2.75	0.95	0.99997
Q2/H	-1.12	0.98	0.99996
Q2/C	2.49	0.95	0.99999
G/H	-0.07	0.95	0.99998
G/C	3.02	0.94	0.99999
P/H	-0.65	0.91	0.99998
P/C	4.77	0.91	0.99997

[a] Q, G and P represent quartz, glass and plastic cuvette, respectively; while H and C represent heating and cooling, respectively.

Table 2-4 Calibrated phase transition temperature and error for different cuvettes

Cuvette/temperature program[a]	CP_H or CP_C for PDEGMA /°C				CP_H or CP_C for $PEtOx_{20}$-$PnPrOx_{80}$ /°C			
	Block	Probe	Calibrated	Error[b]	Block	Probe	Calibrated	Error[b]
Q1/H	26.46	25.45	24.33	1.12	66.80	64.65	62.90	1.75
Q1/C	23.74	24.21	25.40	1.19	64.33	65.17	64.13	1.04
Q2/H	26.81	25.07	25.02	0.05	67.08	63.85	64.29	0.44
Q2/C	23.49	25.27	24.87	0.40	63.80	63.50	63.28	0.22
G/H	26.75	25.46	25.26	0.20	66.79	63.61	63.18	0.43
G/C	24.17	25.41	25.67	0.26	65.42	63.80	64.33	0.53
P/H	28.28	25.49	25.18	0.31	69.68	63.44	63.01	0.43
P/C	21.25	24.54	24.05	0.49	64.21	63.25	63.01	0.24

[a]Q, G and P represent quartz, glass and plastic cuvette, respectively; while H and C represent heating and cooling, respectively. [b]The error is absolute value of the difference between probe and block temperature.

2.2.3 Summary

The influence of the parameters used for turbidimetry measurements of thermoresponsive polymer solution behavior was investigated using PEtOx (Aquazol 50) and PDEGMA as representative examples. The influence of various parameters, such as concentration, heating rate, wavelength of incident light, stirring, position of temperature probe and type of cuvette on the measurement were found can provide in depth information of the thermoresponsive behavior of polymers in solution on the one hand, but can also strongly influence the results leading to erroneous results on the other hand. Hence, based on the analysis of above mentioned parameters, we suggest a uniform condition for turbidimetry measurements of thermoresponsive polymer solutions to make it easier to compare the results reported by different groups. An ambient polymer concentration at 5 mg/ml and heating/cooling rate at 1 K/min with stirring are believed

to give reliable results. The cuvettes and temperature probe mode could be chosen according to the samples, however, a calibration is need to give the real value of the data if a block probe is used for temperature detection. The definition of T_{CP} at 50 % of transmittance on the transmittance versus temperature plot is highly recommended. Regarding to the scientific report of the turbidimetry results, apart from usually reported concentration, heating/cooling rate and wavelength of incident light, the temperature probe mode as well as the utilized cuvette are also suggested to be included to give more information about the measurement.

2.2.4 Experimental section

All chemicals and solvents were commercially available and used as received unless otherwise stated. Dichloromethane (DCM), toluene, dimethylacetamide (DMA), THF, methanol, $CDCl_3$, hexane are from Sigma Aldrich. DCM was distilled before use. Azobisisobutyronitrile (AIBN, 98%, Aldrich) was recrystallized from MeOH (twice) and stored in the freezer. Aquazol 50 (50 kDa, Đ=3-4) was obtained from Polymer Chemistry Innovations Inc.

Size-exclusion chromatography (SEC) was performed on a Agilent 1260-series HPLC system equipped with a 1260 online degasser, a 1260 ISO-pump, a 1260 automatic liquid sampler, a thermostatted column compartment, a 1260 diode array detector (DAD) and a 1260 refractive index detector (RID). Analyses were performed on a PSS Gram30 column in series with a PSS Gram1000 column at 50 ^{o}C. DMAc containing 50 mM of LiCl was used as eluent at a flow rate of 0.6 ml/min. The SEC traces were analysed using the Agilent Chemstation software with the GPC add on. Molar mass and PDI values were calculated against PMMA standards.

Turbidity measurements were performed on a Cary 300 Bio UV-Visible spectrophotometer. The samples were first cooled to a suitable temperature to fully dissolve the copolymer, after which the sample was placed in the instrument and heated to a certain temperature above the lower critical solution temperature.

Poly(di(ethylene glycol) methyl ether methacrylate (PDEGMA) was prepared by reversible addition-fragmentation chain transfer (RAFT) polymerization. Di(ethylene glycol) methyl ether methacrylate, AIBN and 4-cyano-4-(phenylcarbonothioylthio)pentanoic acid were first dissolved in toluene in a schlenk vial. The concentration of monomer was fixed at 2M. After degassing the solution three times by freeze-vacuum-thaw cycles, the schlenk vial was filled with argon and immersed in a preheated oil bath at 70 ^{o}C while stirring. The polymerization was performed for 6 hours and stopped by immersing the schlenk vial into dry ice/isopropanol bath. The resulting polymer was isolated by precipitation in hexane (three times) followed by drying under reduced pressure at 50 ^{o}C. Size exclusion chromatography was used to evaluate the number average molecular weight (Mn) and dispersity (Đ) of the obtained polymers. Mn=5.0 kDa, Đ=1.21.

Chapter 3 Tuning the upper critical solution temperature behavior of poly(methyl methacrylate) in aqueous ethanol

Parts of this chapter were published on:

Q. Zhang, P. Schattling, P. Theato, R. Hoogenboom, *Polymer Chemistry* **2012**, *3*, 1418; Q. Zhang, P. Schattling, P. Theato, R. Hoogenboom, *European Polymer Journal*, DOI: 10.1016/j.eurpolymj.2014.06.029.

My contribution includes the experiments excluding the synthesis and characterization of P(PFPMA-MMA) copolymers, the interpreting of the results and the writing of the manuscripts.

Abstract: Poly(methyl methacrylate) (PMMA) copolymers exhibiting a tunable UCST behavior in ethanol/water solvent mixtures were prepared by post-polymerization modification of poly(MMA-pentafluorophenyl methacrylate) (P(MMA-PFPMA)). The phase transition behavior of the obtained copolymers in aqueous ethanol was evaluated in detail revealing that the UCST transition is highly influenced by the incorporated comonomers. For the copolymers with only 6 mol% of comonomers, the solubility in aqueous ethanol of the copolymer can be strongly increased by the introduction of hydrophilic moieties. When hydrophobic substituents are introduced a decrease in solubility was observed with low content of ethanol and an increase in solubility when adding more ethanol. The UCST behavior of copolymers with both hydrophilic hydroxyethyl and hydrophobic azobenzene substituents also depends on the exact composition. In addition, these azobenzene-containing copolymers are light responsive based on the *cis*-*trans* isomerization of the azobenzene group under UV irradiation. The cloud point temperatures (T_{CP}) of the polymer solutions decreased after UV-irradiation due to the higher dipole moment of the *cis*-isomer of the azobenzene moiety leading to better solubility in ethanol/water solvent mixtures. Furthermore, the UV responsiveness was found to strongly depend on the solvent composition, revealing a higher decrease in cloud point after UV-irradiation in ethanol/water solvent mixture with higher water content.

3.1 Introduction

Thermoresponsive polymers are of great importance in numerous nanotechnological and biomedical applications.[10, 241] The majority of these polymers undergo a reversible phase transition from soluble to insoluble when the environmental temperature is raised above their low critical solution temperature (LCST), driven by dehydration of the polymer chains. However, the reverse behavior would be more beneficial in various applications, for example when the environmental temperature of polymeric nanoparticle carriers would rise above the upper critical solution temperature (UCST) due to a fever, loaded drug could be automatically released due to dissolution of the carrier.

For materials applied in biotechnological applications, biocompatible polymers and low-toxicity solvents are basic requirements. As such, polypeptides,[242-245] poly(*N*-isopropylacrylamide)s,[24, 246-250] poly(oligo(ethylene glycol) methyl ether (meth)acrylate)s (POEG(M)A),[26, 28, 234, 251-254] and poly(2-oxazoline)s [238, 255-257] have been widely reported as biocompatible thermoresponsive LCST polymers in water, which have large potential for application as biomaterials. In addition, non-toxic ethanol/water solvent mixtures exhibit non-ideal mixing behavior leading to UCST behavior of various polymers due to the presence of complex hydration shells around the ethanol molecules.[47-49] For instance, Hoogenboom et al. found that poly(2-phenyl-2-oxazoline) (PPhOx) exhibited an UCST in ethanol/water.[104] Moreover, the solubility of PPhOx and the self-assembly properties of PPhOx copolymers could be significantly altered by changing the composition of the solvent mixture.[258] Based on this binary solvent, UCST behavior of poly(*N*-isopropylacrylamide),[63] POEGMA,[89] poly(acetoacetoxyethyl methacrylate-co-hydroxyethyl methacrylate)[62] and poly(2-methacryloxyethyl phosphorylcholine)[127] has also been reported. It has been demonstrated that PMMA also exhibits a UCST transition in pure ethanol and ethanol/water mixtures,[52, 72, 104, 259] which is tunable by variation of the solvent composition. To further increase the utility of this thermoresponsive polymer system, reactive functional groups can be introduced into the side chains, which allows tuning of the polymer solubility as well as the conjugation of other functional moieties e.g. peptides, drugs and solvatochromic dye molecules onto the polymer backbone.

Besides thermoresponsiveness, polymers have also been designed to respond to other stimuli, such as pH,[260] ions,[40, 261] chemical changes[262, 263] or light,[264, 265] and in recent years the attention is shifting towards dual- or multi-responsive material.[6, 8, 16, 184, 212] Of those dual stimuli-responsive polymers, the combination of thermo and light responsiveness is very popular as these are two easily accessible triggers that can be cycled to induce reversible phase transitions.[8] Moreover, both temperature and light are triggers that commonly occur in natural systems, e.g. during day and night cycles. An early example of a temperature (LCST) and light responsive polymer was reported by Irie et al[144] based on azobenzene containing poly(*N*-isopropylacrylamide) (PNIPAM) copolymers. Such azobenzene groups are known to undergo a reversible isomerization from *trans*- to *cis*-configuration upon UV irradiation.[266, 267] In the excited *cis*-configuration, the

higher dipole moment leads to an increase of polarity of the polymer chain, which has been used to increase the cloud point termperature (T_{CP}) of LCST polymers.[268] Many other examples of dual thermo- and light responsive polymers have been reported after Irie's work.[6, 8, 144, 269-272] For example, Theato et al. have incorporated azobenzene groups into either the polymer side chain or as end group through post-polymerization modification reactions.[234, 264] Higher T_{CP}s values were measured after UV-irradiation of the aqueous polymer solutions depending on the polymer molar mass and the azobenzene content. Lodge and Watanabe have investigated the UCST behavior of PNIPAM copolymers with randomly distributed azobenzene groups in ionic liquids.[273] The T_{CP} could be decreased by 43 ^{o}C upon UV-irradiation as measured by turbidimetry. However, to the best of our knowledge, this is the only report of a UV-responsive polymer with UCST behavior and there are no light responsive polymers reported with UCST behavior in aqueous solution.

Various examples of reactive polymer side chains for post-polymerization modification are presented in the literature, including aldehyde,[274, 275] azide or acetylene/alkene,[276, 277] and activated ester.[278-280] However, few examples concern the application of a reactive comonomer for tuning the thermoresposive behavior of the polymer.[275, 281] Murray et al. have prepared poly(oligo(ethylene glycol) methyl ether methacrylate)-*co*-(methacrylate p-(methacryloxyethoxy) benzaldehyde) containing reactive aldehyde functions, which were reacted with alkoxyamines and hydrazides to tune the LCST behavior. Though this work represents a good example on tuning LCST behavior, most alkoxyamines or hydrazides need to be synthesized beforehand by a two-step reaction. According to previous work of Theato et al., the incorporation of pentafluorophenyl methacrylate (PFPMA) and pentafluorophenyl 4-vinylbenzoate within polymer chains results in high reactivity toward amines.[278-280] Due to the commercially availability of a wide range of amines, PFPMA is an excellent comonomer for PMMA to introduce a reactive functional side chain.

In this chapter, PMMA-PFPMA containing activated ester comonomers was modified by nucleophilic substitution to incorporate various side chain moieties onto the polymer backbone with different amines, including hydrophilic (ethanol amine and ethylenediamine) as well as hydrophobic (isopropylamine, cyclohexylamine and benzylamine) groups. A systematical study on the cloud point temperature upon cooling (T_{CPC}) and clearance point temperature upon heating (T_{CPH}) of the PMMA copolymers in aqueous ethanol was performed revealing the dependence of the UCST transition on the concentration of ethanol, temperature and structure of introduced amines. Moreover, PMMA copolymers prepared by nucleophilic substitution of PMMA-PFPMA with amino-functionalized azobenzenes containing amines were performed. The UCST behavior of PMMA with different side-chain content of photochromic azobenzene groups will be discussed as well as their dual thermo and light responsive behavior in ethanol/water solvent mixtures.

3.2 Tuning the upper critical solution temperature behavior of poly(methyl methacrylate) in aqueous ethanol by comonomers

3.2.1 Synthesis and post-polymerization modification of PMMA-PFPMA

Poly(methyl methacrylate-*co*-pentafluorophenyl methacrylate) (PMMA-PFPMA, P1, see Table 3-1) was prepared by free radical polymerization initiated by AIBN. The content of reactive ester for the polymer was determined by ^{1}H-NMR and FT-IR spectroscopy to be 6 mol-% (spectra not included). P1 was then used to generate PMMA copolymers with different side chain groups by nucleophilic substitution with five different amines.

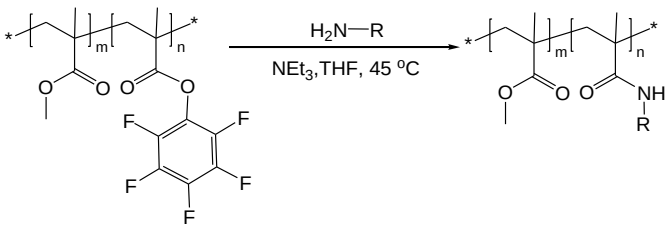

Scheme 3-1 Schematic representation of the nucleophilic substitution of PMMA-PFPMA with amines.

The polymer modification reactions are performed in THF, with triethylamine as catalyst (see Scheme 3-1). Five amines with different R groups were selected for the substitution, ranging from hydrophilic (ethanol amine and ethylenediamine) to hydrophobic (isopropylamine, cyclohexylamine and benzylamine). Ethanol amine and ethylenediamine with hydroxyl and amino groups were employed to enhance the hydrophilicity of PMMA in the aqueous solvent mixture. Two amines with different aliphatic hydrophobic R groups, namely isopropylamine and cyclohexylamine, were also selected to tune the solubility of PMMA in solvent mixtures according to the structure of the R group. Finally, benzylamine was chose to investigate the effect of the hydrophobic aromatic moiety on the UCST behavior of PMMA in ethanol/water solvent mixtures. The obtained copolymers (Table 3-1, P2-P6) were characterized by SEC, FT-IR and ^{19}F NMR spectroscopy (see Table 3-1 and Figure 3-1, FT-IR data not shown) indicated no remarkable difference between polymers before and after substitution). The SEC results revealed that P1 has a polydispersity index (PDI) of 1.98 as expected form free radical polymerization. The PDI decreased to around 1.5 after the activated ester groups were substituted by the amines; most likely due to fractionation during repetitive precipitation. The ^{19}F NMR spectra demonstrated that the peaks originating from PFPMA completely disappeared indicating full conversion of PFPMA to methacrylamide (Figure 3-1).

3.2.2 Turbidity study of the PMMA copolymers in aqueous ethanol

The T_{CPC} of the polymers represents the temperature where the polymer solution undergoes a transition from a clear one-phase regime to an opaque demixed two-phase regime upon cooling. For PMMA in

ethanol/water mixtures, it was demonstrated that the polymer chains are hydrated above the UCST transition due to hydrogen bond formation between the polymer carbonyl groups and water protons leading to the dissolution of PMMA, as shown in Figure 3-2. [52, 65]

Table 3-1 Structure, M_n and polydispersity indices of PMMA-PFPMA and the corresponding substituted PMMA copolymers.

Copolymer	Copolymer structure	Mn [kDa] *	PDI *
P1	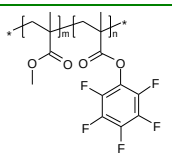	22.1	1.98
P2	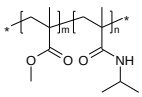	35.0	1.51
P3	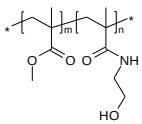	33.5	1.62
P4	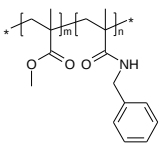	36.1	1.45
P5	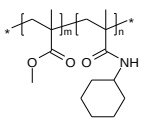	34.7	1.53
P6	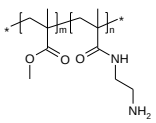	33.4	1.60

* Determined by SEC using DMA with LiCl as eluent and PMMA standards.

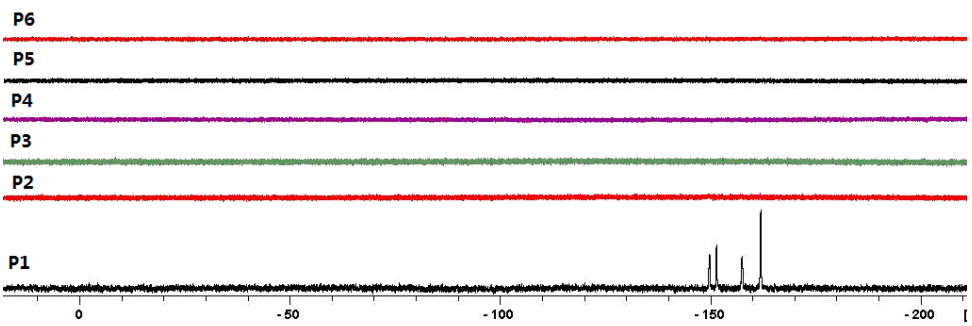

Figure 3-1 ^{19}F NMR spectra of PMMA-PFPMA, P1 and the corresponding substituted PMMA copolymers, P2-P6

Typical transmittance versus temperature plots resulting from turbidimetry are shown in Figure 3-2 for P2 during the cooling run from 75 ^{o}C to 0 ^{o}C revealing a sharp transition from high transmittance (about 100 %) to low transmittance (about 0 %) indicating demixing of the solution and the aggregation of the copolymer. The increase of transmittance of the sample in pure ethanol at temperatures below 65^{o}C can be ascribed to sticking of the copolymer to the cuvette wall leading to higher transmittance as confirmed by visual inspection. The figure also reveals a shift of the polymer phase transition to lower temperatures upon addition of water to ethanol (up to 15 vol-%), followed by an increase in transition temperature when further increasing the water content of the solvent mixture. Similar results were also observed for P3-P6. The high dependence of the T_{CPC} on the water content is due to the co-solvency effect for the polymer resulting from hydration of the ester groups resulting in a kind of 'compatibilizing' hydration layer in between the polymer and the solution, as shown in Figure 3-2, bottom right.[72] The polymer P2 revealed the highest solubility in aqueous solvent with 85 vol-% of ethanol since in this solvent mixture mostly single, non-clustered water molecules are present that can effectively hydrate the polymers without breaking the stronger water-water hydrogen bonds.[48] Further increasing the amount of water leads to the formation of water clusters, which decreases the polymer solubility by the necessity of breaking water-water hydrogen bonds for the formation of a hydration shell; while decreasing the content of water also suppresses the formation of a hydration shell leading to reduced polymer solubility. [52, 65]

The UCST behavior of the different copolymers was compared based on the T_{CPC}, upon cooling as well as the T_{CPH} upon heating, at a polymer concentration of 5 mg/ml. The T_{CPC} and T_{CPH} values obtained by turbidimetry are plotted as a function of ethanol content in the solvent mixtures in Figure 3-3 for P2-P6 as well as PMMA (Mn=27.4 kDa, PDI=1.43) as reference.

The influence of the ethanol content of the solvent mixtures on the phase transitions was evaluated for PMMA and all the PMMA copolymers. The T_{CPC} and T_{CPH} of PMMA-PFPMA were also measured in solvent mixtures with different ethanol content. However, these results were found to be irreproducible most likely due to partial hydrolysis of the pentafluorophenyl esters during the measurements as indicated by the lower dissolution temperatures of the second heating and cooling cycles.

As can be seen from Figure 3-3, the phase diagrams of P2 and P5 exhibit similar trends as PMMA, i.e. the T_{CPC} and T_{CPH} values of the polymers in ethanol decreases upon adding a small amount of water until reaching maximum solubility around 85 vol-% ethanol content. Further additional of water results in an increase of T_{CPC} and T_{CPH}. Moreover, the hysteresis between cooling and heating reversed by variation of the ethanol content. For the good solvent mixture, i.e. for the lower transition temperatures dissolution upon heating occurs at a higher temperature than precipitation upon cooling indicating that the hydrated polymer chains are energetically more favourable than the two-phase system with polymer aggregates in the ethanol/water solvent. The lower T_{CPC} compared with T_{CPH} is because, in this regime, the water molecules in

ethanol are present as indicated, non-clustered molecules[48] resulting in favourable hydrogen bonding of water to the polymer ester groups since these hydrogen bonds of water are stronger than the hydrogen bonds of water with ethanol molecules in solution. For P5, the ester groups are partially shielded by the steric bulk of the cyclohexyl groups resulting in weaker hydrogen bonding with water than for P2 leading to significantly higher T_{CPC} compared with P2 while T_{CPH} is only slightly increased. In contrast, in pure ethanol and ethanol containing a small amount of water, the polymer phase transition is mainly driven by the change in solvent polarity upon heating and the hydration of the polymer is less important. As such, the entropy loss upon solvation of the polymer chains during heating is not overcompensated by strong specific hydration of the ester groups resulting in a slightly lower T_{CPH} compared with T_{CPC}. In solvent mixtures containing less than 70 vol-% ethanol, the T_{CPH} is also lower than T_{CPC}, which is due to the formation of water clusters in solution. As such, the hydrogen bonds between the water molecules are stronger than those between water molecules and the polymeric ester groups resulting in higher T_{CPC} compared to T_{CPH}. Besides P2 and P5, the solubility of P4 also has a similar dependence on ethanol contents as PMMA, but with much higher T_{CPC} and T_{CPH} indicating that the benzyl group has a stronger negative effect on the solubility compared to the cyclohexyl and isopropyl groups, proposedly due to the larger steric bulk of the phenyl rings that hinders solvation of the polymeric ester and amide moieties. In fact, P4 does not dissolve in pure ethanol or 95 vol-% ethanol upon heating to 75 ^{o}C. Furthermore, almost negligible hysteresis is observed for P4 between heating and cooling, which might also be due to less effective hydration, thereby also suppressing hydration effects that are responsible for the hysteresis. On the other hand, the introduction of hydrophilic amines provided much better solubility to PMMA as indicated by the phase diagrams of P3 and P6 in Figure 3-3. In fact, P3 and P6 do not phase separate even at 0 ^{o}C with 70 to 90 vol-% ethanol and 70 to 95 vol-% ethanol, respectively. Despite the highly increased solubility, the T_{CPC} and T_{CPH} revealed similar trends as PMMA in the regions that the copolymer shows thermoresponsive properties; except the T_{CPH} of P6 in pure ethanol which is underestimated due to sticking of the polymer to the quartz cuvette wall as confirmed by visual inspection.

From the previous discussion, it becomes strikingly clear that the phase transition temperatures of PMMA are strongly affected by incorporating and variation of just 6 % of comonomers. In addition, it was found that the hysteresis also varies upon changing the substituted group. For instance, the hysteresis between T_{CPC} and T_{CPH} is 13.3 ^{o}C for P2 in 85 ethanol vol-% solvent while it is only 2.3 ^{o}C for P4.

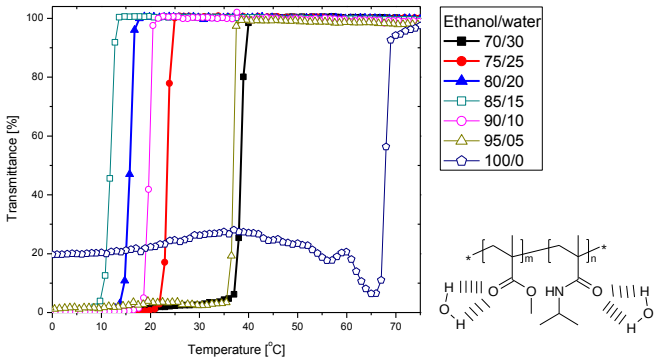

Figure 3-2 Transmittance versus temperature plots for 5 mg/ml P2 solutions in different ethanol/water solvent mixtures obtained during the second cooling run, showing precipitation of the polymer from solution. A schematic representation of the proposed structure of the hydrated P2 is also shown at the bottom right.

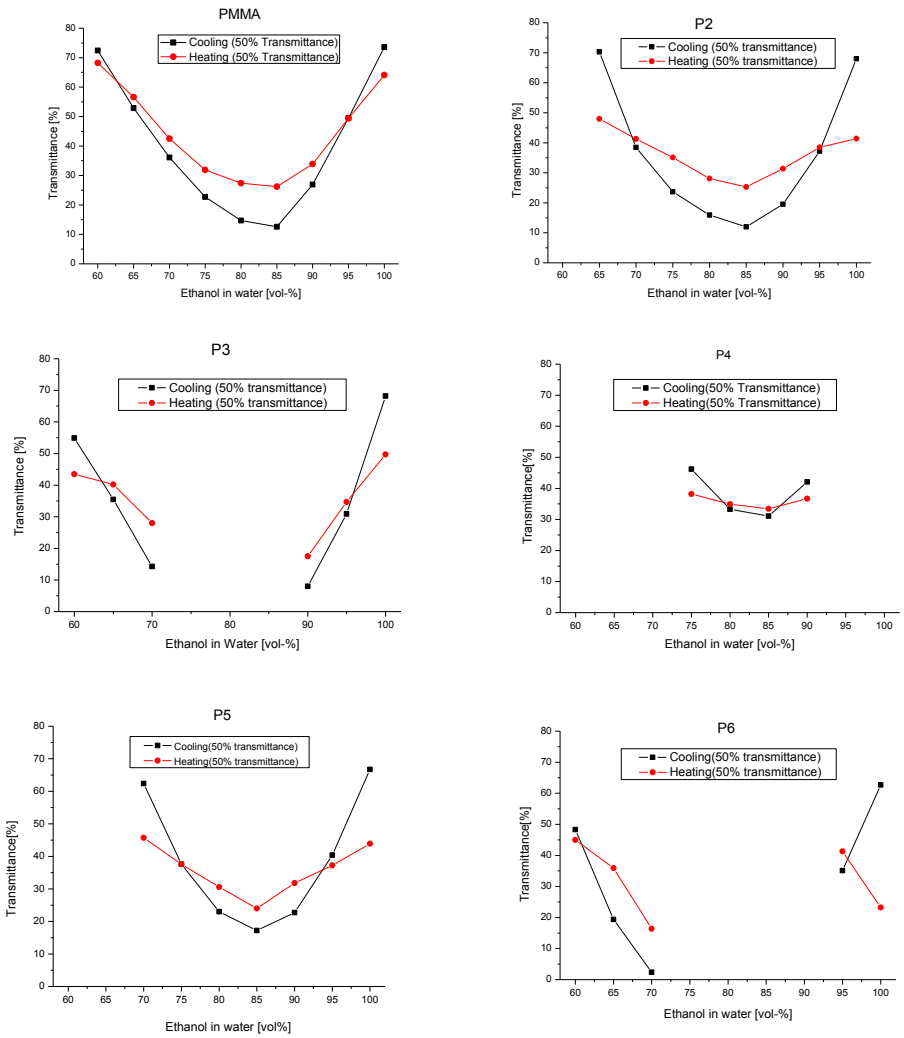

Figure 3-3 Clearance point temperatures upon heating and cloud point temperatures upon cooling as a function of ethanol content for 0.5 mg/ml aqueous solutions of PMMA, P2, P3, P4, P5 and P6.

To further evaluate the influence of these minor side chains on the phase transitions, the T_{CPC} and T_{CPH} of the five substituted copolymers P2-P6 are plotted as a function of amine substituent in 70, 85 and 95 vol-% ethanol in Figure 3-4, together with PMMA as a reference. In general, the introduction of hydrophilic moieties increases the solubility of PMMA in aqueous ethanol leading to lower T_{CPC} and T_{CPH}, while hydrophobic substituents reveal more complex effects on the PMMA solubility diagram, i.e. a decrease in solubility with low content of ethanol and an increase in solubility when adding more ethanol compared to PMMA. Two kinds of hydrophilic groups, hydroxyethyl and aminoethyl, have been introduced to the side chain of the PMMA copolymer, respectively, which improved the solubility of PMMA to different extent, i.e. P3 (hydroxyethyl functionalized) showed a higher phase transition temperature than P6 (aminoethyl functionalized) in 70 vol-% ethanol and, in contrast, a lower T_{CPC}/T_{CPH} in 90 vol-% ethanol. These oppositing solubility trends can be ascribed to the different phase transition mechanism between 70 and 90 ethanol vol-% solvent as previously described. In pure ethanol and ethanol containing a minor water fraction, the interactions between the polymer chain and the solvent are mainly polarity driven rather than specific hydration of the polymer, which results in a better solubility of P3 because of its higher polarity. In contrast, at lower ethanol content, the hydration effects are predominant for the dissolution process due to hydrogen bond formation between water, ethanol and the polymer side chains. As such, P6 reveals a lower phase transition temperature since the amino group can offer two protons for hydrogen bonding with water while the hydroxy groups of P3 only have one proton for hydrogen bonding. Another interesting set of copolymers to compare is P4/P5. Higher solubility might be expected for benzyl functioned PMMA compared to cyclohexyl functioned PMMA due to the lower polarity of the cyclohexyl group. However, P5 was found to be much better soluble than P4, which can be ascribed to the higher steric bulk of the benzyl side chains. The cyclohexyl group is much more flexible and compact than the benzyl group. As a result, hydration of the amide group in P5 is more efficient than for P4, in which this amide group is shielded from the surrounding solvent by the benzyl group.

3.2.3 Metastability between T_{CPC} and T_{CPH}

According to the transmittance versus temperature plot for P5 in 70 vol-% ethanol solvent mixture, the polymer aggregates during cooling at 62.4 ^{o}C while it already dissolves at 45.7 ^{o}C upon heating (Figure 3-3) indicating significant hysteresis pointing towards metastability of the solution within these temperatures. To evaluate the metastability, isothermal turbidity measurements were performed at 59 ^{o}C, both after heating and cooling at 1 ^{o}C/min (Figure 3-5b). Upon heating, P5 dissolved at 45.7 ^{o}C and remained in solution during the isothermal measurement at 59 ^{o}C as demonstrated by the constant transmittance at approximately 75 %. In contrast, the polymer precipitated at 62.4 ^{o}C during cooling and redissolved upon isothermal treatment at 59 ^{o}C as demonstrated by an increase in transmittance. These results clearly demonstrate that P5 is soluble in between T_{CPC} and T_{CPH} in thermodynamic equilibrium. However, upon cooling a metastable

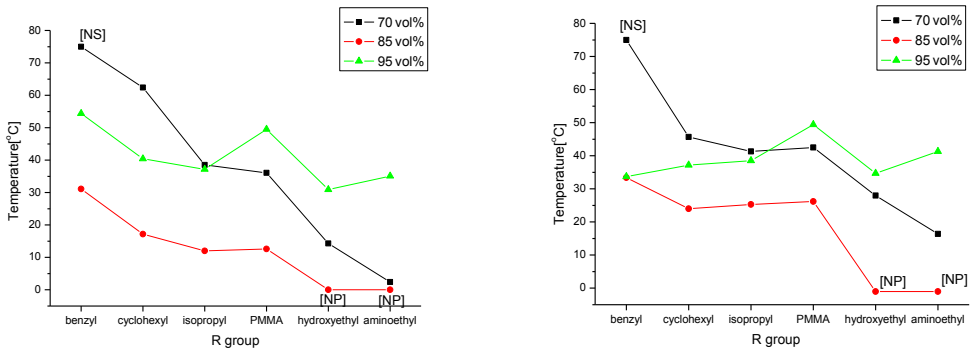

Figure 3-4 Cloud point temperatures upon cooling (left) and clearance point temperatures upon heating (right) for P2-P6 as a function of amine substituent at 5 mg/ml in different solvent composition, with PMMA data as reference. *NP* and *NS* in square brackets represent *no precipitation* and *not soluble*, respectively.

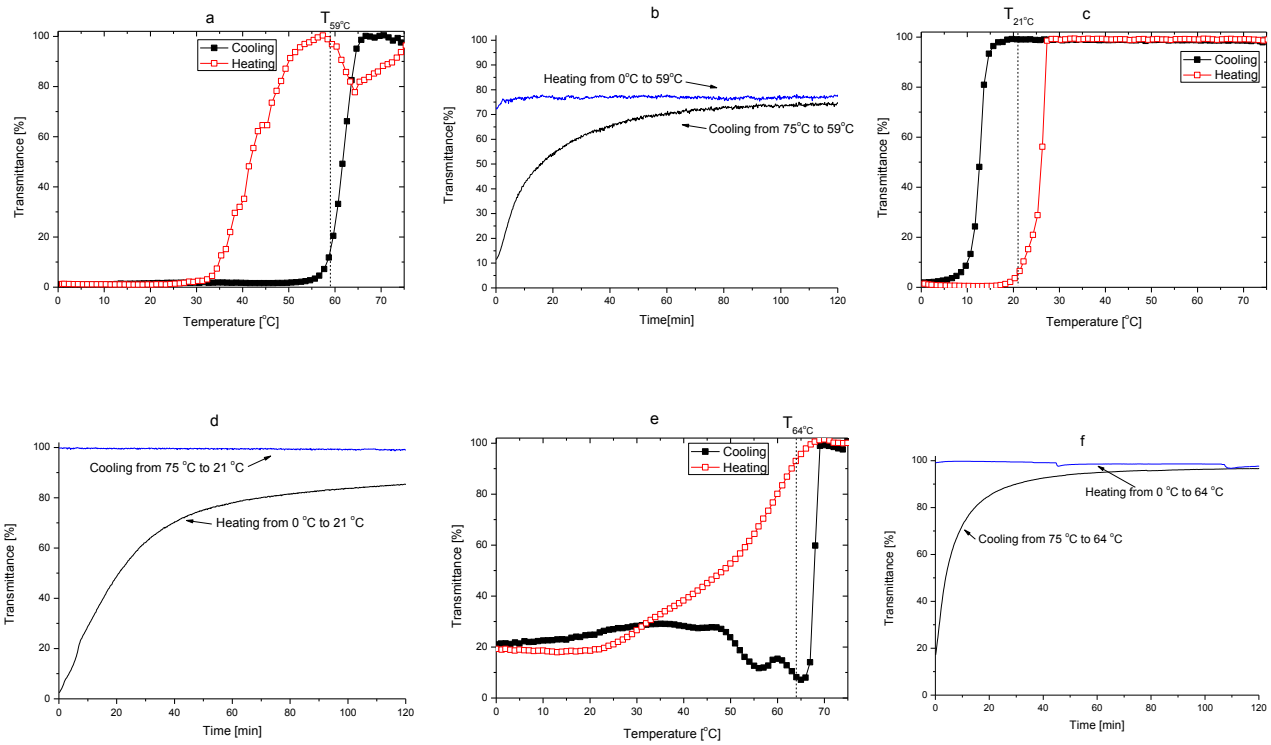

Figure 3-5 Transmittance as a function of temperature and isothermal transmittance as a function of time (after heating or cooling progress) in aqueous ethanol, (a and b) P5 in 70 vol -% ethanol solvent mixture, (c and d) PMMA in 85 vol-% ethanol solvent mixture, and (e and f) P3 in pure ethanol. were shown on the left side

two-phase system is formed in between T_{CPC} and T_{CPH}, which returns to the equilibrium state, i.e. dissolution of the polymer, when given enough time. Apparently, the continuous decrease in chain mobility upon cooling at 1 ^{o}C/min leads to easier dehydration of the polymer chains while allowing time for polymer

relaxation leads to rehydration. In addition, the non-ideal ethanol/water solvent mixture itself might become metastable during this temperature sweeps and, thus, might also influence the polymer solubility.

Isothermal turbidity measurements have also been performed for PMMA in an 85 vol-% ethanol solvent mixture and for P3 in pure ethanol (Figure 3-5d and f). These specific polymer solutions were chosen to cover, together with P5 in 70 vol-% ethanol, all three different hysteresis regions in the polymer solution phase diagrams in aqueous ethanol, namely higher T_{CPH} at low and high ethanol content and higher T_{CPC} at intermediate ethanol content. P3 in ethanol shows similar metastability as P5 in 70 vol-% ethanol, i.e. a metastable precipitated state is obtained just below T_{CPC} upon cooling, whereby the polymer redissolves during the isothermal measurement. The hysteresis of PMMA in 85 vol-% ethanol is reversed compared to the two previously discussed metastable regimes, i.e. $T_{CPH} > T_{CPC}$. The observed metastable behavior of this polymer solution is also reversed and cooling to 21 ^{o}C leads to a clear solution that remains clear during the isothermal measurement. In contrast, upon heating to 21 ^{o}C the polymer remains unsoluble in a metastable two-phase system that converts into a clear one-phase solution during the isothermal measurement. In this case, the hydration of the collapsed polymer aggregates during heating is most likely too slow leading to this observed hysteresis.

3.3 UV-tunable upper critical solution temperature behavior of azobenzene containing poly(methyl methacrylate) in aqueous ethanol

3.3.1 Synthesis of azobenzene-containing PMMA copolymers

To investigate the UV-sensitive thermoresponsive behavior in ethanol/water solvent mixtures of PMMA copolymers with varying content of azobenzene chromophores without interference of the effect of polymer chain length, we have opted for side-chain incorporation of the azobenzene moieties via a post-polymerization modification step of activated ester with amines.[280, 282] For this purpose, poly(methyl methacrylate-*co*-pentafluorophenyl methacrylate) (P(MMA–*co*–PFPMA)) was first prepared by free radical copolymerization initiated by AIBN. The content of the PFPMA moiety was estimated by ^{1}H NMR to be 14 mol-%.

The subsequent post-polymerization modification was performed with an amine functionalized azobenzene moiety followed by reaction of the remaining pentafluorphenyl esters with a large excess of a small amine, as shown in Scheme 3-2. Therefore, the P(MMA– *co*–PFPMA) copolymer was first dissolved in DMF and allowed to react at 60 ^{o}C with *N*-(2-aminoethyl)-4-(2-phenyldiazenyl) benzamide in the presence of triethylamine (TEA). After 7 days (for DP1) or 14 days (for DP2 and DP3), an excess amount of ethanolamine (for DP1 and DP2) or isopropylamine (for DP3) was added and allowed to react for another 24 h to guarantee complete conversion of the pentafluorophenyl esters, respectively. All the reaction solutions were first precipitated by adding excess of diethyl ether. The crude polymers DP1 and DP3 were then re-

dissolved in dichloromethane followed by precipitation in a mixture of diethyl ether and hexane. The crude polymer DP2, prepared with ethanolamine, was not well soluble in dichloromethane and, therefore, was first dissolved in an ethanol/water solvent mixture (ethanol/water with 80/20 in volume) and then precipitated by adding more ethanol. The composition of the resulting purified polymers was analyzed in detail. Full conversion of the pentafluorophenyl groups was confirmed by the complete vanishing of the signal from the activated ester group in the ^{19}F NMR spectra (see Figure 3-6). Additionally, ^{1}H NMR spectroscopy revealed that the copolymers DP1, DP2 and DP3 contained 6.0 mol-%, 7.6 mol-% and 8.1 mol-% azobenzene comonomer units, respectively, while the remainder of activated esters were converted to *N*-isopropyl methacrylamide or hydroxyethyl methacrylamide units respectively (Table 3-2). The slightly reduced incorporated amount of azobenzene moieties compared with the 14% PFPMA content is most likely due to steric hindrance limiting or, at least, severely slowing down further modification. Applying harsher conditions during the post-polymerization modification step was not done as this would result in partial hydrolysis of the activated esters, thereby affecting the copolymer composition even further by incorporation of methacrylic acid units. The two different low molar mass amines isopropylamine and ethanolamine were chosen to modify the overall hydrophilicity of the PMMA copolymer as well as to remove the labile pentafluorophenyl esters that lead to irreproducible thermal transitions due to hydrolysis (see section 3.2).[87] Size-exclusion chromatography (SEC) revealed that the starting P(MMA– *co*–PFPMA) copolymer had a dispersity (Đ) of 1.83, as expected from free radical polymerizations. However Đ decreased to around 1.4 after the post-polymerization modification reactions due to fractionation that is removal of low molar mass chains, during repetitive precipitation (see Table 3-2).

3.3.2 Dual-responsive behavior of PMMA copolymers

After the successful incorporation of the azobenzene moieties into PMMA, the light-induced isomerization of the chromophoric azobenzene group was investigated in ethanol/water solvent mixtures. The UV/Vis spectra of DP1 recorded in an ethanol/water solvent mixture with 80 wt-% of ethanol, before and after UV irradiation serves as representative example for all three polymers (Figure 3-7). After 1 hour irradiation of the solution of copolymer DP1 with 360 nm UV-light, a large increase of the absorption band at 440 nm was observed, which is indicative for the cis-isomer. Only a minor further increase in absorbance at 440 nm could be detected after another 1 h of illumination indicating that the majority of chromophoric azobenzene side groups have been converted to the *cis*-configuration after only 1h of UV-irradiation.

The *trans* to *cis* isomerization of azobenzene is associated with a change in dipole moment of the molecular structure. Azobenzene groups have a dipole moment of 0 Debye in the trans-configuration, while azobenzene molecules in the cis-configuration have a dipole moment of 3 Debye due to loss of the symmetry (see Figure 3-7).[268] As this change in dipole moment upon UV-induced isomerization has been demonstrated to lead to an increase in T_{CP} of azobenzene modified LCST copolymers in aqueous solutions, it was

hypothesized that the *trans* to *cis* isomerization can also induce a better solubility of azobenzene containing PMMA in ethanol/water solvent mixtures due to an increase in polarity leading to a lower T_{CP}. To investigate the UCST behavior of the synthesized azobenzene containing PMMA copolymers DP1 – DP3, turbidimetry of the copolymer solutions in ethanol/water solvent mixtures was performed in a UV-Vis spectrometer. Thus the transmittance of incident light at a wavelength of 600 nm through the sample was monitored as a function of temperature. Typical transmittance versus temperature plots resulting from turbidimetry are shown in Figure 3-8 for DP1. During the cooling runs from 50 °C to 2 °C, a sharp transition from high transmittance (about 100%) to low transmittance (about 0%) was detected indicating phase separation of the solution and the aggregation of the copolymer. Similarly, a reversed transition from low transmittance to high transmittance was also recorded during heating indicating dissolution of the copolymer. Irradiation of the DP1 solution with UV light leads to a shift of both the cooling and heating curves to lower temperatures due to the *trans* to *cis* isomerization of the azobenzene group indicating that the increase in azobenzene polarity indeed leads to the proposed enhanced solubility of the copolymer in the ethanol/water solvent mixture. Besides the enhanced polarity of the azobenzene moiety, the *cis* isomer also acts as better hydrogen bond acceptor compared to the more shielded *trans* isomer, which may further improve the solubility of the copolymer (see Figure 3-7).

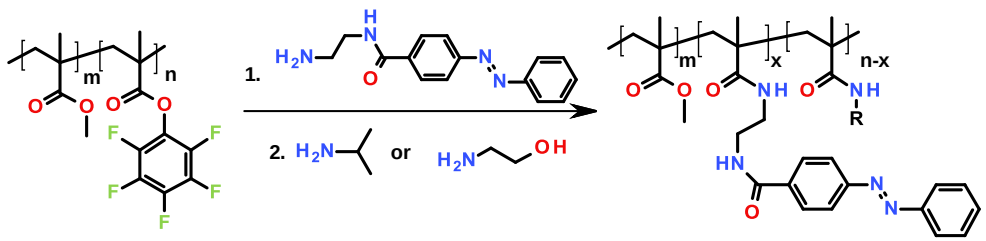

Scheme 3-2 Schematic representation of post-polymerization modification of P(MMA–*co*–PFPMA) with an amino-functionalized azobenzene moiety followed by reaction of the remaining pentafluorophenyl groups with isopropylamine (DP1 and DP3) or ethanolamine (DP2).

Table 3-2 Analytical data of the synthesized copolymers

Copolymer	R groups	Mn [kDa][a]	Đ[a]	Amount of azobenzene [mol-%][b]	Amount of R group [mol-%][c]
P(MMA-PFPMA)	N/A	16.2	1.83	0	0
DP1	OH	52.9	1.42	6.0	8
DP2	OH	54.5	1.46	7.6	6.4
DP3		58.9	1.40	8.0	6

[a] Determined by SEC using PMMA standards; [b] Determined by ^{1}H NMR spectroscopy; [c] Determined as amount of R group = 14- Amount of azobenzene

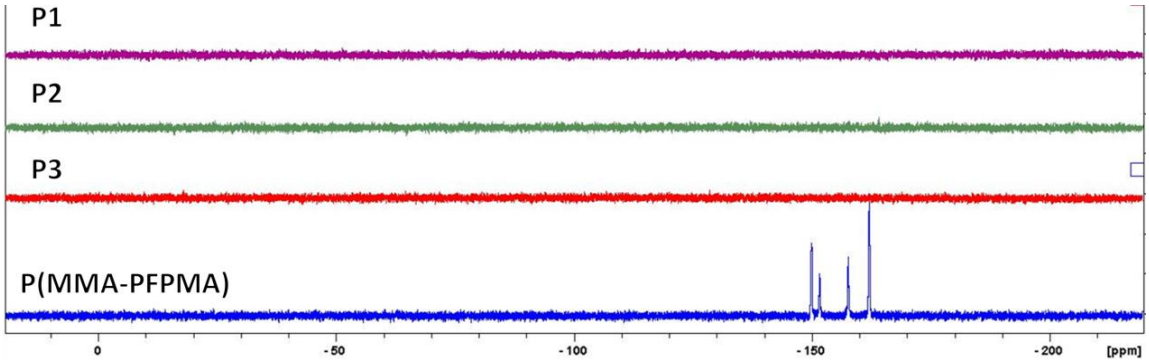

Figure 3-6 ^{19}F NMR spectra of P(MMA–PFPMA) and the corresponding substituted copolymers

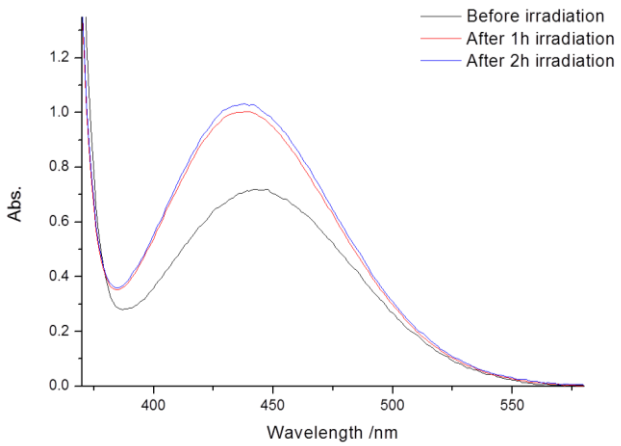

Figure 3-7 Evolution of the UV/Vis spectra of DP1 in an ethanol/water solvent mixture with 80 wt-% of ethanol (2 mg/mL) before and after irradiation at 360 nm for 1 h or 2h. The increase in UV-absorbance corresponds to isomerization of the azobenzene unit from *trans* to *cis* as shown in the inset.

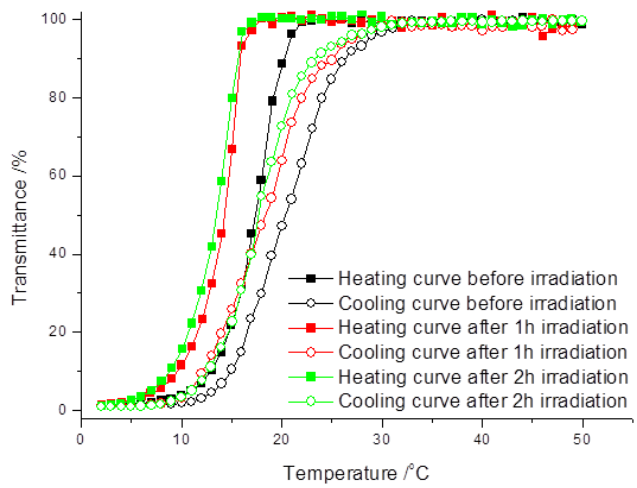

Figure 3-8 Transmittance versus temperature plots for DP1 in ethanol/water solvent mixture (2 mg/mL; 80 wt-% ethanol) before and after irradiation at 360 nm for 1 h or 2h.

For a more quantitative comparison of the polymer phase transitions before and after irradiation, ΔUCST is defined as the decrease of T_{CPC} or T_{CPH} upon UV-irradiation to evaluate the light responsiveness of the polymer solutions. Table 3-3 provides an overview of the effect of polymer structure, concentration and UV-irradiation on T_{CPC} and T_{CPH} in an ethanol/water solvent mixture with 80 wt-% ethanol.

It is evident that the T_{CPC}'s and T_{CPH}'s of the copolymers DP1–DP3 exhibit a strong dependence on the amount of azobenzene and the nature of the side-chain moieties that are introduced besides the azobenzene groups. The T_{CP}s greatly increased (> 10 °C) when the amount of azobenzene was slightly increased from 6.0 % (DP1) to 7.6 % (DP2) due to the hydrophobic character of trans-azobenzene as well as the corresponding decrease of the number of hydrophilic hydroxyethyl side chains. The large influence of minor changes in azobenzene content on the UCST is in good agreement with our previous observation that a PMMA copolymer with only *ca.* 6% of *N*-hydroxyethyl acrylamide comonomer units is completely soluble at 2 or 5 mg/ml in the ethanol/water (80 wt.% ethanol) solvent mixture at all temperatures (see section 3.2). When replacing the hydroxyethyl groups (DP2) with more hydrophobic isopropyl groups (DP3) and keeping the amount of azobenzene groups constant, the copolymer (DP3) becomes too hydrophobic making it insoluble in the ethanol/water solvent mixtures.

Both the T_{CPC}'s and T_{CPH}'s of the soluble polymers DP1 and DP2 were found to be 1-3 °C lower after UV-irradiation indicating enhanced solubility of polymer chain resulting from the more polar *cis* isomer of azobenzene. Even though this is a minor change in T_{CP}s upon UV irradiation, it is similar to the effect of azobenzene isomerization on the T_{CP}s of related LCST polymers.[89, 264]

In contrast to the dramatic influence of minor changes in azobenzene content on the T_{CP}s, the ΔUCST of DP1 and DP2 in the ethanol/water solvent mixture with 80 wt-% ethanol are rather similar (Table 3-3). When increasing the concentrations of DP1 and DP2, the T_{CP}s increased as expected, but the ΔUCST was not significantly affected.

Table 3-3 Thermo- and light-responsive behavior of the copolymers DP1 to DP3 in an ethanol/water (80 wt-% ethanol) solvent mixture.

Polymer	UCST transition before irradiation [°C]		UCST transition after 1h irradiation at 360 nm [°C]		Δ UCST [°C]	
	T_{CPH}	T_{CPC}	T_{CPH}	T_{CPC}	Δ T_{CPH}	Δ T_{CPC}
DP1 (2 mg/ml)	20.4	17.4	18.4	14.5	2.0	2.9
DP1 (5 mg/ml)	24.5	23.2	23.9	20.4	0.6	2.8
DP2 (2 mg/ml)	35.4	31.5	33.1	30.2	2.3	1.3
DP2 (5 mg/ml)	44.5	43.5	44.0	41.5	0.5	2.0
DP3 (2 or 5 mg/mL)	Insoluble	Insoluble	Insoluble	Insoluble	N/A	N/A

Subsequently, we have determined the light- and thermoresponsive behavior of copolymers DP1 in ethanol/water solvent mixtures with various ethanol contents as this has been previously found to strongly influence the T_{CP}s of PMMA (co)polymers. DP2 was not further evaluated as it showed poor solubility in pure ethanol and in 60 wt-% ethanol severely limiting the solvent range that can be evaluated. In general, the phase diagrams of DP1 before (Figure 3-9a) and after UV-irradiation (Figure 3-9b) exhibit similar dependence of T_{CPC}'s and T_{CPH}'s as PMMA homopolymers,[65] that is the T_{CPC} and T_{CPH} values of the copolymers in ethanol decrease when water is added until the maximum solubility is reached at an ethanol content of around 80 wt-%, which has been ascribed to the presence of individual water molecules at this composition leading to efficient hydration and solubilization of the polymer.[48] Further addition of water resulted in an increase of the T_{CPC} and the T_{CPH} due to the formation of water clusters that need to be broken before the polymer can be hydrated in combination with the higher polarity of the solvent mixture. Moreover, the hysteresis between cooling and heating reversed upon variation of the ethanol content: in the case of the good solvent mixtures, the dissolution induced by heating occurs at a higher temperature than the precipitation upon cooling. A smaller hysteresis is found for DP1 in good solvents when compared with the PMMA homopolymer due to shielding of the hydrogen bond accepting ester groups by the large hydrophobic azobenzene groups, which was previously also found for PMMA copolymers with 6 mol-% of benzyl or cyclohexyl side chains (see section 3.2). The T_{CPC} and T_{CPH} values slightly decreased after UV-irradiation in all solvent mixture with varying amounts of ethanol.

A closer look at the effect of UV-irradiation at the T_{CPC} values revealed an unexpected, clear trend (Figure 3-10). The ΔUCST values for the decrease in T_{CPC} were found to, approximately, linearly increase by addition of water in the solvent mixture from pure ethanol to 40 wt-% of water indicating a strong influence of water on the light responsiveness. In fact, no remarkable change of cloud point could be detected in pure ethanol, while a 7 ^{o}C decrease in T_{CPC} was found in the ethanol/water solvent mixture with 40 wt-% of water. This clear dependence of T_{CPC} on solvent composition can be rationalized by considering the hydrogen bond accepting capacity of the azo-group, especially for water molecules as this will enhance the solubility of the copolymer by increasing the overall polarity of the hydrated polymer chains. As such the better availability of this azo-group for solvent molecules in the *cis* isomer will lead to improved solubility when more water is present in comparison to the *trans* isomer where the azo–group is shielded from the solvent by the hydrophobic benzene rings.

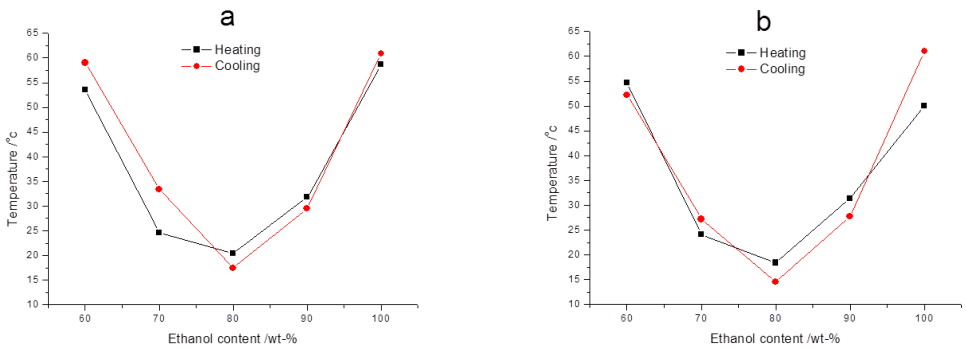

Figure 3-9 Clearance point temperatures upon heating and cloud point temperatures upon cooling as a function of ethanol content for 2 mg ml^{-1} in aqueous solutions of DP1 a) before and b) after 1h of UV irradiation.

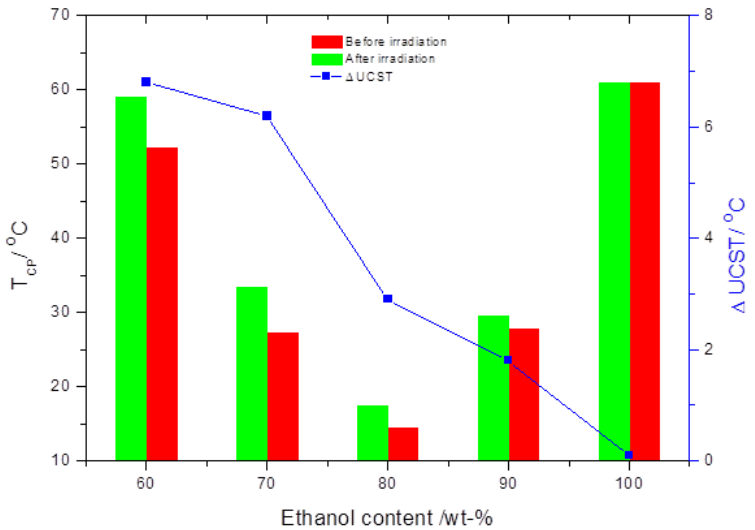

Figure 3-10 Cloud point temperatures upon cooling as a function of ethanol content for 2 mg ml^{-1} aqueous solutions of DP1 before and after 1h of UV irradiation, the blue data points shows the difference in cloud point temperature before and after UV irradiation (ΔUCST).

3.4 Summary

A series of PMMA copolymers containing hydrophilic (aminoethyl or hydroxyethyl), hydrophobic (isopropyl, cyclohexyl or benzyl) or azobenzene functionalized methacrylamide comonomers were synthesized by nucleophilic substitution of PMMA-*stat*-PFPMA with the corresponding amines. The UCST behavior of the obtained copolymers in different compositions of aqueous ethanol was studied in detail revealing that the T_{CPC}, T_{CPH} and hysteresis between heating and cooling of the copolymers were strongly affected by 6% or 14% of the minority of methacrylamide comonomer units. In general, the introduction of hydrophilic moieties increases the solubility of PMMA in aqueous ethanol, while hydrophobic substituent

(isopropyl, cyclohexyl or benzyl) decrease the solubility of PMMA in solvent mixtures with a low ethanol content and increase the solubility in solvent mixtures with a high ethanol content ascribed to the non-ideal solvent behavior of the ethanol/water solvent mixtures. The azobenzene containing PMMA copolymers (DP1 and DP2, also containing hydrophilic hydroxyethyl groups) also exhibited UCST behavior in ethanol/water solvent mixtures and pure ethanol, whereby the T_{CP} depended strongly on the incorporated amount of azobenzene groups; while DP3 (having azobenzene and isopropyl side chains) could not be dissolved in ethanol/water solvent mixtures due to too high hydrophobicity. The UCST transitions of DP1 and DP2 were found to be highly tunable by either the solvent composition or to a lesser extent by UV-irradiation. Furthermore, a larger decrease of cloud point induced by UV-irradiation was found in ethanol/water solvent mixture with increasing content of water from 0 wt-% to 40 wt-% indicating a solvent dependence of light-responsiveness.

To conclude, we have presented the synthesis and characterization of a series of PMMA copolymers with tunable UCST behavior in ethanol/water solvent mixtures. It is found that only 6 mol% of the methacrylamide comonomer can result in a dramatic change of the UCST behavior of the corresponding PMMA in aqueous ethanol. In addition, light and thermo responsive behavior in ethanol-water solvent mixtures was prepared, which represents, to the best of our knowledge, the first example of a dual responsive copolymer combining light responsiveness with UCST behavior in an aqueous solvent mixture.

3.5 Experimental Section

3.5.1 Materials and Instrumentation

All chemicals and solvents are commercially available and were used as received unless otherwise stated. Dichloromethane (DCM), tetrahydrofuran (THF), diethyl ether, methanol, triethylamine (TEA), ethanol, *N*,*N*-dimethylformamide (DMF), *N*,*N*-dimethylacetamide (DMA) and hexane were obtained from Sigma Aldrich. Deuterated chloroform and methanol are supplied by Eurisotop. Isopropylamine and ethanolamine were purchased from Acros Organics. THF and diethyl ether were distilled over sodium before use. TEA was dried over calcium chloride and distilled before use. Azobis(isobutyronitrile) (AIBN) was recrystallized from diethyl ether and stored at -7 ^{o}C.

^{1}H NMR spectra were recorded on a Bruker 300 MHz FT-NMR spectrometer in deuterated solvents. ^{19}F NMR spectra of PMMA-PFPMA and PFPMA were recorded on a Bruker 400 MHz FT-NMR spectrometer. And ^{19}F NMR spectra of PMMA analogues were recorded on a Bruker Avance 282.23 MHz spectrometer in deuterated chloroform. Chemical shifts (δ) were given in ppm relative to TMS.

Size-exclusion chromatography (SEC) was performed on a Agilent 1260-series HPLC system equipped with a 1260 online degasser, a 1260 ISO-pump, a 1260 automatic liquid sampler, a thermostatted column compartment, a 1260 diode array detector (DAD) and a 1260 refractive index detector (RID). Analyses were

performed on a PSS Gram30 column in series with a PSS Gram1000 column at 50 °C. DMA containing 50 mM of LiCl was used as eluent at a flow rate of 1 ml/min. The SEC traces were analysed using the Agilent Chemstation software with the GPC add on. Molar mass and PDI values were calculated against PMMA standards.

Turbidity measurements were performed on a Cary 300 Bio UV-Visible spectrophotometer at a wavelength of 600 nm. The samples in plastic disposable cuvettes were first heated to a suitable temperature to fully dissolve the copolymer, after which the sample was placed in the instrument and heated to a certain temperature above the upper critical solution temperature. The transmittance was measured during at least two controlled cooling/heating cycle with a cooling/heating rate of 1 °C/min controlled by block temperature mode while stirring. T_{CPC} and T_{CPH} are given as the temperature where the transmittance goes through 50%. The metastability study was first performed by heating the sample to 75 °C or cooling to 0 °C following by cooling or heating to the set temperature at 1 °C/min followed by isothermal measurement at the transmittance for 2 hours.

UV-irradiation of the solution for the isomerization experiments was performed by placing the solution in a metal cylindrical container with 300 nm UV lamps (8 x 25 W).

3.5.2 Synthesis of pentafluorophenyl methacrylate (PFPMA)

Pentafluorophenol (35.0g; 0.19 mol) and triethylamine (20.2g; 0.20 mol) were dissolved in 550 ml diethylether. To this mechanically stirred solution, acryloyl chloride (20.9g; 0.20 mol) was added dropwise at 0 ℃. After stirring for 3 additional hours at room temperature, the precipitated salt was removed by filtration. The solvent was removed under reduced pressure and the crude product was further purified via column chromatography (silica gel, solvent: petroleum ether). 45.5g (0.18 mol, 95 %) of a colorless liquid was obtained. ^{1}H-NMR ($CDCl_3$): δ /ppm: 6.43 (t, 1 H, J=1.5 Hz), 5.89 (t, backbone), ^{19}F ($CDCl_3$) δ/ppm: -152.76 (d, 2F), -158.21 (t, 1F), -162.5 (t, 2F), FT-IR (ATR-Mode): 1761 cm^{-1} (C=O, reactive ester band), 1520 cm^{-1} (aromatic band).

3.5.3 Synthesis of N-(2-Aminoethyl)-4-(2-phenyldiazenyl)benzamide

The azobenzene derivative was synthesized according to a method published recently.[264] yield: 83% ^{1}H-NMR ($CDCl_3$): δ/ppm: 8.62 (s, 1H), 8.06 (d, 2H), 7.93 (m, 4H), 7.60 (m, 3H), 3.30 (q, 2H), 2.71 (t, 2H); FT-IR (ATR-mode): υ_{max}/ cm^{-1} 3296 (N-H), 1634 (C=O), 1539 (C=O)

3.5.4 Synthesis of Poly(MMA-stat-PFPMA) (PMMA-PFPMA)

Methyl methacrylate (MMA; 3g; 29 mmol)), pentafluorophenyl methacrylate (0.39g; 1.6 mmol) and AIBN (68mg; 0.4 mmol) were dissolved in 5ml of freshly distilled dioxane and placed in a Schlenk flask.

After four freeze-pump-thaw cycles, the flask was filled with argon, immersed in a preheated oil bath of 80 ℃ and stirred for 15 hours. After the solution was cooled down to room temperature, the polymer was precipitated in ice-cold methanol. The crude polymer was dissolved in THF and precipitated again in ice-cold methanol. This procedure was repeated two more times. The polymer was centrifuged and finally dried under reduced pressure.

3.5.5 PMMA-PFPMA modification

Nucleophilic substitution of PMMA-PFPMA with the amine was performed in THF at 45 ^{o}C with triethylamine as catalyst. 200mg of polymer was dissolved in 10ml THF, and then 0.3 ml of amine and 0.3 ml of triethylamine were added. The solution was placed in a preheated oil bath and stirred for 5 days at 45 ^{o}C. The resulting polymer was isolated by precipitation in cyclohexane (three times) and was dried under reduced pressure.

For the preparation of azobenzene containing copolymers, the copolymer was first allowed to react with the azobenzene containing amine, and then the resulting copolymers were modified by small amines to completely remove the PFPMA moieties. To a solution containing P(MMA-PFPMA) and triethyl amine in DMF, solid N-(2-aminoethyl)-4-(2-phenyldiazenyl)benzamide was added and the mixture was stirred for 14 days (7 days for DP1) under nitrogen atmosphere at 60 ^{o}C. Afterwards, excess of ethanolamine (DP1 and DP2) or isopropylamine (DP3) was added to the flask. After additional 24h of stirring, the solutions were precipitated by addition of diethyl ether and the precipitated polymer was isolated by filtration. The polymer was redissolved in dichloromethane (DP1 and DP3) and precipitated in a hexane-diethyl ether mixture for another 3 times. DP2 was redissolved in ethanol/water (80-20 wt-%) and precipitated by addition of ethanol for another three times. The final resulting polymers were dried under reduced pressure for 24 h at 50 ^{o}C before further analysis.

Chapter 4 Polyampholytes prepared by copolymerization of cationic and anionic monomers: Synthesis, Thermoresponsive behavior and Micellization

Abstract: Polyampholytes with controlled ratio of charges were synthesized by reversible addition-fragmentation chain transfer (RAFT) copolymerization of cationic and anionic monomers. Fine-tuning of the feed ratio of the two monomers to compensate for the different relativities of the two monomers allows the synthesis of quasi-random copolymers. The resulting polyampholytes with equal numbers of cationic and anionic charges were found to show UCST type thermoresponsive behavior in ethanol/water and methanol/water solvent mixtures. In addition, the UCST of the copolymers can be well tuned by varying the composition of the alcohol/water solvent mixtures. Finally, the temperature induced self-assembly of a polyampholyte with oligo(ethylene glycol) side chains was investigated in ethanol and isopropanol.

4.1 Introduction

Thermoresponsive polymers represent polymers that undergo a reversible phase transition at the lower critical solution temperature (LCST) or the upper critical solution temperature (UCST). The most commonly studied and firstly reported thermoresponsive polymer in aqueous solution is poly(*N*-isopropylacrylamide) (PNIPAM) with an LCST of *ca.* 32 °C,[24, 169] which is close to human body temperature. Besides, poly(oligo(ethylene glycol)(meth)acrylate),[20, 26-29] poly(2-oxazoline),[3, 30] poly(vinyl ether)s[31] and polypeptide[32, 33] have also been widely studied and have found various applications as smart materials. Compared with polymers that undergo an LCST phase transition, polymers exhibiting UCST behavior in aqueous solution have been much less documented as it is more challenging to achieve this behavior in aqueous solutions requiring strong inter polymer attraction in combination with high hydrophilicity.

Alcohol-water solvent mixtures have been considered as promising solvents to obtain UCST behavior for various polymers arising from the presence of complex hydration shells around the ethanol molecules and a decrease in solvent polarity upon heating.[47-49] For instance, poly(methyl methacrylate) (PMMA) and its copolymers were found to show UCST behavior in ethanol/water solvent mixtures with tunable phase transition temperature favored by the co-solvency effect of the binary solvent.[52, 64, 65, 72, 87, 94, 100] Besides, Poly(2-alkyl-2-oxazoline)s with various side chains were also found to show UCST phase transitions in ethanol/water binary solvents.[52, 102, 104] In contrast to the co-solvency effect, the binary solvent mixture can also show co-nonsolvent effects, i.e. decreased solubility of the solute compared with the individual solvents, leading to UCST behavior of, e.g. PNIPAM[63, 90, 126] and Poly[*N*-(4-vinylbenzyl)-*N*,*N*-dialkylamine]s.[90, 113]

Polyampholytes are polymers bearing both cationic and anionic repeat units. The present of anions and cations as well as their intra- and inter- molecular interactions provide special properties making such polymers interesting for various applications.[34, 283] Amongst the different types of polyampholytes, polyzwitterions with cationic and anionic groups bound to the same monomer unit are mostly studied, also referred to as polybetaines.[34] Only few reports describe the polyampholytes prepared by controlled copolymerization of cationic and anionic monomers, although this type of polymers can show special properties by tuning of the ratio and/or distance of the two charges.[284] For instance, polypeptides that combine cationic and anionic monomers widely exist in natural systems and play important roles in their biological activities.

The development of controlled radical polymerization techniques (CRP), such as nitroxide-mediated polymerization (NMP),[285] atom transfer radical polymerization (ATRP),[114, 161, 286] and reversible addition-fragmentation chain transfer (RAFT) polymerization,[116, 117, 221] has provided new tools for the synthesis of well-defined (co)polymers with high tolerance of, e.g., water. Compared with conventional living polymerization techniques, CRP allows direct polymerization of functional monomers. For instance, RAFT

polymerization has been reported to provide good control over the direct radical polymerization of monomers with tertiary amine or carboxylic acid group,[117] which may react with living ionic species during conventional living aninic polymerization. However, the controlled stoichiometric copolymerization of a tertiary amine functionalized monomer and carboxylic acid functionalized monomer has not been reported, to the best of our knowledge. In fact, the copolymerization of the two comonomers may be greatly different from the homo-polymerizations since the strong ionic interaction between the two monomers can severely influence the reactivity ratios of the two monomers.

In this section, we will report the synthesis of a new series of polyampholytes by direct RAFT copolymerization of anionic and cationic monomers. Thermoresponsive behavior of the resulting copolymers will be described in alcohol/water solvent mixtures. Finally, by incorporation of a solvophilic neutral comonomer, temperature controlled self-assembly of the non-block copolymer was achieved in alcoholic solvents.

4.2 Results and discussions

4.2.1 Synthesis of polyampholytes by RAFT polymerization

The synthesis of polyampholytes was performed by RAFT copolymerization due to its high tolerance of functionalities. The copolymerization was first performed with identical equivalents of the two charged comonomers, namely methacrylic acid (MA) and 2-(dimethylamino)ethyl methacrylate (DMAEMA), considering the fact that the two monomers bear similar reactive vinyl groups. However, a preliminary kinetic study with equimolar amounts of the monomers revealed a ratio of the polymerization rate constants of DMAEMA and MA as high as 2.5. Hence, the copolymerization was then performed with an excess of MA to obtain charge neutral polyampholytes. Figure 4-1 shows the kinetics plots of the copolymerizations with feed ratios of MA/DMAEMA at 100/40 and 733/200, respectively, relative to the CTA aiming for different target molecular weights.

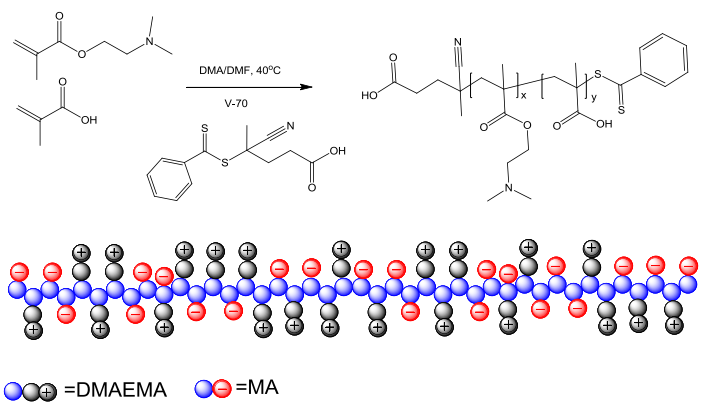

Scheme 4-1 Schematic representation of the synthesis and structure of charge neutral polyampholytes prepared by RAFT copolymerization of anionic and cationic monomers

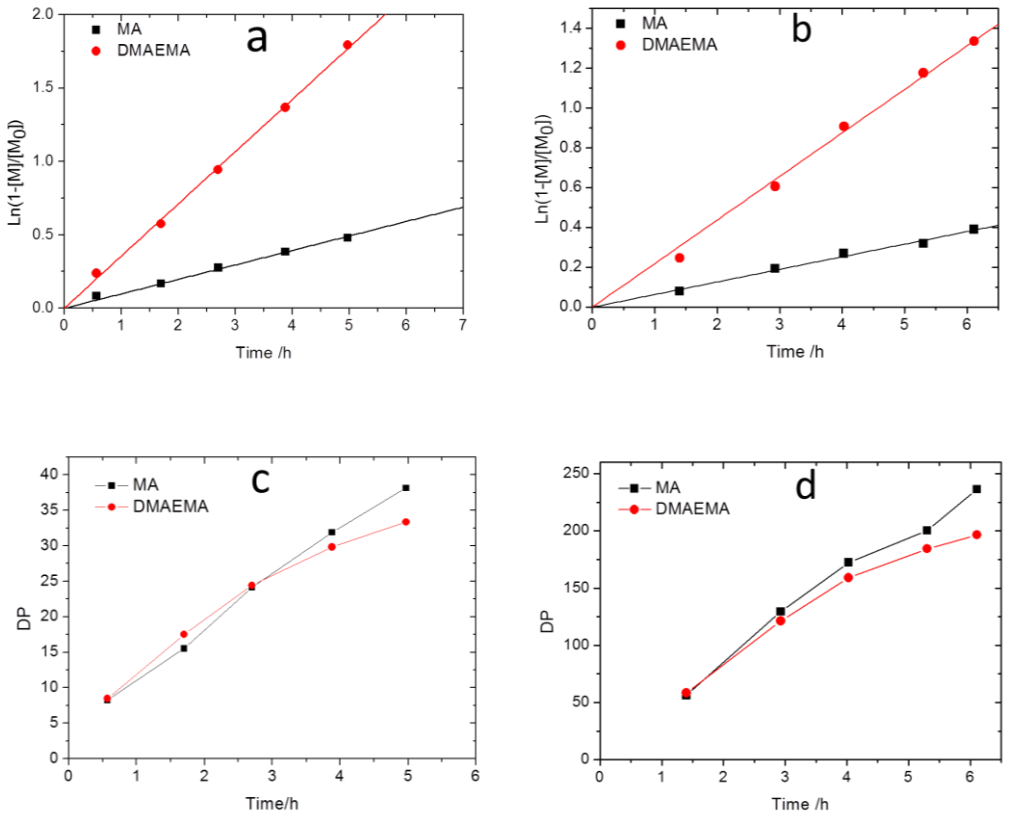

Figure 4-1 a, b) Kinetic plots and c, d) DP versus reaction time plots for copolymerization of MA and DMAEMA with feed ratio of MA: DMAEMA: CTA: V70 at a, c) 100: 40: 1: 0.1 and b, d) 733: 200: 1: 0.2, performed at 40 ^{o}C with V70 as initiator.

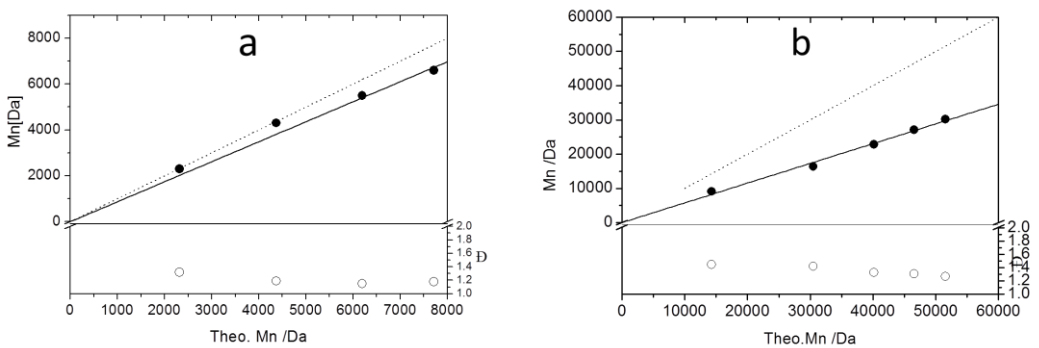

Figure 4-2 Plots of the experimental number-average molar mass (Mn) and dispersity (Đ) versus theoretical Mn for the RAFT copolymerizations of MA and DMAEMA with feed ratios of MA: DMAEMA: CTA: V70 at a) 100: 40: 1: 0.1 and b) 733: 200: 1: 0.2, performed at 40 ^{o}C with V70 as initiator. The dotted lines represent the identical value of the experimental and theoretical Mn; the underestimated of the experimental Mn at high molecular weight range can be ascribed to the collapse of the polymer globules with high Mn due to the strong intra-chain interaction leading to smaller hydrodynamic radius compared to the PMMA standard.

The kinetics of the two copolymerizations revealed linear first order kinetic plots for both monomers indicating a constant free radical concentration indicative for the absence of significant termination reactions. A linear increase of molecular weight with conversion as well as the relatively narrow molar mass distributions (Figure 4-2) further demonstrate good control over the copolymerizations of the two monomers. In addition, the monomer sequence was analyzed by plotting the degree of polymerization (DP) versus time for both monomers. As shown in Figure 4-1c and Figure 4-1d, the DP of both monomers increased similarly during the copolymerization indicating efficient suppression of the gradient formation by controlling the feed ratio of the two monomers providing access to quasi-random copolymer. On the basis of these copolymerization kinetics, a series of well-defined copolymers with different DP and equimolar MA/DMAEMA ratios was prepared (Table 4-1).

Table 4-1 Characterization data of the copolymers with different length and MA/DMAEMA ratios

Code	MA:DMAEMA[a]	DMAEMA/ MA[a]	DMAEMA/ MA[b]	Mn /kDa	Đ	Comonomer
PA1	22 : 24	1.09	1.07	4.1	1.26	
PA2	287 : 288	1.00	1.08	34.1	1.24	
PA3	38 : 38	1.00	1.03	12.9	1.34	with OEGMA comonomer

[a] Determined by GC with DMA as internal standard; [b] Determined by ^{1}H NMR spectroscopy in D_2O;

4.2.2 Thermoresponsive behavior of charge neutral polyampholytes in alcohol/water solvent mixtures

Considering the strong ionic interaction of the two monomers as well as the reported examples of UCST behavior of polybetaines, the copolymers are expected to show an UCST phase transition in water. However, all the synthesized copolymers are well soluble in water above 0 ^oC even for PA2 with high molecular weight. Hence, less polar solvents, namely methanol and ethanol, were added to the aqueous solutions as co-nonsolvent leading to cloud of the solutions at room temperature.

The thermoresponsive behavior of the copolymers was investigated by turbidimetry in alcohol/water solvent mixtures at a concentration of 5 mg/ml. For this purpose polymer solutions in alcohol/water solvent mixtures were heated and cooled between 2 and 80 ℃ (for ethanol/water solvent mixtures) or 60 ℃ (for methanol/water solvent mixtures) at a heating/cooling rate of 1 ℃/min while stirring. Cloud point temperatures (T_{CP}s) were determined at 50% transmittance of light at wavelengths of 600 nm during cooling of the polymer solutions. During the cooling of the polymer solution, a sharp transition from high transmittance (about 100 %) to low transmittance (about 20 %) was detected indicating phase separation of the solution and the aggregation of the copolymer in the binary solvent (Figure 4-3). Figure 4-4 displays the T_{CP}s for PA1 and PA2 in alcohol/water solvent mixtures as a function of alcohol content. Both of the

copolymers show UCST thermoresponsive behavior in a wide range of ethanol content in the ethanol/water solvent mixtures. The T_{CP}s for PA2 are higher than for PA1 in the same solvent mixtures at low content of ethanol indicating the expected molecular weight dependence of the UCST behavior, i.e. the higher the molar mass the stronger the inter chain interaction the higher the T_{CP} .[17, 90] However, the difference between the two polymers decreases with increasing ethanol content and reversed with an ethanol content higher than 70 vol%. The reason for this abnormal molecular weight dependence of UCST T_{CP} at high ethanol content is not yet understood but may be related to the non-ideal solvent behavior of the ethanol/water solvent mixtures. The UCST behavior of PA1 was also investigated in methanol/water solvent mixtures, as shown in Figure 4-4. Higher alcohol content was needed for the polymer to show thermoresponsive behavior in methanol/water solvent mixture due to the higher polarity of methanol leading to better solvation of the polyampholyte.

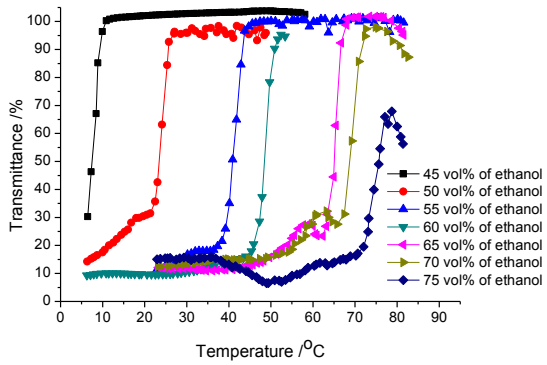

Figure 4-3 Transmittance versus temperature plots for 5 mg/ml PA1 solutions in different ethanol/water solvent mixtures.

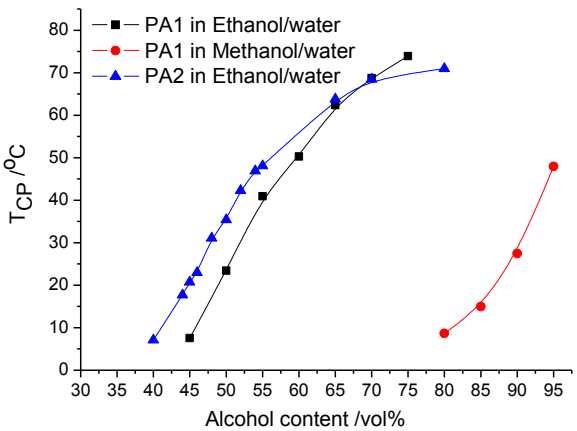

Figure 4-4 UCST phase transition temperatures versus alcohol content for PA1 and PA2 dissolved in alcohol/water solvent mixtures. Lines were added to guide the eyes.

4.2.3 Synthesis and self-assembly of a polyampholyte containing solvophilic comonomer

The tunable thermoresponsive behavior resulting from strong inter- and/or intra- chain electrostatic attraction provides a platform for the preparation of complex copolymers with various architectures, which allow the investigation of temperature controlled self-assembly. As a representative example, a brush copolymer polyampholyte prepared by copolymerization of charged comonomers and a neutral oligo(ethylene glycol) methyl ether methacrylate (OEGMA, Mn=480) comonomer was synthesized, as shown in Scheme 4-2. The statistical copolymer structure was employed in this report because of its much more facile synthesis compared to block copolymers, while self-assembly into well-defined structures is still possible as has been reported recently.[287-289]

The RAFT copolymerization was performed with the ratio of MA: DMAEMA: OEGMA: CTA: V70 at 90: 50: 25: 1: 0.1. Although with MA to DMAEMA ratio of 1.8, copolymer with identical DP of MA and DMAEMA, $MA_{38}DMAEMA_{38}OEGMA_x$, was still obtained. Actually, previous trial with MA to DMAEMA feed ratio at 2.5 was failed to obtain charge balanced copolymer. The reason for the changing of kinetic with third comonomer is still not clear.

The temperature responsive UCST-based self-assembly behavior triggered by temperature change was first evaluated in pure ethanol. A preliminary test of the solubility in ethanol revealed that PA3 is fully soluble in ethanol at room temperature, while PA1 and PA2 are not. Figure 4-5 displays the size distribution of PA3 dissolved in ethanol at 1 mg/ml during cooling from 15 ^{o}C to 5 ^{o}C. The copolymer was completely soluble in ethanol at temperatures higher than 10 ^{o}C as indicated by the small size of 6 nm corresponding to unimers that was detected by dynamic light scattering (DLS). By cooling down to 5 ^{o}C, the particle size dramatically increased to about 45 nm, together with a relatively low PDI (0.28), indicating the formation of defined nanostructure. The UCST-like temperature induced self-assembly of PA3 can be ascribed to collapse of the copolymer due to strong electrostatic interactions of the positive and negative charges, while the solvophilic ethylene glycol side chains serves as solvophilic corona that stabilizes the nano-structures and prevent further agglomeration.

The self-assembly behavior of copolymer PA3 was also investigated in isopropanol at 1 mg/ml while cooling from 60 to 20 ^{o}C, as shown in Figure 4-6. The aggregation of the copolymer in isopropanol happened at 50 ^{o}C, higher than in ethanol due to the lower polarity of the solvent. The particle size increased to about 35 nm when cooling down to 50 ^{o}C, together with the low PDI (0.17) indicating the formation of defined nanostructures. Interestingly, the size of the nanostructures gradually increased upon further cooling of the solution, which most likely due to the formation of larger agglomerates due to further electrostatic assembly indicating that in isopropanol the steric stabilization by the OEG chains is insufficient due to the stronger electrostatic attraction. Noteworthy is that defined nanostructures are obtained at 45 ^{o}C and lower with PDIs below 0.10.

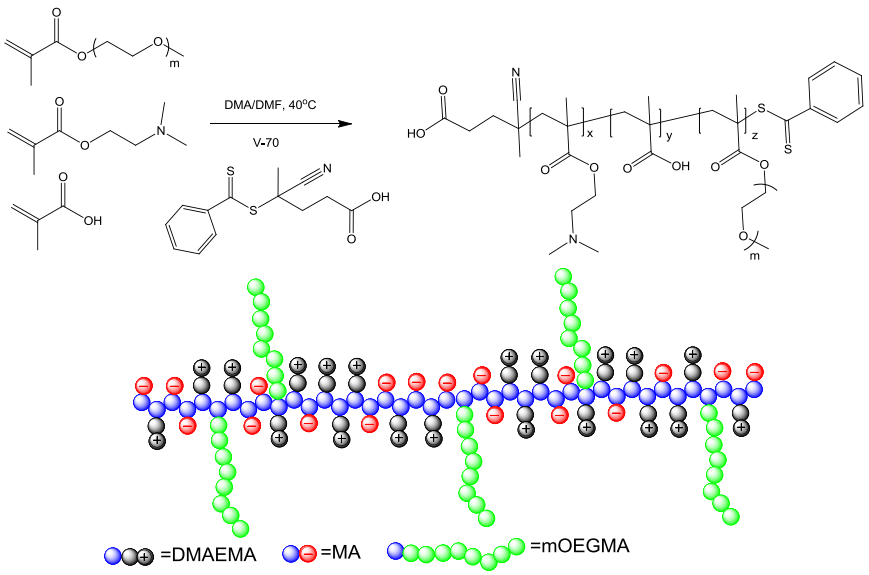

Scheme 4-2 Schematic representation of the synthesis and structure of polyampholyte with solvophilic side chains prepared by RAFT copolymerization of anionic and cationic monomers with oligo(ethylene glycol) methyl ether methacrylate.

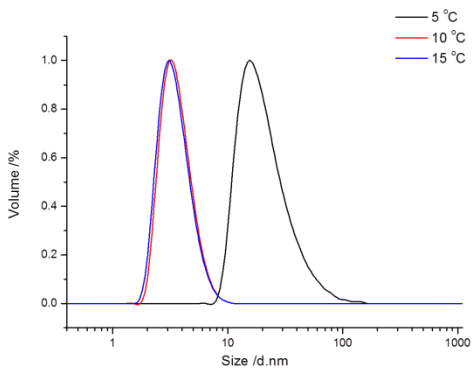

Figure 4-5 Size distribution at various temperatures of a PA3 in ethanol (1g/L) determined by DLS

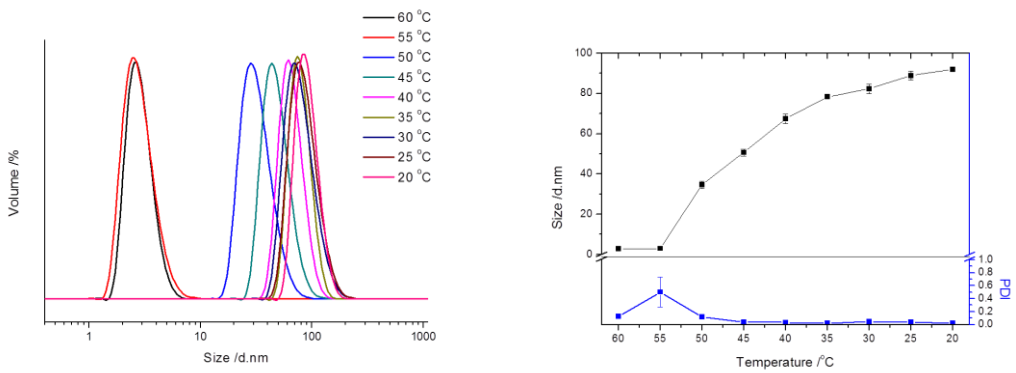

Figure 4-6 Left: Size distribution at various temperatures, and right: Z-average size and PDI versus temperature of a PA3 in isopropanol (1g/L) determined by DLS. Lines were added to guide the eyes.

4.3 Summary

Direct radical copolymerization of cationic and anionic monomers was investigated by reversible addition-fragmentation chain transfer (RAFT) procedure. The reactivity of the two monomers is severely influenced by their strong electronic interaction. However, fine-tuning of the feed ratio of the two monomers could suppress the gradient formation allowing the synthesis of quasi-random copolymers with equimolar amount of the anionic and cationic charge monomers. The resulting charge neutral polyampholytes were found to show UCST behavior in various alcohol/water solvent mixtures. In addition, the UCST of the copolymers can be well tuned by varying the content of alcohol in the solvent mixtures. The temperature-dependent inter- and/or intra-chain electrostatic attraction of the copolymers can be used for the preparation of UCST-based temperature controlled self-assembly. As a proof of concept, a polyampholyte with ethylene glycol side chains was synthesized. The copolymer was found to form defined nano-structures upon cooling in ethanol or isopropanol.

4.4 Experimental section

4.4.1 Materials and Instrumentation

All chemicals and solvents are commercially available and were used as received unless otherwise stated. Methanol, ethanol, isopropanol, *N*,*N*-dimethylformamide (DMF), *N*,*N*-dimethylacetamide (DMA) and diethyl ether were obtained from Sigma Aldrich. Deuterium oxide is supplied by Eurisotop.

^{1}H NMR spectra were recorded on a Bruker 300 MHz FT-NMR spectrometer using D_2O as solvent. Chemical shifts (d) are given in ppm relative to TMS.

Size-exclusion chromatography (SEC) characterization for the copolymers was performed on a Agilent 1260-series HPLC system equipped with a 1260 online degasser, a 1260 ISO-pump, a 1260 automatic liquid sampler (ALS), a thermostatted column compartment (TCC) at 50 ℃ equipped with a PSS Gram30 column in series with a PSS Gram1000 column, a 1260 diode array detector (DAD) and a 1260 refractive index detector (RID). The used eluent was DMA containing 50mM of LiCl at a flow rate of 0.6 ml/min. The spectra were analyzed using the Agilent Chemstation software with the GPC add on. Molar mass and PDI values were calculated against Varian PMMA standards.

Gas chromatography was performed on a 7890A from Agilent Technologies with an Agilent J&W Advanced Capillary GC column (30 m, 0.320 mm, and 0.25 μm). Injections were performed with an Agilent Technologies 7693 auto sampler. Detection was done with a FID detector. Injector and detector temperatures were kept constant at 250 and 280 ^{o}C, respectively. The column was initially set at 50 ^{o}C, followed by two heating stages: from 50 ^{o}C to 100 ^{o}C with a rate of 20 ^{o}C /min and from 100 ^{o}C to 300 ^{o}C with a rate of 40 ^{o}C

/min, and then held at this temperature for 0.5 minutes. Conversion was determined based on the integration of monomer peaks using DMA as internal standard.

Turbidity measurements were performed on a Cary 300 Bio UV-Visible spectrophotometer at a wavelength of 600 nm. The samples were first heated to a suitable temperature to fully dissolve the copolymer (5 mg ml^{-1}), after which the sample was placed in the instrument and cooled to 2 ^{o}C. The transmittance was measured during at least two controlled cooling/heating cycles with a cooling/heating rate of 1 ^{o}C min^{-1} while stirring in PS cuvettes controlled by block temperature probe. The resulting turbidimetry curve and T_{CP}s were calibrated by method developed by section 2.2.

Dynamic light scattering (DLS) was performed on a Zetasizer Nano-ZS apparatus (Malvern Instruments Ltd) using disposable cuvettes. The excitation light source was a He−Ne laser at 633 nm, and the intensity of the scattered light was measured at 173 °. This method measures the rate of the intensity fluctuation and the size of the particles is determined through the Stokes−Einstein equation

$$d(H)= kT/3\pi\eta D \qquad \text{Equation 4-1}$$

where d(H) is the mean hydrodynamic diameter, k is the Boltzmann constant, T is the absolute temperature, η is the viscosity of the dispersing medium, and D is the apparent diffusion coefficient. All samples were filtered through Millipore membranes with pore sizes of 0.2 μm prior to measurement.

4.4.2 Synthesis and characterization

For a typical RAFT copolymerization, methacrylic acid (MA), 2-(dimethylamino)ethyl methacrylate (DMAEMA), 4-cyano-4-(phenylcarbonothioylthio)pentanoic acid and V-70 were first dissolved in a DMF/DMA solvent mixture (80/20 vol) in a schlenk vial. The concentration of monomer was fixed at 2M. After degassing the solution three times by freeze-vacuum-thaw cycles, the schlenk vial was filled with argon and immersed in an oil bath preheated at 40 ^{o}C while stirring. The polymerization was performed for the required time and stopped by immersing the schlenk vial into a dry ice/isopropanol bath. The resulting polymer was isolated by precipitation in ether for three times followed by drying under reduced pressure at room temperature. Conversion of the monomers was analysed by GC with DMA as internal standard. Size exclusion chromatography was used to evaluate number average molar mass (Mn) and dispersity (Đ) of the obtained copolymers. For kinetic studies, samples were withdrawn from the polymerization mixture under a flow of argon at different times.

Chapter 5 UCST behavior of Poly(*N*,*N*-dimethylaminoethyl methacrylate) based on ionic interactions

Parts of this chapter were published on:

Q. Zhang, J.-D. Hong, R. Hoogenboom, *Polymer Chemistry* **2013**, 4, 4322.

My contribution includes the experiments, the interpreting of the results and the writing of the manuscripts.

Abstract: Poly(*N*,*N*-dimethylaminoethyl methacrylate) (PDMAEMA) has been reported to show both UCST and LCST behavior in presence of trivalent metal anions (Müller, 2007), which is attractive for the development of smart materials. In this chapter, the influence of the double thermoresponsive behavior of PDMAEMA by electrostatic interactions is investigated by comparing systems with $[Co(CN)_6]^{3-}$, $[Fe(CN)_6]^{3-}$ and $[Cr(CN)_6]^{3-}$ as trivalent counterions. The tuning of double thermoresponsive behavior of PDMAEMA by incorporating hydrophilic or hydrophobic comonomers will also described in presence of $[Fe(CN)_6]^{3-}$ as trivalent ion. In addition, based on the double thermoresponsive behavior of PMDAEMA, a new class of triple thermoresponsive 'schizophrenic' diblock copolymer that undergoes transitions from conventional micelles (or vesicles) via unimers to reverse micelles (or vesicles) and finally to a precipitated state upon heating is prepared. The various transition temperatures of this copolymer could be well controlled by the concentration of trivalent anion and pH.

5.1 Tuning the LCST and UCST thermoresponsive behavior of poly(*N*,*N*-dimethylaminoethyl methacrylate) by electrostatic interactions with multivalent metal ions and copolymerization

In this section, the tuning of the LCST and UCST behavior of PDMAEMA by electrostatic attractions with different trivalent ions and copolymerization with comonomers will be described. The development of a triple thermoresponsive 'schizophrenic' diblock copolymer based on the dual thermoresponsive behavior of PDMAEMA and LCST behavior of PDEGMA will be described in section 5.2.

5.1.1 Introduction

Thermoresponsive polymers are of great importance in numerous nanotechnological and biomedical applications.[1, 10, 241] The majority of these polymers undergo a reversible phase transition from soluble to insoluble when the environmental temperature is raised above their lower critical solution temperature (LCST), driven by dehydration of the polymer chains. The majority of reported thermoresponsive polymers show LCST type phase transitions, like poly(*N*-isopropyl acrylamide), poly(oligo(ethylene glycol)(meth)acrylate)[20, 26, 27] or poly(2-oxazoline).[3, 30] Polymers with the reverse behavior, i.e. polymers that are solubilized when heated above the upper critical solution temperature (UCST), have been much less documented as it is more challenging to achieve this behavior in aqueous solutions.[17] Only a few examples of polymers exhibiting both an LCST and a UCST have been reported. Examples are poly(vinyl alcohol)[290] and poly(ethylene glycol) (PEG).[291] However, those phase transition temperatures are usually higher than 100^{o}C or lower than 0^{o}C making it difficult to be applied as 'smart' materials.

Poly(*N*,*N*-dimethylaminoethyl methacrylate) (PDMAEMA) has been reported to not only show an LCST transition at around 60 ^{o}C in water, but also a UCST transition when a trivalent anionic hexacyanatocobaltate metal salt is added.[39, 292] This UCST behavior results from the electrostatic interactions between the protonated amine groups of the polymer and the trivalent metal salt, which allows tuning of the UCST transition temperature by varying the concentration of the trivalent counterion. Based on the easy preparation of such double thermoresponsive polymers, PEG/PDMAEMA miktoarm star polymers have been prepared, which self-assembled into spherical aggregates at high and low temperatures whereas molecularly dissolved polymer chains were only present at intermediate temperatures.[293] Similarly, we have prepared poly(di(ethylene glycol) methacrylate)(PDEGMA)-*b*-PDMAEMA block copolymer exhibiting triple thermoresponsive schizophrenic behavior as will be described in section 5.2. Based on the LCST transition of PDEGMA and the double thermoresponsive behavior of PDMAEMA, the copolymer undergoes transitions from conventional micelles via unimers to reversed aggregates (possibly vesicles) and finally to a precipitated state upon heating.

In this section, we will report the influence of the LCST and UCST thermoresponsive behavior of PDMAEMA by screening $[Co(CN)_6]^{3-}$, $[Fe(CN)_6]^{3-}$ and $[Cr(CN)_6]^{3-}$ as trivalent counterions. The tuning of

double thermoresponsive behavior of PDMAEMA in presence of $[Fe(CN)_6]^{3-}$ will also be investigated by incorporating hydrophilic or hydrophobic comonomers.

5.1.2 Results and discussion

The double responsive behavior of PDMAEMA (Table 5-1, DP=64) and its copolymers in aqueous solution were investigated by turbidimetry at pH 8 where only about 20% of the DMAEMA units are protonated and in pH 5 where all DMAEMA units are protonated.[294] Cloud point temperature (T_{CP}s) are defined as the temperature where transmittance passes through 50% during cooling (for UCST type of phase transition) or heating (for LCST type of phase transition). Figure 5-1 displays the T_{CP}s for both UCST and LCST transitions in the presence of different counterions at pH 8 and pH5 as a function of counterion concentration. At both pH values, the UCST-type T_{CP}s increases with addition of small amounts of the trivalent counterions and becomes constant when more ions are added. For the polymer solutions with different trivalent ions, the UCST-type T_{CP}s decreases following the increase of atomic number of the added metallic ions, which can be ascribed to the decreased electronic interaction between metal ions and protonated amines with increasing ion radius of the counterions. Interestingly, the LCST-type T_{CP}s in pH 8 were hardly affected by the type and concentration of counterions. In other words, the UCST transition temperature can be adjusted separately from the LCST transition. When lowering pH from pH 8 to pH 5, the UCST-type of T_{CP}s were found to increase due to the fact that more amine groups are protonated at lower pH leading to stronger electrostatic attraction between the chains. In contrast, the LCST-type T_{CP}s disappear in pH 5 buffer since the polymer is too hydrophilic when most of the amines are protonated.

The dependence of UCST behavior on pH can be utilized to switch the solubility of the polymer by changing the pH leading to pH responsive behavior. Figure 5-2, displays the transmittance of a PDMAEMA solution in presence of $[Fe(CN)_6]^{3-}$ as counterion as a function of pH values at 25 ^{o}C and 37 ^{o}C, obtained by titrating an 0.1 M HCl stock solution to the basic polymer solution. For both of the temperatures, a sharp drop in transmittance, representative for phase separation, was observed upon lowering the pH indicating the pH responsive behavior of the polymer. The phase transition pH shifted from pH 7.7 to pH 7.4 when increasing the temperature from 25 ^{o}C to 37 ^{o}C. The reversibility of pH triggered phase transition was evaluated at 25 ^{o}C by switching the pH between pH 9 and pH 5.5 for 3 times indicating that the pH responsive behavior is fully reversible at least for 3 rounds of pH switching between pH 9 and pH 5.5. This physiological relevant and tunable pH responsive behavior may be of great interesting for bio-related applications as minor changes in temperature can induce a phase transition around the physiological temperature (37 ^{o}C) and pH (7.4).

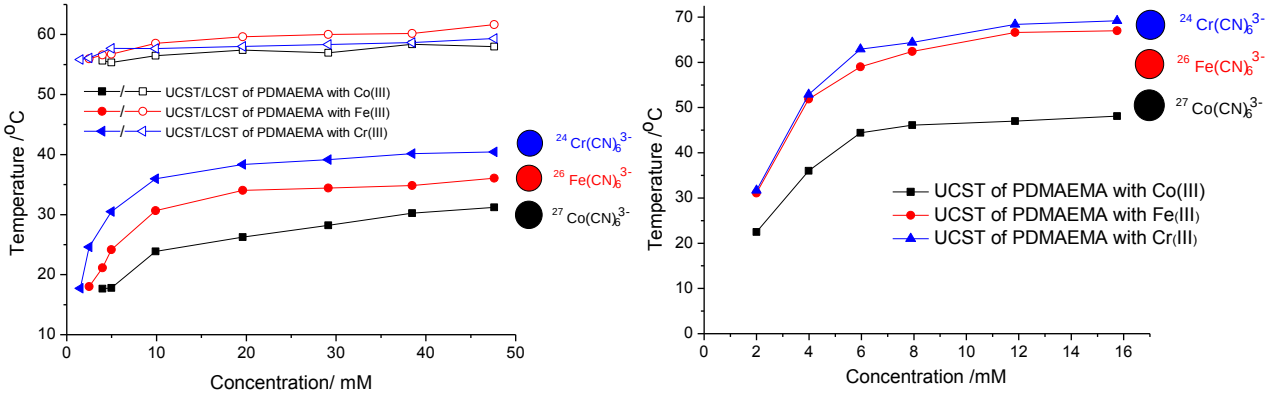

Figure 5-1 Dependence of the UCST and LCST phase transition temperatures of PDMAEMA in (left) pH 8 and (right) pH 5 as a function of trivalent anion salt concentration (polymer concentration was kept at 0.5 mg/ml, with 0.1 M of NaCl) in aqueous solution with $[Co(CN)_6]^{3-}$ (squares), $[Fe(CN)_6]^{3-}$ (circles) and $[Cr(CN)_6]^{3-}$ (triangles) as trivalent ions; closed symbols represent UCST type cloud points, open ones refer to cloud points of the LCST behaviour (lines are a guide to the eye).

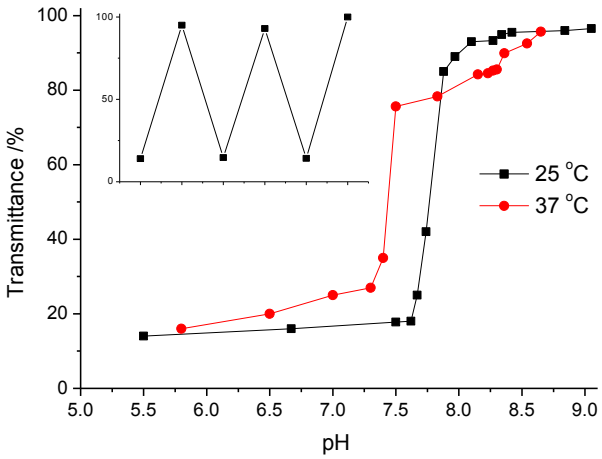

Figure 5-2 Transmittance versus pH for a PDMAEMA solution at 0.5mg/ml in presence of 10 mM $[Fe(CN)_6]^{3-}$ as counterion; the inset shows transmittance as a function of pH changing from 5.5 to 9 for 3 times (lines are a guide to the eye).

For the next step, we evaluated the influence of comonomers on the double thermoresponsive behavior of PDMAEMA. Hence, a series of PDMAEMA copolymers with DEGMA and ethylene glycol methyl ether methacrylate (EGMA) were prepared by reversible addition−fragmentation chain-transfer (RAFT) polymerization at 70 ℃ using a trithiocarbonate-based chain transfer agent (CTA) and azobisisobutyronitrile (AIBN) as initiator in a toluene/*N*,*N*-dimethylacetamide (DMA) (80/20, in volume) solvent mixture (

Scheme 5-1).

The kinetics of the DMAEMA and DEGMA copolymerization was evaluated via gas chromatography (GC) to follow monomer conversion and size exclusion chromatography (SEC) to follow the number average molecular weight (Mn) and dispersity (Đ) of the polymers in time (Figure 5-3). A linear increase of $\ln([M]_0/[M]_t)$ versus time was observed after a short inhibition period that is commonly observed for this RAFT system,[295, 296] whereby both monomers were incorporated in a similar rate. Furthermore, a linear increase of Mn with conversion and relatively low Đ were found, indicating good control over the copolymerization and the generation of near-ideal random copolymers.

Two monomers with different hydrophilicity, namely DEGMA and EGMA, were employed as comonomers for tuning the thermoresponsive behavior of PDMAEMA. Table 5-1 summarizes the properties of the obtained copolymers. SEC characterization of the purified copolymers suggests the formation of well-defined copolymer structures with different ratios of both comonomers as indicated by the low Đ values. To evaluate the composition of the obtained copolymers, ^{1}H NMR spectroscopy was performed on all the purified copolymers. Figure 5-4 and Figure 5-5 display the ^{1}H NMR spectra of the copolymers (normalized on the intensity of peak c) as well as the assignment of the peaks. As shown in Figure 5-4 and Figure 5-5, the content of (D)EGMA units, characterized by the characteristic methoxy peak (a) at around 3.3 *ppm*, was found to increase with increasing amount of the (D)EGMA in the feed ratio indicating the good control over polymer composition by copolymerization. The copolymer composition was quantified by comparing the integral ratio of the dimethyl group of DMAEMA (peak e) and the methyl group of (D)EGMA (peak a), which finely matches with the feed ratio of the two comonomers (see Table 5-1).

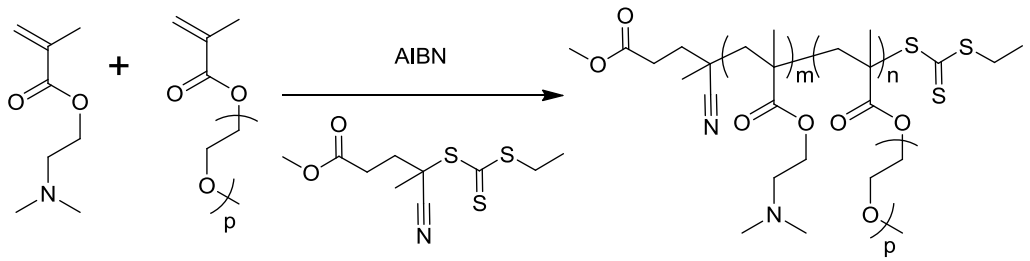

Scheme 5-1 Schematic representation of the synthesis of PDMAEMA copolymers with (D)EGMA via RAFT copolymerization.

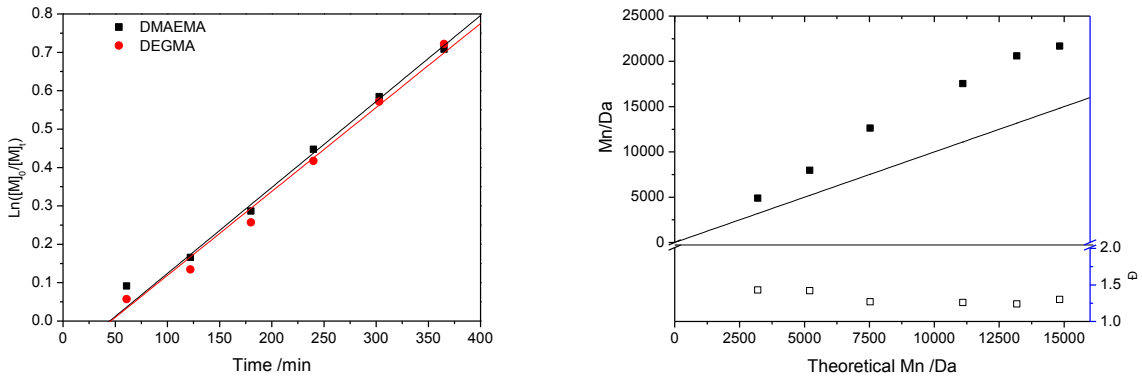

Figure 5-3 Left: Pseudo-first-order kinetic plot for the RAFT copolymerization of DMAEMA and DEGMA with DMAEMA: DEGMA: CTA: AIBN=80: 20: 1: 0.1. Right: Corresponding Mn and Đ versus theoretical Mn plot.

Table 5-1 Polymer composition and properties of the synthesized copolymers in this section

Polymers	Feed ratio DMAEMA:(D)EGMA:CTA	Theoretical DMAEMA content /%	DMAEMA content /%[a]	SEC Mn/kDa	Đ
PDMAEMA	100:0:1	100	100	11.2	1.16
P(DMAEMA$_{90}$-DEGMA$_{10}$)	90:10:1	90	89	14.1	1.19
P(DMAEMA$_{80}$-DEGMA$_{20}$)	80:20:1	80	79	12.8	1.20
P(DMAEMA$_{70}$-DEGMA$_{30}$)	70:30:1	70	69	11.8	1.19
P(DMAEMA$_{60}$-DEGMA$_{40}$)	60:40:1	60	58	11.5	1.21
P(DMAEMA$_{50}$-DEGMA$_{50}$)	50:50:1	50	51	11.5	1.21
P(DMAEMA$_{90}$-EGMA$_{10}$)	90:10:1	90	90	12.8	1.18
P(DMAEMA$_{80}$-EGMA$_{20}$)	80:20:1	80	78	11.4	1.19
P(DMAEMA$_{70}$-EGMA$_{30}$)	70:30:1	70	70	12.9	1.17
P(DMAEMA$_{60}$-EGMA$_{40}$)	60:40:1	60	59	12.1	1.18
P(DMAEMA$_{50}$-EGMA$_{50}$)	50:50:1	50	49	12.1	1.20

[a] Determined by ^{1}H NMR spectra of purified polymers

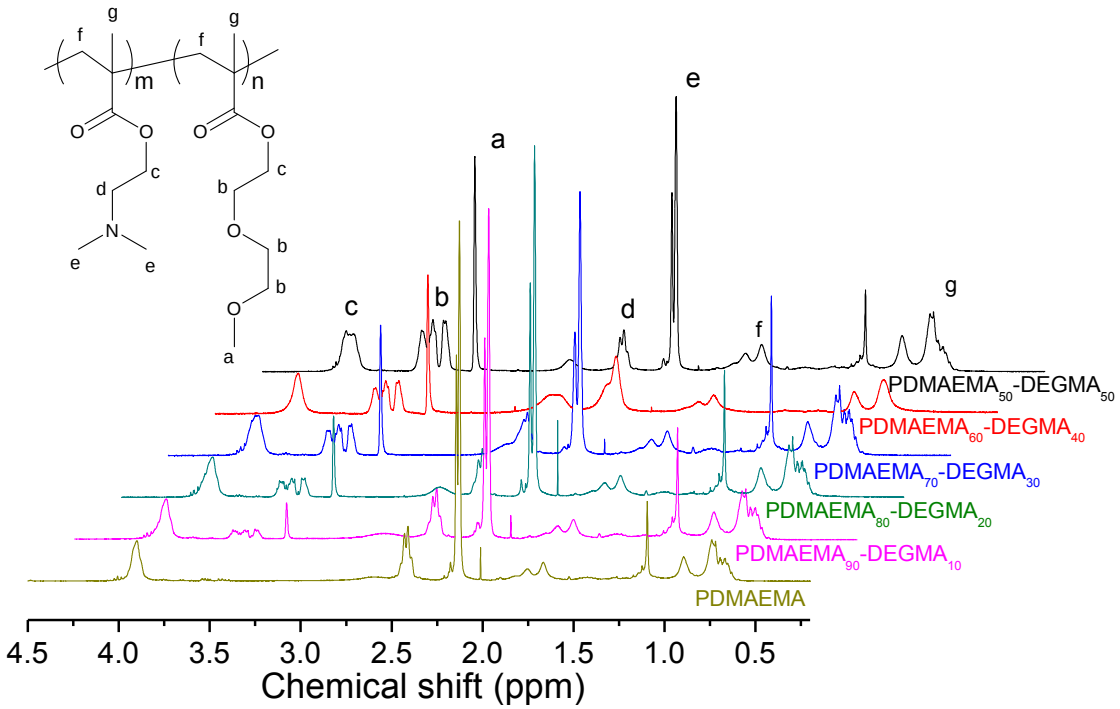

Figure 5-4 ^{1}H NMR spectra for the P(DMAEMA-DEGMA) copolymers

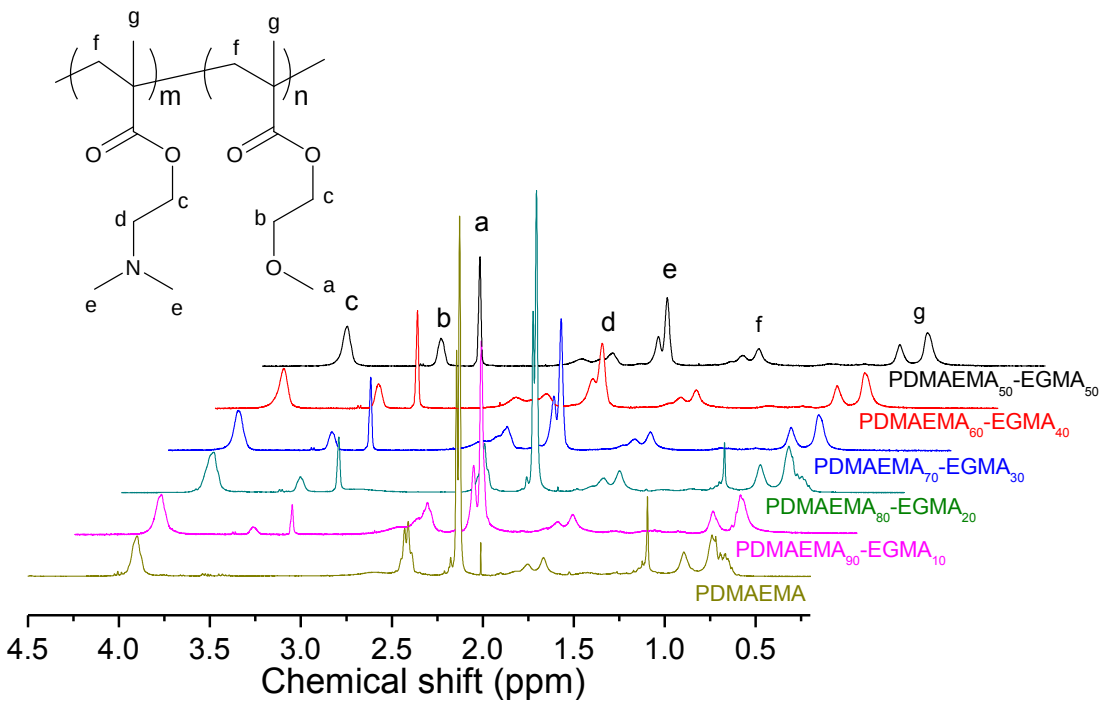

Figure 5-5 ^{1}H NMR spectra for the P(DMAEMA-EGMA) copolymers

After full characterization of the obtained copolymers, the double thermoresponsive behavior of all these copolymers was determined via turbidimetry in the presence of $[Fe(CN)_6]^{3-}$ as trivalent counterion. The iron

based trivalent ion was used because it has very low toxicity, while $[Co(CN)_6]^{3-}$ is very toxic. Figure 5-6 displays the T_{CP}s of P(DMAEMA-DEGMA) copolymers at pH 8 and pH 5. For both of the systems, the UCST-type T_{CP}s of PDMAEMA were significantly decreased with the introduction of DEGMA comonomers, which can be ascribed to the dilution of the (protonated) amine groups on the polymer chain leading to a decrease in electrostatic interactions as well as shielding of the (protonated) amine groups by the relatively long di(ethylene glycol) side chains. With further increasing of DEGMA comonomer content, the phase transition temperature was decreased until the copolymer became fully soluble for $P(DMAEMA_{50}$-$DEGMA_{50}$ (data not shown), since the interaction between protonated amines and trivalent counterions became too weak. In contrast, the LCST-type T_{CP}s at pH 8 are rather independent of polymer composition, which may be ascribed to the similar hydrophilicity of the two monomers. When lowering the pH from pH 8 to pH 5, no LCST-type phase transition of the PDMAEMA copolymers was detected below 110 ^{o}C due to the high hydrophilicity of the fully protonated DMAEMA copolymers.

The influence of the more hydrophobic comonomer, namely EGMA, on the thermoresponsive behavior of PDMAEMA is displayed in Figure 5-7. This comonomer with shorter ethylene glycol side chain has a similar influence on the UCST behavior of PDMAEMA in presence of trivalent counterions as indicated by the decreasing UCST-type T_{CP}s with increasing EGMA comonomer. This decrease in UCST-type T_{CP}s can be ascribed to the balance of two distinct effects of the EGMA comonomer on the PDMAEMA UCST thermoresponsiveness, i.e. lowering of the UCST T_{CP} by diluting the (protonated) amine groups on the one hand and increasing of the UCST T_{CP} due to the hydrophobic nature of the EGMA comonomer on the other hand. The LCST-type T_{CP}s exhibit a clear decrease upon introducing the EGMA comonomer due to the higher hydrophobicity of the EGMA than DMAEMA resulting in the simultaneously decrease of both UCST and LCST phase transition temperatures. No LCST-type phase transition was detected below 110 ^{o}C for any of the copolymers at pH 5 even with 50 % of hydrophobic EGMA copolymers indicating the high solubility of protonated amine groups.

A close comparison on the influence of the two comonomers was performed by plotting T_{CP}s versus comonomer content at pH 8, as shown in Figure 5-8. The UCST-type T_{CP}s for P(DMAEMA-DEGMA) copolymers was found to be lower than for P(DMAEMA-EGMA) copolymers with the same content of comonomers. In contrast, the introduction of DEGMA to PDMAEMA resulted in higher LCST-type T_{CP}s than that of EGMA copolymers leading to a wider of the gap between UCST and LCST for the P(DMAEMA-DEGMA) copolymers.

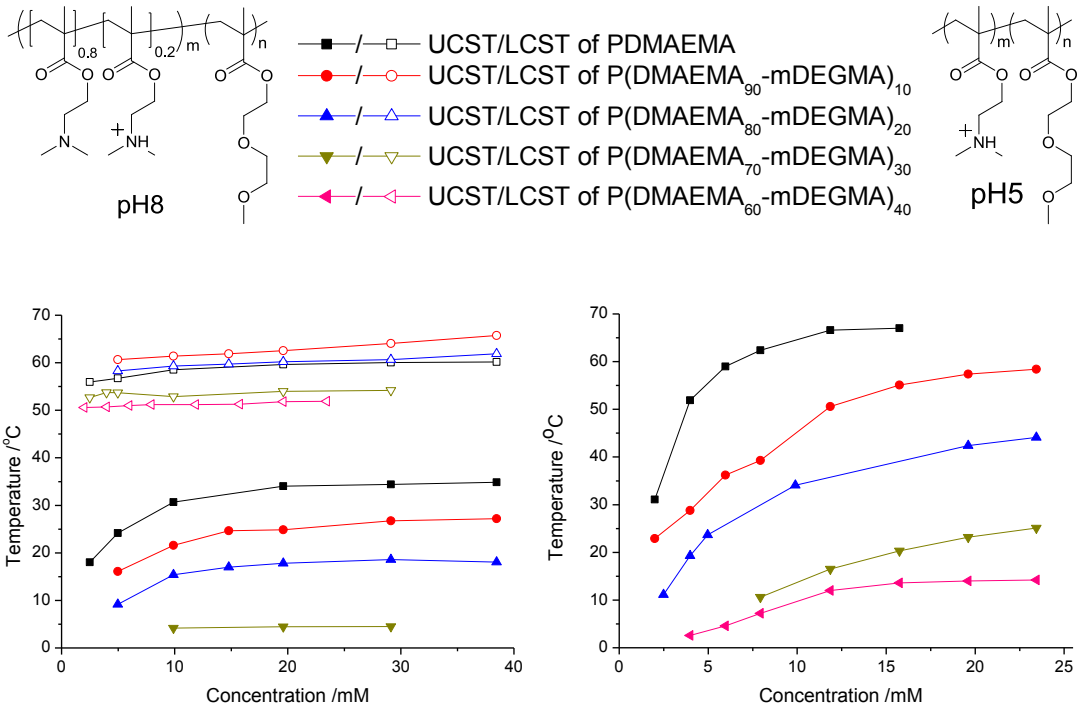

Figure 5-6 Dependence of the UCST and LCST phase transition temperatures for P(DMAEMA-DEGMA) copolymers as a function of counterion concentration (polymer concentration was kept at 0.5 g/L, with 0.1 M of NaCl) in aqueous solution at (Left) pH 8 and (Right) pH 5 with $[Fe(CN)_6]^{3-}$ as counterion; closed symbols represent UCST type cloud points, open symbols refer to cloud points of the LCST behavior (lines are a guide to the eye).

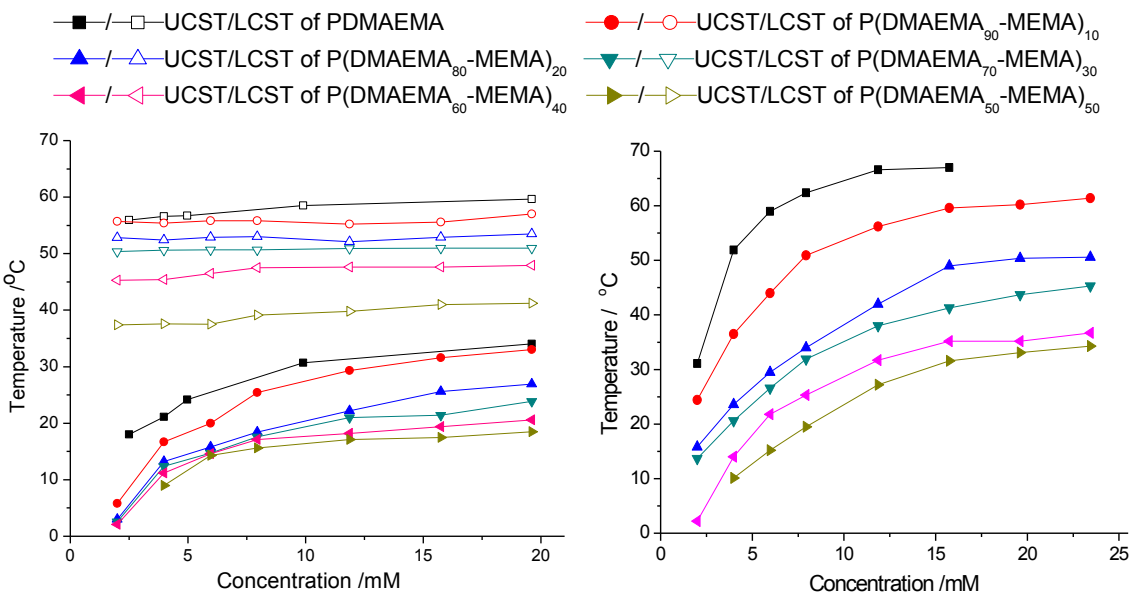

Figure 5-7 Dependence of the UCST and LCST phase transition temperatures of PDMAEMA-EGMA copolymers as a function of counterion concentration (polymer concentration was kept at 0.5 g/L, with 0.1 M of NaCl) in aqueous solution at (Left) pH 8 and (Right) pH 5 with $[Fe(CN)_6]^{3-}$ as trivalent ion; closed symbols represent UCST type cloud points, open symbols refer to cloud points of the LCST behavior (lines are a guide to the eye).

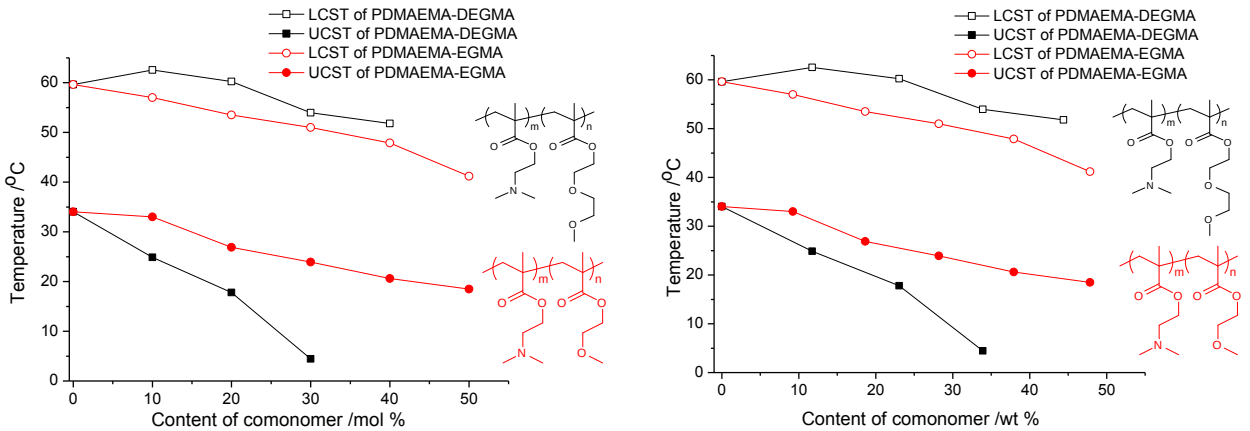

Figure 5-8 LCST and UCST type T_{CP}s for P(DMAEMA-DEGMA) and P(DMAEMA-EGMA) copolymers as a function of (Left) molar percentage and (Right) weight percentage of comonomer content in presence of 20 mM $[Fe(III)(CN)_6]^{3-}$ at pH 8.

5.1.3 Summary

In summary, the tuning of LCST and UCST thermoresponsive behavior of poly(*N*,*N*-dimethylaminoethyl methacrylate) (PDMAEMA) was investigated by electrostatic attractions with various trivalent metal anions and copolymerization with hydrophilic or hydrophobic comonomers.

The UCST T_{CP} of PDMAEMA was found to be highly tunable depending on the utilized counterions revealing an increase in T_{CP} with decreasing atomic number of the trivalent metal ions as a result of stronger electrostatic attraction. In the meantime, the LCST T_{CP}s were hardly affected by the type and concentration of counterions allowing independent adjusting of the UCST behavior of PDMAEMA. A series of DMAEMA statistical copolymers was synthesized by RAFT copolymerization with DEGMA or EGMA as comonomer. The double thermoresponsive behavior of the obtained copolymers was investigated in presence of $[Fe(CN)_6]^{3-}$ as counterions revealing that both the UCST and LCST transitions of PDMAEMA can be well tuned by copolymerization. A close comparison on the influence of the two comonomers revealed that the gap between UCST and LCST of PDMAEMA could be increased by introducing DEGMA as comonomer while EGMA induces a steady decrease at both UCST and LCST transition temperatures.

5.2 A triple thermoresponsive schizophrenic diblock copolymer based on the UCST and LCST behavior of PDMAEMA and LCST behavior of PDEGMA

5.2.1 Introduction

The terminology ‘schizophrenic’ copolymer was first reported by Armes to describe block copolymers that can form micelles and inverted micelles by simply changing the environmental conditions.[297] This first example of a schizophrenic block copolymer was based on poly(diethylaminoethyl methacrylate) as pH

responsive block and poly(2-(*N*-morpholino)ethyl methacrylate) as ionic strength responsive block. Based on their intriguing 'smart' behavior, schizophrenic block copolymers have received considerable interest in the past decade.[35, 298-303] However, the majority of early examples of schizophrenic block copolymers, combined two different response parameters such as pH and ionic strength,[1] or pH and temperature.[300] In 2002, the first examples of schizophrenic block copolymers were reported that could be switched from micelles to inversed micelles only by pH (Armes)[299] or only by temperature (Laschewsky).[35] Especially this latter type of temperature-switchable schizophrenic block copolymer is very attractive since switching can be achieved by simpy changing the temperature with no need to add salts, acids or bases to the solution providing good reversibility.[304-307] However, this type of schizophrenic block copolymers requires the combination of a polymer with quite common lower critical solution temperature (LCST) behavior and a polymer with much less common upper critical solution temperature (UCST) behavior.[3, 11, 17, 21, 36, 39] Up to this moment, all reported fully temperature responsive schizophrenic block copolymers that operate in water were based on sulfobetaines as UCST polymer.

In the current work we aimed to develop 1) fully temperature-responsive schizophrenic diblock copolymers that operate in water without using polybetaines as UCST block and 2) to further extend the thermoresponsive behavior by introducing a third phase transition from the inverted micellar state to a fully precipitated stated upon heating as schematically depicted in Figure 5-9, which is unattainable with polybetaines. Therefore, we will exploit the combined UCST and LCST behavior of PDMAEMA in the presence of hexacyanocobaltate(III) $[Co(CN)_6]^{3-}$ as trivalent counterion as reported by Mueller.[39] This unusual UCST behavior of PDMAEMA can be ascribed to electrostatic interactions between the (partially) protonated PDMAEMA and the trivalent anion leading to supramolecular crosslinks and is, thus, highly tunable by pH and ionic strength of the solution. Poly(oligo(ethylene glycol) methyl ether methacrylate)s (POEGMAs) with two different cloud points (T_{CP}), namely poly(di(ethylene glycol) methyl ether methacrylate) (PDEGMA, T_{CP}=26 °C[29, 182]) and Poly(tri(ethylene glycol) methyl ether methacrylate) (PTEGMA, T_{CP}=52 °C[182, 308]), will be employed as LCST block.

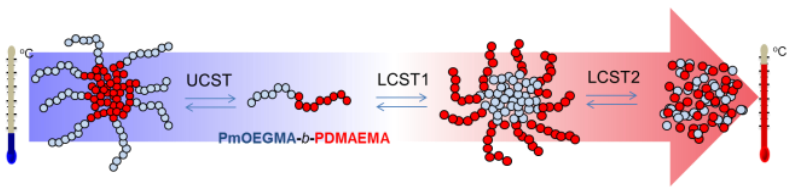

Figure 5-9 Schematic representation of the three proposed thermal transitions from conventional micelles via unimers to reverse micelles and finally a precipitated state by increasing the temperature of a POEGMA-*b*-PDMAEMA solution.

5.2.2 Results and discussions

The POEGMA-b-PDMAEMA block copolymers were synthesized by Reversible Addition Fragmentation Chain Transfer (RAFT) polymerization using methyl 4-cyano-4-[(dodecylsulfanylthiocarbonyl)sulfanyl]propionate as chain transfer agent (CTA) and iso-azobutyronitrile as initiator.[221] Aminolysis of the trithiocarbonate group was performed after the polymerization to remove the hydrophobic dodecyl group originated from the CTA followed by introducing a tri(ethylene glycol) methyl ether acrylate residue by thiol-ene modification (Scheme 5-2)[226, 309]. Kinetic studies of CTA (Figure 5-10) and macroCTA (Figure 5-11) mediated polymerizations revealed pseudo-first-order dependence, together with relatively low dispersity of the polymers, indicating good control of the polymerizations. Based on the kinetics of the polymerizations, a series of copolymers were synthesized, as listed in Table 5-2.

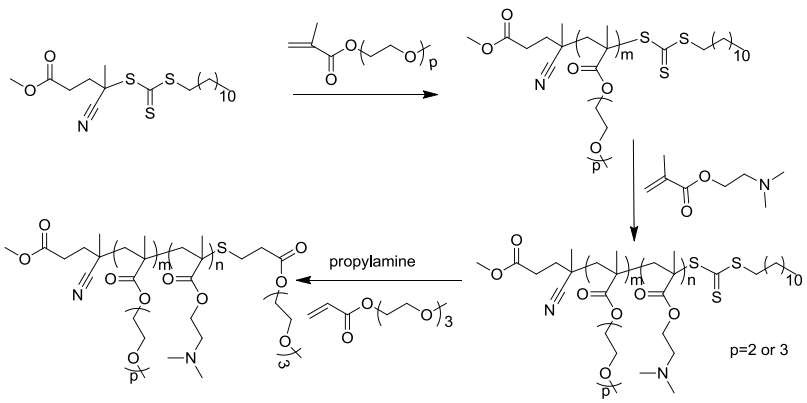

Scheme 5-2 Synthesis of the poly(OEGMA-*b*-DMAEMA) by sequential RAFT polymerization and subsequent aminolysis and thiol-ene modification of the chain end.

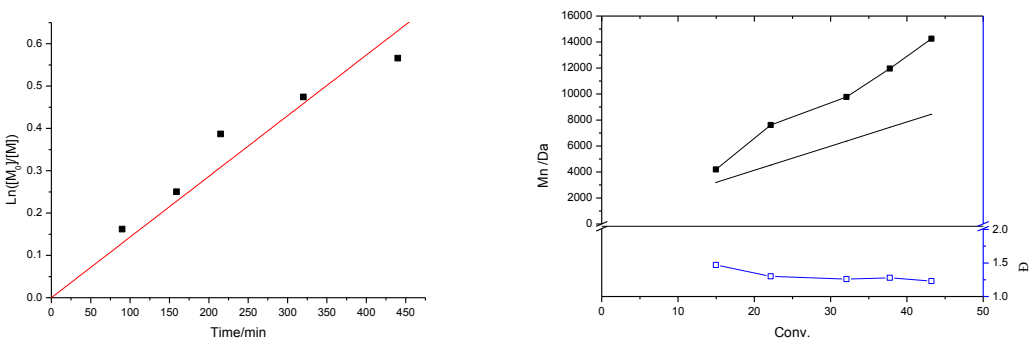

Figure 5-10 Left: Pseudo-first-order kinetic plot for TEGMA RAFT polymerization with monomer: CTA: AIBN=240: 3: 0.4. Right: Corresponding Mn and Đ versus conversion plot. The straight line represents theoretical Mn for different conversions.

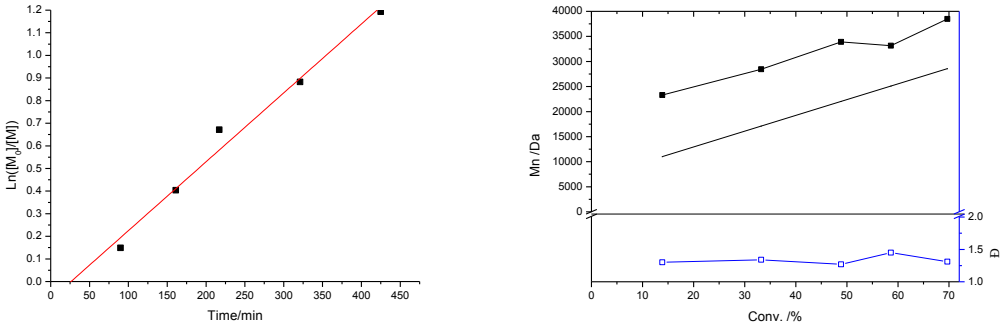

Figure 5-11 Left: Pseudo-first-order kinetic plot for DMAEMA RAFT polymerization with DMAEMA:PDEGMA mCTA: AIBN=200: 1: 0.3. Right: Corresponding Mn and Đ versus conversion. The straight line represents theoretical Mn for different conversions.

Table 5-2 Polymers synthesized by RAFT polymerization

Polymers	SEC		DP by GC conversion		DP by ^{1}H NMR[a]	
	Mn (kDa)	Đ	OEGMA	DMAEMA	OEGMA	DMAEMA
PTEGMA$_{29}$-mCTA	14.6	1.24	35	0	29	0
PDEGMA$_{49}$-mCTA	11.9	1.13	33	0	49	0
PmDMAEMA$_{50}$-mCTA	13.7	1.16	0	52	0	50
PTEGMA$_{29}$-b-PDMAEMA$_{56}$	30.9	1.42	35	80	29	56
PTEGMA$_{29}$-b-PDMAEMA$_{41}$	19.7	1.79[b]	35	50	29	41
PDEGMA$_{49}$-b-PDMAEMA$_{81}$	31.2	1.29	33	64	49	81
PDMAEMA$_{50}$-b-PDEGMA$_{86}$	36.0	1.18	39	52	86	50

[a] DP was calculated based on the ^{1}H NMR spectra of purified polymers; [b] It is not fully clear why this polymer has a larger dispersity, but it might be related to the relatively low DP of both blocks causing incomplete stabilization of the RAFT equilibrium.

PTEGMA$_{29}$-*b*-PDMAEMA$_{56}$ was first evaluated for schizophrenic micellization based on the UCST of PDMAEMA in the presence of $[Co(CN)_6]^{3-}$ at low temperatures and the LCST of PTEGMA at high temperatures. A solution of this polymer in pH5 buffer (at pH 5, PDMAEMA is fully protonated, and does not exhibit LCST behavior) with 0.1 M of NaCl (added to avoid strong variations in ionic strength upon addition of trivalent anion salt) and 1 mM of $K_3[Co(CN)_6]$ clearly revealed the presence of defined micelles with a size of 50 nm and a polydispersity index (PDI) of 0.07 at 10 ^oC (Figure 5-12a). Heating the solution to 30 ^oC led to disruption of the PDMAEMA $[Co(CN)_6]^{3-}$ association (UCST transition) and, thus, individually dissolved polymer chains were observed with a size of ~ 10 nm. Further heating to 61 ^oC induced the LCST transition of the PTEGMA block as indicated by the presence of somewhat polydisperse micellar aggregates (86 nm; PDI = 0.33); particles with this high PDI are possibly anisotropic rather than spherical[298]. However,

the exact structure was not further investigated since in this work we merely focussed on the conceptual ability of this complex schizophrenic block copolymer self-assembly. The temperature-induced phase transitions were studied in further detail by DLS, as shown in Figure 5-12b, revealing that the UCST phase transition occurs at 12 ^{o}C and the LCST phase transition occurs at 57 ^{o}C.

An analogues block copolymer with shorter PDMAEMA block, $PTEGMA_{29}$-b-$PDMAEMA_{41}$, also revealed similar schizophrenic micellization behavior. The polymer solution in pH5 buffer with 1 mM of $[Co(CN)_6]^{3-}$ was prepared and characterized by DLS at various temperatures, as shown in Figure 5-13. The UCST transition from PDMAEMA-cored micelles to individual polymer chains occurred at 7 ^{o}C and the LCST transition to PTEGMA-cored self-assembled structures occurred at 55 ^{o}C. Shortening the PDMAEMA block, thus, lowered both transition temperatures. In particular, the UCST transition is 5 ^{o}C lower, which can be ascribed to the decreased number of electrostatic interactions with the trivalent anion that need to be disrupted. The PDMAEMA-cored micelles of $PTEGMA_{29}$-b-$PDMAEMA_{41}$ at low temperatures are also found to be smaller compared to the $PTEGMA_{29}$-b-$PDMAEMA_{56}$, namely 31 nm instead of 44 nm at 7^{o}C, which is due to shortening of the PDMAEMA block. The size of PTEGMA-cored micelles at elevated temperatures is larger for the polymer with the shorter PDMAEMA block, as expected upon increasing the hydrophobic content. These results indicate that variation of polymer structure allows tuning of the schizophrenic self-assembly behavior.

To confirm the schizophrenic behavior of the $PTEGMA_{29}$-*b*-$PDMAEMA_{56}$ block copolymer, ^{1}H NMR spectra were recorded at various temperatures in D_2O at around pH 6 with 1 mM of $[Co(CN)_6]^{3-}$ and 0.1 M NaCl as shown in Figure 5-14. At 30 ^{o}C, all the signals of both blocks are clearly visible and the integral ratios correspond to the degree of polymerization as expected for fully dissolved block copolymers. However, at 10 ^{o}C the PDMAEMA signals were significantly broadened and highly attenuated, indicating that the PDMAEMA block formed the desolvated and confined state, i.e. the micellar core. In contrast, the peaks from the PTEGMA block were suppressed at 62 ^{o}C, especially signal c close to the hydrophobic polymer backbone, demonstrating the formation of PTEGMA-cored micelles and confirming the schizophrenic behavior of $PTEGMA_{29}$-*b*-$PDMAEMA_{56}$.

In a next step we have evaluated the double responsiveness of the block copolymer as a function of both trivalent anion concentration and pH. As shown in Figure 5-15, the UCST transition from micelles to dissolved polymer chains linearly and significantly relied on the concentration of trivalent $[Co(CN)_6]^{3-}$ anion at constant pH5 and 0.1 M NaCl concentration. Interestingly, the PTEGMA LCST transition temperture was not influenced and remained constant at *ca.* 59 ^{o}C. In other words, the UCST transition temperature can be adjusted separately from the LCST transition.

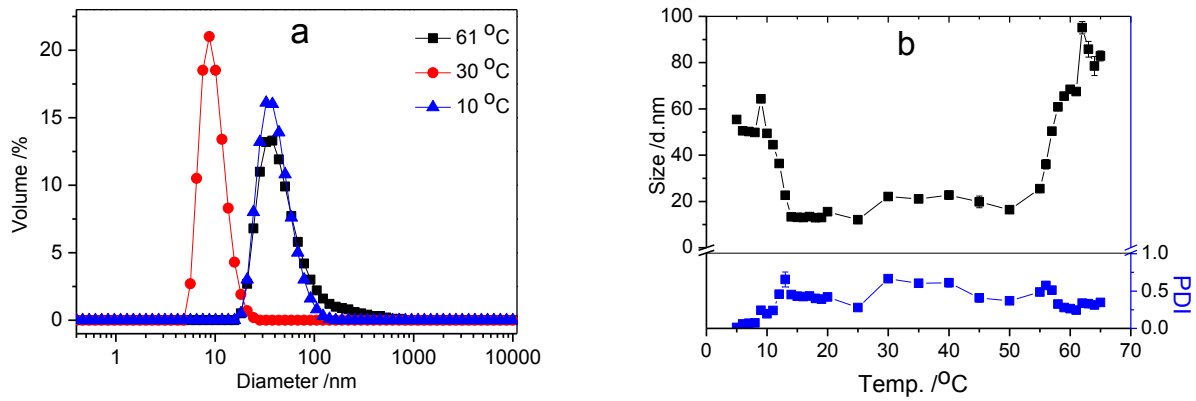

Figure 5-12 Size distribution at various temperatures and b) Z-average size and PDI versus temperture of a PTEGMA$_{29}$-*b*-PDMAEMA$_{56}$ aqueous solution (0.5 g/L in pH5 buffer with 0.1 M of NaCl and 1 mM of $K_3[Co(CN)_6]$) determined by DLS.

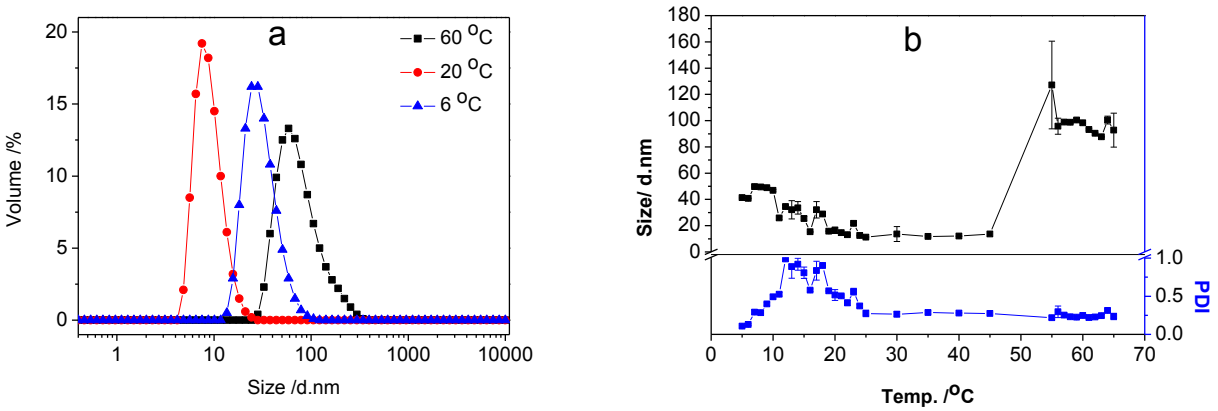

Figure 5-13 a) Micelles and unimers size distribution and b) size versus temperature of PTEGMA$_{29}$-*b*-PDMAEMA$_{41}$ aqueous solution at different temperatures (0.5 g/L in pH5 buffer with 0.1 M of NaCl and 1mM of $K_3[Co(CN)_6]$) determined by DLS.

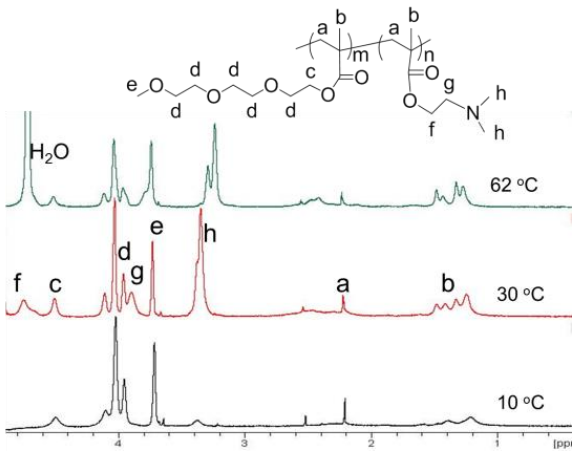

Figure 5-14 ^{1}H NMR spectra of PTEGMA$_{29}$-*b*-PDMAEMA$_{56}$ in deuterated pH 6 buffer recorded at 10, 30 and 62 ℃ with $[Co(CN)_6]^{3-}$ and NaCl at concentrations of 1 mM and 0.1 M, respectively.

Upon increasing the pH of the solution from 5 to 8 (1 mM $[Co(CN_{)6}]^{3-}$; 0.1 M NaCl) the UCST transition from micelles to dissolved chains occurred at 8 °C. However, instead of the formation of distinct micelles at the LCST transition of PTEGMA at 54 °C complete precipitation of the block copolymer sample was observed due to fact that the LCST transition temperature of PDMAEMA is about 60 °C at pH 8, which coincides with the LCST phase transition of PTEGMA[39] (see Figure 5-16).

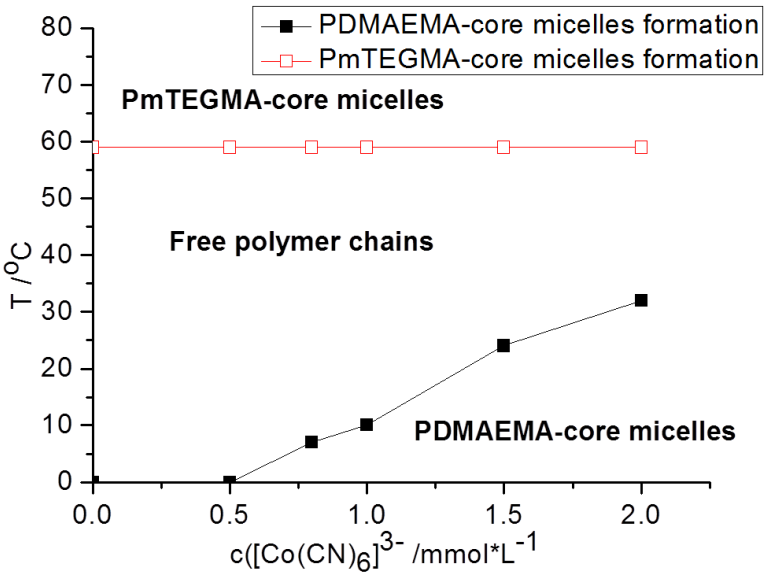

Figure 5-15 Dependence of the transition temperatures of $PTEGMA_{29}$-*b*-$PDMAEMA_{56}$, 0.5 g/L in pH 5 buffer with 0.1 M of NaCl on the concentration of counterion in aqueous solution determined by DLS. (lines are a guide to the eye).

The development of triple thermoresponsive schizophrenic diblock copolymers based on both the UCST transition of PDMAEMA with $[Co(CN)_6]^{3-}$ at low temperatures and the LCST transition of PDMAEMA at 60 °C (at pH 8) cannot be achieved with PTEGMA as second block due to the similarity of the PTEGMA and PDMAEMA LCST collapse temperatures. Therefore, PTEGMA was replaced by PDEGMA, that has a LCST transition around 25 °C, to study the triple thermoresponsive behavior (Scheme 5-2). DLS measurements were performed at different temperatures for the polymer solution of $PDEGMA_{49}$-*b*-$PDMAEMA_{81}$ with $[Co(CN)_6]^{3-}$ (Figure 5-17). Nearly monodisperse aggregates (118 nm; PDI=0.06) were formed at 10 °C, as proposed to be vesicles (not confirmed as mentioned previously). At 20 °C individually dissolved chains were present and at 35 °C self-assembled aggregates with a relatively narrow size distribution (d=481±5 nm, PDI=0.23±0.01) appeared, which is acribed to the LCST transition of PDEGMA resulting in the formation of presumably multilamellar vesicles as was previously reported for related block copolymers in the absence of $[Co(CN)_6]^{3-}$.[310] Further heating of the solution to 40 °C revealed a bimodal size distribution, closely resembling the previously reported observation for the transition from multilamellar vesicles to unilamellar vesicles.[310] Finally, a fully precipitated state as indicated by the very large particles detected by DLS was observed at 60 °C, which is ascribed to the LCST of PDMAEMA at pH8[39]. As such,

this is the first reported example of a triple responsive schizophrenic diblock copolymer, to the best of our knowledge. The more detailed thermoresponsive behavior of this polymer is depicted in Figure 5-17b clearly showing the UCST transition at 12 °C followed by the first LCST transition at 30 °C and the contraction/ conversion of the aggregate structures in between 39 °C and 50 °C followed by macroscopic precipitation at 60 °C. A second run of the measurement showed similar results indicating a good reversibility of this triple thermoresponsive schizophrenic behavior.

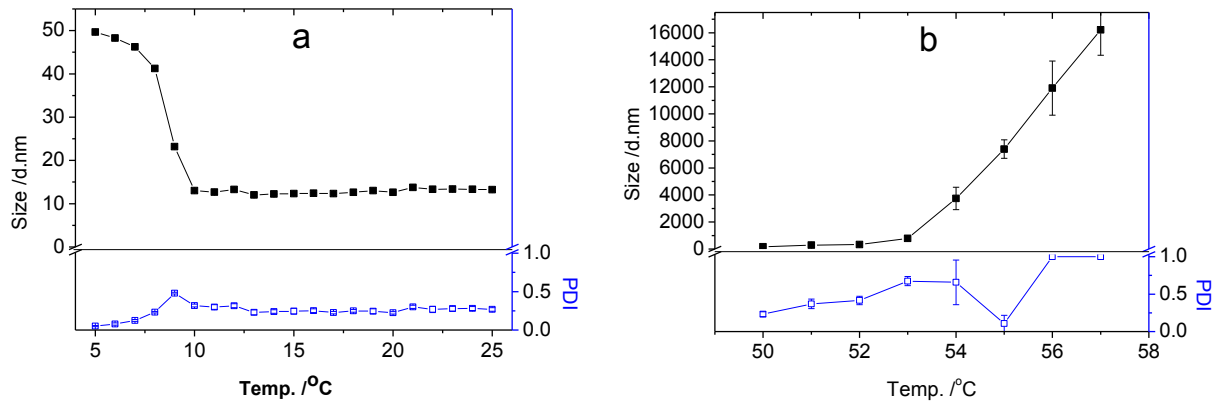

Figure 5-16 Size versus temperature of $PTEGMA_{29}$-*b*-$PDMAEMA_{56}$ aqueous solution at different temperatures (0.5 g/L in pH8 buffer with 0.1 M of NaCl and 1mM of $K_3[Co(CN)_6]$) determined by DLS.

To confirm the triple thermoresponsive and schizophrenic behavior of $PDEGMA_{49}$-*b*-$PDMAEMA_{81}$, ^1H NMR spectra of the polymer solution were recorded at various temperatures in deuterated pH8 buffer (Figure 5-18). It is quite clear that all the peaks corresponding to the polymer are highly suppressed at 62 °C, indicating complete insolubility of the polymer. At 40 °C, peaks related to PDEGMA block were slightly attenuated, especially signal c, due to the formation of aggregated structures, which is similar as observed in our previous report.[310] In the dissolved state at 25 °C all signals are present in the expected integral ratios. Finally, at 10 °C the signals from PDMAEMA were only slightly suppressed, which is different from the result for the block copolymer shown in Figure 5-14 at pH 5. Since the protonation of the PDMAEMA block at pH 8 will be significantly less than at pH 5, the electrostatic assembly with the trivalent anion is less efficient, apparently resulting in higher PDMAEMA mobility in the assembled state inducing less peak broadening/suppression in the ^1H NMR spectrum.

5.2.3 Summary

To Summarize, we have shown a new class of triple thermoresponsive 'schizophrenic' diblock copolymer that undergoes transitions from conventional micelles (or vesicles) via unimers to reverse micelles (or vesicles) and finally to a precipitated state upon heating. The various transition temperatures of this copolymer could well be tuned by varying the concentration of trivalent anion and pH.

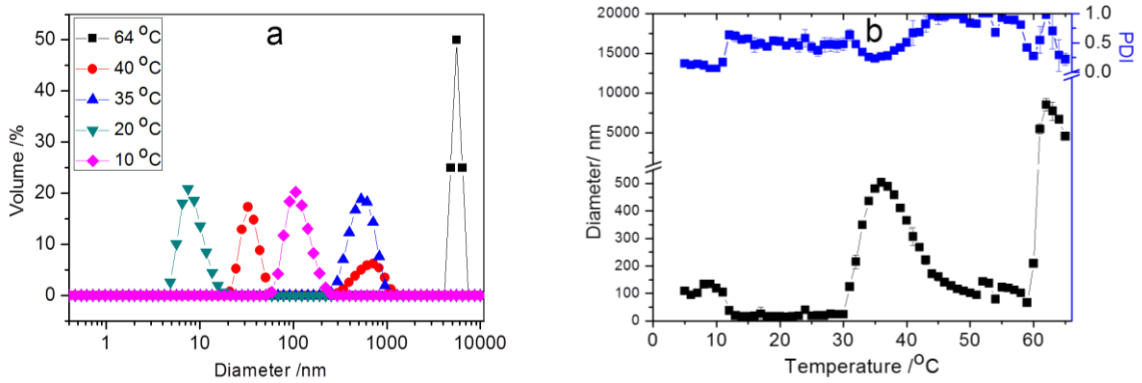

Figure 5-17 a) Size distributions and b) size versus temperature of a PDEGMA$_{49}$-*b*-PDMAEMA$_{81}$ aqueous solution at different temperatures (0.5 g/L in pH8 buffer with 0.1 M of NaCl and 1 mM of $K_3[Co(CN)_6]$) determined by DLS.

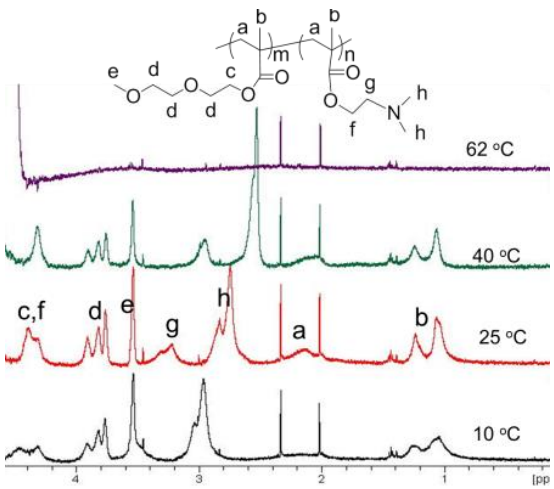

Figure 5-18 ^{1}H NMR spectra of PDEGMA$_{49}$-*b*-PDMAEMA$_{81}$ in deuterated pH8 buffer recorded at 10, 25, 40 and 62 ℃ with 1 mM $[Co(CN)_6]^{3-}$ and 0.1 M NaCl.

5.3 Experimental section

5.3.1 Materials

All chemicals and solvents were commercially available and used as received unless otherwise stated. Dichloromethane (DCM), toluene, *N*,*N*-dimethylacetamide (DMA), THF, methanol, $CDCl_3$, and hexane are obtained from Sigma Aldrich. DCM was distilled before use. Azobisisobutyronitrile (AIBN, 98%, Aldrich) was recrystallized from MeOH (twice) and stored in the freezer. 4-cyano-4-[(dodecylsulfanylthiocarbonyl)sulfanyl]pentanoic acid was purchased from Sigma Aldrich. Potassium hexacyanocobaltate(III) was purchased from Acros Organics. Potassium hexacyanochromate(III) and Potassium hexacyanoferrate(III) were obtained from Sigma Aldrich. pH buffers are obtained from Sigma Aldrich (pH 5) or prepared in the lab (pH 8). All polymerization were performed under an argon atmosphere.

5.3.2 Instrumentation

^{1}H NMR spectra for the structural characterization were recorded on a Bruker 300 MHz FT-NMR spectrometer using $CDCl_3$ as solvent. ^{1}H NMR study of temperature triggered self-assembly of polymers was recorded on a Bruker 500 MHz NMR spectrometer with deuterated pH buffers as solvent. Chemical shifts (d) are given in ppm relative to TMS.

Size-exclusion chromatography (SEC) was performed on an Agilent 1260-series HPLC system equipped with a 1260 online degasser, a 1260 ISO-pump, a 1260 automatic liquid sampler, a thermostatted column compartment, a 1260 diode array detector (DAD) and a 1260 refractive index detector (RID). Analyses were performed on a PSS Gram30 column in series with a PSS Gram1000 column at 50 C. DMA containing 50 mM of LiCl was used as an eluent at a flow rate of 1 ml min^{-1}. The SEC traces were analysed using the Agilent Chemstation software with the GPC add on. Molar mass and Đ values were calculated against PMMA standards.

Gas chromatography was performed on a 7890A from Agilent Technologies with an Agilent J&W Advanced Capillary GC column (30 m, 0.320 mm, and 0.25 μm). Injections were performed with an Agilent Technologies 7693 auto sampler. Detection was done with a FID detector. Injector and detector temperatures were kept constant at 250 and 280 ^{o}C, respectively. The column was initially set at 50 ^{o}C, followed by two heating stages: from 50 ^{o}C to 100 ^{o}C with a rate of 20 ^{o}C /min and from 100 ^{o}C to 300 ^{o}C with a rate of 40 ^{o}C /min, and then held at this temperature for 0.5 minutes. Conversion was determined based on the integration of monomer peaks using DMA as internal standard.

Turbidity measurements were performed on a Cary 300 Bio UV-Visible spectrophotometer at a wavelength of 600 nm. The samples were first cooled to a suitable temperature to fully dissolve the copolymer (5 mg ml^{-1}), after which the sample was placed in the instrument and cooled to 5 ^{o}C. The transmittance was measured during at least two controlled cooling/heating cycles with a cooling/heating rate of 1 ^{o}C min^{-1} while stirring. Cloud point temperatures (T_{CP}s) were calibrated by the method developed in section 2.1.4.

Part of the solubility screening was also performed on a Crystal 16 TM from Avantium Technologies. These samples were analyzed in the temperature range from 0 ℃ to 110 ℃ with heating and cooling ramps of 1 ℃ min^{-1} under stirring. In the Crystal 16 four blocks of four parallel temperature controlled sample holders are connected to a Julabo FP40 cryostat allowing 16 simultaneous measurements. All vials were visually inspected after the heating program to facilitate the interpretation of the observed transmission profiles. Samples that gave unexpected transmission profiles were remeasured.

Dynamic light scattering (DLS) was performed on a Zetasizer Nano-ZS apparatus (Malvern Instruments Ltd) using disposable cuvettes. The excitation light source was a He−Ne laser at 633 nm, and the intensity of

the scattered light was measured at 173 °. This method measures the rate of the intensity fluctuation and the size of the particles is determined through the Stokes−Einstein equation

$$d(H)= kT/3\pi\eta D \qquad \text{Equation 5-1}$$

where d(H) is the mean hydrodynamic diameter, k is the Boltzmann constant, T is the absolute temperature, η is the viscosity of the dispersing medium, and D is the apparent diffusion coefficient. Polymer solutions at different pH were measured at various temperatures. Before starting the measurements, samples were incubated at specific temperature for at least 300s to reach equilibrium. All samples were filtered through Millipore membranes with pore sizes of 0.2 μm prior to measurement.

5.3.3 Synthetic methods

Synthesis of 4-cyano-4-(ethylsulfanylthiocarbonyl)sulfanyl pentanoic acid (ECT)

4-Cyano-4-(ethylsulfanylthiocarbonyl)sulfanylpentanoic acid (ECT), was synthesized as previously described by Convertine et al.[311] At first, ethanethiol (4.72 g, 76 mmol) was added dropwise with stirring over 10 min, to a suspension of sodium hydride (NaH) (60% in oil) (3.15 g, 79 mmol) in 150 mL of diethyl ether at 0 ^{o}C. The reaction was left to stir at 0 ^{o}C for 20 min before the addition of carbon disulfide (CS_2) (6.0 g, 79 mmol). The yellowish crude precipitate of sodium S-ethyl trithiocarbonate was collected by filtration and further reacted with iodine (6.3 g, 25 mmol) in 100 mL of diethyl ether for 1h at room temperature. The resulting solution was filtered, washed with aqueous sodium thiosulfate, dried over sodium sulfate and concentrated under reduced pressure to obtain crude bis(ethylfulfanythiocarbonyl)disulfide. Later, the crude bis(ethylfulfanythiocarbonyl) disulfide (1.37 g, 5.0 mmol) was further refluxed with 4,4′-azobis(4-cyanopentanoic acid) (2.10 g, 7.5 mol) in ethylacetate for 18h to obtain crude ECT. The crude ECT was purified by column chromatography using silica gel as the stationary phase and ethylacetate:hexane (50:50) as the mobile phase. The compound was further recrystallized from hexane to obtain pure ECT as pale yellow powder. ^{1}H NMR (300MHz, $CDCl_3$): δ 1.36 t (SCH_2CH_3); δ 1.88 s ($CCNCH_3$); δ 2.3–2.65 m (CH_2CH_2); δ 3.35 q (SCH_2CH_3).

Synthesis of methyl 4-cyano-4-[(dodecylsulfanylthiocarbonyl)sulfanyl]propionate and methyl 4-cyano-4-(ethylsulfanylthiocarbonyl)sulfanyl propionate

The procedure for the synthesis of *methyl 4-cyano-4-[(dodecylsulfanylthiocarbonyl)sulfanyl]propionate* is described here as representative example. A solution of 4-cyano-4-[(dodecylsulfanylthiocarbonyl)sulfanyl]pentanoic acid (500 mg, 1.24mmol), and methanol (1.5 ml, 37 mmol) in DCM (40 ml) was cooled to 0 ^{o}C in an ice water bath. N-(3-dimethylaminopropyl)-N’-ethylcarbodiimide hydrochloride (285 mg, 1.49 mmol) and 4-dimethylaminopyridine (18.2 mg, 0.15 mmol) in DCM (20 ml) was added dropwise with vigorous stirring. Then the solution was allowed to react for 16 h at room

temperature. After that, the solution was washed with water for two times followed by adding a large amount of sodium sulfate. Then the mixture was filtrated after being stirred for 10 min. The filtrate was collected and dried on a rotary evaporator. The crude product was purified by flash column chromatography using ethyl acetate/hexane (1:1) as solvent system. The yellow product was collected after 24 h drying under reduced pressure (yield 75%). ^{1}H NMR was recorded as shown in Figure 5-19.

Synthesis of PTEGMA macro-CTA, PDEGMA macro-CTA and PDMAEMA macro-CTA

The procedure for TEGMA is described here as representative example. TEGMA, AIBN and CTA were first dissolved in toluene/DMA solvent mixture (80/20 vol) in a schlenk vial. The concentration of monomer was fixed at 2M. After degassing the solution three times by freeze-vacuum-thaw cycles, the schlenk vial was filled with nitrogen and immersed in an oil bath preheated at 70 ^{o}C while stirring. The polymerization was performed for the required time and stopped by immersing the schlenk vial into a dry ice/isopropanol bath. The resulting polymer was isolated by precipitation in hexane (three times) followed by drying under reduced pressure at 50 ^{o}C. Conversion of the monomers was analysed by GC with DMA as internal standard. Size exclusion chromatography was used to evaluate number average molecular weight (Mn) and dispersity (Đ) of the obtained polymers. For kinetic studies, samples were withdrawn from the polymerization mixture under a flow of nitrogen at different times.

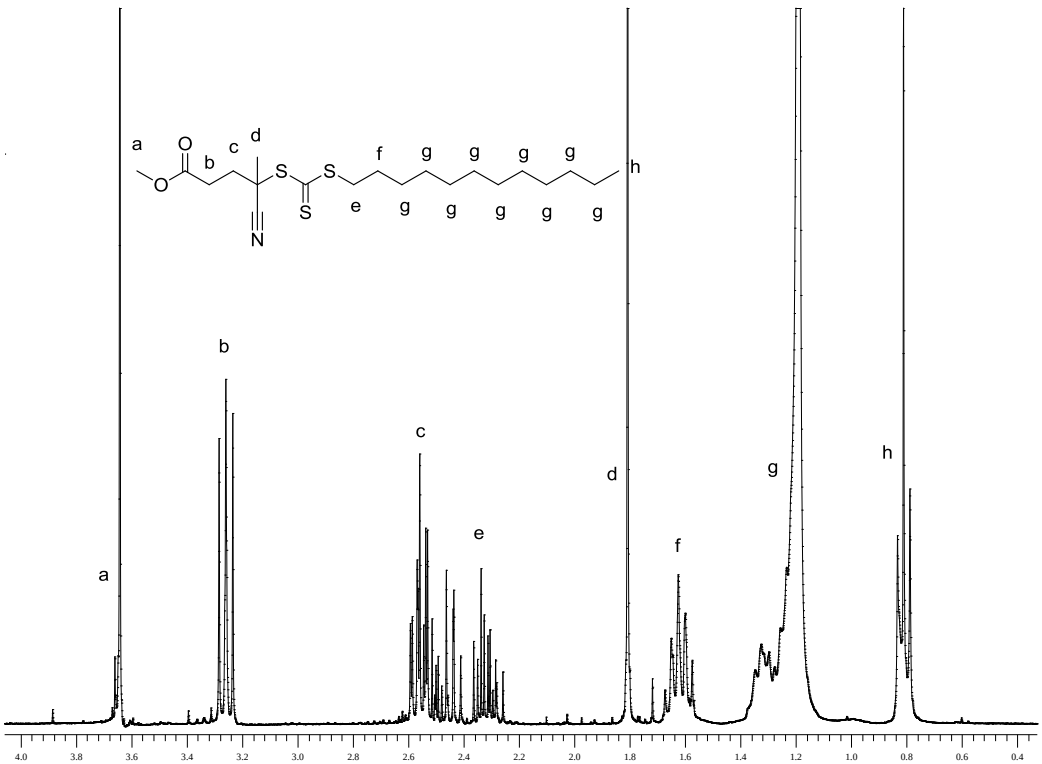

Figure 5-19 ^{1}H NMR spectrum of methyl 4-cyano-4-[(dodecylsulfanylthiocarbonyl)sulfanyl]propionate

Synthesis of PDMAEMA homopolymer, P(DMAEMA-DEGMA) and P(DMAEMA-EGMA)copolymers

ECT, AIBN and monomer(s) were first dissolved in toluene/DMA solvent mixture (80/20 vol) in a schlenk vial. The concentration of monomer(s) was fixed at 2M. After degassing the solution three times by freeze-vacuum-thaw cycles, the schlenk vial was filled with nitrogen and immersed in an oil bath preheated at 70 ^{o}C while stirring. The polymerization was performed for 8h and stopped by immersing the schlenk vial into a dry ice/isopropanol bath. The resulting polymer was isolated by precipitation in hexane/ether (40/60 in volume) for three times followed by drying under reduced pressure at 50 ^{o}C. Size exclusion chromatography was used to evaluate number average molecular weight (Mn) and dispersity (Đ) of the obtained polymers. For kinetic studies, samples were withdrawn from the polymerization mixture under a flow of nitrogen at different times.

Synthesis of block copolymers and subsequently functionalization

The synthesis of PDEGMA-b-PDMAEMA is described here as representative example. DMAEMA, PDEGMA macro-CTA and AIBN were first dissolved in a toluene/DMA mixture solvent (80/20 vol) in a schlenk vial. The concentration of monomer was fixed at 1.5 M. After degassing the solution three times by freeze-vacuum-thaw cycles, the schlenk vial was filled with nitrogen and immersed in an oil bath preheated at 70 ^{o}C while stirring. The polymerization was performed for the required time and stopped by immersing the reaction flask into a dry ice isopropanol bath. The resulting polymer was isolated by precipitation in hexane (three times) followed by drying under reduced pressure. The polymer was dissolved in dichloromethane and excess amount of propylamine/mTEGA (methoxy tri(ethylene glycol) monoacrylate) were then added into the polymerization solution under argon. The solution was then allowed to react overnight for the aminolysis and thiol-ene reaction. The resulting polymer was isolated by precipitation in hexane (three times) followed by drying under reduced pressure. Conversion of the monomers was analysed by GC with DMA as internal standard. Size exclusion chromatography was used to evaluate number average molecular weight (Mn) and dispersity (Đ) of the obtained polymers. For kinetic studies, samples were withdrawn from the polymerization mixture under a flow of nitrogen at different times.

Chapter 6 Cooperative behavior of thermoresponsive polymers

Abstract: LCST polymers undergo a reversible phase transition from hydrophilic to hydrophobic when heated. The interaction between polymer chains during temperature induced aggregation can lead to a cooperative behavior of thermoresponsive polymers.

Fine-tuning the LCST behavior of aqueous polymer solutions via simple mixing of polymers with different T_{CP}s is an attractive strategy since re-synthesis or copolymerization can be avoided. It has been suggested that polymers with molecular weight dependent T_{CP}s are essential to obtain such cooperative behavior (Gibson, 2012). In this section, we will report the cooperative LCST behavior of copoly(2-oxazoline)s with various T_{CP}s ranging from 25 to 90 ^{o}C. The results suggested that the hydrophilicity of the mixed copolymers is also a key factor to control the cooperative behavior of poly(2-oxazoline)s as only mixtures of the most hydrophilic copolymers revealed such cooperative behavior.

The cooperative self-assembly behavior of a thermoresponsive statistical copolymer and a double hydrophilic block copolymer having a permanently hydrophilic block and a thermoresponsive block was also investigated. By adjusting the hydrophilicity of the thermoresponsive statistical copolymers, well defined hybrid nanoparticles were obtained with various ratios of the two species. Importantly, the size of these defined nanoparticles can be accurately tuned from 40 to 300 nm dependent on the T_{CP} and the amount of statistical copolymers in the solution. This developed co-assembly of statistical copolymers and block copolymers method provides a highly tunable platform for the preparation of well-defined polymeric nanoparticles.

6.1 Understanding cooperative lower critical solution temperature behavior based on poly(2-oxazoline)s with systematical variations in hydrophobicity

6.1.1 Introduction

Fine-tuning the lower critical solution temperature (LCST) of aqueous polymer solutions via simple mixing of polymers with different cloud point temperatures (T_{CP}s) is an attractive strategy since re-synthesis or copolymerization can be avoided.[312] Obtaining controlled intermediate T_{CP}s via mixing of two polymers with different T_{CP}s can be referred to as cooperative LCST behavior. It has been suggested by Gibson and coworkers that polymers with molecular weight dependent T_{CP}s are essential to obtain such cooperative behavior based on screening of mixtures of poly(*N*-vinyl pyrrolidone)s, poly(*N*-isopropylacrylamide)s, poly(*N*-vinylcaprolactam)s and poly((oligo(ethyleneglycol) methacrylate)s.[235] However, poly(2-oxazoline)s, as a highly tunable family of thermoresponsive (co)polymers, were not included in the work. In this section, we report a systematical study on the cooperative LCST behavior of copoly(2-oxazoline)s with various hydrophobicity.

6.1.2 Results and discussion

The synthesis of a series of thermoresponsive poly(2-oxazoline) copolymers by living cationic ring opening polymerization of 2-ethyl-2-oxazoline and 2-n-propyl-2-oxazoline was previously performed as described in reference.[238] By variation of the monomer ratios, copolymers with various T_{CP}s were obtained that were used for the cooperative behavior investigation in this study (Scheme 6-1).

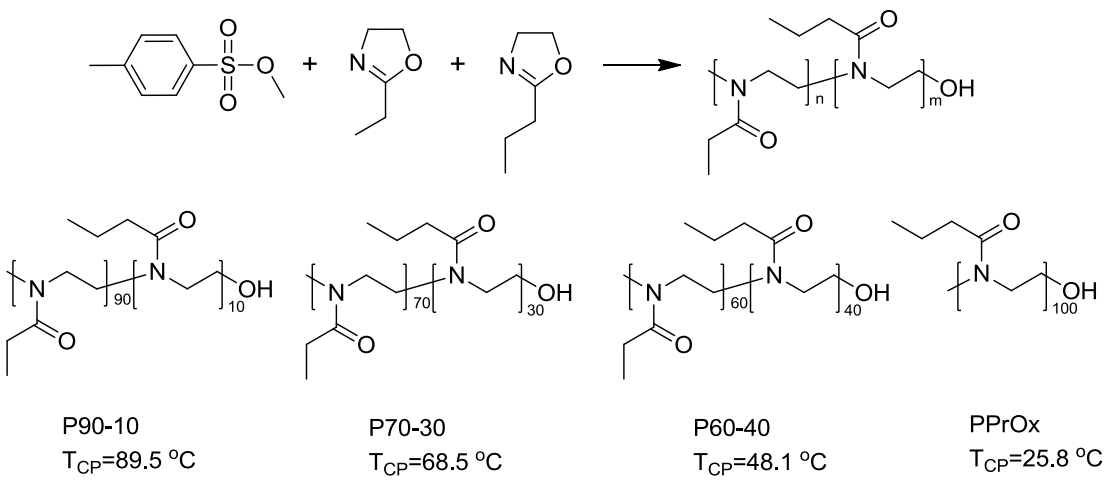

Scheme 6-1 Top) Schematic representation of the methyl tosylate initiated cationic ring-opening copolymerization of 2-ethyl-2-oxazolines and 2-n-propyl-2-oxazoline; Bottom) copolymers used for the cooperative behavior investigation. (T_{CP}s were obtained at 5 mg/ml)

The T_{CP}s of the poly(2-oxazoline) copolymers were reported to decrease with increasing chain length indicating molecular weight dependency, although this was much stronger for more hydrophilic copolymers.[238] According to literature,[235] we may thus expect that mixing of different copoly(2-oxazoline)s gives rise to cooperative LCST behavior. Therefore, the thermoresponsive behavior of copolymer mixtures with various compositions was investigated by turbidimetry at a total copolymer concentration of 5 mg/ml in MilliQ water. The turbidimetry curves for the solutions of polymer mixtures consisting of the most hydrophobic (co)polymers PPrOx and P60-40 are shown in Figure 6-1. The phase transition for pure PPrOx was found to be not influenced by adding P60-40 up to as much as 40 wt% in the total polymer mixture. A slight shift of the turbidimetry curve to higher temperatures could be detected with further increasing of P60-40 content to 80 wt%, which, however, results from the dilution of PPrOx, as was also reported for the mixtures of POEGMAs.[235] The T_{CP} shift of 2 ^{o}C for the polymer blend when going from pure PPrOx to only 20 wt% PPrOx is similar as the shift expected upon dilution of the concentration of PPrOx from 5 mg/ml to 1 mg/ml.[238] These results clearly indicate that molecular weight dependence of T_{CP}s is not the only reason for the cooperative behavior as PPrOx does show molar mass dependent T_{CP}s but no cooperativity. To illuminate the reason for the cooperative behavior, PPrOx was replaced with a more hydrophilic copolymer to study the influence of hydrophobicity.

Figure 6-2 shows the results from mixtures of P70-30 and P60-40 at various compositions. These copolymers with relatively higher hydrophilicity neither showed cooperative behavior as indicated by the unaffected phase transition of P60-40. The tiny increasing of T_{CP}s for polymer mixtures containing more than 40 wt% P70-30 could also be ascribed to the T_{CP} increase of P60-40 upon dilution. Therefore, to further evaluate the influence of hydrophilicity on the cooperative behavior, an even more hydrophilic poly(2-oxazoline) copolymer, namely P90-10 with a T_{CP} at 90 ^{o}C was also mixed with P70-30.

The turbidimetry curves for mixtures of the hydrophilic P90-10 and P70-30 with different compositions are displayed in Figure 6-3. While the individual copolymers show phase transition at 69 and 90 ^{o}C, respectively, mixtures of these copolymers exhibit turbidimetry curves with T_{CP}s lying in between those of the two pure polymers and are controlled by the relative weight fraction of each polymer indicating the cooperative behavior of the polymer mixtures. The change in T_{CP} from of 68 ^{o}C to 77 ^{o}C upon decreasing the amount of P70-30 from 100 to 20 wt% is higher compared to the increase expected from dilution from 5 mg/ml to 1 mg/ml.

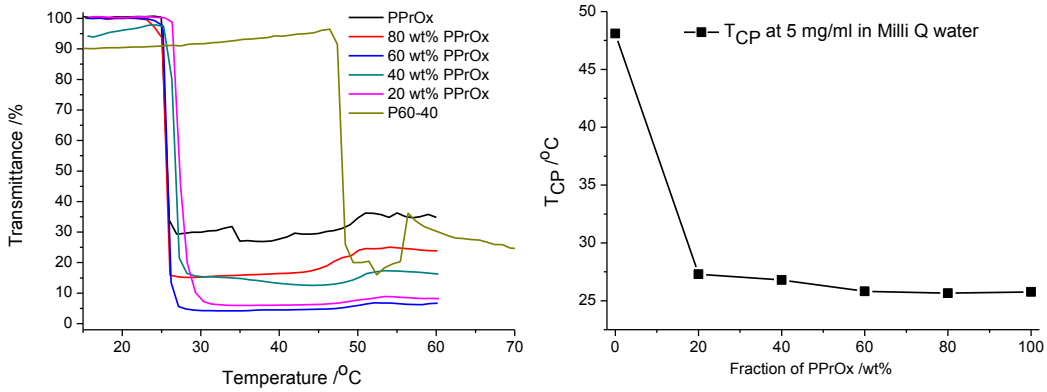

Figure 6-1 Left) Turbidimetry curves of PPrOx and P60-40 at varying compositions at 5 mg/ml; Right) relationship between the cloud points and composition of the polymer mixture

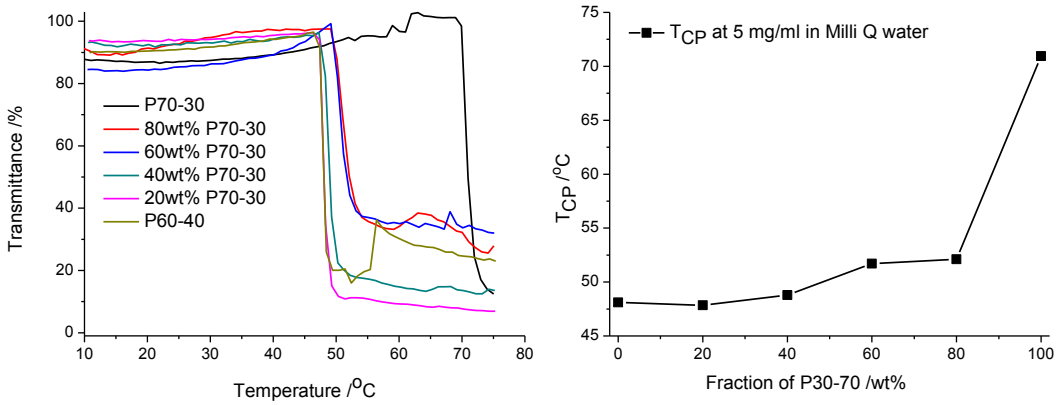

Figure 6-2 Left) Turbidimetry curves of P70-30 and P60-40 at varying compositions at 5 mg/ml; Right) relationship between the cloud points and composition of the polymer mixtures

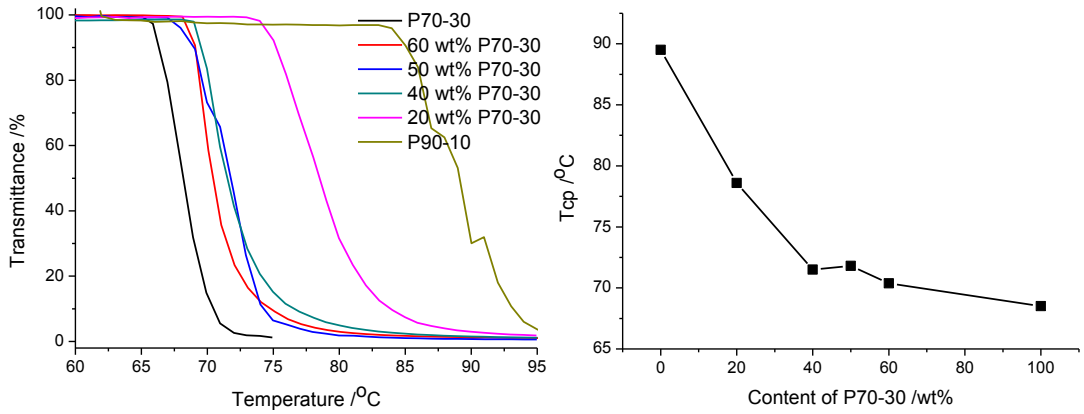

Figure 6-3 Left) Turbidimetry curves of P70-30 and P90-10 at varying compositions at 5 mg/ml; Right) relationship between the cloud points and composition of the polymer mixtures

6.1.3 Summary

A systematical study on the cooperative LCST behavior of copoly(2-oxazoline)s with various T_{CP}s ranging from 25 °C to 90 °C was performed. The results suggest that hydrophilicity is a key factor to control the cooperative behavior of poly(2-oxazoline)s. Further investigations are ongoing to understand the reason for such dependence, whereby it is worth to mention that the majority of reported polymers that exhibit cooperative behavior also had relatively high T_{CP}s.

6.2 Fabrication of novel hybrid polymeric nanoparticles: co-assembly of thermoresponsive polymers and a double hydrophilic thermoresponsive block copolymer

6.2.1 Introduction

Inspired by the ordered structures and functions of biological systems, scientists have been trying for decades to create artificial self-assembled nano- or microstructures using synthetic materials.[313, 314] Block copolymers are ideally suited for this purpose as they can have amphiphilic structures enabling aqueous self-assembly.[315, 316] Various copolymer architectures, e.g. diblock, triblock, comb-like or star shaped copolymers, have been reported to show self-assembly behavior resulting in various shapes of higher-ordered nano- or microstructures.[317, 318] For aqueous self-assembly of any copolymer, an amphiphilic structure with both hydrophilic and hydrophobic blocks are required. Polymers with uniform solubility can hardly self-assemble into an ordered structure since the hydrophobic aggregation cannot be stabilized. In this section, we will present a straightforward method to organize such uniform polymers into ordered structure by co-assembly with a block copolymer (see Figure 6-4). The procedure only requires simple mixing of both the block copolymers and the uniform polymer solutions. To prove the concept, solutions of thermoresponsive statistical copolymer and a double hydrophilic block copolymer with a thermoresponsive block were simply mixed. Temperature triggered co-assembly behavior of the resulting mixed polymer solutions was investigated by DLS. The influence of T_{CP} and concentration of the thermoresponsive statistical copolymer on the co-assembly behavior and resulting nanoparticles was evaluated with one block copolymer of which the concentration was kept constant.

6.2.2 Results and discussion

The block copolymer and statistical copolymers with different T_{CP}s were synthesized by reversible addition−fragmentation chain transfer (RAFT) polymerization (see table 1). By altering the ratio of the two comonomers, namely methoxy di(ethylene glycol) acrylate (mDEGA) and ethoxy di(ethylene glycol) acrylate (eDEGA), statistical copolymers with a wide range of T_{CP}s were obtained that were utilized for this co-assembly study. The block copolymer with one permanent hydrophilic block, namely poly(ethylene

glycol) (PEG, Mn=2000, Đ=1.06), and a P(mDEGA$_{40}$-eDEGA$_{60}$) thermoresponsive block was synthesized using a PEG functionalized macro-CTA.

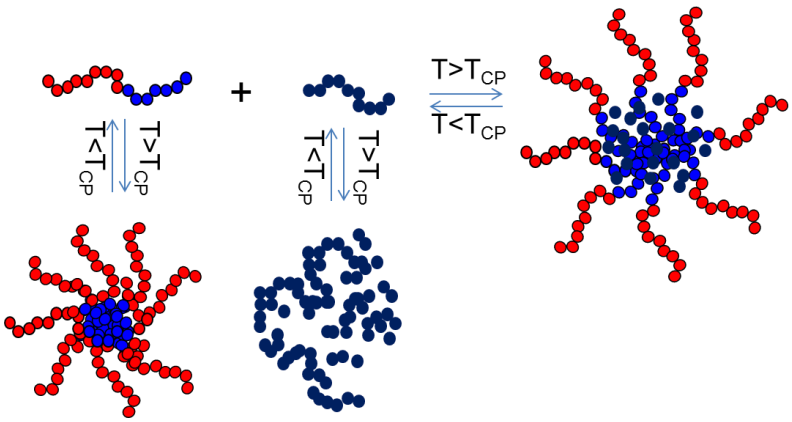

Figure 6-4 Schematic representation of the co-assembly of a thermoresponsive block copolymer and a thermoresponsive statistical copolymer.

Table 6-1 Characterization data of the copolymers synthesized

Polymer	Polymer composition	Mn (kDa)[a]	Đ[a]	mDEGA%[b]	T_{CP}/°C[c]
P20	P(mDEGA$_{20}$-eDEGA$_{80}$)	17.5	1.09	14.3%	20
P40	P(mDEGA$_{40}$-eDEGA$_{60}$)	17.5	1.10	38.8%	26
P50	P(mDEGA$_{50}$-eDEGA$_{50}$)	15.0	1.11	49.2%	29
P60	P(mDEGA$_{60}$-eDEGA$_{40}$)	15.1	1.12	60.0%	33
P80	P(mDEGA$_{80}$-eDEGA$_{20}$)	14.7	1.11	78.6%	40
BP	PEG$_{44}$-*b*-P(mDEGA$_{40}$-eDEGA$_{60}$)	18.4	1.14	40%	29[d]

[a] Determined by SEC; [b] Determined by ^{1}H NMR spectroscopy; [c] Measured by turbidimetry at 5 mg/ml; [d] In this specific situation the phase transition temperature (PTT) was determined by DLS at 1 mg/ml.

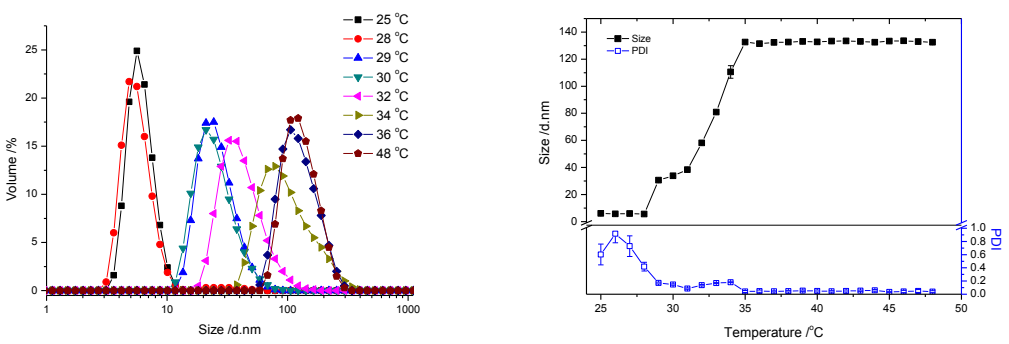

Figure 6-5 a) Size distribution and b) size versus temperature of BP in milliQ water at different temperatures (1 mg/mL) determined by DLS

The temperature induced self-assembly of the block copolymer (BP) was first evaluated by dynamic light scattering (DLS) at 1 mg/ml in aqueous solution. Figure 6-5 displays the size distributions obtained at different temperatures and the evolution of size with temperature of the BP solution during heating from 25 ^{o}C to 48 ^{o}C. A particle size of around 6 nm was observed below 28 ^{o}C indicating the presence of individually dissolved polymer chains, i.e. unimers of the BP. An increase of particle size was detected when the polymer solution was heated above 28 ^{o}C. After a gradual increase of particle size with increasing temperature, the particle size stabilized around 35 ^{o}C at about 130 nm with a very low polydispersity index (PDI=0.05) indicating the formation of defined stabilized nanostructures. Cryogenic transmission electron microscopy (cryo-TEM) was attempted to image the structure of such nanoparticles, but unfortunately, the contrast was insufficient for detection by cryo-TEM most likely due to the high hydrophilicity of the particle core, which is not fully dehydrated in the collapsed state.

The co-assembly behavior of the BP with various statistical copolymers with different T_{CP}s was then investigated by DLS during heating of the aqueous solution with the BP concentration fixed at 1 g/L and varying concentration of the thermoresponsive copolymers. Initial experiments were conducted for assembly of the BP with P20, which has a T_{CP} of 20 ^{o}C being significantly lower than the BP phase transition temperature of 29 ^{o}C. The size and PDI versus temperature at different concentrations are shown in Figure 6-6. Large aggregation was observed when the solution was heated above the solution above T_{CP} of P20, while further heating to temperatures above the phase transition temperature (PTT) of the BP led to stabilization of the aggregates. The mixture of BP and P20 leads to the stabilization and formation of defined nanoparticles of 120 nm and PDI lower than 0.10 when using 0.2 g/L of P20. Co-assembly of P20 with 0.5 g/L polymer already led to the formation of poorly defined nanoparticles while further increasing the concentration led to macroscopic phase separation above the T_{CP} of P20. The mixture of the BP and P40 with a T_{CP} of 26 ^{o}C exhibits similar co-assembly behavior allowing the stabilization of the nanoparticles with the BP at a lower temperature and a larger quantity of the thermoresponsive statistical copolymers could be included in the ordered structures via co-assembly resulting in relatively defined nanoparticles with up to 0.8 g/L of P40. These mixtures of the BP with copolymers having a lower T_{CP} show co-assembly behavior only at temperatures higher than the initial aggregation of the copolymer and only with low loading of the thermoresponsive statistical copolymer. To obtain better co-assembly behavior, P50 with a T_{CP} that equals PTT of the BP was investigated for the co-assembly behavior.

The size and PDI versus temperature plots for mixtures of the BP and P50 were collected by DLS during heating and are displayed in Figure 6-7. The size of the polymers in aqueous solution increased from about 6 nm to 40-250 nm upon heating depending on the ratio of the BP and P50 indicating the successful co-

assembly of the two polymers. It is striking that the co-assembly behavior could be observed with a P50/BP weight ratio up to 10. Well defined hybrid nanoparticles were obtained with various ratios of the two species as demonstrated by the low polydispersity indices of around 0.1 resulting from DLS. Moreover, the size of these defined nanoparticles can be tuned from 40 to 250 nm depending on the amount of P50 in the solution (see Figure 6-8).

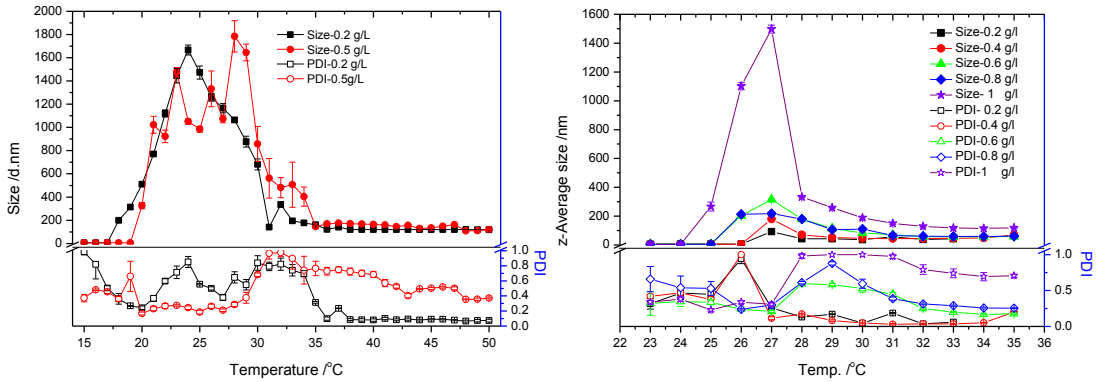

Figure 6-6 The size versus temperature plots of BP with the thermoresponsive copolymers having a T_{CP} lower than the PTT of BP. Left: P20 and BP; Right: P40 and BP. The concentration of BP was kept at 1 mg/ml, the concentrations of homopolymers are indicated in the figure. Data were obtained by DLS.

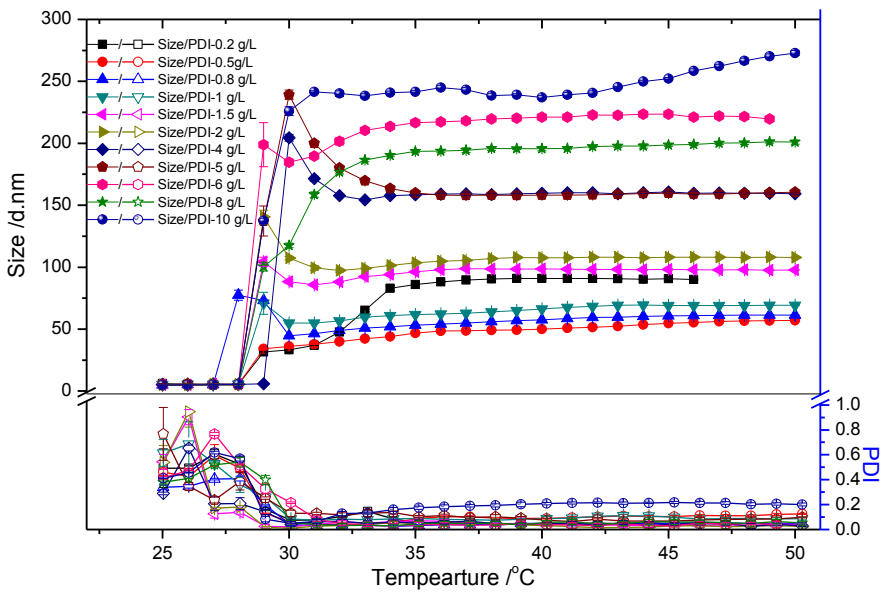

Figure 6-7 The size versus temperature plot of the BP and thermoresponsive polymer P50, both having the same phase transition temperature. The concentration of BP was kept at 1 mg/ml, the concentrations of P50 are indicated in the figure. Data were obtained by DLS.

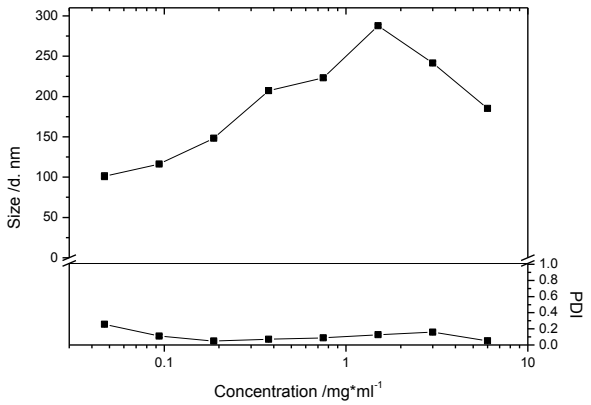

Figure 6-8 Size plotted as a function of concentration of P50 used for the co-assembly of the BP and thermoresponsive copolymer P50. The concentration of BP was kept at 1 mg/ml and the temperature was 37 ^{o}C. Data were obtained by DLS.

The co-assembly behavior of BP with thermoresponsive copolymers having a T_{CP} higher than the PTT of the BP, namely P60 and P80, was also performed with various ratios (see Figure 6-9). Successful co-assembly of the BP and the statistical copolymers was observed as indicated by the increased size of the nanoparticles and very low PDIs (PDI < 0.1). For mixtures of BP and P60, small aggregates with broad size distributions were first formed during the heating of the polymer solutions and the size gradually increased at higher temperatures until the T_{CP} of P60, suggesting the gradual incorporation of the statistical copolymer into the block copolymer micelles during heating. The size of the resulting nanoparticles could also be tuned by varying the ratio of block copolymer and thermoresponsive statistical copolymer in the solution. The collapse of polymer mixtures of BP and P80 leads to less defined nanoparticles as indicated by the high standard deviation and relatively high PDI values, which most likely suggests that less efficient co-assembly occurs due to the big gap between the phase separation temperatures of the two polymers, i.e. BP micelles, co-assembled structures and large P80 aggregates coexist.

The co-assembly behavior of the BP and statistical thermoresponsive copolymers was investigated using polymers having only ethylene glycol and ester groups, which can exclude the occurrence of supramolecular inter- or intra-chain interaction like hydrogen bonding. Hence, only hydrophobic interactions are involved in the co-assembly indicating that such cooperative behavior might be universal.

The hydrophobicity difference between the thermoresponsive statistical copolymers and the thermoresponsive block of the block copolymer plays a vital role in the co-assembly behavior. With regard to a specific block copolymer, the thermoresponsive statistical copolymers used for co-assembly can be divided into three groups, i.e. polymers that aggregate at temperatures lower (i), equal to (ii) and higher (iii) than the phase transition temperature of the block copolymer (Scheme 6-2). For thermoresponsive copolymers with a T_{CP} lower than the phase transition temperature of BP (P20 and P40), the

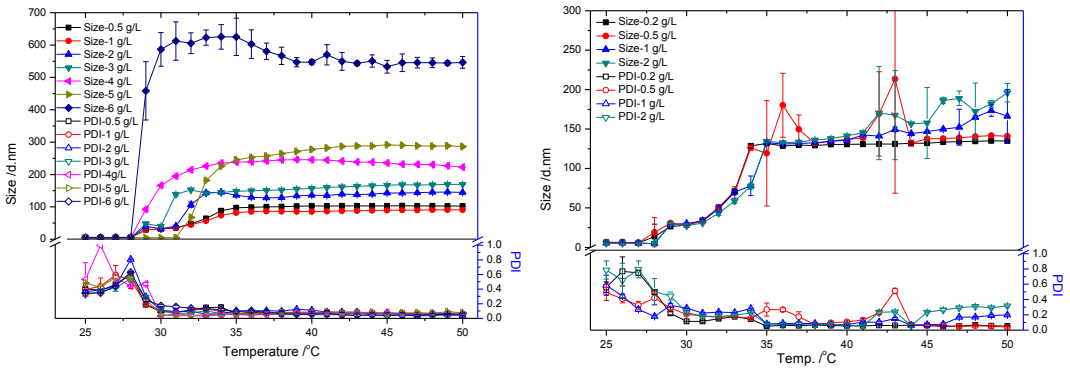

Figure 6-9 The size versus temperature plot of the BP and thermoresponsive polymers with a T_{CP} higher than the PTT of the BP. Left: P60 and BP; Right: P80 and BP, with the concentration of BP kept at 1 mg/ml and the concentrations of homopolymers are indicated in the figure. Data were obtained by DLS.

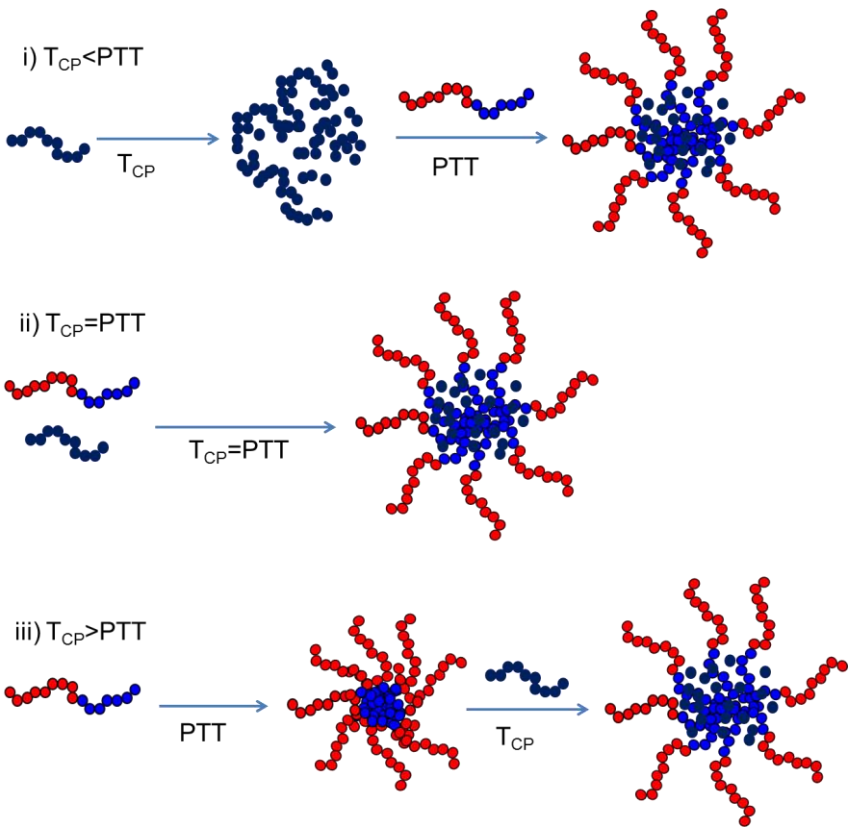

Scheme 6-2 Schematic representation of the mechanism for the co-assembly behaviour of the block copolymer with thermoresponsive statistical copolymers with different T_{CP}s

thermoresponsive statistical copolymers first collapses when heated to its T_{CP} followed by the stabilization of the formed particles by collapse of the block copolymers upon further heating. In this case, the co-assembly behavior is not so efficient since the re-distribution of collapsed thermoresponsive polymers to smaller micelles is required. The most efficient co-assembly behavior was observed when the BP and thermoresponsive statistical copolymer have the same phase transition temperature. During heating of the

polymer mixture, the two polymers collapsed simultaneously leading to the formation of defined well dispersed nanoparticles. For thermoresponsive polymers with a T_{CP} higher than the PTT of the BP, the phase separation for the BP happens before the dehydration of thermoresponsive statistical copolymer resulting in the formation of small micellar particles at a first stage, which gradually increased in size due to the incorporation of the dehydrated thermoresponsive statistical copolymer upon heating. This process was also rather efficient if the T_{CP} of the thermoresponsive statistical copolymer is only slightly higher than the PTT of the BP.

Next, the dynamic co-assembly behavior for BP and P60 with a ratio of 5 was evaluated serving as selected representative example. The polymer sample was heated from 25 ^{o}C to 37 ^{o}C in different rates to induce co-assembly and the size and PDI of the formed nanoparticles were then measured by DLS at 37 ^{o}C. As shown in Figure 6-10, the sizes were found to decrease from 230 nm to 170 nm (all PDI<0.08) when the heating rate increased from 0.1 to 6 ^{o}C/min indicating that the co-assembly behavior and formation of ordered nanoparticles can also be controlled kinetically. The increase of the nanoparticle size with slower heating is due to efficient diffusion of thermoresponsive statistical copolymers into the defined nanoparticles from self-assembly of the BP.

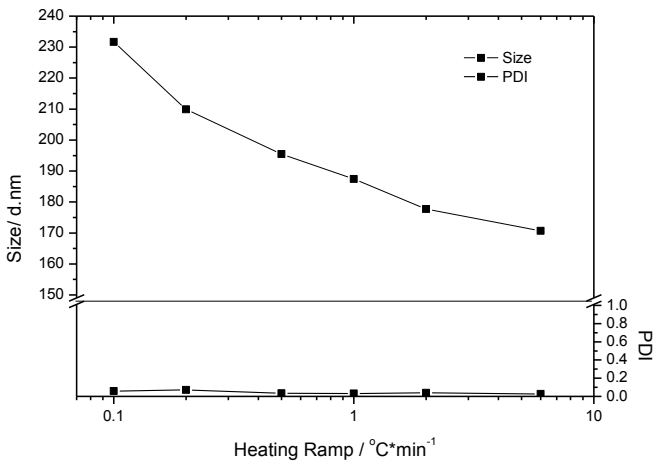

Figure 6-10 Size and PDI as a function of heating rate for co-assembly of BP and P60 in aqueous solution (1 mg/mL of BP and 5 mg/ml of P60) at 37 ^{o}C by DLS, heated from 25 ^{o}C

The overall concentration dependence of the co-assembly behavior was also evaluated for mixtures of BP and P60 with a fixed ratio of 5 serving as selected representative example. The polymer solutions with different concentrations were heated from 25 ^{o}C to 37 ^{o}C at 1 ^{o}C/min and the sizes and PDIs of the resulting nanoparticles were recorded by DLS at 37 ^{o}C, as shown in Figure 6-11. The size of the nanoparticles formed at 37 ^{o}C firstly increased upon dilution from overall 6 mg/ml to 1.5 mg/ml followed by a decrease with even further dilution. One possible reason for this evolution of sizes is the different dependence of the T_{CP} of BP

and P60 on their concentrations, which resulting in slightly different co-assembly behavior of the two polymers. Moreover, the assembled nano-structures could be detected down to about 0.1 mg/ml of polymers indicating a high stability of the hybrid nanoparticles.

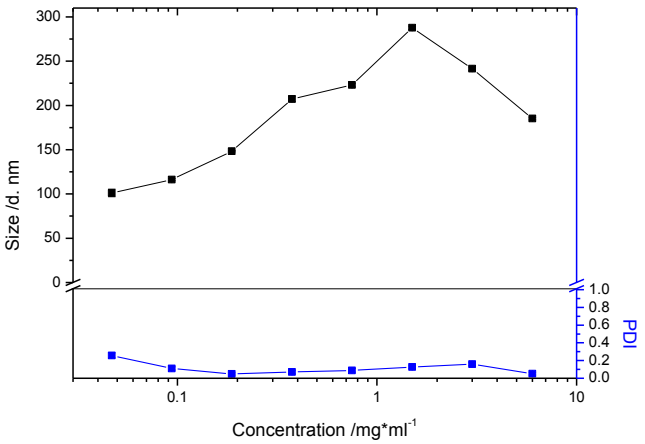

Figure 6-11 Size and PDI as a function of the total concentration of BP and P60 in aqueous solution (with P60:BP=5:1 by weight) at 37 ^{o}C determined by DLS

6.2.3 Summary

In summary, a novel method for the preparation of hybrid polymeric nanoparticles is established through heating induced co-assembly of thermoresponsive statistical copolymers and a double hydrophilic block copolymer having a permanently hydrophilic block and a thermoresponsive block. By adjusting the hydrophilicity of the thermoresponsive statistical copolymer, well defined hybrid micelles with tunable sizes were obtained with various ratios of the two species depending on the T_{CP} and the concentration of the thermoresponsive statistical copolymer in the solution. This developed co-assembly method provides a highly tunable platform for the preparation of well-defined polymeric nanoparticles with potential applications in, e.g. drug delivery systems.[319, 320]

6.3 Experimental section

6.3.1 Materials and Instrumentation

All chemicals and solvents were commercially available and use as received unless otherwise stated. Toluene, *N*,*N*-dimethylformamide (DMF) and $CDCl_3$ are obtained from Sigma Aldrich. Azobisisobutyronitrile (AIBN, 98%, Aldrich) was recrystallized from methanol (twice) and stored in the freezer. 2-(Butylthiocarbonothioylthio)propanoic acid (BCPA) was prepared according to the established procedures.[321]

^{1}H NMR spectra were recorded on a Bruker 300 MHz FT-NMR spectrometer using $CDCl_3$ as solvent. Chemical shifts (d) are given in ppm relative to TMS.

Size-exclusion chromatography (SEC) was performed on a Agilent 1260-series HPLC system equipped with a 1260 online degasser, a 1260 ISO-pump, a 1260 automatic liquid sampler (ALS), a thermostatted column compartment (TCC) at 50 ℃ equipped with a PSS Gram30 column in series with a PSS Gram1000 column, a 1260 diode array detector (DAD) and a 1260 refractive index detector (RID). The used eluent was DMA containing 50mM of LiCl at a flow rate of 1 ml/min. The spectra were analysed using the Agilent Chemstation software with the GPC add on. Molar mass and PDI values were calculated against Varian PMMA standards.

Gas chromatography was performed on a 7890A from Agilent Technologies with an Agilent J&W Advanced Capillary GC column (30 m, 0.320 mm, and 0.25 μm). Injections were performed with an Agilent Technologies 7693 auto sampler. Detection was done with a FID detector. Injector and detector temperatures were kept constant at 250 and 280 ^oC, respectively. The column was initially set at 50 ^oC, followed by two heating stages: from 50 ^oC to 100 ^oC with a rate of 20 ^oC /min and from 100 ^oC to 300 ^oC with a rate of 40 ^oC /min, and then held at this temperature for 0.5 minutes.

Turbidity measurements were performed on a Cary 300 Bio UV-Visible spectrophotometer at a wavelength of 600 nm. The samples were first cooled to a suitable temperature to fully dissolve the copolymer (5 mg ml^{-1}), after which the sample was placed in the instrument and cooled to 5 ^oC. The transmittance was measured during at least two controlled cooling/heating cycles with a cooling/heating rate of 1 $^oC\ min^{-1}$ while stirring in PS cuvettes controlled by block temperature probe.

Dynamic light scattering (DLS) was performed on a Zetasizer Nano-ZS apparatus (Malvern Instruments Ltd) using disposable cuvettes. The excitation light source was a He−Ne laser at 633 nm, and the intensity of the scattered light was measured at 173 °. This method measures the rate of the intensity fluctuation and the size of the particles is determined through the Stokes−Einstein equation

$$d(H)= kT/3\pi\eta D \qquad \text{Equation 6-1}$$

where d(H) is the mean hydrodynamic diameter, k is the Boltzmann constant, T is the absolute temperature, η is the viscosity of the dispersing medium, and D is the apparent diffusion coefficient. All samples were filtered through Millipore membranes with pore sizes of 0.2 μm prior to measurement.

6.3.2 Synthesis and characterization

The synthesis of poly(2-oxazoline) copolymers by living cationic ring opening polymerization of 2-ethyl-2-oxazoline and 2-n-propyl-2-oxazoline is described in reference.[238]

The synthesis of PEG-CTA is described in section 7.4.2.

Synthesis of PEG-P(mDEGA-PeDEGA) block copolymer (performed by Lenny Voorhaar)

The PEG-P(mDEGA-PeDEGA) block copolymer was synthesized via RAFT polymerization using [PEG-CTA]:[eDEGA]:[mDEGA]:[AIBN] = 1:60:40:0.1 and 2M total monomer concentration in DMF. The solution was degassed by five freeze-pump-thaw cycles, put under nitrogen atmosphere and heated to 70 ℃ for two hours. GC showed a monomer conversion of 81% for eDEGA and 83% for mDEGA. The solution was diluted with THF and precipitated three times in a hexane/diethyl ether mixture and dried in a vacuum oven.

Synthesis of P(mDEGA –PeDEGA) copolymers (performed by Lenny Voorhaar)

The P(mDEGA-PmDEGA) copolymers were synthesized via RAFT polymerization using a Chemspeed ASW2000 automated synthesizer equipped with 16 parallel reactors of 13 mL, a Huber Petite Fleur thermostat for heating/cooling, a Huber Ministat 125 for reflux and a Vacuubrand PC 3000 vacuum pump. Stock solutions of BCPA, AIBN, eDEGA and mDEGA in DMF were prepared and bubbled with argon for at least 30 minutes before being introduced into the robot system and then kept under argon atmosphere. The hood of the automated synthesizer was continuously flushed with nitrogen and the reactors were flushed with argon to ensure an inert atmosphere. Before starting the polymerizations, the reactors were degassed through ten vacuum-argon cycles. Stock solutions were transferred to the reactors using the syringe of the automated synthesizer while the reactors were kept at 10 ℃. Reactions were performed using [M]:[BCPA]:[AIBN] = 100:1:0.1 and a total monomer concentration of 2M in DMF with a total volume of 4 mL. The [eDEGA]:[mDEGA] ratio was varied to be 80:20, 60:40, 50:50, 40:60 and 20:80. Each reaction was performed in duplo. A t = 0 minutes, sample was taken from each reaction for later conversion calculation. The reactors were then heated to 70 ℃ to start the polymerizations. During the reactions, 50 μL samples were taken every 20 minutes and transferred into 1.5 mL sample vials containing 1 mL of acetone for GC and SEC measurements. After two hours the reactors were cooled to 10 ℃ to stop the reactions. The solutions were transferred to centrifuge tubes, diluted with distilled water, heated to 60 ℃ and centrifuged for one minute at 7500 RPM. The water was poured off and the polymer was redissolved in cold distilled water, heated to 60 ℃ and centrifuged again for one minute at 7500 RPM. The water was poured of and the polymer dissolved in dichloromethane and dried under reduced pressure before full analysis.

Chapter 7 Dual pH- and temperature-responsive polymers and their biomedical applications

Parts of this chapter were published on:

Q. Zhang, N. Vanparijs, B. Louage, B. G. De Geest, R. Hoogenboom, *Polymer Chemistry* **2014**, 5, 1140.

My contribution includes the experiments excluding the *in vitro* toxicity determination and the SDS-PAGE analysis of the copolymers, the interpreting of the results and the writing of the manuscripts.

Abstract: For biomedical applications of thermoresponsive polymers, clearance from the body is important to avoid accumulation of synthetic polymers in the body. However, this is not the case with most of the reported thermoresponsive polymers as they will remain in the collapsed state at all times at body temperature. In this chapter, we report a new type of dual pH- and temperature-responsive copolymers that undergo phase-transition below body temperature while degrading in time into hydrophilic species, thereby avoiding long-term accumulation in the body.

These dual responsive polymers were developed based on the combination of temperature-responsive and acid labile acetal monomers. Copolymers with tuneable lower critical solution temperature behaviour were found to be hydrolysable depending on pH and polymer hydrophilicity. RAFT copolymerization of these monomers using, respectively, a PEG-functionalized or amine-reactive NHS-functionalized chain transfer agent allows designing of micelles and polymer–protein conjugates with transient solubility properties within a physiologically relevant window.

To make the dual responsive polymers more robust, we optimized the dual responsive copolymers by combining bulky dimethyldioxolane side chains with small hydrophilic hydroxyethyl side chains leading to acid-degradable thermoresponsive polymers that are relatively quickly hydrolyzed under slightly acidic conditions on the one hand while the dioxolane group provides high stability at pH 7.4 on the other hand. These unprecedented properties are ascribed to the good exposure of the hydropohobic degradable dioxolane groups to the aqueous solution making them more prone to acidic hydrolysis. The polymer architecture induced acceleration of hydrolysis are of particular interest in the design of biodegradable polymer since the intrinsic limitation that faster acidic degradation rate of acid-labile groups always goes hand in hand with higher instability at neutral conditions can be overcome.

Dual responsive copolymers using less stable pH-labile linear acetal instead of its cyclic analogue are also investigated. The synthesis, thermoresponsive behavior and pH triggered hydrolysis of such copolymer were performed revealing a relatively fast hydrolysis in acidic environment compared to the copolymers with cyclic acetal groups.

7.1 Dual pH- and temperature-responsive RAFT-based block co-polymer micelles and polymer-protein conjugates with transient solubility

This section describes the synthesis, dual responsive behavior and potential applications. The optimization the dual responsive copolymers by controlling over copolymer architecture and utilizing less stable pH-labile linear acetal will be discussed in sections 7.2 and 7.3, respectively.

7.1.1 Introduction

Temperature-responsive polymers are attractive materials for biomedicine, including drug delivery, tissue engineering and diagnostics[10, 13, 21, 322, 323]. In particular, those polymers exhibiting lower critical solution temperature (LCST) behavior with a hydrophilic-to-hydrophobic phase transition between room and body temperature are highly attractive candidates for the development of "smart" materials to be used in the human body. Within this class of polymers, poly(*N*-isopropyl acrylamide) (PNIPAM)[24, 193] poly(oligo(ethylene glycol) (meth)acrylate)s[26, 27] and poly(2-oxazoline)s[3, 30] are the most intensively studied, being bio-compatible and allowing to tune the LCST by incorporation of more hydrophilic or hydrophobic co-monomers.

However, for biomedical applications, clearance from the body is highly desired to avoid accumulation of synthetic polymers in the body[324]. Unfortunately, this is not the case for the above listed polymers as they will remain in the collapsed state at all times at body temperature. Therefore, there is a clear need for engineered dual responsive polymers that undergo an LCST phase-transition below body temperature while degrading in time into hydrophilic species, thereby avoiding long-term accumulation in the body. With respect to intracellular drug delivery, e.g. for anti-cancer or vaccine delivery, acidic pH is an attractive trigger to induce drug release[13, 325]. Indeed, whereas the extracellular medium has a neutral pH of 7.4, an acidic pH of 4-5 is encountered in intracellular endo/lysosomes (i.e. vesicular organelles in which particulate material becomes located upon phagocytosis) and in the intra-tumor environment.

Here we report a novel class of dual responsive polymers that exhibit LCST behavior and degrade into fully water soluble polymers under mild acidic conditions. These copolymers are designed by combining methoxy tri(ethylene glycol) acrylate (mTEGA) with 2,2-dimethyl-1,3-dioxolane-4-yl)methyl acrylate (DMDMA). Poly(mTEGA) has a cloud point temperature (T_{CP}, *i.e.* the temperature at which the polymer precipitates from solution upon heating due to entropic reasons) of ~ 65 °C and we found that copolymerization with DMDMA allows 'à la carte' tuning of the T_{CP} below physiological temperature by varying the monomer ratio. Importantly, the acetal groups of the DMDMA are acid-labile[326] and can be hydrolyzed into hydrophilic glycerol acrylate moieties at low pH. Up to now, DMDMA has, however, only been used as acid-labile protecting group for glycerol acrylate and not to induce pH-responsivity[327-329]. We demonstrate that copolymerization of mTEGA and DMDMA yields highly biocompatible copolymers with

attractive dual temperature- and pH-responsive, properties. Furthermore, these copolymers can be used to prepare dual-responsive block copolymer micelles[330] and protein conjugates.[331, 332] With respect to the latter, we are, to the best of our knowledge, the first to report on such degradable dual-responsive polymer-protein conjugates that can be prepared in homogeneous aqueous conditions at low temperature while the collapse of the copolymers at body temperature in combination with pH-dependent hydrolysis of the DMDMA units enables slow release of the protein under acidic conditions as found in intracellular vesicles.

7.1.2 Results and discussions

Copolymerization of mTEGA and DMDMA (Scheme 7-1) was performed via reversible addition-framentation chain transfer (RAFT) polymerization at 70 ℃ using a trithiocarbonate-based (macro) chain transfer agent ((M)CTA) and azobisisobutyronitrile (AIBN) as initiator in a toluene/N,N-dimethylacetamide (DMA) (80/20, vol %) mixture. Table 7-1 summarizes the properties of the obtained (block) copolymers. The DMDMA-mTEGA copolymerization kinetics were evaluated via gas chromatography (GC) to follow monomer conversion and size exclusion chromatography (SEC) to follow the number average molecular weight (Mn) and dispersity (Đ) of the polymers in time. A linear increase of $\ln([M_0]/[M_t])$ versus time was observed (See Figure 7-1), whereby both monomers were incorporated in a similar rate. Furthermore, a linear increase of Mn with conversion and relatively narrow Đ were found, indicating good control over the copolymerization and the generation of near-ideal random copolymers.

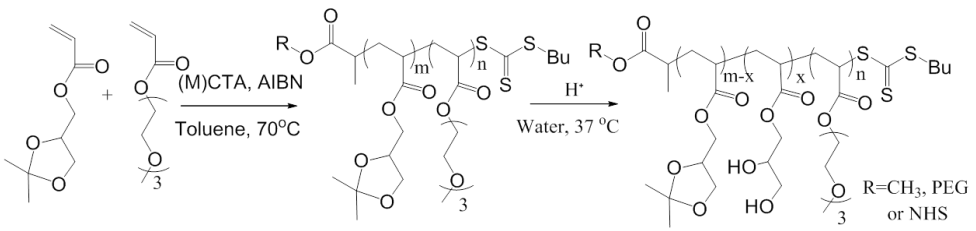

Scheme 7-1 Synthesis and (partial) hydrolysis of pH degradable temperature-responsive copolymers

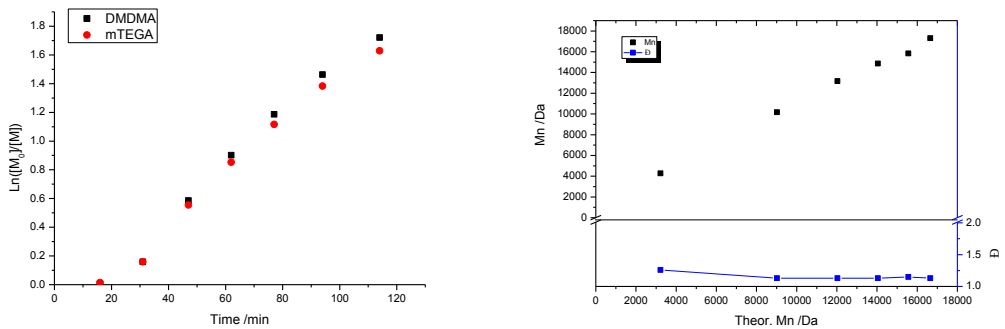

Figure 7-1 Left: Pseudo-first-order kinetic plot of DMDMA and mTEGA for RAFT polymerization with DMDMA: mTEGA: CTA: AIBN=50: 50: 1: 0.1. Right: Corresponding Mn and Đ versus theoretical Mn plot. The CTA used in this kinetics study was MPTTCP

The temperature-responsive properties of the synthesized statistical copolymers were determined via turbidimetry in aqueous medium. Figure 7-2A depicts the transmittance as function of temperature for copolymers with different ratios of DMDMA. When calculating the cloud point temperature (T_{CP}) from the temperature at which the transmittance is 50%, a quasi-linear decrease of the T_{CP} with increasing amount of the hydrophobic DMDMA monomer is found (Figure 7-2B). These phase transition temperatures were confirmed by dynamic light scattering (DLS), showing a significant increase of the hydrodynamic radius at the same temperatures as those determined by turbidimetry (Figure 7-3). The T_{CP}s measured by DLS were found to be 2-3 ^{o}C higher than measured by UV-vis, which can be ascribed to the lower concentration of the DLS measurements. P50 was found to aggregate into rather small and defined aggregates at 9 ^{o}C and these initial aggregates grow in size upon further heating. As such the T_{CP} determined by turbidimetry is higher as this technique only detects aggregates big enough to scatter 600 nm light. This different behavior of P50 compared to the other copolymers, which agglomerate into micrometer-sized agglomerates at the transition temperature, can be ascribed to the higher hydrophobic DMDMA content leading to the formation of a hydrophobic DMDMA core that is stabilized by an mTEGA corona. In other words, P50 acts more like an amphiphilic polymer while the other polymers with less DMDMA behave like statistical random copolymers that full collapse upon heating. We also found that the pH of the aqueous medium slightly affected the T_{CP} of the copolymer, likely due to a change in ionic strength of the solution[92]. However, in all cases, the same linear relationship between T_{CP} and monomer ratio is observed.

Table 7-1 Polymer composition and properties of the synthesized copolymers in this section

Polymer	DP determined by GC			Mn /kDa[b]	Đ[b]	Fraction DMDMA[c]	Fraction DMDMA[d]	Cloud Point temperature/ ^{o}C
	EG[a]	DMDMA	mTEGA					
P50	0	48	48	15.0	1.19	50%	49.5%	13.6
P42	0	36	50	13.8	1.15	42%	42.1%	17.0
P37	0	32	55	14.6	1.18	37%	37.4%	25.6
P30	0	27	63	15.5	1.21	30%	31.2%	33.7
P22	0	20	68	13.5	1.20	22%	22.6%	40.0
HP1	0	0	89	13.5	1.23	0%	0%	67.8
HP2	0	90	0	14.2	1.12	100%	100%	not soluble
P33-NHS	0	28	56	14.4	1.27	33%	32.0%	31.0
P32-NHS	0	7	22	4.5	1.10	32%	35.9%	24.2
BP40	48	36	53	16.1	1.23	40%	41.4%	34.0[e]
BP38	48	32	52	15.5	1.17	38%	36.1%	36.0[e]

[a] 'EG' represents 'ethylene glycol'; [b] Data collected by THF SEC; [c] Calculated by GC using DMA as internal standard; [d] Calculated based on ^{1}H NMR spectroscopy; [e] Micellization temperature based on dynamic light scattering.

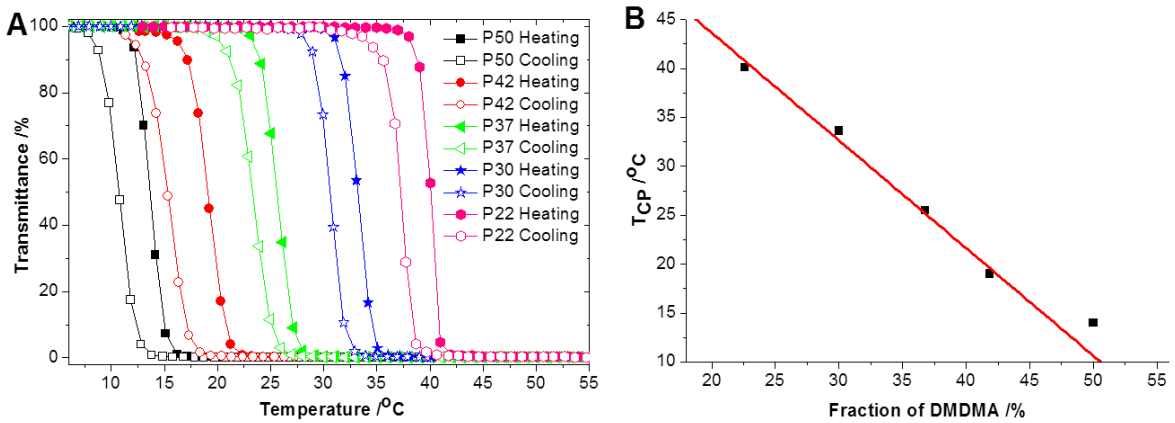

Figure 7-2 (A) Transmittance versus temperature for P50, P42, P37 and P30 in Milli Q water (5 mg/ml). (B) Influence of DMDMA content on the cloud point temperatures (T_{CP}) in water (5mg/ml). Note that the unexpected higher T_{CP} value of P50 is due to different aggregation behavior.

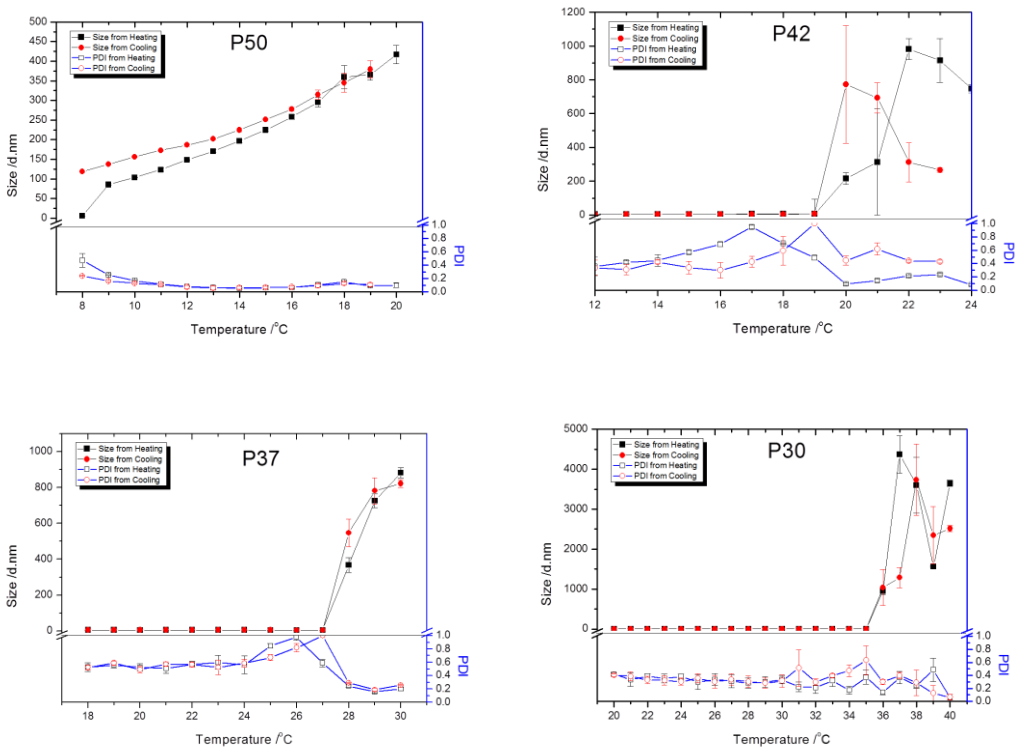

Figure 7-3 Hydrodynamic diameter of P50, P42, P37 and P30 versus temperature, measured by dynamic light scattering. The concentrations of polymers were 1 mg/ml. Error bars correspond to standard deviations based on 5 measurements.

Subsequently, we aimed at elucidating the pH-responsive behavior of the copolymers. Taking into account that the 2,2-dimethyl-1,3-dioxolane group is prone to hydrolysis at acidic pH leading to hydrophilic

glycerol groups,[333, 334] we expected the T_{CP} of the copolymer to increase during hydrolysis. Therefore, we incubated the different copolymers (5 mg/mL) at 37 ℃ (i.e. physiological temperature), buffered at different pH values (i.e. pH4, pH5, pH6 and pH7.4) and measured the T_{CP} of the copolymers as function of time. As shown in Figure 7-4, no major changes in T_{CP} occurred upon incubation at a pH between 5 and 7.5. However, incubation at a pH of 4 leads to hydrolysis of the acetal groups as indicated by the increase of T_{CP} in time for all copolymers. As expected, copolymers with higher acetal content require more time to reach a T_{CP} above physiological temperature. The pH-dependent hydrolysis of the two outermost polymers, i.e. P50 and P30, was also followed by ^{1}H NMR spectroscopy by calculating the integral ratio of the dimethyl group of DMDMA and the methyl group of mTEGA. As shown in Figure 7-4, these experiments fully confirm the trends observed via turbidimetric determination of the T_{CP} proving that the increase in T_{CP} indeed results from hydrolysis of the acetal groups.

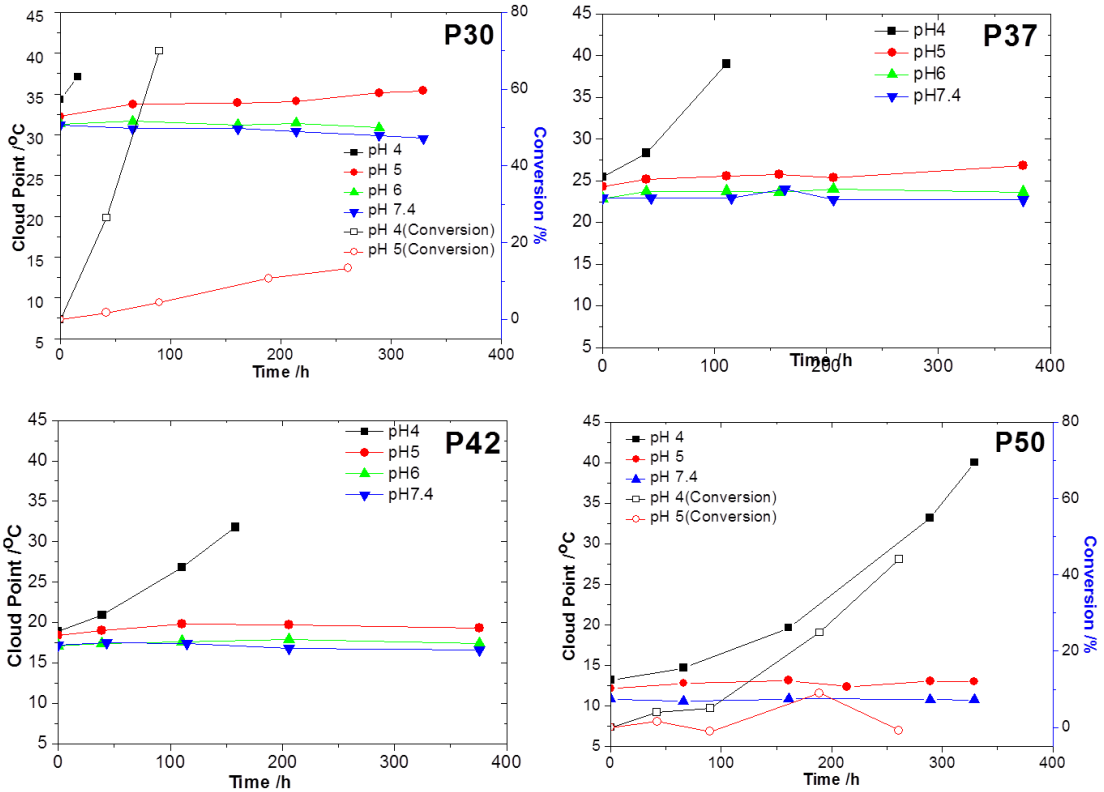

Figure 7-4 Plot of T_{CP} versus hydrolysis time for copolymers with different mTEGA:DMDMA. Conversion of hydrolysis is also shown for P50 and P30 incubated in pH4 and pH5 (open symbols).

After establishing the dual temperature- and pH-responsive properties we aimed in a next part of the work to explore the potential of this type of polymers for biomedical applications. In a first series of experiments, conducted by our collaborators in the group of Prof. Bruno De Geest, we assessed the *in vitro* toxicity of the copolymers on a mouse macrophage (RAW264.7) cell line and a primary dermal fibroblast cell line (HCA2-hTERT). RAW264.7 macrophages are actively phagocyting cells and are well suited to

evaluate the toxicity of the copolymers when envisioning further applications for intracellular drug or vaccine delivery. The HCA2-hTERT fibroblast cell line is used as model for non-phagocyting cells. The toxicity was tested via MTT assay using polymers with different T_{CP}, i.e. below and above the physiological temperature of 37 ℃, allowing evaluating the polymer both in soluble and precipitated state. Additionally, we also tested the polymers after hydrolysis of the acetal groups (assigned in the X-axis legend of Figure 7-5 with an (H)) and supplemented these with the corresponding amount of acetone that is produced as byproduct during the acid hydrolysis. Note that the acetone byproduct was initially removed during isolation of the hydrolyzed polymers. Finally, pure poly(mTEGA) and poly(DMDMA) were also tested, for which we could only test the poly(DMDMA) after hydrolysis as the native polymer could not be dispersed in water.

As shown in Figure 7-5, the MTT assay performed at different polymer concentrations, revealing no significant influence on cell viability of any (co)polymer at any concentration, whereby it should be noted that the lower cell viability for the copolymer with a T_{CP} of 30 ^{o}C at higher concentrations is most likely due to precipitation of the polymer globules on top of the cells. This suggests that, at least *in vitro*, this class of (co)polymers either in soluble, collapsed or hydrolyzed form is very well tolerated by living cells.

Next we evaluated the applicability of the dual responsive polymer system to form block copolymer micelles. Such self-assembled structures are widely used for the delivery and release of hydrophobic drugs due to the high drug-loading capacity of the inner core as well as their prolonged circulation times in the body[335]. Block copolymers having poly(ethylene glycol) (PEG, Mn=2000, Đ=1.06) as hydrophilic block were synthesized using a PEG-functional CTA (Table 7-1, BP38). The temperature triggered self-assembly of the block copolymer was followed by DLS, (Figure 7-6**A-B**) indicating the formation of micelles at 36 ℃, with hydrodynamic diameters ranging from 20 to 25 nm and narrow polydispersity (PDI<0.10). Subsequently, the micelles were loaded with Nile Red as model hydrophobic compound and its pH dependent release was monitored at physiological temperature (i.e. 37 ° C). Due to the temperature-responsive properties of the block copolymers, loading of the micelles is easily achieved by dissolving the block copolymer below its T_{CP} followed by the addition of a small volume of concentrated ethanoic Nile Red solution. Subsequent rapid increase of the temperature above the T_{CP} induces micelle formation, thereby encapsulating the Nile Red in the hydrophobic micellar cavity. As Nile Red exhibits strongly reduced fluorescence in aqueous medium relative to hydrophobic medium, its release can easily be measured via fluorimetry. As shown in Figure 7-6**C**, upon incubation in aqueous buffer at pH 4, Nile Red was almost completely released within 200 hours. At pH 5 the release was significantly slower, while at pH 7 almost no release was observed in 1200 hours (50 days). These data highlight the potential of this class of polymers for acid triggered drug release while ensuring stable encapsulation at physiological pH.

In a last part of this study, again conducted by our collaborators in the group of Prof. Bruno De Geest, we investigated whether low temperature homogeneous aqueous conjugation of the dual responsive copolymers

to proteins allows modulating the solution behavior of the polymer-protein conjugates by altering temperature and/or pH. Therefore, we synthesized copolymers with a T_{CP} of 31 °C using a CTA bearing an amine-reactive NHS group that can be coupled to lysine residues. Two different molecular weight copolymers, i.e. 6 and 18 kDa, were synthesized having a T_{CP} of 24 ^{o}C and 31 ^{o}C, respectively (Table 7-1. P32-NHS and P33-NHS). Lysozyme was used as model protein and the polymers were conjugated below their T_{CP} in aqueous medium buffered at pH 8.3. Gel electrophoresis (SDS-PAGE; Figure 7-7**A**) demonstrated that, relative to native lysozyme (lane 2), the polymer-protein conjugates (lane 3 to 8) exhibited an increase in molecular weight, indicating successful bio-conjugation. As expected, the 6 kDa polymer clearly gave smaller conjugates than the 18 kDa polymer. Increasing the molar ratio of polymer to lysozyme resulted in a larger amount of protein becoming conjugated, likely with multiple chains attached. Control samples (polymer incubated without lysozyme) were not visible on the gel and proteins mixed with unreactive copolymers without NHS-ester end-group did not induce a delay in gel migration (data not shown).

To assess whether copolymer conjugation provides the protein with dual temperature- and pH-responsive properties we measured the electrophoretic mobility of the conjugates in polyacrylamide gel below and above the T_{CP} of the copolymers both before and after acid-triggered hydrolysis of the copolymers. As the presence of SDS in the PAGE experiment strongly increases the T_{CP} of the copolymers, we performed the PAGE under so-called 'native' non-reducing conditions excluding SDS. As shown in Figure 7-7B, when the PAGE is performed below the T_{CP} of the copolymers, no difference in electrophoretic mobility is observed between non-hydrolyzed and hydrolyzed conjugates. Contrary, when the PAGE is performed above the T_{CP} of the copolymers, the non-hydrolyzed conjugates do not migrate on the gel whereas the hydrolyzed conjugates migrated on the gel independently of temperature. These data clearly demonstrate that the copolymer-protein conjugates have dual-responsive properties. Indeed, the conjugates are water soluble below the T_{CP}, precipitate from solution above the T_{CP} while regaining full solubility upon hydrolysis of the acetals into the hydrophilic glycerol moieties.

7.1.3 Summary

In summary, we have introduced a novel class of dual-responsive copolymers, by combining a temperature-responsive monomer with an acid-labile monomer. The T_{CP} of the resulting copolymers could be precisely tailored via the monomer composition to any temperature below physiological temperature. While being stable at physiological pH of 7.4 the copolymers hydrolyzed into fully water soluble polymers under mild acidic conditions (pH 4) resulting in non-toxic byproducts as verified by in vitro cell studies. Block copolymers containing a dual-responsive block were able to form micelles that hold potential for encapsulation and stimuli-responsive release of hydrophobic molecules as demonstrated for Nile Red release. Finally we demonstrated that NHS-functional copolymers could be used for low temperature homogeneous

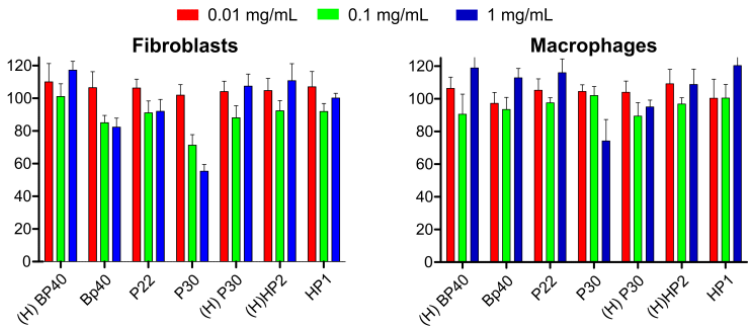

Figure 7-5 Cell viability data measured by MTT assay of HCA2-hTERT human dermal fibroblasts and RAW264.7 macrophages incubated with different concentrations of the respective polymer samples. The '(H)' prefix in the X-axis refers to samples that were subjected to full hydrolysis of the acetal groups.

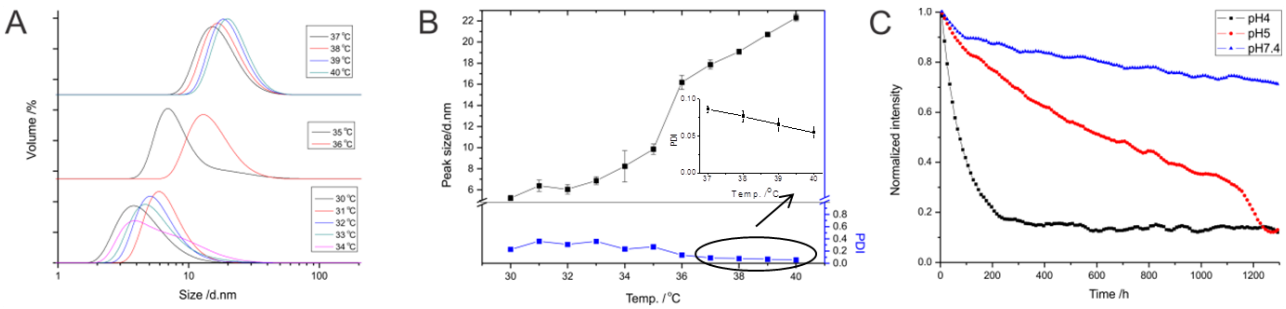

Figure 7-6 (A-B) Hydrodynamic diameter of the BP38 block copolymer versus temperature, measured by dynamic light scattering. (C) Time-dependent change of the fluorescence intensity at 630 nm (Ex at 200 nm) of Nile red loaded in BP38 micelles upon incubation at 37 ℃ and different pH values. The concentration of the BP38 block co-polymer was 1.0 mg/mL.

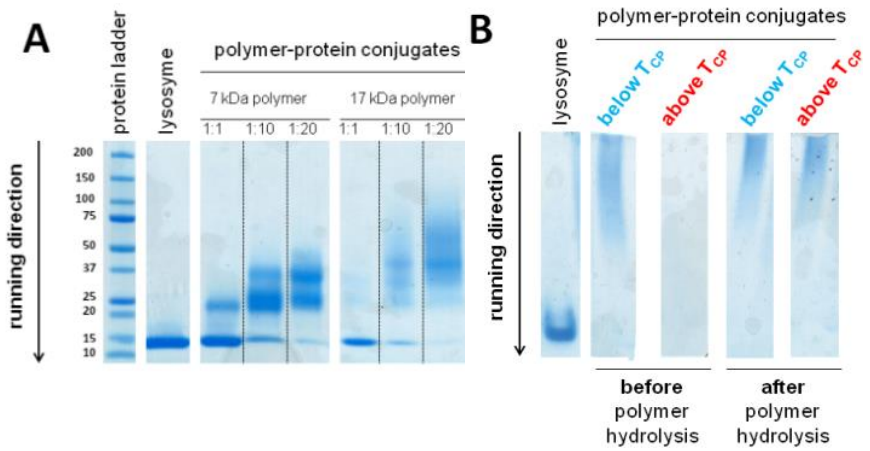

Figure 7-7 (A) SDS-PAGE analysis of the conjugation mixtures. (Lane 2) Native lysozyme (Lane 3 to 5) lysozyme - 6 kDa polymer (P33-NHS) conjugate ratio 1:1, 1:10 and 1:20 (Lane 6 to 8) lysozyme - 18 kDa polymer (P32-NHS) conjugate ratio 1:1, 1:10 and 1:20. (B) Native PAGE of primary and hydrolysed protein-polymer (18 kDa copolymer, ratio 20:1). Below T_{CP} there is no clear difference between both samples. Above T_{CP}, however, the intact polymer conjugates are not visible on the gel due to precipitation in the well.

aqueous bio-conjugation to proteins, engineering them with transient water-soluble/insoluble properties. Such systems are highly attractive for intracellular protein delivery, including nano-particualte vaccine delivery.[336, 337]

7.2 Dual responsive copolymers that combine fast pH triggered hydrolysis and high stability at neutral conditions – on the importance of polymer architecture

7.2.1 Introduction

Polymers that degrade under specific conditions are attractive materials for biomedical applications.[324, 325, 338-342] For instance, drug loaded polymeric micelles that could release their cargo in mild acidic environment are interesting because of the lower pH, in e.g. tumor tissues or the endosomes/lysosomes in cells where nanoparticles typically end up upon endocytosis.[343] For drug delivery applications, such acid-degradable polymers need to be stable at pH 7.4 in the blood stream. To achieve subsequent degradation in acidic medium, labile functional groups, such as ester[344] or cyclic acetal/ketal[236, 237, 333, 334, 345-348] groups, are usually incorporated in the polymer backbone or side chains. However, due to the relatively high stability of these groups, very long degradation times are typically required to render these hydrophobic degradable polymers water soluble (see also section 7.1). Less stable acid labile functional groups, like linear acetal/ketal,[334, 349-351] ortho ester[352-355] or hydrazone groups,[356, 357] have been reported to lead to faster acidic degradation, but notable hydrolysis of those polymers at pH 7.4 is usually also observed leading to premature release of the cargo prior to reaching the target tissue. This can potentially cause side effects resulting from systemic toxicity. Moreover, the instability of these more labile polymers make them very difficult to work with, since the polymer can degrade in aqueous solution or during storage in slight moist conditions. Therefore, polymers with well-balanced stability, i.e. fast hydrolysis in acidic environment and high stability at pH 7.4 are highly desired for intracellular drug delivery applications. However, as stability and degradability go hand in hand, such ideal polymers that are stable at pH 7.4 and quickly degrade at mild acidic conditions are difficult to achieve by tuning of the stability of the degradable moiety.

Stimuli-responsive polymers, also called “smart” polymers, are increasingly used as drug or vaccine carriers.[1, 10, 11, 13, 21, 322, 323, 358] In particular, polymers exhibiting lower critical solution temperature (LCST) behavior with a hydrophilic-to-hydrophobic phase transition between room and body temperature are highly attractive candidates for the development of “smart” biomaterials. Poly(*N*-isopropyl acrylamide) (PNIPAM),[24] poly(oligo(ethylene glycol) (meth)acrylate)s[20, 26, 27] and poly(2-oxazoline)s[3, 30, 238] are prime candidates for such applications based on their good biocompatibility. In section 7.1, we have described a novel type of pH-labile thermoresponsive polymer via copolymerization of a thermoresponsive monomer, mTEGA, and an acid labile acetal monomer, DMDMA.[237] The cloud point temperature (T_{CP}, referred to as the temperature where the transmittance goes through 50% during heating of the polymer solution in water)

of the resulting mTEGA-DMDMA copolymers was increased by hydrolysis of the cyclic acetal side chain groups in acidic conditions, which could trigger the release of Nile Red as model drug cargo. The advantage of combining temperature responsiveness with pH-degradability is that it allows homogeneous aqueous formulation as well as protein conjugation of the copolymers at low temperatures while at 37 °C the polymer becomes hydrophobic and can induce encapsulation of a hydrophobic drug payload. In addition, the kinetics of hydrolysis and, thus, solubilization of the copolymers at 37 °C could be finely tuned by the composition of the copolymers, i.e. copolymers with higher T_{CP} close to 37 °C hydrolyze faster, which was ascribed to the less efficient dehydration of these polymeric globules at 37 °C, i.e. the collapsed polymer globules still contain a significant amount of water molecules required for hydrolysis.

Inspired by these results, we hypothesized that faster hydrolysis might be achieved by incorporating hydroxyl groups into the acid-degradable copolymers, since the hydroxyl group can increase hydration in the collapsed globules by hydrogen bonding with water molecules. Therefore, in this work DMDMA was copolymerized with 2-hydroxethylacrylate (HEA) to prepare dual responsive PHEA-DMDMA copolymers with faster acid triggered hydrolysis (Scheme 7-2) .

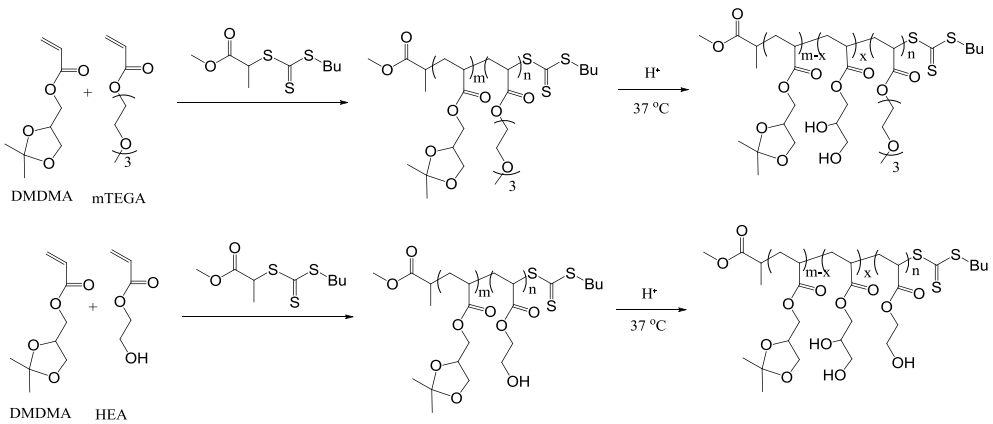

Scheme 7-2 Synthesis and (partial) hydrolysis of the P(mTEGA-DMDMA) (top) and P(HEA-DMDMA) (bottom) copolymers.

7.2.2 Results and discussions

The copolymers were prepared by reversible addition-fragmentation chain transfer (RAFT) copolymerization[116, 117, 221] to ensure the formation of defined copolymers facilitating the correlation of their thermoresponsive behavior with the molecular structure. At first a kinetic study was performed with 25 mol% HEA and 75 mol% DMDMA revealing controlled copolymerizaion with near to ideal random comonomer distribution (Figure 7-8). Subsequently a series of copolymers was prepared with varying ratios of HEA and DMDMA yielding well-defined copolymers with a wide range of monomer compositions (Table 7-2).

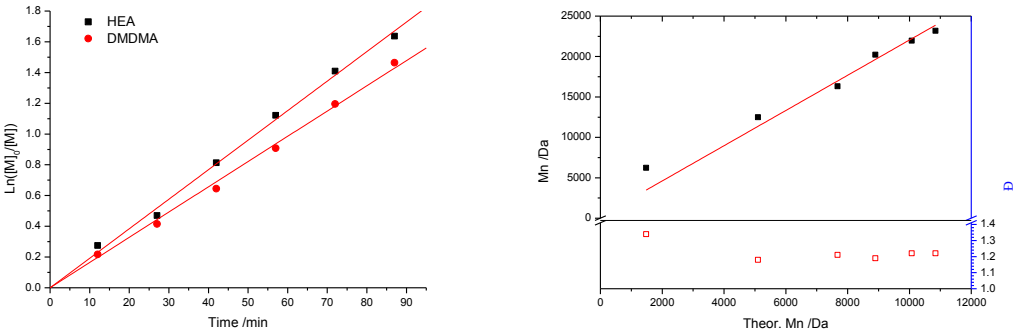

Figure 7-8 Left: Pseudo-first-order kinetic plot for RAFT polymerization of DMDMA and HEA with DMDMA: HEA: MPTTCP: AIBN=75: 25: 1: 0.1. Right: Corresponding Mn and Đ versus theoretical Mn plot.

Table 7-2 Polymer composition and properties of the synthesized copolymers in this section

Polymer	Theoretical DMDMA%[a]	DP[b]			DMDMA%[c]	Mn[d]/kDa	Đ[d]	T_{CP} /°C
		HEA	DMDMA	DMDMA%				
HP0	0%	84	0	0 %	0 %	27.3	1.13	N/A[e]
HP5	5%	81	2	2.4%	4.3%	27.0	1.11	N/A
HP12	12%	75	8	9.6%	10.0%	24.4	1.20	70.0[f]
HP15	15%	72	7	8.8%	11.4%	24.1	1.13	43.5
HP20	20%	69	14	16.9%[g]	15.5%	26.2	1.11	30.1
HP22	22%	71	12	14.5%[g]	16.4%	27.1	1.24	24.2
HP25	25%	61	23	27.0%	21.1%	24.0	1.20	16.6
HP30	30%	58	25	30.1%	26.5%	26.2	1.29	9.0
HP35	35%	55	29	34.5%	35.5%	24.9	1.27	Insoluble

[a] DMDMA% corresponding to the fraction of DMDMA of the copolymers; The theoretical values were determined by the feed ratios of the two monomers. [b] Calculated by GC using DMA as internal standard. [c] Determined by ^{1}H NMR spectroscopy. [d] Data collected by DMA SEC. [e] No phase transition had been detected until heating to 100 °C. [f] Determined by fast heating ramp, slow heating (1 °C/min) revealed no precipitation. [g] HP20 and HP22 bear reversed content of DMDMA obtained by GC could be considered as the error of GC measurement due to the bad solubility of DMDMA in methanol.

The thermoresponsive behavior of these HEA-DMDMA copolymers was evaluated in MilliQ water by turbidimetry at 5 mg/mL and the resulting T_{CP}s are plotted versus DMDMA content in Figure 7-9; the T_{CP}s of our previously reported P(mTEGA-DMDMA) copolymers are also shown for comparison.[237] Surprisingly, there is only a rather narrow composition window that yields thermoresponsive polymers, namely from 10 to ~ 30 mol% DMDMA as less DMDMA yields fully soluble polymers as expected since PHEA is water soluble,[231-233] whereas more DMDMA renders the polymers insoluble. Nonetheless, within this specific range T_{CP} exponentially correlates with DMDMA content. Comparison of P(HEA-DMDMA) with P(mTEGMA-DMDMA) generally revealed lower solubility, that is a lower T_{CP}, for P(HEA-DMDMA) within its thermoresponsive regime. This observation is rather unexpected as PHEA is more hydrophilic than PmTEGA indicating that the thermoresponsive behavior of these copolymers is not solely governed by their

hydrophilic-hydophobic balance. When comparing the schematic polymer structures of P(HEA-DMDMA) and P(mTEGA-DMDMA) it becomes evident that the observed differences in thermoresponsive behavior may result from the copolymer architecture (Figure 7-10). P(HEA-DMDMA) is a pure statistical copolymer in which the HEA side chain is smaller than the DMDMA side chain. On the contrary, the P(mTEGA-DMDMA) copolymer can be considered to be a kind of graft copolymer with large triethylene-glycol side chains that can cover and hide the DMDMA side chains. As such, it is proposed that the exposure of the hydrophobic DMDMA units to the aqueous medium is considerably higher in P(HEA-DMDMA) than in P(mTEGA-DMDMA) leading to a stronger hydrophobic contribution of DMDMA on the overall solubility behavior of P(HEA-DMDMA). This is in agreement with a recent observation from our group for poly(2-oxazoline)s where it was found that introducing more hydrophobic side chains causes a larger suppression of T_{CP} than introducing a more hydrophobic polymer backbone.[359]

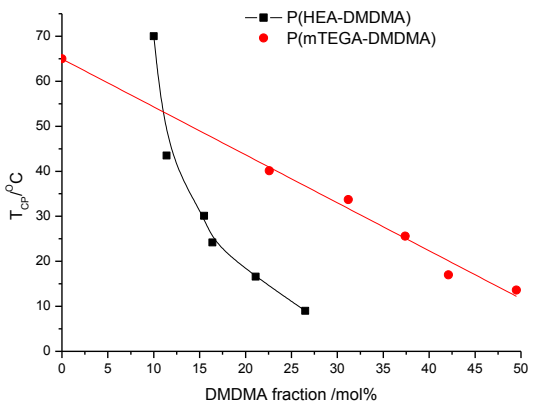

Figure 7-9 Evaluation of cloud point temperatures (T_{CP}) as function of DMDMA content (obtained by ^{1}H NMR spectroscopy) for P(HEA-DMDMA) and P(mTEGA-DMDMA)[237] in MilliQ water (5mg/ml). Lines are a guide for the eye and all polymers have the same end-groups and similar degree of polymerization.

Intrigued by this unusual solubility behavior of the P(HEA-DMDMA) copolymers, we continued to investigate the influence of the high exposure of the DMDMA units to the aqueous solution on the pH-dependent degradability of the copolymers. The hydrolysis of P(HEA-DMDMA) with T_{CP}=24.2 ^oC in milliQ (HP22, Table 7-2 Polymer composition and properties of the synthesized copolymers) in pH5, 6 and 7.4 will be discussed serving as representative example for the P(HEA-DMDMA) copolymer series. The T_{CP}s of the HP22 copolymer were monitored in time as measure for the hydrolysis, whereby the T_{CP} increases as the dioxolane group is hydrolyzed into two hydrophilic alcohol groups under release of acetone leading to higher solubility.[237, 350] For future use of these copolymers for pH-induced drug delivery, it will be important to know when the T_{CP} increases beyond body temperature, 37 ^oC, leading to dissolution of the copolymer. As shown in Figure 7-11a, no major changes in T_{CP} occurred upon incubation of HP22 at the physiological pH of 7.4 for as long as 1000 hours (42 days) indicating high stability of the copolymer at this pH resembling the

pH, in the blood stream. This high stability was expected considering the relatively high stability of the cyclic acetal group and indicates that higher exposure of the dioxolane moiety to the aqueous phase does not compromise this stability.[237, 334] However, incubation of HP22 at the endo/lysosomal pH of 5 resulted in a relatively fast increase of T_{CP} leading to solubility at 37 ^{o}C after ~200 hours. Even incubation of the HP22 copolymer in a pH 6 buffer solution leads to a steady increase in T_{CP} rendering the polymer soluble at 37 ^{o}C at ~1000 hours. It was confirmed by ^{1}H NMR spectroscopy that the increase in T_{CP} directly correlates to the conversion of the acetal moieties (see Figure 7-11a).

A direct comparison of the acid-catalyzed hydrolysis of P(HEA-DMDMA) and P(mTEGA-DMDMA) copolymers with similar T_{CP} of ~17 ^{o}C shows a strikingly faster hydrolysis for the P(HEA-DMDMA) while they both carry the same degradable acetal moieties (Figure 7-11b). After 800 hours there is nearly no hydrolysis of P(mTEGA-DMDMA) even at pH 5 while P(HEA-DMDMA) steadily hydrolyses at both pH 5 and pH 6, respectively, while being stable at pH 7.4. These results indicate that the better exposure of DMDMA in the P(HEA-DMDMA) copolymer allows faster hydrolysis under acidic conditions while the stability at pH 7.4 is unaffected. Moreover, there may be a catalytic effect of the HEA alcohol moieties to activate the acetal groups by hydrogen bonding leading to faster hydrolysis. A more detailed look at the data also revealed that the same degree of hydrolysis conversion leads to a larger T_{CP} increase for P(HEA-DMDMA) compared to PmTEGA-DMDMA.[360] This observation can be ascribed to the fact that hydrolysis of DMDMA in P(HEA-DMDMA) not only results in deprotection of two hydroxyl groups, but also unveils the hidden alcohol groups of the HEA segments. A direct comparison of the hydrolysis in time of P(HEA-DMDMA) (HP22 with T_{CP}=16.2 ^{o}C in pH 5 buffer) in pH 5 buffer with P(mTEGA-DMDMA (P50 with T_{CP}=12.2 ^{o}C in pH 5 buffer) revealed much faster hydrolysis of HP22 than P50, as expected based on the previous observations (Figure 7-11c). To exclude the possibility that the lower T_{CP} of P50 is partially responsible for the slower hydrolysis, a P(mTEGA-DMDMA) copolymer with much higher T_{CP} (P30 with T_{CP}=32.2 ^{o}C in pH 5 buffer) is also included in Figure 7-11c. Even this more hydrophilic P(mTEGA-DMDMA) copolymer revealed much slower hydrolysis than HP22 demonstrating that the presence of HEA is the prime responsible factor for the fast hydrolysis, either by higher exposure of DMDMA to the aqueous phase and/or by autocatalytic action.

7.2.3 Summary

In conclusion, we have demonstrated that by variation of the comonomer, the T_{CP} and pH-degradability of dioxolane containing copolymers can be drastically altered. It was found that hydroxyl functionalized thermo- and pH-responsive copolymers, P(HEA-DMDMA), reveal significantly faster pH triggered hydrolysis while maintaining high stability at neutral conditions compared to P(mTEGA-DMDMA) copolymers. This unexpected result is ascribed to the higher exposure of the dioxolane group in P(HEA-DMDMA) to the aqueous environment, possibly in combination with a catalytic effect of the alcohol groups

of HEA. As the HEA hydroxyl groups are masked by the hydrophobic dioxolane ring, the T_{CP}s of the P(HEA-DMDMA) copolymers were also lower compared to P(mTEGA-DMDMA) copolymers, despite that HEA is a more hydrophilic comonomer than mTEGA.

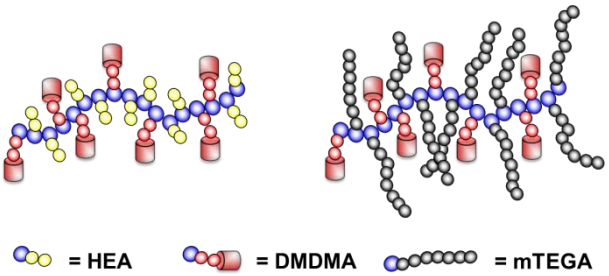

Figure 7-10 Schematic representation of the P(HEA-DMDMA) (left) and P(mTEGA-DMDMA) (right) copolymers.

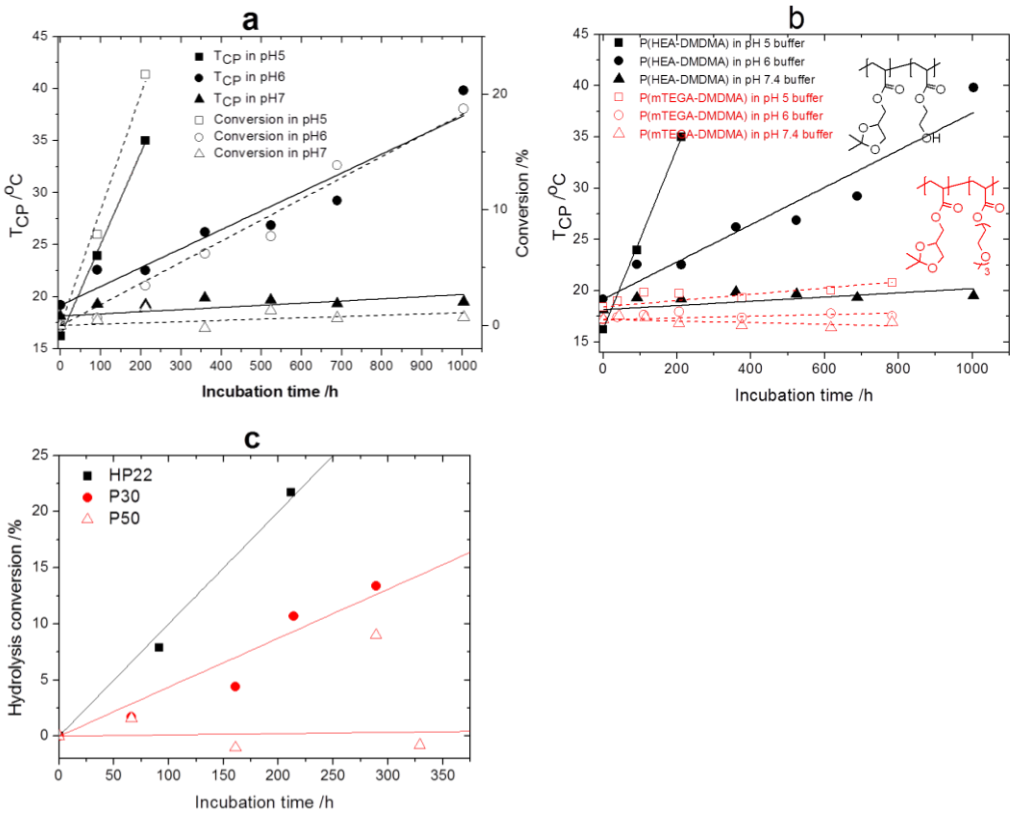

Figure 7-11 a) Plots of T_{CP} (solid symbols) and hydrolysis conversion (hollow symbols) versus time for HP22 incubated in pH 5, 6 and 7.4; b) Plots of T_{CP} versus hydrolysis time for HP22 and P42 at pH 5, 6 and 7.4; and c) Plots of hydrolysis conversion obtained from ^{1}H NMR for HP22, P30 and P50. Data for P42, P30 and P50 were previously reported.[237] (Lines are a guide for the eye)

In summary, we have demonstrated that control over copolymer architecture allows the use of relatively stable pH-degradable moieties to obtain polymers that are highly stable at pH 7.4 while readily degrading at pH 5 and 6. Importantly, the high stability of the dioxolane group facilitates synthesis and handling of these copolymers. Therefore, the developed P(HEA-DMDMA) copolymers are highly attractive for biomedical

applications such as intracellular drug or vaccine delivery.[336, 337] Further studies are in progress to evaluate the anti-cancer drug encapsulation and internalization of nanocarriers based on these dual responsive copolymer.

7.3 Dual responsive polymers based on pH labile linear acetals

7.3.1 Introduction

Thermoresponsive polymers with pH-labile groups developed in our group have been proved to be promising biomaterials for drug delivery systems (see section 7.1and 7.2). However, the pH induced hydrolysis of the cyclic acetal groups still requires a long period of time due to the intrinsic stability of the group even for the copolymers with HEA. In this section, we will describe the synthesis and hydrolysis behavior of dual pH- and temperature-responsive polymers with relatively fast hydrolysis in acidic environment based on the less stable linear acetal group.

7.3.2 Results and discussion

The new pH labile monomer, namely 2-(1-ethoxyethoxy) ethyl acrylate (EEEA), was prepared according to the literature (Scheme 7-3).[361] The synthesis was performed in ambient conditions resulting in a high yield (*ca.* 90%). After the purification of the functional monomer by distillation, its copolymerization with mTEGA was performed via reversible addition-framentation chain transfer (RAFT) polymerization at 70 ℃ using a trithiocarbonate-based chain transfer agent (CTA) and azobisisobutyronitrile (AIBN) as initiator in a toluene/*N*,*N*-dimethylacetamide (DMA) (80/20, vol %) solvent mixture yielding copolymers with tunable compositions, as listed in Table 7-3. The thermoresponsive behavior of the two copolymers was investigated by turbidimetry indicating the expected dependence of T_{CP} on the composition of the copolymers, which is lower T_{CP} with higher fraction of the hydrophobic acetal comonomer (Table 7-3).

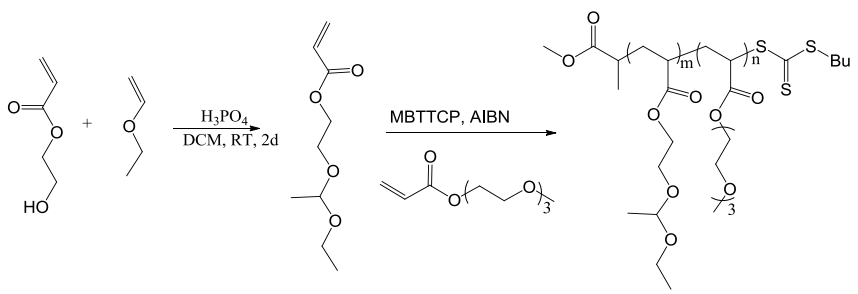

Scheme 7-3 Synthesis of 2-(1-ethoxyethoxy) ethyl acrylate (EEEA) and pH labile thermoresponsive copolymers

The pH induced hydrolysis was investigated by incubating the different copolymers (5 mg/mL) at 37 ℃ (i.e. physiological temperature), in pH 5 and pH 7.4 buffers. The linear acetal group from EEEA was previously reported to hydrolyze in acidic conditions giving hydroxyl group on polymer chains leading to a better solubility in water.[333, 334] Hence, the hydrolysis was followed by measuring the T_{CP} of the copolymers

as function of time. As shown in Figure 7-12, no major changes in T_{CP} occurred upon incubation at a pH of 7.4 indicating relatively high stability in neutral condition. However, incubation at pH 5 leads to quite fast hydrolysis of the acetal groups as indicated by the increase of T_{CP} in time for the copolymers. The hydrolysis of the two copolymers at pH 5 was also followed by ^{1}H NMR spectroscopy by calculating the integral ratio of the methyl group (the one directly connected to methylene group) of EEEA and the methyl group of mTEGA. As shown in Figure 7-12, these experiments fully confirm the trends observed via turbidimetry of the T_{CP} proving that the increase in T_{CP} is indeed resulted from hydrolysis of the acetal groups.

Table 7-3 Polymer composition and properties of the synthesized copolymers in this section

Code	Polymer	DP[a]		SEC		T_{CP} (°C)[b]
		EEEA	mTEGA	Mn/kDa	Đ	
CPET1	P($EEEA_{35}$-$mTEGA_{54}$)	35	54	14.2	1.27	29.5
CPET2	P($EEEA_{34}$-$mTEGA_{34}$)	34	34	13.2	1.16	19.9

[a]Determined by GC; [b]Determined by turbidimetry with 5 mg/ml in MilliQ water.

Compared to DMDMA-contained dual-responsive copolymers (section 7.1), P(EEEA-mTEGA) (CPET) copolymers exhibit much faster increase of T_{CP} due to the faster hydrolysis of the functional linear acetal group.[334] For instance, starting from the same T_{CP}, CPET1 exhibits a fast increase of T_{CP} at pH 5 from 25 °C to 43 °C in about 70h, while P37 (section 7.1) shows no evident increase of T_{CP} by incubation in the same pH buffer. ^{1}H NMR spectroscopy also reveals the faster hydrolysis of the linear acetal than the cyclic one by comparison on the hydrolysis rate of CPET2 and P50, both exhibiting T_{CP} at around 15 °C in pH5 buffer (section 7.1). After 250 hours there is nearly no hydrolysis of P50 at pH 5, while CPET2 steadily hydrolyzed at pH 5 up to 90 % conversion in 140 hours.

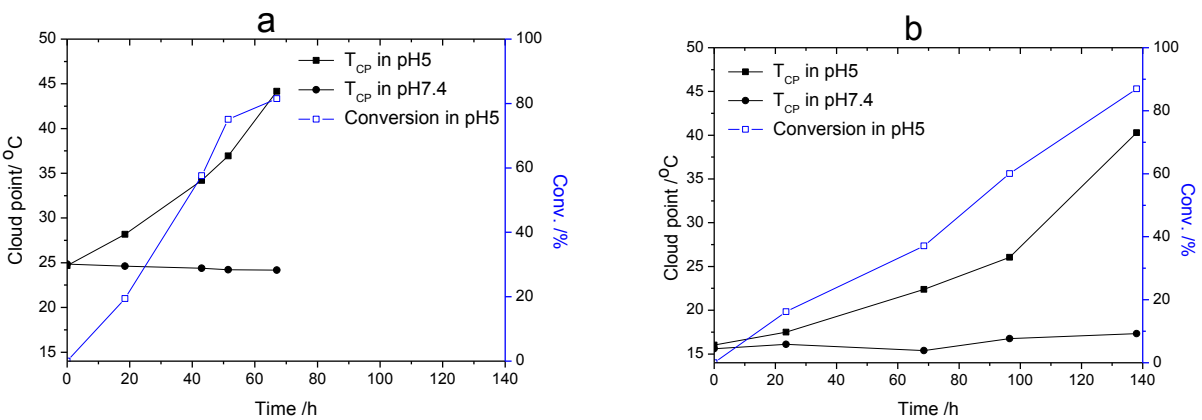

Figure 7-12 Plots of T_{CP}s versus hydrolysis time for copolymers (a) CPET1 and (b) CPET2 incubation in pH 5 and pH 7.4, respectively; conversion of hydrolysis is also shown for copolymers incubated in pH 5 (open symbols)

7.3.3 Summary

In summary, dual pH- and temperature-responsive polymers with a linear acetal comonomer were prepared by RAFT copolymerization. Due to the intrinsic lower stability of the linear acetal group compared to its cyclic analogue, the copolymers exhibit a faster hydrolysis in acidic conditions. This new class of dual responsive copolymer is highly attractive in biomedical applications.

7.4 Experimental section

7.4.1 Materials and Instrumentation

All chemicals and solvents were commercially available and used as received unless otherwise stated. Dichloromethane (DCM), toluene, *N*,*N*-dimethylacetamide (DMA), THF, methanol, $CDCl_3$, hexane are obtained from Sigma Aldrich. DCM was distilled before use. Azobisisobutyronitrile (AIBN, 98%, Aldrich) was recrystallized from MeOH (twice) and stored in the freezer. 2-(Butylthiocarbonothioylthio)propanoic acid and methyl-2-(n-pentyltrithiocarbonyl)propanoate (MPTTCP) were prepared according to the established procedures.[321] pH4 buffer was prepared by mixing 100 ml 0.1 M potassium hydrogen phthalate and 0.2 ml of 0.1 M HCl; pH 5 buffer was prepared by mixing 100 ml 0.1 M potassium hydrogen phthalate and 45.2 ml of 0.1 M NaOH; pH6/pH7.4 buffers was prepared by mixing 100 ml 0.1 M KH_2PO_4 and 11.2 ml/78.2 ml of 0.1 M NaOH, distilled water was added to these solutions to yield 200ml of buffers. Poly(ethylene glycol) monomethyl ether (average Mn ~2,000, Sigma Aldrich) was characterized by size exclusion chromatography with THF as eluent (Mn=2400, PDI=1.06) and ^{1}H NMR spectroscopy using $CDCl_3$ as solvent (DP=48). All polymerization were performed under a nitrogen atmosphere.

^{1}H NMR spectra were recorded on a Bruker 300 MHz FT-NMR spectrometer using $CDCl_3$ as solvent. Chemical shifts (d) are given in *ppm* relative to TMS.

Size exclusion chromatography (SEC) characterization for P(mTEGA-DMDMA) copolymers was carried out in THF at 45 ^{o}C at a flow rate of 1 mL/min with a SFD S5200 auto sampler liquid chromatogram pH equipped with a SFD refractometer index detector 2000. The PL gel 5 lm (105 Å, 104 Å, 103 Å, and 100 Å) columns were calibrated with polystyrene standards.

Size-exclusion chromatography (SEC) characterization for P(HEA-DMDMA) and P(EEEA-mTEGA) copolymers was performed on a Agilent 1260-series HPLC system equipped with a 1260 online degasser, a 1260 ISO-pump, a 1260 automatic liquid sampler (ALS), a thermostatted column compartment (TCC) at 50 ℃ equipped with a PSS Gram30 column in series with a PSS Gram1000 column, a 1260 diode array detector (DAD) and a 1260 refractive index detector (RID). The used eluent was DMA containing 50mM of LiCl at a flow rate of 1 ml/min. The spectra were analysed using the Agilent Chemstation software with the GPC add on. Molar mass and PDI values were calculated against Varian PMMA standards.

Gas chromatography was performed on a 7890A from Agilent Technologies with an Agilent J&W Advanced Capillary GC column (30 m, 0.320 mm, and 0.25 μm). Injections were performed with an Agilent Technologies 7693 auto sampler. Detection was done with a FID detector. Injector and detector temperatures were kept constant at 250 and 280 ^{o}C, respectively. The column was initially set at 50 ^{o}C, followed by two heating stages: from 50 ^{o}C to 100 ^{o}C with a rate of 20 ^{o}C /min and from 100 ^{o}C to 300 ^{o}C with a rate of 40 ^{o}C /min, and then held at this temperature for 0.5 minutes. Conversion was determined based on the integration of monomer peaks using DMA as internal standard.

Turbidity measurements were performed on a Cary 300 Bio UV-Visible spectrophotometer at a wavelength of 600 nm. The samples were first cooled to a suitable temperature to fully dissolve the copolymer (5 mg ml^{-1}), after which the sample was placed in the instrument and cooled to 5 ^{o}C. The transmittance was measured during at least two controlled cooling/heating cycles with a cooling/heating rate of 1 ^{o}C min^{-1} while stirring in a plastic disposable cuvette with block temperature probe.

Dynamic light scattering (DLS) was performed on a Zetasizer Nano-ZS apparatus (Malvern Instruments Ltd) using disposable cuvettes. The excitation light source was a He−Ne laser at 633 nm, and the intensity of the scattered light was measured at 173 °. This method measures the rate of the intensity fluctuation and the size of the particles is determined through the Stokes−Einstein equation

$$d(H)= kT/3\pi\eta D \qquad \text{Equation 7-1}$$

where d(H) is the mean hydrodynamic diameter, k is the Boltzmann constant, T is the absolute temperature, η is the viscosity of the dispersing medium, and D is the apparent diffusion coefficient. All samples were filtered through Millipore membranes with pore sizes of 0.2 μm prior to measurement.

Fluorescence measurements were carried out on a Cary Eclipse fluorescence spectrophotometer (Agilent Technologies) equipped with a Varian Cary Temperature Controller. The emission spectra resulting from excitation by a 200 nm laser were monitored from 520 - 700 nm, and the slit width was kept at 5 nm during the measurements.

7.4.2 Synthesis and characterization

Synthesis of (2,2-dimethyl-1,3-dioxolane-4-yl)methyl acrylate (DMDMA) monomer

The synthesis of this monomer was performed in two steps based on reported methods[345]. For the first step, glycerol (92 g, 1 mol), acetone (52g, 0.9 mol) p-toluenesulfonic acid monohydrate (0.1 g) and hexane (300 ml) were placed in a 500 ml flask and refluxed for 48h. 20ml of acetone were added after 12, 24 and 36 hours during reaction. Then the reaction solution was neutralized by adding potassium bicarbonate (0.22 g, 2.6 mmol) followed by filtration. The filtrate was dried under reduced pressure. Then 85.2 g (64%) of acetone glycerol was collected by distillation under reduced pressure. ^{1}H NMR (300 MHz, $CDCl_3$), δ (ppm):

4.19 (m, 1H, CH_2CHCH_2), 3.49–4.04 (m, 4H, $HOCH_2CHCH_2$), 2.52–2.75 (br, 1H, *H*O), 1.25-1.45 (d, 6H, $C(CH_3)_2$).

For the second step, a solution of acetone glycerol (22.36 ml, 180 mmol) and triethylamine (25.1 ml, 180.0 mmol) in anhydrous dichloromethane (DCM, 100 mL) was cooled to 0 ^oC in an ice water bath. Acryloyl chloride (16.2 ml, 200 mmol) in DCM (30 mL) was added dropwise with vigorous stirring. After 12h of reaction, the solution was filtered. The filtrate was washed twice with distilled water after neutralization by adding sodium hydroxide solution (0.1 M). Then the residual water and DCM were evaporated under reduced pressure. 26.0 ml (*ca*. 78%) DMDMA was purified by reduced-pressure distillation in the presence of hydroquinone as inhibitor. ^1H NMR (300 MHz, $CDCl_3$), δ (ppm): 5.70–6.40 (m, 3H, CH_2CH), 3.65–4.32 (m, 5H, CH_2CHCH_2), 1.25-1.42 (d, 6H, $C(CH_3)_2$).

Synthesis of methoxy tri(ethylene glycol) acrylate (mTEGA) monomer

The preparation procedure of mTEGA was similar as reported in literature.[362] A solution of triethylene glycol monomethyl ether (32 ml, 0.2 mol) and triethylamine (33.47 ml, 2.4 mol) in DCM (240 ml) was cooled to 0 ^oC in an ice water bath. Acryloyl chloride (19.4 ml, 0.24 mol) in DCM (60 mL) was added dropwise with vigorous stirring. After 12h of reaction, *ca*. 20g of silica gel was added to the solution. The mixture was purified by column chromatography using silica gel as stationary phase and DCM as eluent. Then the solvent was evaporated under reduced temperature. The product was finally purified by reduced-pressure distillation in the presence of hydroquinone as inhibitor. Yield: 33g (76%). 1H NMR (300 MHz, $CDCl_3$), δ (ppm): 5.70–6.42 (m, 3H, CH_2CH), 4.20–4.30 (m, 2H, $CH_2CHCOOCH_2$), 3.42-3.72 (m, 10H, $CH_2(OCH_2CH_2)_2OCH_3$), 3.3 (s. 3H. CH_3). WARNING: THIS MONOMER MIGHT CAUSE CHEMICAL BURNS WHEN IN DIRECT CONTACT WITH SKIN!

Synthesis of poly(ethylene glycol) macro chain transfer agent PEG-CTA

A solution of 2-(butylthiocarbonothioylthio)propanoic acid (1.43g, 6 mmol) and poly(ethylene glycol) monomethyl ether (10g) in DCM (100 ml) was cooled to 0 ^oC in an ice water bath. N-(3-dimethylaminopropyl)-N'-ethylcarbodiimide hydrochloride (1.15g, 6 mmol) and 4-dimethylaminopyridine (61.08 mg, 0.5 mmol) in DCM (40 ml) was added dropwise with vigorous stirring. Then the solution was allowed to react for 16 h in room temperature. After that, the solution was washed with water for two times and dried under reduced pressure. The solid residue was dissolved in DCM and precipitated for three times in hexane/diethyl ether mixture (80/20 *vol*). PEG-CTA was collected by drying under reduced pressure at room temperature for 48h. Mn (THF SEC)= 2600, Đ=1.06. ^1H NMR spectra of PEG and PEG-CTA are shown in Figure 7-13.

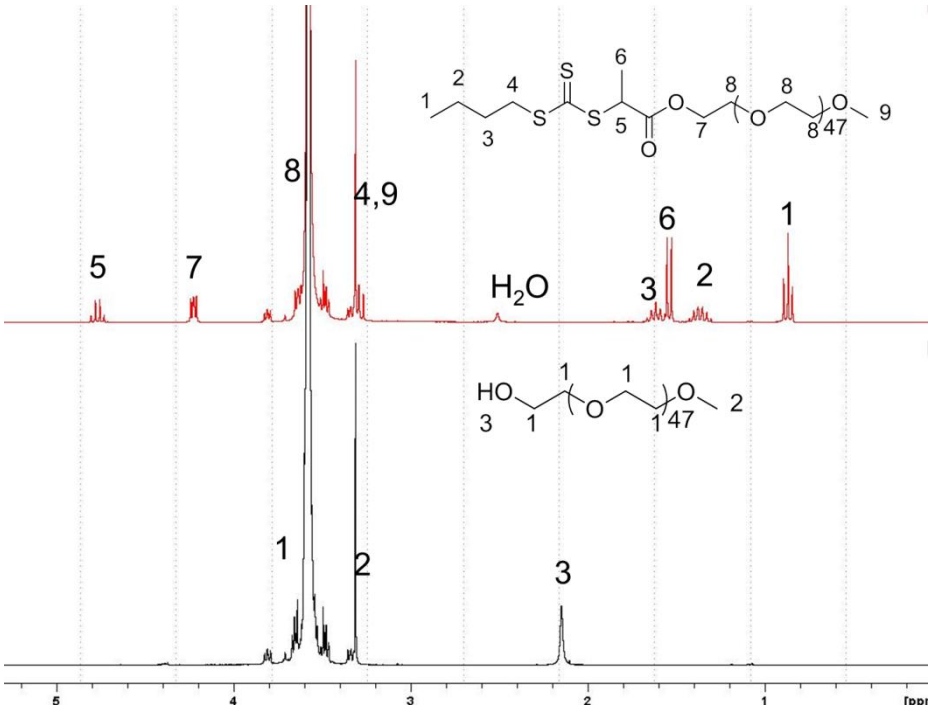

Figure 7-13 ^{1}H NMR spectra of PEG and PEG-CTA in $CDCl_3$

Synthesis of 2-(1-ethoxyethoxy)ethyl acrylate (EEEA)

Under a nitrogen atmosphere, hydroxylethyl acrylate was added slowly at 0 ℃ to a mixture of ethyl vinyl ether phosphoric acid as a catalyst. The mixture was stirred at room temperature for 48 h. The catalyst was then removed by passing through an aluminum oxide column. Then the excess vinyl ether was evaporated. The product was distilled at reduced pressure with hydroquinone as inhibitor. Yields are about 90%. ^{1}H NMR (500 MHz, $CDCl_3$), δ (ppm): 5.70–6.40 (m, 3H, CH_2C*H*), 4.8 (m, 1H, C*H*), 4.3 (t, 2H, COOCH_2), 3.6–3.8 (m, 4H, COOCH$_2$CH_2 & OCH_2CH$_3$), 1.25-1.4 (m, 6H, CHCH_3 & CH$_2$CH_3).

Synthesis of poly(DMDMA-co-mTEGA)

DMDMA, mTEGA azobisisobutyronitrile (AIBN) and MPTTCP were first dissolved in toluene/DMA solvent mixture (80/20 *vol*) in a schlenk vial. The concentration of monomer was fixed at 2M in different ratios. After degassing the solution three times by freeze-vacuum-thaw cycles, the schlenk vial was filled with argon and immersed in a preheated oil bath at 70 ^{o}C while stirring. The polymerization was performed for about 2 hours and stopped by immersing the schlenk vial into a dry ice/isopropanol bath. The resulting polymer was isolated by precipitation in hexane (three times) followed by drying under reduced pressure at 50 ^{o}C. Conversion of the monomers was analysed by GC with DMA as internal standard. Size exclusion chromatography was used to evaluate number average molecular weight (Mn) and dispersities (Đ) of the obtained polymers. For kinetic studies, samples were withdrawn from the polymerization mixture under a flow of argon at different times.

Synthesis of PEG-block-poly(DMDMA-co-mTEGA)

DMDMA, mTEGA, AIBN and PEG-CTA were first dissolved in toluene/DMA solvent mixture (80/20 *vol*) in a schlenk vial. The concentration of monomer was fixed at 1.5 M. After degassing the solution three times by freeze-vacuum-thaw cycles, the schlenk vial was filled with argon and immersed in a preheated oil bath at 70 ^{o}C while stirring. The polymerization was performed for 2 hours and stopped by immersing the reaction flask into dry ice isopropanol bath. The resulting polymer was isolated by precipitation in hexane (three times) followed by drying under reduced pressure. Conversion of the monomers was analysed by GC with DMA as internal standard. Size exclusion chromatography was used to evaluate number average molecular weight (Mn) and dispersities (Đ) of the obtained polymers.

Synthesis of poly(HEA-DMDMA) copolymers

DMDMA, HEA, AIBN and MPTTCP were first dissolved in DMA/DMF solvent mixture (80/20 *vol*), or toluene/DMA solvent mixture (80/20 *vol*) in a schlenk vial. The concentration of monomer was fixed at 2M and a ratio [M]:[MPTTCP]:[AIBN] of 100:1:01 was used. After degassing the solution three times by freeze-vacuum-thaw cycles, the schlenk vial was filled with nitrogen and immersed in a preheated oil bath at 70 ^{o}C while stirring. The polymerization was performed for about 90 min and stopped by immersing the schlenk vial into dry ice/isopropanol bath. The resulting polymer was isolated by precipitation in diethyl ether (three times) followed by drying under reduced pressure at room temperature. Conversion of the monomers was analyzed by GC with DMF or DMA as internal standard. Size exclusion chromatography was used to evaluate number average molecular weight (Mn) and dispersities (Đ) of the obtained polymers. For the kinetic study, samples were withdrawn from the polymerization mixture under a flow of nitrogen at different times.

Synthesis of poly(EEEA-mTEGA) copolymers

EEEA, mTEGA, AIBN and MPTTCP were first dissolved in Toluene/DMA solvent mixture (80/20 *vol*) in a schlenk vial. The concentration of monomer was fixed at 2M and a ratio [M]:[MPTTCP]:[AIBN] of 100:1:01 was used. After degassing the solution three times by freeze-vacuum-thaw cycles, the schlenk vial was filled with nitrogen and immersed in a preheated oil bath at 70 ^{o}C while stirring. The polymerization was performed for about 100 min and stopped by immersing the schlenk vial into dry ice/isopropanol bath. The resulting polymer was isolated by precipitation in hexane/diethyl ether solvent mixture (80/20 in volume) followed by drying under reduced pressure at room temperature. Conversion of the monomers was analyzed by GC with DMA as internal standard. Size exclusion chromatography was used to evaluate number average molecular weight (Mn) and dispersities (Đ) of the obtained polymers.

7.4.3 Methods

pH triggered hydrolysis of poly(DMDMA-co-mTEGA)

Hydrolysis of poly(DMDMA-*co*-mTEGA) was performed in pH buffers (pH=4, 5, 6, and 7.4 respectively) at a concentration of 5 mg/ml at 37 ^{o}C in test tubes. Samples for cloud point measurement were taken directly from the hydrolysis solution. For ^{1}H NMR measurements, 10 ml of hydrolysis solution was taken from the tube and was first neutralized by adding NaOH solution. The mixture of inorganic salt and polymer was directly used for the ^{1}H NMR analysis after evaporating the water under reduced pressure and dissolving the residue in MeOH-*d*4.

Acid-triggered release of Nile red.

The acid-triggered release of Nile red was studied in three pH buffers, pH4, pH5 and pH7.4. In general, 0.1 ml of Nile red in ethanol (3mg/mL) was mixed with 0.9 mL of an aqueous solution with 10 mg block copolymer at room temperature. After 1 min of incubation with stirring, the solution was put in a preheated water bath at 50 ^{o}C and incubated for 1 min. Then the solutions were transferred back to a water bath at 37 ^{o}C. 9 ml of pH buffer (preheated to 37 ^{o}C) was added to the solution to dilute the polymer solution to 1 mg/ml in different pH buffers, pH4, pH5 and pH7.4. The emission spectrum of the solution was recorded at 37 ℃ for every half an hour by fluorescence spectroscopy.

Cell viability assay (MTT) (performted by collaborators)

Dulbecco's Phosphate-Buffered Saline (DPBS), Dulbecco's Modified Eagle Medium (DMEM), fetal bovine serum (FBS), L-glutamine, sodium pyruvate, penicillin and streptomycin were purchased from Invitrogen. Dimethyl sulfoxide (DMSO) and 3-(4,5-dimethylthiazol-2-yl)-2,5-diphenyltetrazolium bromide (MTT) were commercially available at Sigma Aldrich. Acetone was purchased from Fischer Chemical. Membrane filters (0.22 μm) were obtained from Whatman. HCA2-hTERT human fibroblasts were kindly provided by C. Jones (Cardiff University, UK). RAW 264.7 mouse macrophages were obtained from ATCC. The MTT assay was executed in 96-well titer plates purchased from TPP. Absorbance was measured on a Perkin Elmer microplate reader.

HCA2-hTERT human fibroblasts and RAW264.7 mouse macrophages were cultured in DMEM, supplemented with 10% FBS, 2 mM L-glutamine, 1 mM sodium pyruvate and antibiotics (50 units/mL penicillin and 50 μg/mL streptomycin). Cells were incubated at 37 ℃ in an controlled, sterile environment of 95% relative humidity and 5% CO2.

Polymer stock solutions of 5mg/ml were prepared by dissolving 20mg of polymer in 4ml cold (4 ℃) culture medium. Acetone was added to stock solutions of fully hydrolyzed polymers (polymer 1, 5 and 6) in accordance to the amount that would be released after hydrolysis of the corresponding non-hydrolyzed

polymer. Stock solutions were sterilized by membrane filtration. With these obtained stock solutions, two dilutions in culture medium were made to reach a concentration of 0.5 and 0.05 mg/mL, respectively.

MTT stock solution consisted of 250mg MTT, dissolved in 50ml of PBS. For MTT assay, MTT solution was prepared by a fivefold dilution of MTT stock solution in culture medium. The MTT assay was performed according to established procedures. Briefly, HCA2-hTERT human fibroblasts and RAW264.7 mouse macrophages were seeded into 96-well titer plates (10 000 cells per well, suspended in 200µl of culture medium) and incubated for 24h. Thereupon, 50µl of polymer solution (5, 0.5 or 0.05 mg/mL), DMSO (positive control = 0% viability) or culture medium (negative control = 100% viability) was added. After 24h of incubation, medium was aspirated and cells were washed with 250 µL PBS. After aspiration, 200 µL of MTT solution was added for 4h. MTT solution was removed and the purple formazan crystals were dissolved in 50µl of DMSO. Absorbance was determined at 590nm on a microplate reader. The absorbance of the positive control was subtracted from all values. Cell viability (%) was defined as absorbance of the test polymer divided by absorbance of negative control times 100% . Experiments were carried out in quintuplicate.

Protein bioconjugation (performted by collaborators)

PAGE experiments were conducted using the Bio-Rad mini-PROTEAN tetra set-up. A typical conjugation procedure was as follows. A lysozyme (from hen egg white, Sigma) solution in DI water (0.25 mL, 8.56×10^{-5} mmol, 5 mg mL^{-1}) was added to different volumes of a NHS-terminated p(DMDMA28-mTEGA56) solutions in DI water (10 mg mL^{-1} for the 7 kDa polymer and 20 mg mL^{-1} for the 17 kDa polymer), respectively in a 1:1, 1:10 and 1:20 molar ratio. The total volume was brought to 2 mL with a 0.1 M sodium bicarbonate buffer of pH 8.3. The solutions were kept at room temperature with gentle shaking overnight. Polymer solution without lysozyme was included as a control. Moreover half of the conjugation mixture was brought to pH 3 with 0.1 M HCl and kept in a heating block at 56 ℃ overnight, in order to hydrolyze the polymer under accelerated conditions. The undiluted conjugation mixtures were analyzed by SDS-PAGE. To confirm LCST behavior, native page was performed at room temperature and at 45 ℃ by placing the PAGE set-up in an oven.

Chapter 8 Polymeric temperature sensor with a broad sensing regime

Abstract: In this chapter, we will report some preliminary results on the development of polymeric temperature sensor with a broad sensing regime in aqueous solution. Two strategies, namely including gradient within the polymer chain and incorporation of high polar hydroxyl functionality, are used to broader the phase transition rang of dye-functional thermoresponsive copolymers. Disperse red 1 is chosen as solvatochromic dye as it allows a ratiometric signal for a temperature read-out, which is much less concentration dependent. The influence of polymer gradient and the presence of hydroxyl groups on the sensing regime of the thermometer will be investigated.

8.1 Introduction

Polymeric temperature sensors have attracted increasing attention during the last decades mainly due to the wide applicability and importance of temperature determination.[143] The combination of solvatochromic dyes and thermoresponsive polymers that undergo a temperature induced phase transition provides access to thermosensors wtih an easy read-out as well as high adaptability of the sensing behavior towards different applications.

After about 20 years of development, polymeric temperature sensors have been reported for various applications.[143] Uchiyama et al. have reported the intracellular thermometry with a fluorescent nanogel thermometer based on the thermoresponsiveness of PNIPAM in combination with environmentally sensitive fluorophores.[191, 206, 207] Polymeric thermometers that simultaneously sense temperature and pH were reported by Hoogenboom[184] and Chung.[199] However, the temperature sensing regime of LCST-based sensors is often limited to a narrow temperature range (around 10 to 20 ^{o}C) resulting from the sharp entropic LCST phase transition. Hoogenboom et al. reported temperature sensors by combination of disperse red 1 (DR1) or pyrene[100] and thermoresponsive PMMA, which exhibit UCST behavior in ethanol/water solvent mixtures.[52, 65, 87] These sensors exhibit a much broader temperature sensing regime of 30 ^{o}C due to the broader enthalpic UCST phase transition.

In this section, we will report some preliminary results on the development of a polymeric temperature sensor with a broader temperature sensing regime in waetr. Hence, a polymer is required with a broad phase transition range. Therefore, gradient LCST thermoresponsive polymer sensors are developed aiming for gradual dehydration and collapse of the copolymer chains.[232] In addition, hydroxyl groups are introduced in the LCST polymer sensor to investigate their effect on the LCST phase transition process.

8.2 Results and discussion

The synthesis of the DR1-labeled copolymer was performed using Cu(0)-mediated polymerization to ensure the preparation of well-defined copolymers allowing a straightforward interpretation of the sensing results. The kinetics of the gradient copolymerization of 2‑hydroxyethyl acrylate (HEA) or mTEGA and 2‑methoxyethyl acrylate (MEA) using ethyl α-bromoisobutyrate (EBiB) as initiator and tris[2-(dimethylamino)ethyl]amine (Me_6TREN) as ligand was first investigated in presence of disperse red 1 acrylate (DR1-A). The copolymerization reactions were initiated by the addition of copper wire to the mixture of HEA (or mTEGA): DR1-A: EBiB: Me_6TREN: $CuBr_2$ in DMSO in a ratio of 80: 3:1:0.18:0.05 mixtures in DMSO at room temperature following our recently optimized protocol.[230] The continuous addition of 80 equivalents of MEA dissolved in DMF to the reaction mixture was started after 15 minutes (syringe pump). After the addition of MEA over 60 min, the polymerization was allowed to run for another 20 min. The conversion of HEA (or mTEGA) and MEA were followed in time by gas chromatography (GC)

with DMSO and DMF as internal standard, respectively. As shown in Figure 8-1, the two gradient copolymers exhibit similar gradients as indicated by the same evolution of cumulative composition of MEA versus DP. HEA-MEA copolymerization was found to be faster than the mTEGA-MEA copolymerization leading to a longer copolymer chain in the same time frame. The characterization details of the resulting gradient copolymers, namely HEA_{45}-*grad*-MEA_{23}-DR1 and $mTEGA_{38}$-*grad*-MEA_{13}-DR1 with relatively narrow molecular weight distributions are listed in Table 8-1. A statistical copolymer, namely HEA_{16}-*st*-MEA_{27}-DR1, was also synthesized by Cu(0)-mediated polymerization to serve as reference of non-gradient copolymer (Table 8-1). The DR1 dye was successfully incorporated into the copolymers as determined by ^{1}H NMR spectroscopy. The defined structure of the resulting gradient and statistical copolymers as indicated by relatively low Đ values make these copolymers good candidates for the investigation of temperature sensing property.

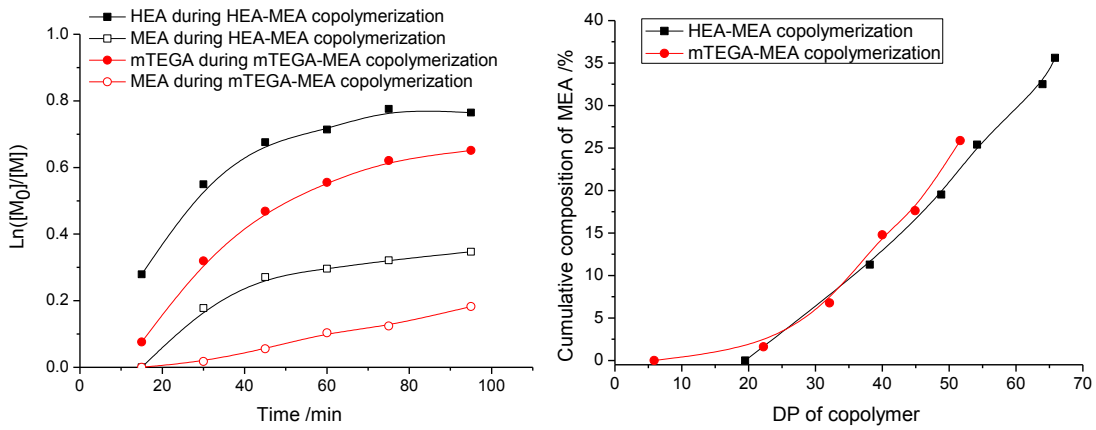

Figure 8-1 Left) kinetic plots for the gradient copolymerization with continuous addition of MEA; Right) Calculated monomer distributions of the investigated HEA-MEA and mTEGA-MEA gradient copolymer

Table 8-1 Polymer composition and properties of the synthesized copolymers in this section

Polymers	MEA% by GC	MEA% by ^{1}H NMR	SEC Mn/kDa	Đ
HEA_{45}-*grad*-MEA_{23}-DR1	33.8%	34.5%	23.2	1.14
HEA_{16}-*st*-MEA_{27}-DR1	62.8%	N/A	12.9	1.34
$mTEGA_{38}$-*grad*-MEA_{13}-DR1	25.5%	N/A	15.3	1.23

To quantify the temperature sensing ability of the DR1-functionalized HEA_{45}-*grad*-MEA_{23}-DR1 in aqueous solution, UV/vis absorption spectra were recorded at different temperatures during heating of the polymer solution in water (0.2 mg/ml). The spectra (Figure 8-2) clearly show the intensity change of the two absorption maxima of the DR1 dye at 291 nm ($\pi^*\leftarrow\pi$ (n)) and 500 nm ($\pi^*\leftarrow\pi$). At 14 ^{o}C, when the polymer

is completely dissolved in water, the polymer revealed the lowest absorbance at both absorption maxima and no scattering was observed above 650 nm as expected for molecularly dissolved polymer chains. The precipitation of the polymer started at about 30 ^{o}C leading to a clear intensity increase of both the absorption maxima, which is most likely due to solvation of the DR1 moiety in the less polar precipitated polymer agglomerate. However, the intensity at 290 nm increases more steeply than the intensity at 500 nm in line with previous reports.[100, 184]

The intensity ratio of the ($\pi^*\leftarrow\pi$ (n)) and ($\pi^*\leftarrow\pi$) transitions of HEA_{45}-*grad*-MEA_{23}-DR1 are plotted as a function of temperature in Figure 8-2. The use of intensity ratio instead of individual absorption intensity as sensing signal is believed to make the sensor more robust since this ratio will be less dependent on the polymer concentration compared to absolute intensity. The ratio significantly increased from 0.45 to about 0.86 as the temperature increased from 30 to 60 ^{o}C indicating a broad sensing regime of about 30 ^{o}C, which is much higher compared to most of the reported polymeric thermometer based on LCST phase transition, specially the previous reports using DR1 with POEGMAs.

To elucidate the reason for the broad sensing regime, we also evaluated the sensor behavior of the gradient copolymer without hydroxyl groups, namely $mTEGA_{38}$-*grad*-MEA_{13}-DR1, and the statistical copolymer with hydroxyl groups, namely HEA_{16}-*st*-MEA_{27}-DR1 by UV-Vis spectroscopy. Figure 8-3 displays the UV-Vis absorption of $mTEGA_{38}$-*grad*-MEA_{13}-DR1 and the absorption ratio as a function of temperature. The enhancement of absorption ratio increased about 4 fold due to increasing of temperature, which is higher than that found for HEA_{45}-*grad*-MEA_{23}-DR1 (2 folds) due to the lower hydrophilicity of mTEGA than HEA.[189] However, the sensing regime of the copolymer solution, which is about 15 ^{o}C, is much narrower compared to the HEA gradient copolymer analogue. These results indicate that the monomer gradient might not be the reason for the broader sensing regime of HEA_{45}-*grad*-MEA_{23}-DR1.

Next, the sensing ability of the statistical copolymer with hydroxyl groups, namely HEA_{16}-*st*-MEA_{27}-DR1, was also followed by UV-Vis spectroscopy during heating. The statistical copolymer exhibits a much higher MEA content compared to HEA_{45}-*grad*-MEA_{23}-DR1. Nonetheless, the two hydroxyl-functional copolymers exhibit similar phase transition temperature due to their different polymer architecture making the statistical copolymer a perfect reference of the gradient HEA-MEA copolymer. As shown in Figure 8-4, the absorption ratio increased from about 0.46 to 0.86 when heating the polymer aqueous solution from 30 ^{o}C to 60 ^{o}C indicating a broad sensing regime of *ca.* 30 ^{o}C and a two-fold increase revealing that the hydroxyl groups are in fact responsible for the broader temperature sensing regime. We propose that the hydroxyl group can hydrogen bond with water significantly slowing down the dehydration during the thermal induced LCST phase transition. Further heating of the polymer solution induced gradual exclusion of the water in polymer globules leading to a slow increase of the absorption ratio of the DR1 dye.

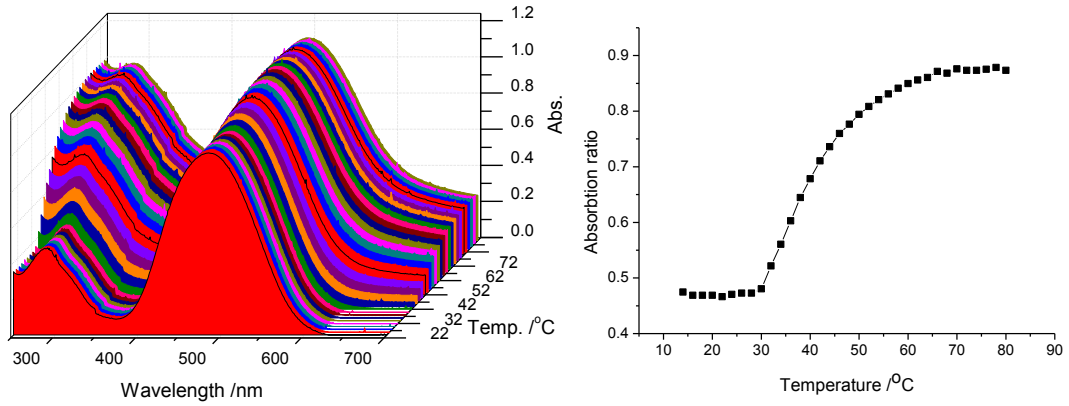

Figure 8-2 Left) UV-Vis spectra of HEA_{45}-*grad*-MEA_{23}-DR1 in aqueous solution at 0.2 mg/ml; and Right) temperature dependence of the absorption ratio (π*←π (n)/π *←π)

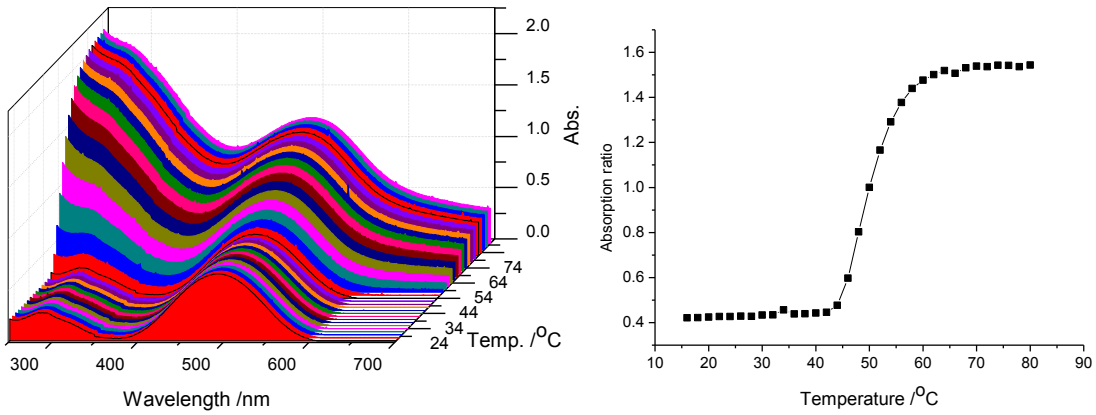

Figure 8-3 Left) UV-Vis spectra of $mTEGA_{38}$-*grad*-MEA_{13}-DR1 in aqueous solution at 0.2 mg/ml; and Right) temperature dependence of the absorption ratio (π*←π (n)/π *←π)

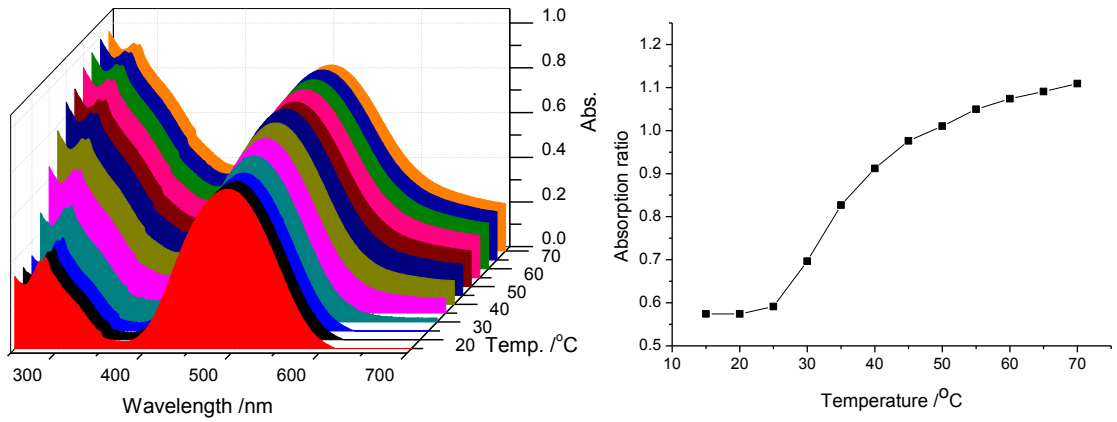

Figure 8-4 Left) UV-Vis spectra of HEA_{16}-*st*-MEA_{27}-DR1 in aqueous solution at 0.2 mg/ml; and Right) temperature dependence of the absorption ratio (π*←π (n)/π *←π)

8.3 Summary and outlook

In summary, we developed polymeric temperature sensors with a broad sensing regime in aqueous solution and investigated the influence of gradient structure and the presence of hydroxyl groups on their sensing regime. By comparison on the sensory properties of copolymers with and without gradient and hydroxyl groups, respectively, the broad sensing regime could be ascribed to the hydrogen bonding of the hydroxyl group with water, which induces slower, more gradual dehydration of the copolymer globules leading to a broader phase transition range. Further analysis is needed to confirm this proposed mechanism.

8.4 Experimental section

8.4.1 Materials and Instrumentation

All chemicals and solvents were commercially available and use as received unless otherwise stated. Ethyl α-bromoisobutyrate (EBiB, 98%), tris[2-(dimethylamino)ethyl]amine (Me_6TREN) were obtained from Sigma Aldrich. Pre-cut copper wire (Sigma-Aldrich, 99.9%) was pretreated with diluted sulphuric acid and milliQ water to remove the oxidized copper. After drying under a nitrogen flow, the copper wire was stored in a nitrogen atmosphere. 2-Methoxyethyl acrylate (MEA, 98%) and 2‑hydroxyethyl acrylate (HEA) were purchased from Sigma-Aldrich and purified by passing over a neutralized aluminium oxide column to remove the inhibitor. Copper(II) bromide (CuBr2, 99%) was purchased from Fluka and used as received.

^{1}H NMR spectra were recorded on a Bruker 300 MHz FT-NMR spectrometer using deuterated dimethyl sulfoxide (DMSO-d6) as solvent. Chemical shifts (d) are given in ppm relative to TMS.

Size-exclusion chromatography (SEC) characterization was performed on a Agilent 1260-series HPLC system equipped with a 1260 online degasser, a 1260 ISO-pump, a 1260 automatic liquid sampler (ALS), a thermostatted column compartment (TCC) at 50 ℃ equipped with a PSS Gram30 column in series with a PSS Gram1000 column, a 1260 diode array detector (DAD) and a 1260 refractive index detector (RID). The used eluent was DMA containing 50mM of LiCl at a flow rate of 0.6 ml/min. The spectra were analysed using the Agilent Chemstation software with the GPC add on. Molar mass and PDI values were calculated against Varian PS standards.

Gas chromatography was performed on a 7890A from Agilent Technologies with an Agilent J&W Advanced Capillary GC column (30 m, 0.320 mm, and 0.25 μm). Injections were performed with an Agilent Technologies 7693 auto sampler. Detection was done with a FID detector. Injector and detector temperatures were kept constant at 250 and 280 ^{o}C, respectively. The column was initially set at 50 ^{o}C, followed by two heating stages: from 50 ^{o}C to 100 ^{o}C with a rate of 20 ^{o}C /min and from 100 ^{o}C to 300 ^{o}C with a rate of 40 ^{o}C /min, and then held at this temperature for 0.5 minutes. Conversion was determined based on the integration of monomer peaks using DMSO or DMF as internal standard.

UV-Vis spectra were collected on a Cary 300 Bio UV-Visible spectrophotometer with wavelength range from 700 to 250 nm.

8.4.2 Synthesis and characterization

Synthesis of (2-{N-ethyl-N-[4-(4-nitrophenylazo)phenyl]amino}ethyl acrylate) (DR1-A).

To a solution of disperse red 1 (DR1, 1 equivalent.) in anhydrous DCM, triethylamine (2 equivalents) were added followed by dropwise addition of acryloyl chloride (2 equivalents). The resulting mixture was stirred at 0 ℃ and allowed to warm to room temperature overnight. Subsequently, the reaction solution was washed with water. After evaporation of the DCM, the crude product DR1-A was purified by silica gel chromatography eluting with n-hexane/diethyl ether (25:75).

Cu(0)-mediated synthesis of gradient copolymer

HEA (or mTEGA), DR1-A, EBiB, Me_6TREN and $CuBr_2$ were first dissolved in DMSO in a schlenk vial. After degassing the solution three times by freeze-vacuum-thaw cycles, the polymerization was initiated by adding copper wire in the solution under nitrogen atmosphere. After 15 min of reaction, the continuous addition of MEA dissolved in DMF to the reaction mixture was started (syringe pump). The addition of MEA finished in 60 min, after which the polymerization was allowed to proceed for another 20 min. The copolymerization was stopped by immersing the schlenk vial into liquid nitrogen. After addition of DCM to the frozen solution, the mixture was incubated at room temperature to allowed melting of the frozen solution. A neutralized aluminium oxide column eluting with DCM was used to remove the copper salts. The resulting polymers were isolated by precipitation in n-hexane/diethyl ether (75/25) for three times followed by drying under reduced pressure at room temperature. The conversion of HEA (or mTEGA) and MEA were followed in time by gas chromatography (GC) with DMSO and DMF as internal standards, respectively.

The synthesis of the HEA-MEA statistical copolymer was performed using Cu(0)-mediated copolymerization in a similar procedure as the synthesis of the gradient copolymers.

Chapter 9 General conclusions and outlook

Thermoresponsive polymers are widely used as smart materials in a variety of fields, including biomedicine, temperature sensing and nanotechnology. The use of controlled radical polymerization (CRP) techniques and/or post-polymerization modification allows the synthesis of defined polymers with accurately tunable thermoresponsive behavior making such polymers very attractive.

In this thesis, the development of novel thermoresponsive smart materials with UCST behavior, multi-responsive materials as well as co-assembly of different responsive polymers were described. With regard to applications, dual pH- and temperature polymers for drug delivery purposes and polymeric temperature sensors with broad temperature sensing regime were also discussed.

In **Chapter 1** we reviewed the current developments of thermoresponsive polymers. In particular, the development of polymers that undergo phase separation upon cooling, so-called UCST behavior in alcohol/water solvent mixtures and polymeric temperature sensors were discussed in detail.

In **Chapter 2** we discussed the methods concerning the synthesis of well-defined polymers and the investigation of thermoresponsive behavior of polymers. A one-pot procedure that straightforwardly combines RAFT polymerization and end group transformation to remove the RAFT end-groups was developed for the synthesis of well-defined polymers. This procedure only requires the addition of excess primary amine after the standard RAFT polymerization procedure, which eliminates the need for separation and purification of the intermediate polymers and hence leads to extreme reduction of the working time and utilized solvents. In addition, the influence of the parameters used for turbidimetry measurements of thermoresponsive polymer solution behavior was investigated. Various parameters, such as concentration, heating rate, wavelength of incident light, stirring, position of temperature probe and type of cuvette can provide in depth information of the thermoresponsive behavior of polymers in solution on the one hand, but can also strongly influence the results leading to erroneous results on the other hand. Finally, the "best" condition for the turbidimetry measurement was proposed.

In **Chapter 3** we have presented the synthesis and characterization of a series of PMMA copolymers with tunable UCST behavior in ethanol/water solvent mixtures. It is found that only 6 mol% of the methacrylamide comonomer can result in a dramatic change of the UCST transition temperature of the corresponding PMMA copolymers in aqueous ethanol. In addition, we synthesized and studied the dual responsive behavior of azobenzene-containing PMMA copolymers, which represent, to the best of our knowledge, the first example of a dual responsive copolymer combining light responsiveness with UCST behavior in an aqueous solvent mixture.

In **Chapter 4** we developed a novel type of polyampholytes with UCST behavior prepared by copolymerization of cationic and anionic monomers. Direct radical copolymerization of cationic and anionic monomers was investigated by RAFT procedure. The reactivity of the two monomers is severely influenced by their strong electrostatic attraction. Nonetheless, fine-tuning of the feed ratio of the two monomers could suppress the gradient formation allowing the synthesis of quasi-random copolymers with equimolar amounts of the anionically and cationically charged monomers. The resulting charge neutral polyampholytes were found to show UCST behavior in various alcohol/water solvent mixtures. In addition, the UCST transition of the copolymers can be well tuned by varying the content of alcohol in the solvent mixtures. The temperature-dependent inter- and/or intra-chain electrostatic attraction of the copolymers can be used for UCST-based temperature controlled self-assembly. As a proof of concept, a polyampholyte with ethylene glycol side chains was synthesized, which was found to form defined nano-structures upon cooling in ethanol or isopropanol.

In **Chapter 5** we first discussed the tuning of the LCST and UCST thermoresponsive behavior of poly(*N*,*N*-dimethylaminoethyl methacrylate) by electrostatic interactions with multivalent metal ions and copolymerization. The UCST T_{CP} of PDMAEMA was found to be highly tunable depending on the particle size of the trivalent ion, while the LCST transition was hardly affected by the type and concentration of counterions. The influence of comonomers on the double thermoresponsive behavior of PDMAEMA was also investigated revealing that both the hydrophobicity and side chain length can influence the UCST behavior of PDMAEMA, while the LCST behavior of PDMAEMA is only affected by the hydrophobicity of the comonomer. In addition, we have shown a new class of triple thermoresponsive 'schizophrenic' diblock copolymers that undergoes transitions from conventional micelles (or vesicles) via unimers to reverse micelles (or vesicles) and finally to a precipitated state upon heating. The various transition temperatures of this copolymer could well be tuned by varying the concentration of trivalent anion and pH.

In **Chapter 6** we discussed the cooperative behavior of thermoresponsive (co)polymers. A systematical study on the cooperative LCST behavior of copoly(2-oxazoline)s with various T_{CP}s ranging from 25 ^{o}C to 90 ^{o}C was performed. The results suggest that hydrophilicity is a key factor to control the cooperative behavior of poly(2-oxazoline)s. Based on the cooperative behavior of a thermoresponsive polymer and a double hydrophilic thermoresponsive block copolymer, a novel method for the preparation of hybrid polymeric nanoparticles is established through heating induced co-assembly of thermoresponsive statistical copolymers and a double hydrophilic block copolymer having a permanently hydrophilic block and a thermoresponsive block. By adjusting the hydrophilicity of the thermoresponsive statistical copolymer, well defined hybrid micelles with tunable sizes were obtained with various ratios of the two species depending on the T_{CP} and the concentration of the thermoresponsive statistical copolymer in the solution.

In **Chapter 7** we report a new type of dual pH- and temperature-responsive copolymers that undergo phase-transition below body temperature while degrading in time into hydrophilic species, which can avoid long-term accumulation in the body. The polymers were prepared by RAFT copolymerization of a temperature-responsive monomer or water soluble monomer with an acid-labile monomer. The T_{CP} of the resulting copolymers could be precisely tailored via the monomer composition. While being stable at physiological pH of 7.4, the copolymers hydrolyzed into fully water soluble polymers under mild acidic conditions resulting in non-toxic byproducts as verified by in vitro cell studies. Block copolymers containing a dual-responsive block were able to form micelles that hold potential for encapsulation and stimuli-responsive release of hydrophobic molecules as demonstrated for Nile Red. NHS-functional copolymers could be used for low temperature homogeneous aqueous bio-conjugation to proteins, engineering them with transient water-soluble/insoluble properties. In addition, the acceleration of hydrolysis was investigated by controlling the copolymer architecture or employing a less stable pH-labile comonomer. It was found that the introduction of a hydroxyl containing comonomer to the dual responsive copolymer can significantly accelerate pH triggered hydrolysis while maintaining high stability at neutral condition. This unexpected result is ascribed to the higher exposure of the dioxolane group in hydroxyl functionalized copolymer to the aqueous environment, possibly in combination with a catalytic effect of the alcohol groups of hydroxyl group. The usage of a linear acetal instead of cyclic acetal as pH labile group also led to a faster pH triggered hydrolysis due to intrinsically lower stability of linear acetals than cyclic ones. This new class of dual responsive copolymers is highly attractive in biomedical applications.

In **Chapter 8** we demonstrated a polymeric temperature sensor with a broad sensing regime in aqueous solution and investigated the influence of polymer gradient and the presence of hydroxyl groups on the sensing regime of the thermometer. By comparing the sensing abilities of copolymers with and without gradient and with and without hydroxyl groups, respectively, the broad sensing regime could be ascribed to the hydrogen bonding ability of the hydroxyl group with water, which allows the gradual dehydration of the copolymer globules. Further analysis will be needed to confirm this proposed mechanism.

To summarize, we have reported the synthesis, characterization, thermoresponsive and cooperative behavior and applications of thermoresponsive polymers as smart materials in this thesis. We have shown that polymers with UCST behavior in ethanol/water solvent mixtures are promising smart systems with highly tunable properties upon changing the temperature, solvent composition and polymer structures. By investigating the double thermoresponsive behavior of PDMAEMA, we have shown the versatility of this polymer to be used as smart materials. With the study on co-assembly behavior of block copolymer and homopolymer, we proposed a new method for the fabrication of novel hybrid polymeric nanoparticles, which may find a variety of applications as smart materials. Moreover, the co-assembly of block copolymers and homopolymers may extent to the polymers that don’t show stimuli-responsive behavior, which can be

triggered by the change of solvent compositions. With regards to the applications, the introduction of degradability to thermoresponsive polymers makes such polymers safer for body, which is essential for biomaterials. The study of polymeric sensor with broad sensing regime not only gives access of an advanced sensor system, but also provides insights into the structural conformation of the hydroxyl-containing polymer chains during the LCST phase transition.

With more than 40 years of development, thermoresponsive polymers are now a large group of functional/smart polymers and have found applications in various fields. For the future trends, the copolymer is becoming more 'smart' with combination of other stimuli-responsive factors, such as the development of dual- or multiresponsive polymers. Moreover, the development of supramolecular chemistry and advanced polymerization techniques will dramatically contribute to the development of thermoresponsive polymers or even stimuli-responsive polymers giving access to more subtle smart systems. Apart from thermoresponsive behavior in solution, the development of thermoresponsive nano-materials, 2D or even 3D bulky materials may be more interesting and important and give access to more applications. Finally, I am convinced that thermoresponsive polymers will become more and more 'smart' in the future.

References and Notes

1 D. Roy, W. L. A. Brooks and B. S. Sumerlin, *Chem. Soc. Rev.*, 2013, **42**, 7214.

2 M. A. Ward and T. K. Georgiou, *Polymers*, 2011, **3**, 1215.

3 C. Weber, R. Hoogenboom and U. S. Schubert, *Prog. Polym. Sci.*, 2012, **37**, 686.

4 Y. Li, G. H. Gao and D. S. Lee, *Adv. Healthc. Mater.*, 2013, **2**, 388.

5 V. Aseyev, H. Tenhu and F. M. Winnik, *Adv. Polym. Sci.*, 2011, **242**, 29.

6 P. Schattling, F. D. Jochum and P. Theato, *Polym. Chem.*, 2014, **5**, 25.

7 J. Thevenot, H. Oliveira, O. Sandre and S. Lecommandoux, *Chem. Soc. Rev.*, 2013, **42**, 7099.

8 F. D. Jochum and P. Theato, *Chem. Soc. Rev.*, 2013, **42**, 7468.

9 S. Maji, G. Vancoillie, L. Voorhaar, Q. Zhang and R. Hoogenboom, *Macromol. Rapid. Commun.*, 2014, **35**, 214.

10 C. D. H. Alarcon, S. Pennadam and C. Alexander, *Chem. Soc. Rev.*, 2005, **34**, 276.

11 E. S. Gil and S. M. Hudson, *Prog. Polym. Sci.*, 2004, **29**, 1173.

12 D. Roy, J. N. Cambre and B. S. Sumerlin, *Prog. Polym. Sci.*, 2010, **35**, 278.

13 M. A. C. Stuart, W. T. S. Huck, J. Genzer, M. Mueller, C. Ober, M. Stamm, G. B. Sukhorukov, I. Szleifer, V. V. Tsukruk, M. Urban, F. Winnik, S. Zauscher, I. Luzinov and S. Minko, *Nat. Mater.*, 2010, **9**, 101.

14 E. G. Kelley, J. N. L. Albert, M. O. Sullivan and I. I. I. T. H. Epps, *Chem. Soc. Rev.*, 2013, **42**, 7057.

15 L. Zhai, *Chem. Soc. Rev.*, 2013, **42**, 7148.

16 J. Zhuang, M. R. Gordon, J. Ventura, L. Li and S. Thayumanavan, *Chem. Soc. Rev.*, 2013, **42**, 7421.

17 J. Seuring and S. Agarwal, *Macromol. Rapid. Commun.*, 2012, **33**, 1898.

18 M. I. Gibson and R. K. O'Reilly, *Chem. Soc. Rev.*, 2013, **42**, 7204.

19 R. L. Bartlett and A. Panitch, *Biomacromolecules*, 2012, **13**, 2578.

20 G. Vancoillie, D. Frank and R. Hoogenboom, *Prog. Polym. Sci.*, 2014, **39**, 1074.

21 D. Schmaljohann, *Adv. Drug Deliver. Rev*, 2006, **58**, 1655.

22 S. Dai, P. Ravi and K. C. Tam, *Soft Matter*, 2009, **5**, 2513.

23 J. S. Scarpa, D. D. Mueller and I. M. Klotz, *J. Am. Chem. Soc.*, 1967, **89**, 6024.

24 H. G. Schild, *Prog. Polym. Sci.*, 1992, **17**, 163.

25 H. Wei, S.-X. Cheng, X.-Z. Zhang and R.-X. Zhuo, *Prog. Polym. Sci.*, 2009, **34**, 893.

26 J.-F. Lutz, *J. Polym. Sci. Pol. Chem.*, 2008, **46**, 3459.

27 J.-F. Lutz, *Adv. Mater.*, 2011, **23**, 2237.

28 J.-F. Lutz, O. Akdemir and A. Hoth, *J. Am. Chem. Soc.*, 2006, **128**, 13046.

29 J.-F. Lutz and A. Hoth, *Macromolecules*, 2005, **39**, 893.

30 R. Hoogenboom, *Angew. Chem. Int. Edit.*, 2009, **48**, 7978.

31 S. Aoshima, S. Kanaoka and B. Springer-Verlag, in *Adv. Polym. Sci.*, 2008, vol. 210, pp. 169.

32 A. Chilkoti, M. R. Dreher and D. E. Meyer, *Adv. Drug Deliver. Rev*, 2002, **54**, 1093.

33 J. Huang and A. Heise, *Chem. Soc. Rev.*, 2013, **42**, 7373.

34 S. Kudaibergenov, W. Jaeger and A. Laschewsky, in *Adv. Polym. Sci.*, Springer Berlin Heidelberg, 2006, vol. 201, pp. 157.

35 M. Arotçaréna, B. Heise, S. Ishaya and A. Laschewsky, *J. Am. Chem. Soc.*, 2002, **124**, 3787.

36 J. Seuring and S. Agarwal, *Macromolecules*, 2012, **45**, 3910.

37 E. Karjalainen, V. Aseyev and H. Tenhu, *Macromolecules*, 2014, **47**, 2103.

38 X. Jia, D. Chen and M. Jiang, *Chem. Commun.*, 2006, 1736.

39 F. A. Plamper, A. Schmalz and A. H. E. Müller, *J. Am. Chem. Soc.*, 2007, **129**, 14538.

40 Q. Zhang, J.-D. Hong and R. Hoogenboom, *Polym. Chem.*, 2013, **4**, 4322.

41 T. Ueki and M. Watanabe, *Bull. Chem. Soc. Jpn.*, 2012, **85**, 33.

42 M. Singh, *J. Dispersion Sci. Tech.*, 2007, **28**, 583.

43 K. Pagonis and G. Bokias, *Polymer*, 2004, **45**, 2149.

44 K.-I. Seno, A. Date, S. Kanaoka and S. Aoshima, *J. Polym. Sci. Pol. Chem.*, 2008, **46**, 4392.

45 H. Shimomoto, D. Fukami, S. Kanaoka and S. Aoshima, *J. Polym. Sci. Pol. Chem.*, 2011, **49**, 2051.

46 W.-M. Wan, F. Cheng and F. Jäkle, *Angew. Chem. Int. Edit.*, 2014, **53**, 8934.

47 F. Franks and D. J. G. Ives, *Q. Rev. Chem. Soc.*, 1966, **20**, 1.

48 S. Y. Noskov, G. Lamoureux and B. Roux, *J. Phys. Chem. B*, 2005, **109**, 6705.

49 H. S. Frank and M. W. Evans, *J. Chem. Phys.*, 1945, **13**, 507.

50 P. Bustamante, J. Navarro, S. Romero and B. Escalera, *J. Pharm. Sci.*, 2002, **91**, 874.

51 F. Sardari and A. Jouyban, *J. Chem. Eng. Data*, 2012, **57**, 2848.

52 R. Hoogenboom, S. Rogers, A. Can, C. R. Becer, C. Guerrero-Sanchez, D. Wouters, S. Hoeppener and U. S. Schubert, *Chem. Commun.*, 2009, 5582.

53 P. J. Roth, T. P. Davis and A. B. Lowe, *Polym. Chem.*, 2012, **3**, 2228.

54 N. J. Hornung, G. R. Choppin and G. Renovitch, *Appl. Spectrosc. Rev.*, 1974, **8**, 149.

55 H. E. Stanley and J. Teixeira, *J. Chem. Phys.*, 1980, **73**, 3404.

56 K. A. Sharp and J. M. Vanderkooi, *Acc. Chem. Res.*, 2010, **43**, 231.

57 N. Galamba, *J. Phys. Chem. B*, 2013, **117**, 589.

58 H. S. Frank and W.-Y. Wen, *Discuss. Faraday Soc.*, 1957, **24**, 133.

59 G. Lamoureux, A. D. MacKerell and B. t. Roux, *J. Chem. Phys.*, 2003, **119**, 5185.

60 J. B. Escalera, P. Bustamante and A. Martin, *J. Pharm. Pharmacol.*, 1994, **46**, 172.

61 S. Romero, A. Reillo, B. Escalera and P. Bustamante, *Chem. Pharm. Bull.*, 1996, **44**, 1061.

62 V. Boyko, Y. Lu, A. Richter and A. Pich, *Macromol. Chem. Phys.*, 2003, **204**, 2031.

63 R. O. R. Costa and R. F. S. Freitas, *Polymer*, 2002, **43**, 5879.

64 J. M. G. Cowie, I. J. McEwen and M. T. Garay, *Polym. Commun.*, 1986, **27**, 122.

65 R. Hoogenboom, C. R. Becer, C. Guerrero-Sanchez, S. Hoeppener and U. S. Schubert, *Aust. J. Chem.*, 2010, **63**, 1173.

66 S. Dixit, J. Crain, W. C. K. Poon, J. L. Finney and A. K. Soper, *Nature*, 2002, **416**, 829.

67 T. Takamuku, K. Saisho, S. Aoki and T. Yamaguchi, *Z. Naturforsch. A Phys. Sci.*, 2002, **57**, 982.

68 T. Takamuku, H. Maruyama, K. Watanabe and T. Yamaguchi, *J. Solution Chem.*, 2004, **33**, 641.

69 A. R. Shultz and P. J. Flory, *J. Am. Chem. Soc.*, 1953, **75**, 5681.

70 B. A. Wolf and G. Blaum, *J. Polym. Sci, Polym. Phys. Ed.*, 1975, **13**, 1115.

71 F. Ikkai, N. Masui, T. Karino, S. Naito, K. Kurita and M. Shibayama, *Langmuir*, 2003, **19**, 2568.

72 J. M. G. Cowie, M. A. Mohsin and I. J. McEwen, *Polymer*, 1987, **28**, 1569.

73 A. Can, S. Hoeppener, P. Guillet, J.-F. Gohy, R. Hoogenboom and U. S. Schubert, *J. Polym. Sci. Pol. Chem.*, 2011, **49**, 3681.

74 B. A. Wolf and M. M. Willms, *Makromol.Chem.*, 1978, **179**, 2265.

75 H. G. Schild, M. Muthukumar and D. A. Tirrell, *Macromolecules*, 1991, **24**, 948.

76 S. Katayama, Y. Hirokawa and T. Tanaka, *Macromolecules*, 1984, **17**, 2641.

77 T. Amiya, Y. Hirokawa, Y. Hirose, Y. Li and T. Tanaka, *J. Chem. Phys.*, 1987, **86**, 2375.

78 S. Hirotsu, *J. Chem. Phys.*, 1988, **88**, 427.

79 T. López-León, D. Bastos-González, J. L. Ortega-Vinuesa and A. Elaïssari, *ChemPhysChem*, 2010, **11**, 188.

80 F. M. Winnik, H. Ringsdorf and J. Venzmer, *Macromolecules*, 1990, **23**, 2415.

81 G. Zhang and C. Wu, *Phys. Rev. Lett.*, 2001, **86**, 822.

82 M. Liu, F. Bian and F. Sheng, *Eur. Polym. J.*, 2005, **41**, 283.

83 F. Tanaka, T. Koga and F. M. Winnik, *Phys. Rev. Lett.*, 2008, **101**, 028302.

84 F. Tanaka, T. Koga, H. Kojima and F. M. Winnik, *Macromolecules*, 2009, **42**, 1321.

85 H. Kojima, F. Tanaka, C. Scherzinger and W. Richtering, *J. Polym. Sci. Polym. Phys.*, 2013, **51**, 1100.

86 C. Weber, S. Rogers, A. Vollrath, S. Hoeppener, T. Rudolph, N. Fritz, R. Hoogenboom and U. S. Schubert, *J. Polym. Sci. Pol. Chem.*, 2013, **51**, 139.

87 Q. Zhang, P. Schattling, P. Theato and R. Hoogenboom, *Polym. Chem.*, 2012, **3**, 1418.

88 P. J. Roth, M. Collin and C. Boyer, *Soft Matter*, 2013, **9**, 1825.

89 P. J. Roth, F. D. Jochum and P. Theato, *Soft Matter*, 2011, **7**, 2484.

90 L. Liu, T. Wang, C. Liu, K. Lin, G. Liu and G. Zhang, *J. Phys. Chem. B*, 2013, **117**, 10936.

91 M. M. Bloksma, D. J. Bakker, C. Weber, R. Hoogenboom and U. S. Schubert, *Macromol. Rapid. Commun.*, 2010, **31**, 724.

92 Y. J. Zhang, S. Furyk, D. E. Bergbreiter and P. S. Cremer, *J. Am. Chem. Soc.*, 2005, **127**, 14505.

93 Z. Zhang, S. Maji, A. B. d. F. Antunes, R. De Rycke, Q. Zhang, R. Hoogenboom and B. G. De Geest, *Chem. Mater.*, 2013, **25**, 4297.

94 S. Piccarolo and G. Titomanlio, *Makromol. Chem. Rapid. Commum.*, 1982, **3**, 383.

95 S. K. Jewrajka, U. Chatterjee and B. M. Mandal, *Macromolecules*, 2004, **37**, 4325.

96 T. Terashima, M. Ouchi, T. Ando, M. Kamigaito and M. Sawamoto, *Macromolecules*, 2007, **40**, 3581.

97 K. Kubota, K. M. Abbey and B. Chu, *Macromolecules*, 1983, **16**, 137.

98 E. E. Dormidontova, *Macromolecules*, 2004, **37**, 7747.

99 Q. Zhang, P. Schattling, P. Theato and R. Hoogenboom, *Eur. Polym. J.* 2014, DOI: 10.1016/j.eurpolymj.2014.06.029

100 C. Pietsch, R. Hoogenboom and U. S. Schubert, *Polym. Chem.*, 2010, **1**, 1005.

101 R. Hoogenboom and H. Schlaad, *Polymers*, 2011, **3**, 467.

102 H. M. L. Lambermont-Thijs, H. P. C. v. Kuringen, J. P. W. v. d. Put, U. S. Schubert and R. Hoogenboom, *Polymers*, 2010, **2**, 188.

103 R. Hoogenboom, H. M. L. Thijs, M. W. M. Fijten, B. M. van Lankvelt and U. S. Schubert, *J. Polym. Sci. Pol. Chem.*, 2007, **45**, 416.

104 R. Hoogenboom, H. M. L. Thijs, D. Wouters, S. Hoeppener and U. S. Schubert, *Soft Matter*, 2008, **4**, 103.

105 H. M. L. Lambermont-Thijs, R. Hoogenboom, C.-A. Fustin, C. Bomal-D'Haese, J.-F. Gohy and U. S. Schubert, *J. Polym. Sci. Pol. Chem.*, 2009, **47**, 515.

106 C. Diehl, I. Dambowsky, R. Hoogenboom and H. Schlaad, *Macromol. Rapid. Commun.*, 2011, **32**, 1753.

107 C.-A. Fustin, H. M. L. Thijs-Lambermont, S. Hoeppener, R. Hoogenboom, U. S. Schubert and J.-F. Gohy, *J. Polym. Sci. Pol. Chem.*, 2010, **48**, 3095.

108 K. Knop, R. Hoogenboom, D. Fischer and U. S. Schubert, *Angew. Chem. Int. Edit.*, 2010, **49**, 6288.

109 H. Otsuka, Y. Nagasaki and K. Kataoka, *Adv. Drug Deliver. Rev*, 2003, **55**, 403.

110 F. M. Veronese and G. Pasut, *Drug Discov. Today*, 2005, **10**, 1451.

111 S. Saeki, N. Kuwahara, M. Nakata and M. Kaneko, *Polymer*, 1976, **17**, 685.

112 D. L. Ho, B. Hammouda, S. R. Kline and W. R. Chen, *J. Polym. Sci. Pol. Phys.*, 2006, **44**, 557.

113 Y. Su, M. Dan, X. Xiao, X. Wang and W. Zhang, *J. Polym. Sci. Pol. Chem.*, 2013, **51**, 4399.

114 K. Matyjaszewski and N. V. Tsarevsky, *J. Am. Chem. Soc.*, 2014, **136**, 6513.

115 W. A. Braunecker and K. Matyjaszewski, *Prog. Polym. Sci.*, 2007, **32**, 93.

116 S. Perrier and P. Takolpuckdee, *J. Polym. Sci. Pol. Chem.*, 2005, **43**, 5347.

117 G. Moad, E. Rizzardo and S. H. Thang, *Aust. J. Chem.*, 2009, **62**, 1402.

118 G. B. H. Chua, P. J. Roth, H. T. T. Duong, T. P. Davis and A. B. Lowe, *Macromolecules*, 2012, **45**, 1362.

119 D. H. Seuyep N, D. Szopinski, G. A. Luinstra and P. Theato, *Polym. Chem.*, 2014, **5**, 5823.

120 D. H. Seuyep N, G. A. Luinstra and P. Theato, *Polym. Chem.*, 2013, **4**, 2724.

121 H.-N. Lee, B. M. Rosen, G. Fenyvesi and H. B. Sunkara, *J. Polym. Sci. Pol. Chem.*, 2012, **50**, 4311.

122 Z. M. O. Rzaev, S. Dincer and E. Piskin, *Prog. Polym. Sci.*, 2007, **32**, 534.

123 S. Dhanya, D. Bahadur, G. C. Kundu and R. Srivastava, *Eur. Polym. J.*, 2013, **49**, 22.

124 B. Trzebicka, B. Robak, R. Trzcinska, D. Szweda, P. Suder, J. Silberring and A. Dworak, *Eur. Polym. J.*, 2013, **49**, 499.

125 K. Mukae, M. Sakurai, S. Sawamura, K. Makino, S. W. Kim, I. Ueda and K. Shirahama, *J. Phys. Chem.*, 1993, **97**, 737.

126 M. J. A. Hore, B. Hammouda, Y. Li and H. Cheng, *Macromolecules*, 2013, **46**, 7894.

127 Y. Matsuda, M. Kobayashi, M. Annaka, K. Ishihara and A. Takahara, *Polym. J.*, 2008, **40**, 479.

128 K. Dušek, *Collect. Czech. Chem. Commun.*, 1969, **34**, 3309.

129 K. Dušek and B. Sedláček, *Collect. Czech. Chem. Commun.*, 1971, **36**, 1569.

130 T. Terashima, M. Ouchi, T. Ando and M. Sawamoto, *J. Polym. Sci. Pol. Chem.*, 2010, **48**, 373.

131 S. Aoshima, H. Oda and E. Kobayashi, *J. Polym. Sci. Pol. Chem.*, 1992, **30**, 2407.

132 Z. J. Liu, K. Inomata and Y. L. Guo, *Colloid Polym. Sci.*, 2011, **289**, 1917.

133 A. Sehlinger, O. Kreye and M. A. R. Meier, *Macromolecules*, 2013, **46**, 6031.

134 M. Passerini, *Gazz. Chem. Ital.*, 1921, **51**, 126.

135 T. Gelbrich, M. Feyen and A. M. Schmidt, *Macromolecules*, 2006, **39**, 3469.

136 B. Adhikari and S. Majumdar, *Prog. Polym. Sci.*, 2004, **29**, 699.

137 C. Li and S. Liu, *Chem. Commun.*, 2012, **48**, 3262.

138 J. Hu and S. Liu, *Macromolecules*, 2010, **43**, 8315.

139 A. M. Horgan, J. D. Moore, J. E. Noble and G. J. Worsley, *Trends Biotechnol.*, 2010, **28**, 485.

140 U. Lange, N. V. Roznyatouskaya and V. M. Mirsky, *Anal. Chim. Acta*, 2008, **614**, 1.

141 M. I. J. Stich, L. H. Fischer and O. S. Wolfbeis, *Chem. Soc. Rev.*, 2010, **39**, 3102.

142 C. Reichardt, *Chem. Rev.*, 1994, **94**, 2319.

143 C. Pietsch, U. S. Schubert and R. Hoogenboom, *Chem. Commun.*, 2011, **47**, 8750.

144 D. Kungwatchakun and M. Irie, *Makromol. Chem. Rapid. Commum.*, 1988, **9**, 243.

145 P. Vyskocil, J. Ricka and T. Binkert, *Helv. Phys. Acta*, 1989, **62**, 243.

146 F. M. Winnik, *Macromolecules*, 1990, **23**, 233.

147 H. G. Schild and D. A. Tirrell, *Macromolecules*, 1992, **25**, 4553.

148 L. Tang, J. K. Jin, A. J. Qin, W. Z. Yuan, Y. Mao, J. Mei, J. Z. Sun and B. Z. Tang, *Chem. Commun.*, 2009, 4974.

149 S. W. Hong, D. Y. Kim, J. U. Lee and W. H. Jo, *Macromolecules*, 2009, **42**, 2756.

150 A. Balamurugan, V. Kumar and M. Jayakannan, *Chem. Commun.*, 2014, **50**, 842.

151 R. X. Liu, M. Fraylich and B. R. Saunders, *Colloid Polym. Sci.*, 2009, **287**, 627.

152 X.-d. Wang, O. S. Wolfbeis and R. J. Meier, *Chem. Soc. Rev.*, 2013, **42**, 7834.

153 A. M. Breul, M. D. Hager and U. S. Schubert, *Chem. Soc. Rev.*, 2013, **42**, 5366.

154 M. Beija, M.-T. Charreyre and J. M. G. Martinho, *Prog. Polym. Sci.*, 2011, **36**, 568.

155 X. J. Lu, L. F. Zhang, L. Z. Meng and Y. H. Liu, *Polym. Bull.*, 2007, **59**, 195.

156 M. A. Gauthier, M. I. Gibson and H.-A. Klok, *Angew. Chem. Int. Edit.*, 2009, **48**, 48.

157 P. Theato, *J. Polym. Sci. Pol. Chem.*, 2008, **46**, 6677.

158 H. C. Kolb, M. G. Finn and K. B. Sharpless, *Angew. Chem. Int. Edit.*, 2001, **40**, 2004.

159 C. R. Becer, R. Hoogenboom and U. S. Schubert, *Angew. Chem. Int. Edit.*, 2009, **48**, 4900.

160 K. Matyjaszewski and J. Xia, *Chem. Rev.*, 2001, **101**, 2921.

161 J.-S. Wang and K. Matyjaszewski, *J. Am. Chem. Soc.*, 1995, **117**, 5614.

162 C. Li, Y. Zhang, J. Hu, J. Cheng and S. Liu, *Angew. Chem. Int. Edit.*, 2010, **49**, 5120.

163 J. M. Hu, X. Z. Zhang, D. Wang, X. L. Hu, T. Liu, G. Y. Zhang and S. Y. Liu, *J. Mater. Chem.*, 2011, **21**, 19030.

164 L. Liu, W. Li, K. Liu, J. Yan, G. Hu and A. Zhang, *Macromolecules*, 2011, **44**, 8614.

165 X. W. Zhang, X. M. Lian, L. Liu, J. Zhang and H. Y. Zhao, *Macromolecules*, 2008, **41**, 7863.

166 A. Laukkanen, F. M. Winnik and H. Tenhu, *Macromolecules*, 2005, **38**, 2439.

167 W. Zhang, Z. Zhang, Z. Cheng, Y. Tu, Y. Qiu and X. Zhu, *J. Polym. Sci. Pol. Chem.*, 2010, **48**, 4268.

168 F. H. Schacher, P. A. Rupar and I. Manners, *Angew. Chem. Int. Edit.*, 2012, n/a.

169 M. Heskins and J. E. Guillet, *J. Macromol. Sci. A*, 1968, **2**, 1441.

170 Y. S. Avlasevich, V. N. Knyukshto, O. G. Kulinkovich and K. N. Solovyov, *J. Appl. Spectrosc.*, 2000, **67**, 663.

171 K. Iwai, K. Hanasaki and M. Yamamoto, *J. Lumin.*, 2000, **87-9**, 1289.

172 S. Uchiyama, Y. Matsumura, A. P. de Silva and K. Iwai, *Anal. Chem.*, 2003, **75**, 5926.

173 S. Uchiyama, Y. Matsumura, A. P. de Silva and K. Iwai, *Anal. Chem.*, 2004, **76**, 1793.

174 K. Iwai, Y. Matsumura, S. Uchiyama and A. P. de Silva, *J. Mater. Chem.*, 2005, **15**, 2796.

175 N. Jordão, R. Gavara and A. J. Parola, *Macromolecules*, 2013, **46**, 9055.

176 A. Nagai, K. Kokado, J. Miyake and Y. Cyujo, *J. Polym. Sci. Pol. Chem.*, 2010, **48**, 627.

177 Y. Shiraishi, R. Miyamoto and T. Hirai, *Org. Lett.*, 2009, **11**, 1571.

178 Y. Zhao, L. Tremblay and Y. Zhao, *J. Polym. Sci. Pol. Chem.*, 2010, **48**, 4055.

179 G. Liu, W. Zhou, J. Zhang and P. Zhao, *J. Polym. Sci. Pol. Chem.*, 2012, **50**, 2219.

180 Y. Shiraishi, R. Miyarnoto and T. Hirai, *Langmuir*, 2008, **24**, 4273.

181 K. Van Durme, G. Van Assche and B. Van Mele, *Macromolecules*, 2004, **37**, 9596.

182 S. Han, M. Hagiwara and T. Ishizone, *Macromolecules*, 2003, **36**, 8312.

183 C. Pietsch, A. Vollrath, R. Hoogenboom and U. S. Schubert, *Sensors*, 2010, **10**, 7979.

184 C. Pietsch, R. Hoogenboom and U. S. Schubert, *Angew. Chem. Int. Edit.*, 2009, **48**, 5653.

185 R. París, I. Quijada-Garrido, O. García and M. Liras, *Macromolecules*, 2011, **44**, 80.

186 B. H. Lessard, E. J. Y. Ling and M. Marić, *Macromolecules*, 2012, **45**, 1879.

187 S. Inal, J. D. Kolsch, F. Sellrie, J. A. Schenk, E. Wischerhoff, A. Laschewsky and D. Neher, *J. Mater. Chem. B*, 2013, **1**, 6373.

188 S. Y. Lee, S. Lee, I. C. Youn, D. K. Yi, Y. T. Lim, B. H. Chung, J. F. Leary, I. C. Kwon, K. Kim and K. Choi, *Chem. Eur. J.*, 2009, **15**, 6103.

189 S. Inal, J. D. Kolsch, L. Chiappisi, D. Janietz, M. Gradzielski, A. Laschewsky and D. Neher, *J. Mater. Chem. C*, 2013, **1**, 6603.

190 C. Gota, S. Uchiyama and T. Ohwada, *Analyst*, 2007, **132**, 121.

191 C. Gota, K. Okabe, T. Funatsu, Y. Harada and S. Uchiyama, *J. Am. Chem. Soc.*, 2009, **131**, 2766.

192 K. Okabe, N. Inada, C. Gota, Y. Harada, T. Funatsu and S. Uchiyama, *Nat. Commun.*, 2012, **3**, 705.

193 L. Yin, C. He, C. Huang, W. Zhu, X. Wang, Y. Xu and X. Qian, *Chem. Commun.*, 2012, **48**, 4486.

194 C.-Y. Chen and C.-T. Chen, *Chem. Commun.*, 2011, **47**, 994.

195 Y. Matsumura and K. Iwai, *Polymer*, 2005, **46**, 10027.

196 G. Moad, E. Rizzardo and S. H. Thang, *Chem. Asian j.*, 2013, **8**, 1634.

197 J. Hu, C. Li and S. Liu, *Langmuir*, 2010, **26**, 724.

198 W. Z. Wang, R. Wang, C. Zhang, S. Lu and T. X. Liu, *Polymer*, 2009, **50**, 1236.

199 C. Y.-S. Chung and V. W.-W. Yam, *Chem. Eur. J.*, 2013, **19**, 13182.

200 Q. Yan, J. Y. Yuan, W. Z. Yuan, M. Zhou, Y. W. Yin and C. Y. Pan, *Chem. Commun.*, 2008, 6188.

201 T. Wu, G. Zou, J. Hu and S. Liu, *Chem. Mater.*, 2009, **21**, 3788.

202 S.-I. Yusa, T. Endo and M. Ito, *J. Polym. Sci. Pol. Chem.*, 2009, **47**, 6827.

203 L. Liu, W. Li, J. Yan and A. Zhang, *J. Polym. Sci. Pol. Chem.*, 2014, **52**, 1706.

204 Y. Y. Li, H. Cheng, J. L. Zhu, L. Yuan, Y. Dai, S. X. Cheng, X. Z. Zhang and R. X. Zhuo, *Adv. Mater.*, 2009, **21**, 2402.

205 H. Kobayashi, M. Nishikawa, C. Sakamoto, T. Nishio, H. Kanazawa and T. Okano, *Anal. Sci.*, 2009, **25**, 1043.

206 S. Uchiyama, K. Kimura, C. Gota, K. Okabe, K. Kawamoto, N. Inada, T. Yoshihara and S. Tobita, *Chem. Eur. J.*, 2012, **18**, 9552.

207 C. Gota, S. Uchiyama, T. Yoshihara, S. Tobita and T. Ohwada, *J. Phys. Chem. B*, 2008, **112**, 2829.

208 J. Yin, C. Li, D. Wang and S. Liu, *J. Phys. Chem. B*, 2010, **114**, 12213.

209 C. Li and S. Liu, *J. Mater. Chem.*, 2010, **20**, 10716.

210 T. Liu, J. Hu, J. Yin, Y. Zhang, C. Li and S. Liu, *Chem. Mater.*, 2009, **21**, 3439.

211 Q. Yan, J. Yuan, Y. Kang, Z. Cai, L. Zhou and Y. Yin, *Chem. Commun.*, 2010, **46**, 2781.

212 P. Schattling, F. D. Jochum and P. Theato, *Chem. Commun.*, 2011, **47**, 8859.

213 S. Uchiyama, N. Kawai, A. P. de Silva and K. Iwai, *J. Am. Chem. Soc.*, 2004, **126**, 3032.

214 Z. Q. Guo, W. H. Zhu, Y. Y. Xiong and H. Tian, *Macromolecules*, 2009, **42**, 1448.

215 G. Pasparakis, M. Vamvakaki, N. Krasnogor and C. Alexander, *Soft Matter*, 2009, **5**, 3839.

216 D. J. Keddie, *Chem. Soc. Rev.*, 2014, **43**, 496.

217 M. Semsarilar and S. Perrier, *Nat. Chem.*, 2010, **2**, 811.

218 G. Moad, E. Rizzardo and S. H. Thang, *Aust. J. Chem.*, 2006, **59**, 669.

219 G. Moad, E. Rizzardo and S. H. Thang, *Aust. J. Chem.*, 2005, **58**, 379.

220 G. Moad, E. Rizzardo and S. H. Thang, *Polym. Int.*, 2011, **60**, 9.

221 J. Chiefari, Y. K. Chong, F. Ercole, J. Krstina, J. Jeffery, T. P. T. Le, R. T. A. Mayadunne, G. F. Meijs, C. L. Moad, G. Moad, E. Rizzardo and S. H. Thang, *Macromolecules*, 1998, **31**, 5559.

222 D. Smith, A. C. Holley and C. L. McCormick, *Polym. Chem.*, 2011, **2**, 1428.

223 C. Boyer, V. Bulmus, T. P. Davis, V. Ladmiral, J. Liu and S. Perrier, *Chem. Rev.*, 2009, **109**, 5402.

224 M. Ahmed and R. Narain, *Prog. Polym. Sci.*, 2013, **38**, 767.

225 M. A. Harvison, P. J. Roth, T. P. Davis and A. B. Lowe, *Aust. J. Chem.*, 2011, **64**, 992.

226 H. Willcock and R. K. O'Reilly, *Polym. Chem.*, 2010, **1**, 149.

227 V. Lima, X. Jiang, J. Brokken-Zijp, P. J. Schoenmakers, B. Klumperman and R. Van Der Linde, *J. Polym. Sci. Pol. Chem.*, 2005, **43**, 959.

228 X.-P. Qiu and F. M. Winnik, *Macromol. Rapid. Commun.*, 2006, **27**, 1648.

229 C. R. Becer, A. M. Groth, R. Hoogenboom, R. M. Paulus and U. S. Schubert, *QSAR Comb. Sci.*, 2008, **27**, 977.

230 L. Voorhaar, S. Wallyn, F. E. Du Prez and R. Hoogenboom, *Polym. Chem.*, 2014, **5**, 4268.

231 W. Steinhauer, R. Hoogenboom, H. Keul and M. Moeller, *Macromolecules*, 2010, **43**, 7041.

232 W. Steinhauer, R. Hoogenboom, H. Keul and M. Moeller, *Macromolecules*, 2013, **46**, 1447.

233 R. Hoogenboom, A.-M. Zorn, H. Keul, C. Barner-Kowollik and M. Moeller, *Polym. Chem.*, 2012, **3**, 335.

234 F. D. Jochum, L. zur Borg, P. J. Roth and P. Theato, *Macromolecules*, 2009, **42**, 7854.

235 N. S. Ieong, M. Hasan, D. J. Phillips, Y. Saaka, R. K. O'Reilly and M. I. Gibson, *Polym. Chem.*, 2012, **3**, 794.

236 S. Monge, S. Antoniacomi, V. Lapinte, V. Darcos and J.-J. Robin, *Polym. Chem.*, 2012, **3**, 2502.

237 Q. Zhang, N. Vanparijs, B. Louage, B. G. De Geest and R. Hoogenboom, *Polym. Chem.*, 2014, **5**, 1140.

238 R. Hoogenboom, H. M. L. Thijs, M. J. H. C. Jochems, B. M. van Lankvelt, M. W. M. Fijten and U. S. Schubert, *Chem. Commun.*, 2008, 5758.

239 V. Chytry and K. Ulbrich, *J. of Bioact. and Compat.*, 2001, **16**, 427.

240 F. Kohori, K. Sakai, T. Aoyagi, M. Yokoyama, Y. Sakurai and T. Okano, *J. Control Release.*, 1998, **55**, 87.

241 L. Klouda and A. G. Mikos, *Eur. J. Pharm. Biopharm.*, 2008, **68**, 34.

242 W. Agut, A. Brulet, C. Schatz, D. Taton and S. Lecommandoux, *Langmuir*, 2010, **26**, 10546.

243 C. S. Xiao, C. W. Zhao, P. He, Z. H. Tang, X. S. Chen and X. B. Jing, *Macromol. Rapid. Commun.*, 2010, **31**, 991.

244 T. D. Craggs, *Chem. Soc. Rev.*, 2009, **38**, 2865.

245 A. Karatzas, P. Bilalis, H. Iatrou, M. Pitsikalis and N. Hadjichristidis, *React. Funct. Polym.*, 2009, **69**, 435.

246 T. L. Sun and G. Y. Qing, *Adv. Mater.*, 2011, **23**, H57.

247 C. Chang, H. Wei, Q. A. Li, B. Yang, N. Chen, J. P. Zhou, X. Z. Zhang and R. X. Zhuo, *Polym. Chem.*, 2011, **2**, 923.

248 J. H. Holtz and S. A. Asher, *Nature*, 1997, **389**, 829.

249 B. Jeong, Y. H. Bae, D. S. Lee and S. W. Kim, *Nature*, 1997, **388**, 860.

250 T. Tang, V. Castelletto, P. Parras, I. W. Hamley, S. M. King, D. Roy, S. Perrier, R. Hoogenboom and U. S. Schubert, *Macromol. Chem. Phys.*, 2006, **207**, 1718.

251 C. Lavigueur, J. G. Garcia, L. Hendriks, R. Hoogenboom, J. Cornelissen and R. J. M. Nolte, *Polym. Chem.*, 2010, **2**, 333.

252 D. Fournier, R. Hoogenboom, H. M. L. Thijs, R. M. Paulus and U. S. Schubert, *Macromolecules*, 2007, **40**, 915.

253 C. R. Becer, S. Hahn, M. W. M. Fijten, H. M. L. Thijs, R. Hoogenboom and U. S. Schubert, *J. Polym. Sci. Pol. Chem.*, 2008, **46**, 7138.

254 K. Bebis, M. W. Jones, D. M. Haddleton and M. I. Gibson, *Polym. Chem.*, 2011, **2**, 975.

255 C. Diehl and H. Schlaad, *Macromol. Biosci.*, 2009, **9**, 157.

256 S. Huber and R. Jordan, *Colloid Polym. Sci.*, 2008, **286**, 395.

257 J. Park, Y. Akiyama, F. Winnik and K. Kataoka, *Macromolecules*, 2004, **37**, 6786.

258 R. Hoogenboom, H. M. L. Lambermont-Thijs, M. Jochems, S. Hoeppener, C. Guerlain, C. A. Fustin, J. F. Gohy and U. S. Schubert, *Soft Matter*, 2009, **5**, 3590.

259 S. Piccarolo and G. Titomanlio, *Makromol. Chem. Rapid. Commum.*, 1982, **3**, 383.

260 S. Nowag and R. Haag, *Angew. Chem. Int. Edit.*, 2014, **53**, 49.

261 J. P. Magnusson, A. Khan, G. Pasparakis, A. O. Saeed, W. Wang and C. Alexander, *J. Am. Chem. Soc.*, 2008, **130**, 10852.

262 D. Han, O. Boissiere, S. Kumar, X. Tong, L. Tremblay and Y. Zhao, *Macromolecules*, 2012, **45**, 7440.

263 P. Schattling, I. Pollmann and P. Theato, *React. Funct. Polym.*, 2014, **75**, 16.

264 F. D. Jochum and P. Theato, *Polymer*, 2009, **50**, 3079.

265 H.-i. Lee, W. Wu, J. K. Oh, L. Mueller, G. Sherwood, L. Peteanu, T. Kowalewski and K. Matyjaszewski, *Angew. Chem. Int. Edit.*, 2007, **46**, 2453.

266 K. G. Yager and C. J. Barrett, *J. Photochem. Photobiol. A*, 2006, **182**, 250.

267 G. S. Hartley, *Nature*, 1937, **140**, 281.

268 G. S. Hartley and R. J. W. Le F èvre, *J. Am. Chem. Soc.*, 1939, 531.

269 H. Akiyama and N. Tamaoki, *J. Polym. Sci. Pol. Chem.*, 2004, **42**, 5200.

270 H. Akiyama and N. Tamaoki, *Macromolecules*, 2007, **40**, 5129.

271 T. Shimoboji, E. Larenas, T. Fowler, S. Kulkarni, A. S. Hoffman and P. S. Stayton, *Proc. Natl. Acad. Sci. U.S.A.*, 2002, **99**, 16592.

272 C. Luo, F. Zuo, X. Ding, Z. Zheng, X. Cheng and Y. Peng, *J. Appl. Polym. Sci.*, 2008, **107**, 2118.

273 T. Ueki, Y. Nakamura, A. Yamaguchi, K. Niitsuma, T. P. Lodge and M. Watanabe, *Macromolecules*, 2011, **44**, 6908.

274 S. K. Yang and M. Weck, *Macromolecules*, 2008, **41**, 346.

275 B. S. Murray, A. W. Jackson, C. S. Mahon and D. A. Fulton, *Chem. Commun.*, 2010, **46**, 8651.

276 D. Fournier, R. Hoogenboom and U. S. Schubert, *Chem. Soc. Rev.*, 2007, **36**, 1369.

277 R. Hoogenboom, *Angew. Chem. Int. Edit.*, 2010, **49**, 3415.

278 K. Nilles and P. Theato, *J. Polym. Sci. Pol. Chem.*, 2010, **48**, 3683.

279 P. J. Roth, F. D. Jochum, F. R. Forst, R. Zentel and P. Theato, *Macromolecules*, 2010, **43**, 4638.

280 M. Eberhardt, R. Mruk, R. Zentel and P. Theato, *Eur. Polym. J.*, 2005, **41**, 1569.

281 F. D. Jochum and P. Theato, *Macromolecules*, 2009, **42**, 5941.

282 M. Beija, Y. Li, A. B. Lowe, T. P. Davis and C. Boyer, *Eur. Polym. J.*, 2013, **49**, 3060.

283 S. E. Kudaibergenov and A. Ciferri, *Macromol. Rapid. Commun.*, 2007, **28**, 1969.

284 K. S. Pafiti, M. Elladiou and C. S. Patrickios, *Macromolecules*, 2014, **47**, 1819.

285 E. E. Malmström and C. J. Hawker, *Macromol. Chem. Phys.*, 1998, **199**, 923.

286 K. Matyjaszewski, *Macromolecules*, 2012, **45**, 4015.

287 K. Sui, X. Zhao, Z. Wu, Y. Xia, H. Liang and Y. Li, *Langmuir*, 2011, **28**, 153.

288 D. Hu, Z. Cheng, J. Zhu and X. Zhu, *Polymer*, 2005, **46**, 7563.

289 L. Li, K. Raghupathi, C. Song, P. Prasad and S. Thayumanavan, *Chem. Commun.*, 2014, **50**, 13417.

290 B. J. Pae, T. J. Moon, C. H. Lee, M. B. Ko, M. Park, S. Lim, J. Kim and C. R. Choe, *Korea Polym. J.*, 1997, **5**, 126.

291 B. Hammouda, D. Ho and S. Kline, *Macromolecules*, 2002, **35**, 8578.

292 F. A. Plamper, C. V. Synatschke, A. P. Majewski, A. Schmalz, H. Schmalz and A. H. E. Mueller, *Polimery*, 2014, **59**, 66.

293 F. A. Plamper, J. R. McKee, A. Laukkanen, A. Nykanen, A. Walther, J. Ruokolainen, V. Aseyev and H. Tenhu, *Soft Matter*, 2009, **5**, 1812.

294 H. Lee, S. H. Son, R. Sharma and Y.-Y. Won, *J. Phys. Chem. B*, 2011, **115**, 844.

295 Y. K. Chong, J. Krstina, T. P. T. Le, G. Moad, A. Postma, E. Rizzardo and S. H. Thang, *Macromolecules*, 2003, **36**, 2256.

296 G. Moad, E. Rizzardo and S. H. Thang, *Polymer*, 2008, **49**, 1079.

297 V. Bütün, N. C. Billingham and S. P. Armes, *J. Am. Chem. Soc.*, 1998, **120**, 11818.

298 V. Bütün, S. Liu, J. V. M. Weaver, X. Bories-Azeau, Y. Cai and S. P. Armes, *React. Funct. Polym.*, 2006, **66**, 157.

299 S. Liu and S. P. Armes, *Angew. Chem. Int. Edit.*, 2002, **41**, 1413.

300 S. Liu, N. C. Billingham and S. P. Armes, *Angew. Chem. Int. Edit.*, 2001, **40**, 2328.

301 J. Z. Du and R. K. O'Reilly, *Macromol. Chem. Phys.*, 2010, **211**, 1530.

302 D. Roy, J. N. Cambre and B. S. Sumerlin, *Chem. Commun.*, 2009, 2106.

303 Y. F. Zhang, L. Hao, J. M. Hu, C. H. Li and S. Y. Liu, *Macromol. Rapid. Commun.*, 2009, **30**, 941.

304 J. Virtanen, M. Arotçarména, B. Heise, S. Ishaya, A. Laschewsky and H. Tenhu, *Langmuir*, 2002, **18**, 5360.

305 J. V. M. Weaver, S. P. Armes and V. Butun, *Chem. Commun.*, 2002, **0**, 2122.

306 Y. Maeda, H. Mochiduki and I. Ikeda, *Macromol. Rapid. Commun.*, 2004, **25**, 1330.

307 Y. J. Shih, Y. Chang, A. Deratani and D. Quemener, *Biomacromolecules*, 2012, **13**, 2849.

308 G. Coullerez, A. Carlmark, E. Malmström and M. Jonsson, *J. Phys. Chem. A*, 2004, **108**, 7129.

309 J. Xu, J. He, D. Fan, X. Wang and Y. Yang, *Macromolecules*, 2006, **39**, 8616.

310 C. Pietsch, U. Mansfeld, C. Guerrero-Sanchez, S. Hoeppener, A. Vollrath, M. Wagner, R. Hoogenboom, S. Saubern, S. H. Thang, C. R. Becer, J. Chiefari and U. S. Schubert, *Macromolecules*, 2012, **45**, 9292.

311 A. J. Convertine, D. S. W. Benoit, C. L. Duvall, A. S. Hoffman and P. S. Stayton, *J. Control Release.*, 2009, **133**, 221.

312 F. Fernandez-Trillo, J. C. M. van Hest, J. C. Thies, T. Michon, R. Weberskirch and N. R. Cameron, *Chem. Commun.*, 2008, 2230.

313 D. E. Discher and A. Eisenberg, *Science*, 2002, **297**, 967.

314 A. Sorrenti, O. Illa and R. M. Ortuno, *Chem. Soc. Rev.*, 2013.

315 J. D. Hartgerink, E. Beniash and S. I. Stupp, *Science*, 2001, **294**, 1684.

316 A. H. Gröschel, F. H. Schacher, H. Schmalz, O. V. Borisov, E. B. Zhulina, A. Walther and A. H. E. Müller, *Nat. Commun.*, 2012, **3**, 710.

317 J. Zhang, X.-F. Chen, H.-B. Wei and X.-H. Wan, *Chem. Soc. Rev.*, 2013, **42**, 9127.

318 G. Riess, *Prog. Polym. Sci.*, 2003, **28**, 1107.

319 Q. Chen, K. Osada, T. Ishii, M. Oba, S. Uchida, T. A. Tockary, T. Endo, Z. Ge, H. Kinoh, M. R. Kano, K. Itaka and K. Kataoka, *Biomaterials*, 2012, **33**, 4722.

320 S. Uchida, K. Itaka, Q. Chen, K. Osada, T. Ishii, M.-A. Shibata, M. Harada-Shiba and K. Kataoka, *Mol Ther*, 2012, **20**, 1196.

321 N. P. Truong, Z. Jia, M. Burgess, L. Payne, N. A. J. McMillan and M. J. Monteiro, *Biomacromolecules*, 2011, **12**, 3540.

322 S. Ganta, H. Devalapally, A. Shahiwala and M. Amiji, *J. Control Release.*, 2008, **126**, 187.

323 A. K. Bajpai, S. K. Shukla, S. Bhanu and S. Kankane, *Prog. Polym. Sci.*, 2008, **33**, 1088.

324 R. Langer and D. A. Tirrell, *Nature*, 2004, **428**, 487.

325 S. Binauld and M. H. Stenzel, *Chem. Commun.*, 2013, **49**, 2082.

326 N. Murthy, Y. X. Thng, S. Schuck, M. C. Xu and J. M. J. Frechet, *J. Am. Chem. Soc.*, 2002, **124**, 12398.

327 P. Cai-Yuan, T. Lei and W. De-Cheng, *J. Polym. Sci. Pol. Chem.*, 2001, **39**, 3062.

328 N. A. A. Rossi, Y. Zou, M. D. Scott and J. N. Kizhakkedathu, *Macromolecules*, 2008, **41**, 5272.

329 Q. Zhang, C. Wang, L. Qiao, H. Yan and K. Liu, *J. Mater. Chem.*, 2009, **19**, 8393.

330 C. J. F. Rijcken, O. Soga, W. E. Hennink and C. F. van Nostrum, *J. Control Release.*, 2007, **120**, 131.

331 K. L. Heredia and H. D. Maynard, *Org. Biomol. Chem.*, 2007, **5**, 45.

332 H. Li, A. P. Bapat, M. Li and B. S. Sumerlin, *Polym. Chem.*, 2011, **2**, 323.

333 E. M. Bachelder, T. T. Beaudette, K. E. Broaders, J. Dashe and J. M. J. Fréchet, *J. Am. Chem. Soc.*, 2008, **130**, 10494.

334 R. A. Shenoi, J. K. Narayanannair, J. L. Hamilton, B. F. L. Lai, S. Horte, R. K. Kainthan, J. P. Varghese, K. G. Rajeev, M. Manoharan and J. N. Kizhakkedathu, *J. Am. Chem. Soc.*, 2012, **134**, 14945.

335 G. Gaucher, M. H. Dufresne, V. P. Sant, N. Kang, D. Maysinger and J. C. Leroux, *J. Control Release.*, 2005, **109**, 169.

336 S. De Koker, B. N. Lambrecht, M. A. Willart, Y. van Kooyk, J. Grooten, C. Vervaet, J. P. Remon and B. G. De Geest, *Chem. Soc. Rev.*, 2011, **40**, 320.

337 J. J. Moon, B. Huang and D. J. Irvine, *Adv. Mater.*, 2012, **24**, 3724.

338 J. Luten, C. F. van Nostruin, S. C. De Smedt and W. E. Hennink, *J. Control Release.*, 2008, **126**, 97.

339 K. Dan and S. Ghosh, *Angew. Chem. Int. Edit.*, 2013, **52**, 7300.

340 C. C. Lee, J. A. MacKay, J. M. J. Frechet and F. C. Szoka, *Nat. Biotechnol.*, 2005, **23**, 1517.

341 L. S. Nair and C. T. Laurencin, *Prog. Polym. Sci.*, 2007, **32**, 762.

342 Y. Wu, W. Chen, F. Meng, Z. Wang, R. Cheng, C. Deng, H. Liu and Z. Zhong, *J. Control Release.*, 2012, **164**, 338.

343 C. Oerlemans, W. Bult, M. Bos, G. Storm, J. F. W. Nijsen and W. E. Hennink, *Pharm. Res.*, 2010, **27**, 2569.

344 W. Amass, A. Amass and B. Tighe, *Polym. Int.*, 1998, **47**, 89.

345 D. Zhang, H. Zhang, J. Nie and J. Yang, *Polym. Int.*, 2010, **59**, 967.

346 Y. Zou, D. E. Brooks and J. N. Kizhakkedathu, *Macromolecules*, 2008, **41**, 5393.

347 H. Morinaga, H. Morikawa, Y. Wang, A. Sudo and T. Endo, *Macromolecules*, 2009, **42**, 2229.

348 X.-N. Huang, F.-S. Du, B. Zhang, J.-Y. Zhao and Z.-C. Li, *J. Polym. Sci. Pol. Chem.*, 2008, **46**, 4332.

349 K. E. Broaders, J. A. Cohen, T. T. Beaudette, E. M. Bachelder and J. M. J. Fréchet, *Proc. Natl. Acad. Sci. U.S.A.*, 2009, **106**, 5497.

350 L. Cui, J. L. Cohen, C. K. Chu, P. R. Wich, P. H. Kierstead and J. M. J. Fréchet, *J. Am. Chem. Soc.*, 2012, **134**, 15840.

351 J. A. Cohen, T. T. Beaudette, J. L. Cohen, K. E. Broaders, E. M. Bachelder and J. M. J. Fréchet, *Adv. Mater.*, 2010, **22**, 3593.

352 Z.-Y. Qiao, F.-S. Du, R. Zhang, D.-H. Liang and Z.-C. Li, *Macromolecules*, 2010, **43**, 6485.

353 X. Huang, F. Du, J. Cheng, Y. Dong, D. Liang, S. Ji, S.-S. Lin and Z. Li, *Macromolecules*, 2009, **42**, 783.

354 R. Tang, W. Ji, D. Panus, R. N. Palumbo and C. Wang, *J. Control Release.*, 2011, **151**, 18.

355 J. Heller, J. Barr, S. Y. Ng, K. S. Abdellauoi and R. Gurny, *Adv. Drug Deliver. Rev*, 2002, **54**, 1015.

356 T. s. Etrych, M. Šírová, L. Starovoytova, B. Říhová and K. Ulbrich, *Mol. Pharm.*, 2010, **7**, 1015.

357 H. Krakovičová, T. Etrych and K. Ulbrich, *Eur. J. Pharm. Sci.*, 2009, **37**, 405.

358 B. Jeong and A. Gutowska, *Trends Biotechnol.*, 2002, **20**, 305.

359 M. M. Bloksma, R. M. Paulus, H. P. C. van Kuringen, F. van der Woerdt, H. M. L. Lambermont-Thijs, U. S. Schubert and R. Hoogenboom, *Macromol. Rapid. Commun.*, 2012, **33**, 92.

360 For instance, only 22% hydrolysis of HP22 can contribute to T_{CP} increasing of 18.8 ^{o}C (from 16.2 to 35.0 ^{o}C), while for P(mTEGA-DMDMA) with T_{CP} of 13.2 ^{o}C, around 50% of hydrolysis is needed to obtain the same increasing of T_{CP} (from 13.2 to 32.0 ^{o}C). Even considering the influence of the different start T_{CP} before hydrolysis and different pH buffer solutions (HP22 in pH5, P(mTEGA-DMDMA) in pH4) of the two copolymers, the contrast is still remarkable.

361 W. Van Camp, F. E. Du Prez and S. A. F. Bon, *Macromolecules*, 2004, **37**, 6673.

362 J.-H. Ryu, R. Roy, J. Ventura and S. Thayumanavan, *Langmuir*, 2010, **26**, 7086.

Scientific publications during PhD

Peer-reviewed publications:

1. **Q. Zhang**, P. Schattling, P. Theato, R. Hoogenboom, *UV-tunable upper critical solution temperature behavior of azobenzene containing poly(methyl methacrylate) in aqueous ethanol*, **European Polymer Journal**, DOI: 10.1016/j.eurpolymj.2014.06.029.
2. M. Dierendonck, K. Fierens, R. De Rycke, L. Lybaert, S. Maji, Z. Zhang, **Q. Zhang**, R. Hoogenboom, B. N. Lambrecht, J. Grooten, J. P. Remon, S. De Koker, B. G. De Geest, *Nanoporous Hydrogen Bonded Polymeric Microparticles: Facile and Economic Production of Cross Presentation Promoting Vaccine Carriers*, **Advanced Functional Materials** 2014, 24, 4634-4644
3. **Q. Zhang,** N. Vanparijs, B. Louage, B. G. De Geest, R. Hoogenboom, *Dual pH- and temperature-responsive RAFT-based block co-polymer micelles and polymer-protein conjugates with transient solubility*, **Polymer Chemistry** 2014, 5, 1140-1144.
4. S. Maji, G. Vancoillie, L. Voorhaar, **Q. Zhang**, R. Hoogenboom, *RAFT Polymerization of 4-Vinylphenylboronic Acid as the Basis for Micellar Sugar Sensors*, **Macromolecular Rapid Communications** 2014, 35, 214-220.
5. **Q. Zhang**, J.-D. Hong, R. Hoogenboom, *A triple thermoresponsive schizophrenic diblock copolymer*, **Polymer Chemistry** 2013, 4, 4322-4325
6. Z. Zhang, S. Maji, A. B. d. F. Antunes, R. De Rycke, **Q. Zhang**, R. Hoogenboom, B. G. De Geest, *Salt Plays a Pivotal Role in the Temperature-Responsive Aggregation and Layer-by-Layer Assembly of Polymer-Decorated Gold Nanoparticles*, **Chemistry of Materials** 2013, 25, 4297-4303
7. V. S. Joseph, S. Kim, **Q. Zhang**, R. Hoogenboom, J.-D. Hong, *Multilayer films composed of a thermoresponsive cationic diblock copolymer and a photoresponsive dye*, **Polymer** 2013, 54, 4894-4901
8. **Q. Zhang**, P. Schattling, P. Theato, R. Hoogenboom, *Tuning the upper critical solution temperature behavior of poly(methyl methacrylate) in aqueous ethanol by modification of an activated ester comonomer*, **Polymer Chemistry** 2012, 3, 1418-1426

Manuscripts submitted or in preparation:

1. **Q. Zhang**, G. Vancoillie, R. Hoogenboom, *Polymeric temperature sensors*, book chapter in Thermometry at the Nanoscale, submitted.

2. B. Louage, **Q. Zhang**, N. Vanparijs, L. Voorhaar, S. Vande Casteele, Y. Shi, W. E. Hennink, J. Van Bocxlaer, R. Hoogenboom, B. G. De Geest, Dual-responsive ketal-based block copolymer nanoparticles: systematic design, self-assembly, paclitaxel loading and in vitro evaluation, Submitted
3. N. Vanparijs, S. Maji, B. Louage, L. Voorhaar, D. Laplace, **Q. Zhang**, Y. Shi, W. E. Hennink, R. Hoogenboom, B. G. De Geest, *Polymer-protein conjugation via a RAFT-based 'grafting-to' approach - a comparative study of the performance of protein-reactive raft chain transfer agents*, Submitted
4. **Q. Zhang,** R. Hoogenboom, *Polymers with upper critical solution temperature in alcohol/water solvent mixtures,* in preparation
5. **Q. Zhang,** R. Hoogenboom, *Polyampholytes prepared by copolymerization of cationic and anionic monomers: Synthesis, Thermoresponsive behavior and Micellization*, submitted
6. **Q. Zhang,** F. Tosi, S. Üğdüler, S. Maji and R. Hoogenboom, *Tuning the LCST and UCST thermoresponsive behavior of poly(N,N-dimethylaminoethyl methacrylate) by electrostatic interactions with trivalent metal hexacyanide anions and copolymerization*, submitted.
7. **Q. Zhang** et al. *One-Pot preparation of inert well-defined polymers combining RAFT polymerization in situ and end group transformation*, in preparation.
8. **Q. Zhang,** B. Louage, N. Vanparijs, B. G. De Geest, R. Hoogenboom, *Acid-labile thermoresponsive copolymers that combine fast pH triggered hydrolysis and high stability at neutral condition – on the importance of polymer architecture*, Submitted.
9. **Q. Zhang**, G. Vancoillie and R. Hoogenboom, Polymeric temperature sensor with a broad sensing regime, Submitted
10. **Q. Zhang,** L. Voorhaar, B. Fatma Yeşil and R. Hoogenboom, Fabrication of novel hybrid polymeric nanoparticles: co-assembly of thermoresponsive polymers and a double hydrophilic thermoresponsive block copolymer, in preparation

Conference contributions:

1. **Q. Zhang**, P. Schattling, P. Theato, R. Hoogenboom, *UV-tunable upper critical solution temperature behavior of azobenzene containing poly(methyl methacrylate) in aqueous ethanol solutions,* 248 ACS national meeting, 10-14th, August 2014, San Francisco, USA *Poster*
2. **Q. Zhang**, R. Hoogenboom, *Tuning the LCST and UCST thermoresponsive behavior of Poly(N,N-dimethylaminoethyl methacrylate) by electrostatic interactions and copolymerization,* 248 ACS national meeting, 10-14th, August 2014, San Francisco, USA *Oral presentation by R. Hoogenboom*
3. **Q. Zhang,** B. Louage, N. Vanparijs, B. G. De Geest, R. Hoogenboom, *pH degradable thermoresponsive polymers for biomedical applications,* 248 ACS national meeting, 10-14th, August 2014, San Francisco, USA *Poster*
4. **Q. Zhang**, R. Hoogenboom, *Understanding cooperative lower critical solution temperature behavior based on poly(2-oxazoline)s with systematical variations in hydrophobicity,* 248 ACS national meeting, 10-14th, August 2014, San Francisco, USA *Poster*

5. **Q. Zhang**, R. Hoogenboom, *Fabrication of novel hybrid polymeric micelles: co-assembly of thermoresponsive homopolymers and a double hydrophilic block copolymer*, 248 ACS national meeting, 10-14th, August 2014, San Francisco, USA *Poster*

6. **Q. Zhang**, P. Schattling, P. Theato, R. Hoogenboom, *UV-tunable upper critical solution temperature behavior of poly(methyl methacrylate) in aqueous ethanol*, ESF Research Networking Programme Precision Polymer Materials (P2M), 2nd P2M Conference, 25- 28th Aug. 2013, Ghent, Belgium *Poster*

7. **Q. Zhang**, B. G. De Geest, R. Hoogenboom, *pH degradable thermoresponsive polymer*, European Polymer Congress EPF 16-21st, Jun 2013, Pisa, Italy *Poster*

8. **Q. Zhang**, R. Hoogenboom, *A triple thermoresponsive schizophrenic diblock copolymer*, COST workshop, 2-3rd, May 2013, Leuven, Belgium *Oral presentation*

9. **Q. Zhang**, B. G. De Geest, R. Hoogenboom, *pH degradable thermoresponsive polymer*, MacroBeGe-Belgian-German (Macro)Molecular Meeting, 3-4th, Dec. **2012**, Houffalize, Belgium *Poster*

10. **Q. Zhang**, R. Hoogenboom, *Thermoresponsive polymers based on poly(meth)acrylate scaffolds*, BPG 2012 - Annual Meeting of the Belgian Polymer Group, 10-11th, May **2012**, Blankenberge, Belgium *Oral presentation*

11. **Q. Zhang**, P. Schattling, P. Theato, R. Hoogenboom, *Tuning the UCST behavior of PMMA in aqueous ethanol by modification of an activated ester comonomer*, KVCV Biannual meeting, **2012**, Blankenberge, Belgium *Poster*

12. **Q. Zhang**, P. Schattling, P. Theato, R. Hoogenboom, *Tuning the UCST behavior of PMMA in aqueous ethanol by modification of an activated ester comonomer*, IUPAC 9th International Conference on Advanced Polymers via Macromolecular Engineering (APME 2011), 5-8th, Sep. **2011**, Cappadocia, Turkey *Poster*

13. **Q. Zhang**, P. Schattling, P. Theato, R. Hoogenboom, *Tuning the UCST behavior of PMMA in aqueous ethanol by modification of an activated ester comonomer*, BPG 2011 - Annual Meeting of the Belgian Polymer Group, 12-13th, May **2011**, Houffalize, Belgium *Poster*